Soils and Rocks Volume 34, N.1 2011

ISSN 1980-9743

Soils and Rocks

Soils and Rocks

An International Journal of Geotechnical and Geoenvironmental Engineering

Volume 34, N. 1
January-April 2011

Soils and Rocks is an International Journal of Geotechnical and Geoenvironmental Engineering published by

ABMS - Brazilian Association for Soil Mechanics and Geotechnical Engineering
Av. Prof. Almeida Prado, 532, IPT/DEC-Prédio 54
05508-901 São Paulo, SP
Brazil

SPG – Portuguese Geotechnical Society
LNEC, Avenida do Brasil, 101
1700-066 Lisboa
Portugal

Issue Date: *April 2011*

Issue: *3,200 copies*

Manuscript Submission: *For review criteria and manuscript submission information, see Instructions for Authors at the end.*

SOILS and ROCKS

An International Journal of Geotechnical and Geoenvironmental Engineering

Editor André Pacheco de Assis - University of Brasília, Brazil

Co-editor Ricardo Oliveira - COBA, Portugal

Soils and Rocks publishes papers in English in the broad fields of Geotechnical Engineering, Engineering Geology and Geo-environmental Engineering. The Journal is published in April, August and December. Subscription price is US$ 90.00 per year. The journal, with the name "Solos e Rochas", was first published in 1978 by the Graduate School of Engineering-Federal University of Rio de Janeiro (COPPE-UFRJ). In 1980 it became the official magazine of the Brazilian Association for Soil Mechanics and Geotechnical Engineering (ABMS), acquiring the national character that had been the intention of its founders. In 1986 it also became the official Journal of the Brazilian Association for Engineering Geology and the Environment (ABGE) and in 1999 became the Latin American Geotechnical Journal, following the support of Latin-American representatives gathered for the Pan-American Conference of Guadalajara (1996). In 2007 the journal acquired the status of an international journal under the name of Soils and Rocks, published by the Brazilian Association for Soil Mechanics and Geotechnical Engineering (ABMS), Brazilian Association for Engineering Geology and the Environment (ABGE) and Portuguese Geotechnical Society (SPG). In 2010, ABGE decided to publish its own journal and left the partnership.

Soils and Rocks

1978,	1 (1, 2)
1979,	1 (3), 2 (1,2)
1980-1983,	3-6 (1, 2, 3)
1984,	7 (single number)
1985-1987,	8-10 (1, 2, 3)
1988-1990,	11-13 (single number)
1991-1992,	14-15 (1, 2)
1993,	16 (1, 2, 3, 4)
1994-2010,	17-33 (1, 2, 3)
2011,	**34 (1**

ISSN 1980-9743 CDU 624.131.1

ISSN 1980-9743

SOILS and ROCKS

An International Journal of Geotechnical and Geoenvironmental Engineering

Publication of

ABMS - Brazilian Association for Soil Mechanics and Geotechnical Engineering

SPG - Portuguese Geotechnical Society

Volume 34, N. 1, January-April 2011

Table of Contents

Victor de Mello Lecture

The Victor de Mello Lecture was established in 2008 by the Brazilian Association for Soil Mechanics and Geotechnical Engineering (ABMS), the Brazilian Association for Engineering Geology and the Environment (ABGE) and the Portuguese Geotechnical Society (SPG) to celebrate the life and professional contributions of Prof. Victor de Mello. Prof. de Mello was a consultant and academic for over 5 decades and made important contributions to the advance of geotechnical engineering. Each year a worldwide acknowledged geotechnical expert is invited to deliver this special lecture. It is a privilege to have Dr. Harry G. Poulos (Coffey Geotechnics, Australia) delivering the second edition of the Victor de Mello Lecture. Dr. Poulos and Prof. de Mello were close friends for decades and in his lecture he reviews the contributions of the late Victor de Mello to foundation engineering and highlights the insights that he provided in a number of key areas.

Prof. HARRY POULOS AM FAA FTSE, DScEng is a Senior Principal with the geotechnical consulting company of Coffey Geotechnics in Sydney Australia, and an Emeritus Professor at the University of Sydney. He has been involved in a large number of major projects in Australia and overseas including the Egnatia Odos highway project in Greece, the Burj Khalifa tower in Dubai, and the Dubai tower in Doha, Qatar. He was elected a Fellow of the Australian Academy of Science in 1988 and a Fellow of The Australian Academy of Technological Sciences and Engineering in 1996. He has received a number of awards and prizes, including the Kevin Nash Gold Medal of the International Society of Soil Mechanics and Geotechnical Engineering in 2005. He was the Rankine Lecturer in 1989 and the Terzaghi Lecturer in 2004, and was selected as the Australian Civil Engineer of the Year for 2003 by the Institution of Engineers, Australia. In 1993, he was made a Member of the Order of Australia for his services to engineering, and in 2010, he was elected a Distinguished Member of the American Society of Civil Engineers.

Soils and Rocks
v. 34, n. 1

The de Mello Foundation Engineering Legacy

Harry G. Poulos

Abstract. This paper reviews the contributions of the late Victor de Mello to foundation engineering and attempts to highlight the insights that he provided in a number of key areas, including foundation design principles, the bearing capacity of shallow foundations, the axial load capacity of deep foundations, and the behaviour of foundations incorporating settlement reducing piles. In each case, de Mello challenged some of the existing concepts and as a consequence, subsequent research has clarified the profession's understanding and has led to the development and implementation of improved methods of design. Some examples of developments in the above areas, and their application to practice, are described.

Keywords: bearing capacity, design criteria, foundations, piles, piled raft, settlement.

1. Introduction

The late Victor de Mello was no ordinary man. He was not only one of the world's pre-eminent geotechnical engineers, but also a person with an enormous breadth and depth of knowledge, and with passionate but considered views of many aspects of human society and existence. As a consequence, he was a vibrant and stimulating colleague and friend. His personal qualities have been described fully and eloquently by Professor John Burland in his first de Mello Lecture (Burland, 2008) and I can only add that I was privileged, as was Professor Burland, to have the encouragement of this giant of our profession in the early stages of my career. He was extraordinarily well-read, both in his professional field and in many other areas of intellectual endeavour, and could debate with equal authority the finer points of soil behaviour and the competing virtues of various philosophers of the enlightenment.

De Mello was an expert in several areas of geotechnical engineering, and in particular, embankment dams, and his 1977 Rankine Lecture dealt with this topic in an authoritative and expansive way. He also had a major influence on foundation engineering, and it is this aspect that will be explored in this paper. In particular, there are two pivotal papers that will be referred to frequently here, his State of the Art Report at the 7th International Conference in Mexico City in 1969, entitled "Foundations of Buildings in Clay", and his General Report with Burland & Broms at the 9th International Conference in Tokyo entitled "Behaviour of Foundations and Structures". An indication of his breadth of reading is evidenced by the very large number of references in these papers, 344 in the first and 333 in the second. Mention can also be made here of his epic treatise on the Standard Penetration Test (de Mello, 1971) which contained no less than 353 references, his 1994 Terzaghi Oration at the 13th International Conference in New Delhi, and in a different vein, his paper in 2000 uniquely entitled "Overview of hypotheses not plucked or pursued. Merit recanting or rechanting?"

I will attempt in this paper to summarize the engineering philosophy of Victor de Mello and then to examine some areas within foundation engineering in which he made notable contributions, and in which he identified shortcomings. The questions that he raised have been addressed subsequently by both researchers and practitioners, and have led to a better understanding of foundation behaviour and to more robust practical methods of analysis and design. The areas that will be discussed include the bearing capacity of shallow foundations, the load capacity and settlement of piles under axial loading, and the behaviour and design of settlement reducing piles.

2. Some Aspects of the De Mello Philosophy

2.1. Broad views

Victor de Mello expounded his philosophical views on a number of issues, some related directly to foundation engineering, and some to broader issues of design, education and the role of the engineer in society. Burland (2008) succinctly summarized de Mello's philosophy in terms of five Design Principles (DP). These were oriented towards embankment dam design, but can perhaps be generalised as follows:

1. DP1 - Aim to design out any risk from behaviour triggered by local phenomena – *Robustness.*
2. DP2 - Use a dominant feature to cut across uncertainties – *Change the problem*
3. DP3 - Aim at homogenization – *Redundancy.*
4. DP4 - Minimize rapid uncontrolled loading – *Observational control.*
5. DP5 - Question each design assumption and the consequences of departure from it – *Ask "what if" questions.*

Beyond these broad design principles, there were a number of other viewpoints that de Mello expressed (often very forcefully), and a small selection of these views is presented below, based on his published papers. Most of the

Harry G. Poulos, Coffey Geotechnics, Sydney, Australia. e-mail: harry_poulos@coffey.com.
Submitted on February 8, 2011; Final Acceptance on February 21, 2011; Discussion open until August 31, 2011.

quotations are self-explanatory and require little or no comment.

2.2. False conclusions from data

De Mello was highly critical of people who drew inappropriate conclusions from available data, and illustrated his point with the following example (de Mello, 1984):

"Most persons die in bed; therefore bed is the single most dangerous place for humans".

2.3. Use and abuse of statistics

Statistics was viewed by de Mello as a useful tool but one that was frequently mis-used or abused. The following quotation sets out his views on this subject.

"We must shun statistics at random, and choose to apply statistical adjustments to our reasonable theories. The temporary application of a presumed theory does not preclude that it is not satisfactory, and consequently revising it, or even proposing an entirely different one; what cannot be condoned is the attempt to extract conclusions from data at random and spurious statistics, without any theory, however nominal, or any design and purpose, since such efforts prove sterile and may even lead to dangerous conclusions" (de Mello, 1984).

2.4. The costs of undue conservatism and the problem of codes

An enduring theme in de Mello's publications was his extreme distaste for excessive conservatism brought about by a lack of understanding of geotechnical and foundation behaviour and the shelter that codes and standards provided for those who lacked such understanding.

"Two fundamental challenges in geotechnical civil engineering have been neglected under the avalanche of the published word in scientific quantifications. One is the nurturing of past experience of individual cases. The other is the global resulting cost to society of the constructed facility, with due inclusion of the costs of risk and of discredited professional prestige" (de Mello, 1994).

"Do the learned writers of prescriptions and codes realize how much and how unjustifiably they increase the conservatism of driven piling?" (de Mello, 1995).

"Misunderstood pronouncements, and a few visible failures, have weighed a thousand times more than the trernendously more important silent record of cases that did not merit study or publication".

"How can committees, discussing Codes, lightly banter around with changes of FS values (*e.g.* from 1.5 to 2.0, or vice-versa) without any statistical data to evaluate the magnitudes of the consequences?" (de Mello, 1995).

2.5. The philosophy of design

"We recognise two distinct phases of study, firstly, the adjustment of parameters and computational models and methods, so as to be able to predict deformations or other behaviour reasonably. The second problem is one of decision: how acceptable are the displacements predicted or observed" (de Mello, 1983).

"Of the many absurdities in design practices, one lies in requiring the same FS per pile whether it is alone in supporting a column, or is one of a group for that task" (de Mello, 1995).

2.6. Role of computers and computations

"The computer has diverted a great proportion of attention from real-life field geotechnics – paper is easily generated and imprinted, and checking proof positive for mental models is simpler" (de Mello, 2004).

"Computations (analytic or numerical) are a means and not ends, in service of engineering" (de Mello, 1992).

2.7. Importance of knowing the ground conditions

"A prime requirement for foundation design and construction will always be a knowledge of the soil profile and groundwater conditions across the site. No amount of detailed laboratory testing or sophisticated analysis can compensate for such knowledge" (Burland *et al.*, 1977).

2.8. Professional communications

"Let us not make the mistake of speaking within our closed circle, to ourselves; it is to our clients that we must speak., and convincingly we must have the courage to separate some of the adulterated data that most often surround us" (de Mello, 1983).

2.9. Case histories

"Although we emphasize the importance of analysing case histories, in order to avoid chaotic conclusions, or conclusions dominated by subjective and/or wishful thinking, it is even more important to run such case history back-analyses objectively, expurgating the inexorable subjective and deterministic reasonings" (de Mello, 1983).

2.10. The failings of contemporary civil engineering education

"Am I becoming old and grouchy when I complain that universities are no longer producing the civil geotechnical engineers, but mostly young technocrats who are absolutely sure of their theories, and armed with computers, absolutely sure of their numbers, to several decimal places?" (de Mello, 1985).

2.11. Specifications

"It is fundamental to reject once and for all the often cited, and even lauded, method specification. It is illogical.

The only valid principle acceptable is the end product specification". (de Mello, 2000).

2.12. Lack of proper progress in geotechnical engineering

De Mello was passionate about the folly of pursuing unnecessary refinements that did not lead to material progress, but rather to the perpetuation of irrelevant problem-solving. The following quotation expresses very clearly his frustrations with the perceived lack of direction in progressing geotechnical engineering.

"For better setting our line of sight, it is imperative that we keep revising our origins and reappraising our goals of service to society. We move imperceptibly from finding adequate solutions to significant problems, to seeking illusory refinements of solutions, to finding problems in solution, and to seeking problems in problems. *Quo Vadis, Geotecnica*?" (de Mello, 1995).

3. Foundation Design Principles and Criteria

3.1. Introduction

De Mello thought carefully and critically about commonly used design principles, design methods and design criteria. As mentioned in Section 2.3 above, he was particularly hostile to the unthinking acceptance of the provisions of codes and standards that contained criteria that were excessively conservative or that were not consistent with practical experience. Some of his views on design principles and design criteria are summarized below, together with later views by other authors.

3.2. Design principles

A paper published in the Salas memorial volume in 2000 set out de Mello's views on the shortcomings of common design practices for piling. Among the issues upon which he commented were the following:

• The lack of benefit granted by codes to the design of pile groups, in comparison with single piles.

• The probability of failure or unsatisfactory behaviour decreased greatly with large groups, yet this was not taken into account in the codes of which he was aware. He therefore urged "earnest reconsideration of the historical arbitrary fixed FS numbers".

• "A building's performance doesn't know whether it is founded on footings, piles, piers or rafts; why is it that the settlement-limited codified prescriptions are so much tighter for piles than for footings?"

• Whatever the desirability may be, in 99% of practical cases, prior testing of preliminary piles is not feasible, in contrast to the recommendation of the ISSMFE subcommittee

• The standards for pile load testing lack rationality in the specified testing procedures. It is not necessary to wait for settlements to stabilize beyond the working dead load, as the emphasis is then on the pile capacity and checking the factor of safety. Accordingly, it would be more rational to employ a constant, and rapid, rate of penetration test, rather than a conventional incremental loading test.

It is clear that de Mello was greatly concerned about the lack of rationality of foundation design methods, and in particular, the rather ad-hoc choices that designers made for the factor of safety against failure. The following section describes one attempt to place this issue on a more rational and logical basis.

3.3. The de Mello principles applied in a design code

The recently – released Australian Piling Code, AS2159-2009, incorporates a risk assessment procedure for obtaining the partial factor of safety (or its reciprocal, the geotechnical strength reduction factor) when designing piles against failure. This code adopts a limit state approach, and the key requirement for the ultimate limit state (*i.e.* the design against geotechnical failure) requires the following condition to be satisfied:

$$R_{d,g} \geq E_d \tag{1}$$

where $R_{d,g}$ = design geotechnical strength of the pile and E_d = design action effect, *i.e.* the factored-up load combination.

$R_{d,g}$ is computed as follows:

$$R_{d,g} = \gamma_g R_{d,ug} \tag{2}$$

where $R_{d,ug}$ = ultimate geotechnical strength (capacity) of pile and γ_g = geotechnical reduction factor.

The geotechnical reduction factor is given by:

$$\gamma_g = \gamma_{gb} + (\gamma_{tf} - \gamma_{gb})K \geq \gamma_{gb} \tag{3}$$

where γ_{gb} = basic geotechnical strength reduction factor; γ_{tf} = intrinsic test factor: 0.9 for static load testing, 0.75, for rapid load testing, 0.8, for dynamic load testing of preformed piles, 0.75, for dynamic load testing of other than preformed piles, 0.85, for bi-directional load testing, and γ_{gb}, for no testing; K = testing benefit factor: $1.33p/(p + 3.3) \leq 1$, for static or rapid load testing, $1.13p/(p + 3.3) = 1$, for dynamic load testing, and p = percentage of the total piles that are tested and meet the specified acceptance criteria

The basic geotechnical strength reduction factor (γ_{gb}) is calculated using the following risk assessment procedure:

(a) Each risk factor shown in Table 1 is rated by the designer on a scale from 1 to 5 for the nature of the site, the available site information and the pile design and installation procedures adopted. This will produce an individual risk rating *(IRR)* according to the level of risk assessed by the designer, as set out in Table 2.

(b) The overall design average risk rating *(ARR)* is obtained using the weighted average of the product of all of the risk weighting factors (w_i) shown in column 2 of Table 2, times the relevant individual risk rating *(IRR),* as follows:

$$ARR = \frac{\sum w_i IRR_i}{\sum wI} \quad (4)$$

(c) The basic geotechnical strength reduction factor (γ_{gb}) is then obtained from Table 3, depending on the level of redundancy in the piling system. Systems with a high degree of redundancy would include large pile groups under large caps, piled rafts and pile groups with more than 4 piles. Systems with a low level of redundancy would in-

Table 1 - Weighting factors and individual risk ratings for risk factors (AS2159-2009).

Risk factor	Weighting factor (w_i)	Typical description of risk circumstances for individual risk rating (IRR)		
		1 (Very low risk)	3 (Moderate)	5 (Very high risk)
Site				
Geological complexity of site	2	Horizontal strata, well-defined soil and rock characteristics	Some variability over site, but without abrupt changes in stratigraphy	Highly variable profile or presence of karstic features or steeply dipping rock levels or faults present on site, or combinations of these
Extent of ground investigation	2	Extensive drilling investigation covering whole site to an adequate depth	Some boreholes extending at least 5 pile diameters below the base of the proposed pile foundation level	Very limited investigation with few shallow boreholes
Amount and quality of geotechnical data	2	Detailed information on strength compressibility of the main strata	CPT probes over full depth of proposed piles or boreholes confirming rock as proposed founding level for piles	Limited amount of simple in situ testing (*e.g.*, SPT) or index tests only
Design				
Experience with similar foundations in similar geological conditions	1	Extensive	Limited	None
Method of assessment of geotechnical parameters for design	2	Based on appropriate laboratory or in situ tests or relevant existing pile load test data	Based on site-specific correlations or on conventional laboratory or in situ testing	Based on non-site-specific correlations with (for example) SPT data
Design method adopted	1	Well-established and soundly based method or methods	Simplified methods with well-established basis	Simple empirical methods or sophisticated methods that are not well established
Method of utilizing results of in situ test data and installation data	2	Design values based on minimum measured values on piles loaded to failure	Design methods based on average values	Design values based on maximum measured values on test piles loaded up only to working load, or indirect measurements used during installation, and not calibrated to static loading tests
Installation				
Level of construction control	2	Detailed with professional geotechnical supervision, construction processes that are well established and relatively straight forward	Limited degree of professional geotechnical involvement in supervision, conventional construction procedures	Very limited or no involvement by designer, construction processes that are not well established or complex
Level of performance monitoring of the supported structure during and after construction	0.5	Detailed measurements of movements and pile loads	Correlation of installed parameters with on-site static load tests carried out in accordance with this Standard	No monitoring

The pile design includes the risk circumstances for each individual risk category and consideration of all of the relevant site and construction factors.

clude isolated heavily loaded piles and piles set out at large spacings.

The approach is based on an earlier paper that developed a reliability-based approach to pile capacity design (Poulos, 2004). It is considered that the approach incorporates a number of the aspects of foundation design philosophy that de Mello advocated, including:

• Proper consideration of the various geotechnical risks involved, including the site conditions, the design process and the construction procedure.

• The application of engineering judgement by the designer.

• Allowance for the benefits of doing pile load testing to reduce uncertainties.

3.4. Foundation settlement criteria for design

In his State of the Art paper in 1969, de Mello had commented that "a great number of truly outstanding cases of buildings and other projects successfully designed on clays, under conditions so adverse as to challenge responsibility to the point of daring, attest to the fact that there has been a very considerable progress in the field."

The subsequent paper by Burland *et al.* (1977) was highly influential in promoting a more rational approach to design criteria in relation to allowable foundation movements, and furthering the profession's appreciation of the importance not only of the type of structure, but also of the nature of the deformations. For example, following on the work of Burland & Wroth (1974), the 1977 paper emphasized that brick walls subjected to "hogging" deformations were more susceptible to damage than the same walls subjected to "sagging" movements.

They also summarized some of the available information relating building damage to foundation movements, including the following:

Skempton & MacDonald (1956) had recommended safe limits of total settlements of 40 mm for isolated foundations, and 40-65 mm for rafts, maximum differential settlements of 25 mm and a relative rotation (angular distortion) of 1/500. In sands, settlement takes place rapidly under load, and therefore these criteria may be conservative. Indeed, no cases of damage to buildings founded on sand had been reported up to that time.

Table 2 - Individual Risk Rating (IRR).

Risk level	Individual risk rating (IRR)
Very low	1
Low	2
Moderate	3
High	4
Very high	5

For buildings on isolated foundations on clay, some cases of slight damage had been reported for total settlements in excess of 150 mm and differential settlements in excess of 50 mm.

For buildings founded on rafts in clay, no damage had been reported for total settlements less than 250 mm and differential settlements less than 125 mm.

The movements quoted above are well in excess of the allowable values that are commonly adopted for foundation design, and prompted the authors to question "who is limiting the settlements and why."

More recent work by Zhang & Ng (2006) has confirmed that the conclusions reached by Burland *et al.* (1977), and their recommendations are summarized in Table 4. Even these recommendations may be somewhat conservative in light of the fact that a number of buildings in Frankfurt founded on piled rafts in clay have settled well in excess if 100 mm without any visible signs of distress.

4. Bearing Capacity of Shallow Foundations

4.1. Introduction

In his state-of-the art lecture at the 7th International Conference in 1969, de Mello introduced a degree of scepticism in relation to the theory of bearing capacity of a shallow foundation, and wrote as follows: "Notwithstanding the great importance of the determination of the ultimate bearing capacity of a foundation, it is evident that the theo-

Table 3 - Basic geotechnical strength reduction factor (γ_{gb}) for average risk rating.

Range of average risk rating (*ARR*)	Overall risk category	γ_{gb} for low redundancy systems	γ_{gb} for high redundancy systems
ARR ≤1.5	Very low	0.67	0.76
1.5 < *ARR* ≤2.0	Very low to low	0.61	0.70
2.0 < *ARR* ≤2.5	Low	0.56	0.64
2.5 < *ARR* ≤3.0	Low to moderate	0.52	0.60
3.0 < *ARR* ≤3.5	Moderate	0.48	0.56
3.5 < *ARR* ≤4.0	Moderate to high	0.45	0.53
4.0 < *ARR* ≤4.5	High	0.42	0.50
> 4.5	Very high	0.40	0.47

Table 4 - Suggested serviceability criteria for structures (Zhang & Ng, 2006).

Quantity	Value	Comments
Limiting tolerable Settlement mm	106	Based on 52 cases of deep foundations. Std. Deviation = 55 mm. Factor of safety of 1.5 recommended on this value
Observed intolerable Settlement mm	349	Based on 52 cases of deep foundations. Std. Deviation = 218 mm
Limiting tolerable angular distortion rad	1/500 1/250 (H < 24 m) 1/330 (24 < H < 60 m) 1/500 (60 < H < 100 m) 1/1000(H > 100 m)	Based on 57 cases of deep foundations. Std. Deviation = 1/500 rad From Chinese Code (MOC, 2002) H = building height
Observed intolerable angular distortion rad	1/125	Based on 57 cases of deep foundations. Std. Deviation = 1/90 rad

retical solutions to the problems are still subject to discussion, both in comparison between them, and in comparisons with controlled tests designed to check their validity". This scepticism proved to be well-founded, as subsequent work demonstrated significant dispersion of theoretical solutions and also disturbing differences between theoretical and measured behaviour. Some of these differences are discussed below.

4.2. Conventional theory

The traditional Terzaghi bearing capacity theory (Terzaghi, 1943) expresses the ultimate bearing capacity, q_u, of a shallow footing as follows:

$$q_u = c.\,N_c + 0.5\gamma B.N_\gamma + \gamma D.\,N_q \tag{5}$$

where c = soil cohesion, γ = soil unit weight, B = footing width, D = depth of embedment of base of footing below surface, N_c, N_γ and N_q are bearing capacity factors that depend on the angle of internal friction γ of the soil.

Terzaghi derived the bearing capacity factors from a limit equilibrium analysis. Subsequently, Davis & Booker (1971) obtained solution for the bearing capacity factors N_c, N_γ and N_q from plasticity theory, and compared these with the traditional Terzaghi theory. As shown in Fig. 1, the Terzaghi theory overestimates the bearing capacity factors considerably as compared with the more rigorous

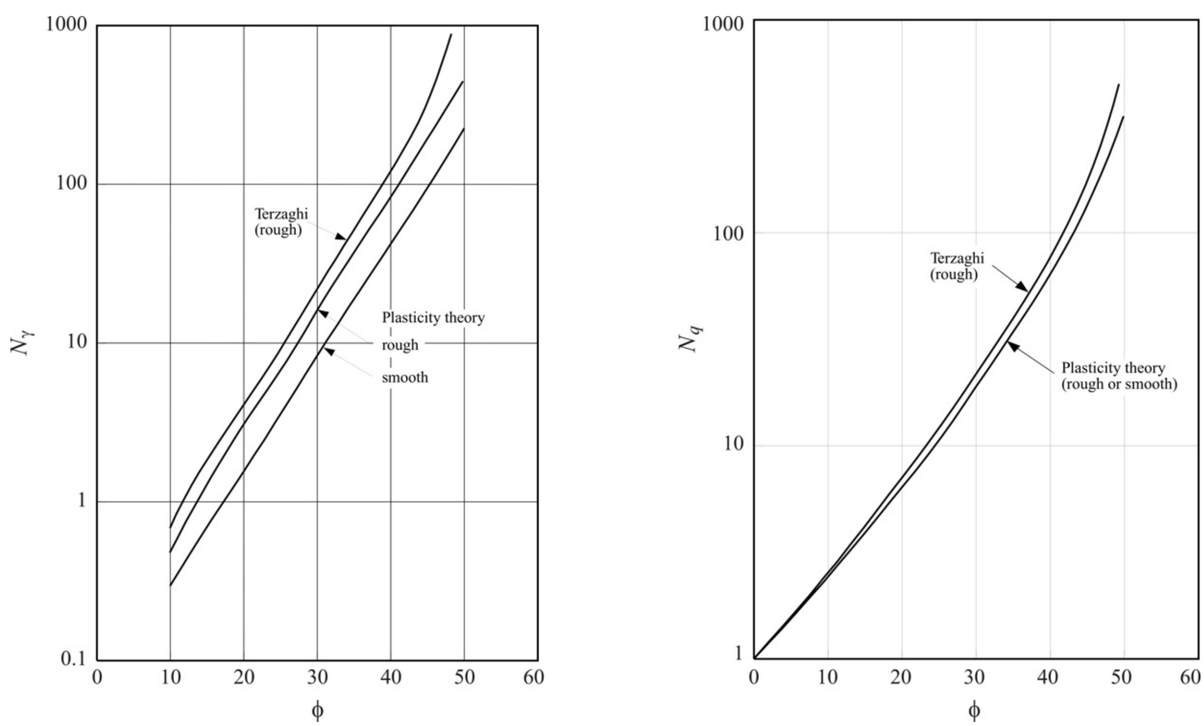

Figure 1 - Comparison between Terzaghi (1943) and Davis & Booker (1971) solutions for shallow footing bearing capacity.

plasticity solutions of Davis & Booker, with the difference being particularly marked for the factor N_γ for a smooth footing.

The superposition of the three components of bearing capacity in Eq. (3) has been recognised as being an approximation and Poulos *et al.* (2001) point out that the highly non-linear behaviour of real soils may mean that the superposition is at best approximate. They also note that while the traditional bearing capacity approach is based on plasticity theory, there is a significant amount of empiricism to allow for practical complicating factors that make a rigorous solution intractable or very difficult to obtain, for example, the effects of footing shape, load inclination, and soil surface inclination.

4.3. Effects of soil compressibility

A further issue was raised by Vesic (1973) who demonstrated the critical importance of soil compressibility in determining foundation bearing capacity. While the traditional bearing capacity theories for a rigid plastic material might be satisfactory for stiff clays under undrained conditions, they could seriously over-predict the bearing capacity of footings on relatively compressible soils such as loose calcareous sediments. Vesic introduced compressibility correction factors for the traditional bearing capacity factors that were a function of the rigidity index I_r, defined as follows:

$$I_r = G / (c + q.\tan\gamma) \tag{6}$$

where G = soil shear modulus, c = cohesion, q = vertical pressure, γ = angle of internal friction.

Terzaghi had in fact recognised this shortcoming in describing the mechanism of "local shear" failure for compressible sands. He recommended that, in such cases, a reduced angle of friction of about 2/3 of the actual friction angle be employed. An illustrative case of the importance of soil compressibility was presented by Poulos & Chua (1985) who compared the bearing capacity of a shallow circular model footing on silica sand and then the same footing on calcareous sand. The calcareous sand had a much greater compressibility, as indicated by the load-settlement curves in Fig. 2. Figure 3 shows the measured bearing capacity as a function of the relative density of the soil. The more compressible calcareous soil has a markedly smaller bearing capacity than the silica sand at the same relative density.

Figures 4 and 5 compare the measured bearing capacities with three different computed values:

• That computed from Terzaghi's conventional rigid plastic theory (general shear), using the measured angle of internal friction;

• That computed from Terzaghi's bearing capacity, using a friction angle reduced to 2/3 of the measured value;

• That computed from cavity expansion theory.

These comparisons show that, for both the silica sand and the calcareous sand, Terzaghi's conventional theory significantly over-estimates the bearing capacity, whereas the latter two methods of calculation give a more satisfactory level of agreement with the measurements.

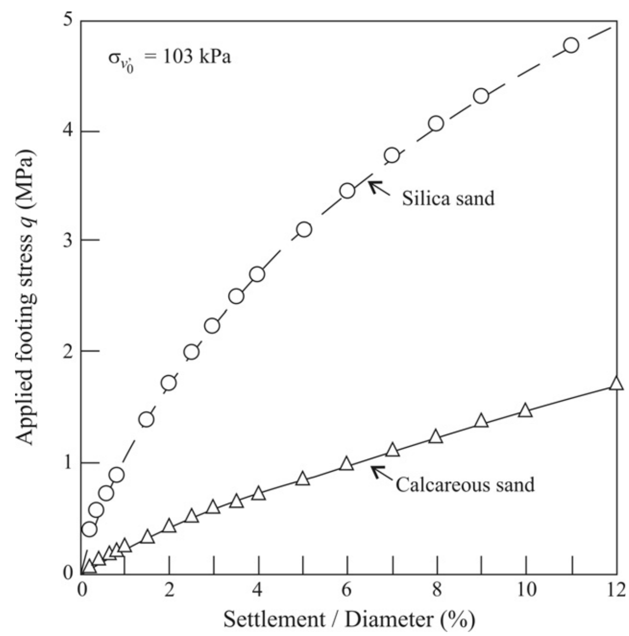

Figure 2 - Load-settlement curves for model footing on silica sand and calcareous sand (Poulos & Chua, 1985).

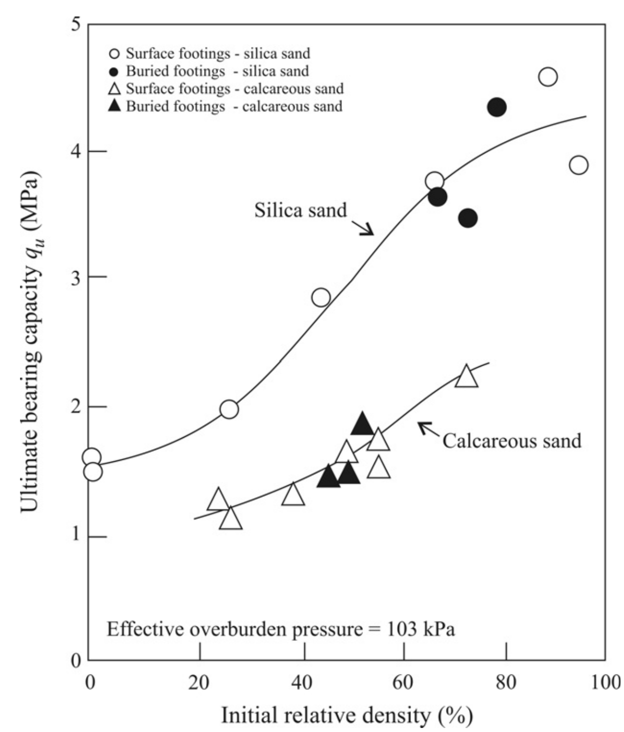

Figure 3 - Bearing capacity of model footings on silica sand and calcareous sand (Poulos & Chua, 1985).

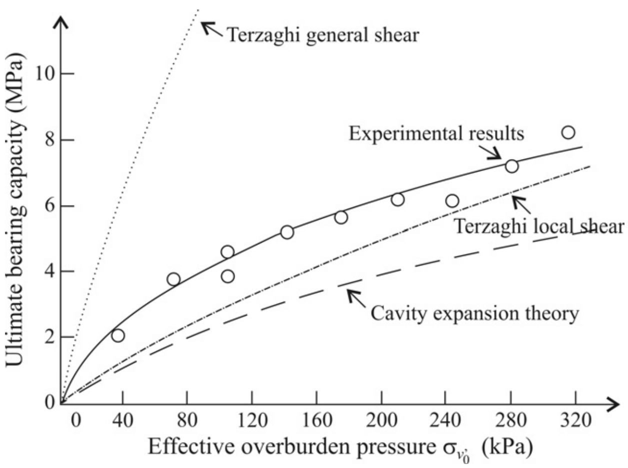

Figure 4 - Comparison between measured and calculated bearing capacity of footing on silica sand (Poulos & Chua, 1985).

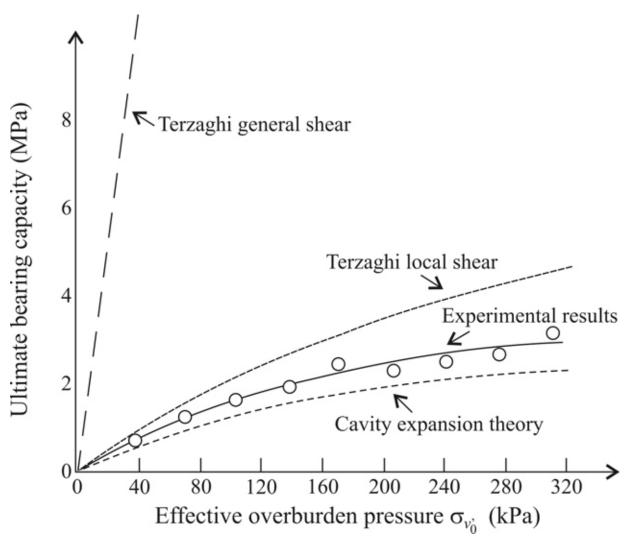

Figure 5 - Comparison between measured and calculated bearing capacity of footing on calcareous sand (Poulos & Chua, 1985).

4.4. Combined vertical, lateral and moment loadings

The Terzaghi equation does not directly consider the effects of horizontal or moment loading, and is confined to purely vertical applied load on a shallow footing. A variety of approximations have been developed to cater for combined loading, and a review of some of these was made by Poulos *et al.* (2001). An equation describing the failure locus in terms of all three components of the load was proposed by Taiebat & Carter (2000a) and was expressed as follows:

$$f = \left(\frac{V}{V_u}\right)^2 + \left(\frac{M}{M_u}\left(1-\alpha_1\frac{H\,M}{H_u\,|M|}\right)\right)^2 + \left|\left(\frac{H}{H_u}\right)^3\right| - 1 = 0 \quad (7)$$

where V_u, M_u and H_u are the ultimate vertical, moment and horizontal load capacities of the footing, and α_1 is a factor that depends on the soil profile.

For a homogeneous soil, a value of $\alpha_1 = 0.3$ provides a good fit to the bearing capacity predictions from the numerical analysis. The three-dimensional failure locus described by Eq. (7) will not tightly match the numerical predictions over the entire range of loads, especially around the abrupt changes in the failure locus that occur when the horizontal load is high. However, overall the approximation is satisfactory, conservative and sufficient for many practical applications.

For a footing subjected to eccentric vertical loading, there is no exact expression to evaluate the effects of eccentricity of the load applied to a foundation. However, the effective width method is commonly used in the analysis of foundations subjected to eccentric loading (*e.g.*, Vesic, 1973; Meyerhof, 1951, 1953). In this method, the bearing capacity of a foundation subjected to an eccentrically applied vertical loading is assumed to be equivalent to the bearing capacity of another foundation with a fictitious effective area on which the vertical load is centrally applied.

Comparisons presented by Poulos *et al.* (2001) showed that the effective width method, commonly used in the analysis of foundations subjected to eccentric loading, provides good approximations to the collapse loads, and that its continued use in practice therefore appears justified.

4.5. Differences between theory and experiment

According to the classical bearing capacity theory, the bearing capacity q_u of a footing of width B on the surface of a soil layer with zero cohesion is given by:

$$q_u = \gamma B N_\gamma / 2 \quad (8)$$

where γ = soil unit weight and N_γ = bearing capacity factor depending on the friction angle γ.

This equation implies that the larger the footing width B, the larger is the unit bearing capacity q_u. Unfortunately, there is now considerable evidence that demonstrates that this theoretical conclusion is not borne out in practice. For example, Decourt (2008) has re-plotted data from tests on footings of various sizes and found that, when normalized with respect to settlement/diameter (S/B), the load-settlement curves are unique and not dependent on the footing size nor on the relative density (Fig. 6). Similar conclusions have been reached from recent centrifuge test carried out on model footings by Gavin *et al.* (2009). In Fig. 7, the ratio of bearing pressure to cone resistance is plotted against S/B, and again, a relatively unique relationship is derived, regardless of footing size (for prototype footings ranging between 1 and 3 m in width). Akbas & Kulhawy (2009) have arrived at similar conclusions to those of Decourt and Gavin *et al.*

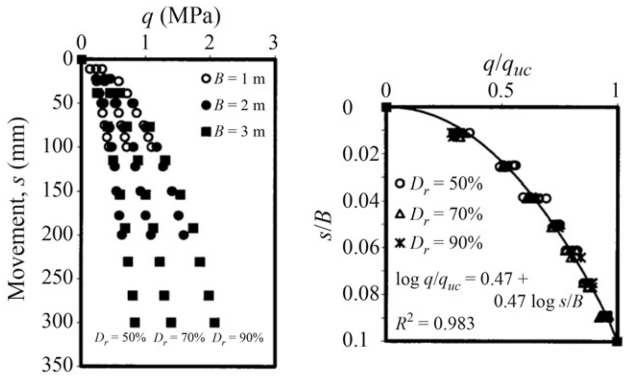

Figure 6 - Load-settlement curves for footings of various diameter on sand (Decourt, 2008).

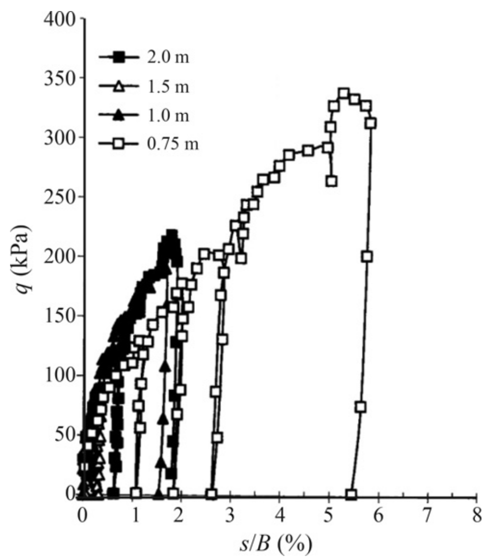

Figure 7 - Load-settlement curves for footings on sand at shenton park, site C (Gavin *et al.*, 2009).

4.6. Summary

De Mello's doubts in 1969 regarding the applicability of Terzaghi's theory to practice appear to have been well-founded. Experience now demonstrates that:

• The original Terzaghi bearing capacity factors were not entirely accurate;

• Soil compressibility plays a major role in bearing capacity and the use of the original rigid plastic theory may tend to overestimate bearing capacity significantly for granular soils.

• The "N_γ" term in the Terzaghi bearing capacity equation implies that the bearing capacity of a surface footing increases in proportion to its size. However, this does not appear to be the case in reality.

It is interesting to note that, 31 years after his 1969 classic paper, de Mello bemoaned the persistent adherence by the geotechnical profession to conventional bearing capacity theories, as follows: "My questions and objections to be raised in these matters are unfortunately repeated from a distant candid outcry (de Mello, 1969). I appeal for an unabashed abandonment of plasticity theory solutions, their postulates and results to be courageously recanted".

5. Axial Load Capacity of Pile Foundations

5.1. Introduction

The 1969 General Report by de Mello highlighted a number of important issues that were emerging in relation to the axial load capacity of piles. These issues included the following:

• The pile installation method can have a significant effect on the axial capacity;

• The displacement required to mobilize the ultimate shaft resistance is independent of pile diameter, whereas that required to mobilize the base resistance is roughly proportional to pile diameter.

• The ultimate skin friction of piles in sand does not increase linearly with depth, as would be inferred from conventional methods of calculation. Rather, the work of Vesic (1965) indicated that a limiting average skin friction would be reached at some depth, typically 10-20 diameters.

• The shaft friction in compression is different from that in tension, which had been frequently overlooked in attempts to establish skin friction values from field tests.

• It is desirable to develop a load-settlement curve for a pile, not only an estimate of the ultimate load. Emerging methods of analysis, such as those published by Seed & Reese (1955) and Poulos & Davis (1968) were mentioned.

For piles in clay, de Mello reproduced data from Kerisel (1965) that related the ratio of ultimate skin friction (f_s) to undrained shear strength (s_u), as a function of s_u. This ratio (which de Mello referred to as β but is more commonly given the symbol α) was recognized by de Mello as "a rough indication which must be subject to "a considerable latitude of judgement".

De Mello concluded that there was a need to develop improved approaches to the estimation of pile shaft friction in place of the rudimentary methods existing at that time. Some of these developments are outlined below.

5.2. Methods of estimation of pile shaft friction

5.2.1. Total stress approach

One of the traditional methods of estimating the ultimate shaft friction in compression, f_s, involves the use of the total stress ("alpha") method for piles in clay soils. This method relates f_s to the undrained shear strength s_u as:

$$f_s = \alpha s_u \tag{9}$$

where α = adhesion factor.

Poulos *et al.* (2001) summarize several approaches for assessing the adhesion factor α, most of which involve relating α to s_u; for example, Kulhawy & Phoon (1993) suggest the following approximation:

$$\alpha = 0.21 + 0.26\,(p_a/s_u)\,(\leq 1.0) \quad (10)$$

where p_a = atmospheric pressure.

It must be admitted that relatively limited progress has been made with total stress approaches since de Mello's report, the possible exception being the approach developed by Fleming *et al.* (1992) in which α is related not to s_u but to the ratio of undrained shear strength to vertical effective stress, s_u/σ_v':

$$\alpha = (s_u/\sigma_v)^{0.5}\,(s_u/\sigma_v)^{-0.5} \text{ for } (s_u/\sigma_v') \leq 1 \quad (11)$$

$$\alpha = (s_u/\sigma_v)^{0.5}\,(s_u/\sigma_v)^{-0.25} \text{ for } (s_u/\sigma_v') \geq 1 \quad (12)$$

5.2.2. Effective stress approaches

The effective stress ("beta") method can be applied for piles in any soil type. f_s is related to the in-situ effective stresses as follows:

$$f_s = K_s \tan\delta\,\sigma'_v \quad (13)$$

where K_s = lateral stress coefficient; δ = pile-soil friction angle; σ'_v = effective vertical stress at level of point under consideration.

Several of the more recent effective stress methods have employed cavity expansion theories in an attempt to model the effects of installation and subsequent loading of the pile (for example, Randolph *et al.*, 1979; Carter *et al.*, 1979b). While the results of such studies have been illuminating and have indicated the important effects of initial installation and subsequent dissipation of excess pore pressures, they appear to have had relatively little impact on design practice, due largely to the need to have reasonably detailed knowledge of the initial stress conditions within the soil, as well as the soil strength and compressibility characteristics. A detailed and intensive discussion of effective stress approaches to estimating the ultimate shaft friction is given by O'Neill (2001).

An alternative approach has been adopted by a number of researchers, in which attempts have been made to develop more reliable methods of estimating the lateral stress coefficient K_s. Notable among such methods is the approach of Jardine & Chow (1996), who have related K_s to the cone resistance, the distance from the pile tip, and the dilatant increase in normal stress during pile loading. Different expressions have been derived for driven piles in sand and clay soils, and the case of open-ended piles has also been considered. These expressions have been based on carefully instrumented pile data and a close appreciation of the fundamental behaviour of soils and pile-soil interfaces. Alternative methods have been developed more recently and these are summarised conveniently by Seo *et al.* (2009). Most of these recent methods have been developed for the offshore industry and involve the use of data from cone penetration testing. Where such data are available, comparisons between measured and computed shaft friction values indicate more satisfactory agreement than with the earlier procedures.

Seo *et al.* (2009) have presented an interesting comparison of the computed shaft capacities for an H-pile in a layered soil profile consisting of interbedded clays, silts and sands. The comparison is shown in Table 5, together with the measured shaft capacity. The computed values are for the assumption that the friction is mobilized around the outer shaft perimeter, rather than around the full interface contact perimeter. It can be seen that five of the seven methods considered tend to over-estimate the shaft capacity, and that there is a factor of almost 3 between the largest and smallest estimates of capacity.

Thus, despite almost 40 years of research and application, there is still great uncertainty in predicting the shaft capacity of a single pile in a realistic layered soil profile.

In addition, a number of issues raised by de Mello in 1969 still remain to be clarified for practical pile designers in relation to the ultimate shaft friction on piles. Such issues include the following:

- Does a limiting value of f_s actually exist, especially for piles in sandy soils?
- How does the value of f_s in uplift compare to the value of f_s for compression?
- Can laboratory testing be used to provide a more reliable estimate of f_s?

The results of recent research over the past decade or so can shed some light on these issues.

5.3. Limiting f_s values for piles in sandy soils

The concept of limiting ultimate shaft resistance in sandy soils was developed by Kerisel (1961), Vesic (1967) and BCP (1971). It arose from tests on instrumented piles in which it appeared that the average ultimate shaft friction reached a limiting value for depths in excess of between 5 and 20 pile diameters from the top of the pile. This was attributed to an arching phenomenon around the shaft, and led to the adoption of a practice of specifying limiting f_s val-

Table 5 - Measured and computed shaft capacities for an H-pile in layered soil (after Seo *et al.*, 2009).

Prediction method	Shaft capacity (kN)
Fleming *et al.* (1992) & API (1993)	1314
Foye *et al.* (2009) and API (1993)	1724
Aoki & Velloso (1975) – SPT	1179
Aoki & Velloso (1975) – CPT	868
Bustamante & Gianeselli (1982) – CPT	638
NGI (Clausen *et al.*, 2005) – CPT	1281
ICP (Jardine *et al.*, 2005) - CPT	1228
Measured value	1053

ues in design (*e.g.*, Vesic, 1969; Meyerhof, 1976; Poulos & Davis, 1980).

The existence of such a limiting value has been questioned critically by a number of authors subsequently (*e.g.*, Kulhawy, 1984; Fellenius, 1984). The apparent limiting values of f_s have been attributed to at least two factors:

• The existence of residual stresses in the piles before the measurements of shaft resistance were made. This leads to the shaft friction in the lower part of the pile appearing to be lower than the true value;

• The overconsolidation of the soil near the surface, which gives rise to higher values of in-situ lateral stress, and hence values of shaft resistance. The effects of overconsolidation become less with increasing depth, and hence the rate of increase of shaft resistance with depth becomes less.

Attempts to reproduce theoretically the apparent limiting shaft friction have been unsuccessful, although a reduction in the rate of increase of shaft resistance has been obtained by consideration of the effects of compressibility of the soil, and the reduction of the soil friction angle (and hence the interface friction angle) with increasing effective pressure and depth.

The conclusion to be drawn from research into this aspect is that a limiting value of f_s probably does not exist, although the rate of increase of f_s with depth is not linear. However, from the viewpoint of practical design, the adoption of a suitable limiting value of f_s is a conservative approach which at least avoids predicting unrealistically large shaft friction values at great depths within a sandy soil.

5.4. Shaft resistance in uplift and compression

It is generally accepted that the uplift shaft resistance for piles in clay is similar to that for compressive loading. However, there is conflicting evidence in relation to piles in sand, with some early researchers indicating similar values for both compression and uplift, while others found the values in uplift to be less than in compression.

A significant advance in understanding of this problem was made by de Nicola & Randolph (1993) who showed that the ratio of the uplift resistances in uplift and compression, f_{su}/f_{sc}, was dependent on the relative compressibility of the pile, via the Poisson effect. The relationship they derived is as follows:

$$\frac{f_{su}}{f_{sc}} = \left\{1 - 0.2\log_{10}\left[\frac{100}{L/d}\right]\right\}(1 - 8\eta - 25\eta^2) \qquad (14)$$

where L = pile length; d = pile diameter; η = dimensionless compressibility factor = $\nu_p.\tan\sigma.(L/d).(G_{av}/E_p)$; ν_p = pile Poisson's ratio; σ = pile-soil interface friction angle; G_{av} = average soil shear modulus along pile shaft; E_p = Young's modulus of pile material. For piles in medium dense to dense sands, this ratio typically ranges between 0.7 and 0.9, but tends towards unity for relatively short piles.

5.5. Use of laboratory testing for f_s

It has generally been accepted by practitioners that there is no suitable laboratory test which can be used reliably to measure the ultimate shaft friction f_s. However, there has been a significant development over the past 10-15 years in direct shear testing of interfaces, with the development of the "constant normal stiffness" (CNS) test (Ooi & Carter, 1987; Lam & Johnston, 1982). The basic concept of this test is illustrated in Fig. 8, and involves the presence of a spring of appropriate stiffness against which the normal stress on the interface acts. This test provides a closer simulation of the conditions at a pile-soil interface than the conventional constant normal stress direct shear test. The normal stiffness K_n can be "tuned" to represent the restraint of the soil surrounding the pile, and is given by:

$$K_n = \frac{4G_s}{d} \qquad (15)$$

where G_s = shear modulus of surrounding soil; d = pile diameter.

The effects of interface volume changes and dilatancy can be tracked in a CNS test, and the results are particularly enlightening when cyclic loading is applied, as they demonstrate that the cyclic degradation is due to the reduction in normal stress arising from the cyclic displacements applied to the interface.

Some success has been achieved in applying CNS testing to the estimation of skin friction f_s for large diameter piles in Middle East soft carbonate rocks. Figure 9 shows comparisons between values of ultimate static shaft friction from CNS tests and measured mobilized values of shaft friction from full-scale pile load tests for the Emirates Towers (Poulos & Davids, 2005). There is a tendency for the CNS data to be somewhat higher than the measured mo-

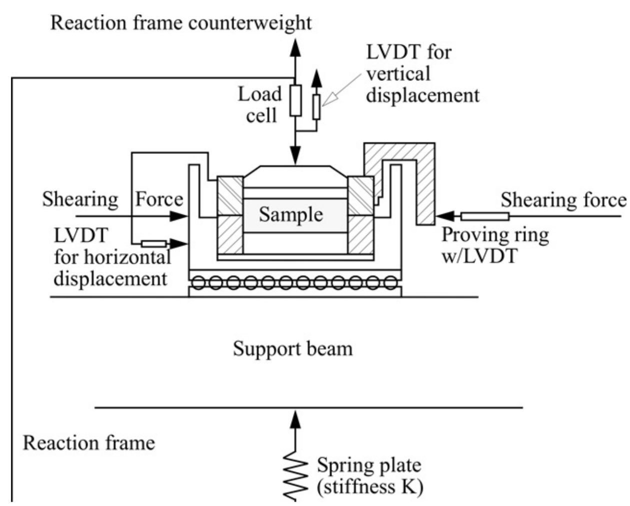

Figure 8 - Constant normal stiffness direct shear apparatus (Tabucanon *et al.*, 1995).

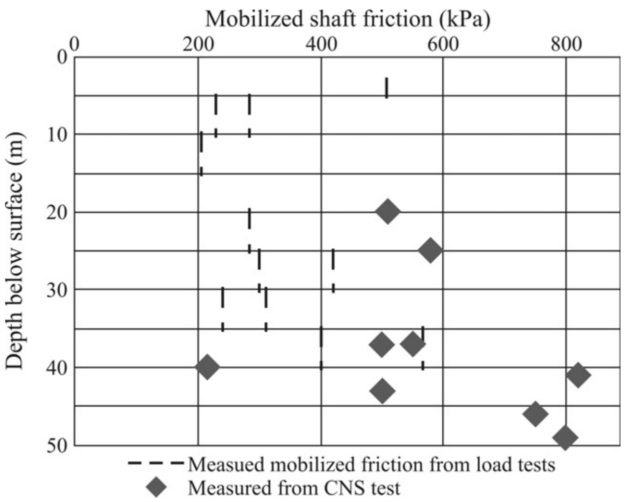

Figure 9 - Shaft friction data from Emirates project, Dubai (after Poulos & Davids, 2005).

bilized values, but it must be pointed out that the full pile capacity had not been mobilized when the maximum test load was reached. Hence, the actual ultimate shaft friction values may well have been similar to those measured from the CNS testing. In any case, as a consequence of both the laboratory testing and the subsequent pile load tests, the design values of shaft friction were increased considerably over the values that had previously been adopted in Dubai.

5.6. Methods of estimation of pile end bearing

In the total stress approach, the ultimate end bearing resistance f_b is given by:

$$f_b = N_c\ s_u \tag{16}$$

where N_c = bearing capacity factor.

This approach is almost universally used for piles founded in clay, but clearly is inapplicable to piles founded in granular materials or rock. For piles in granular materials, or for long-term bearing capacity generally, an effective stress approach must be used, and the following approximate relationship is commonly adopted:

$$f_b = \sigma_v'.N_q \tag{17}$$

where σ_v' = vertical effective stress at level of pile base and N_q = bearing capacity factor.

Figure 10 reproduces a figure that appeared in the classic text by Lambe & Whitman (1969) and demonstrated an alarming spread of theoretical solutions for the bearing capacity factor N_q for deep foundations. For a typical angle of internal friction of 35 degrees, this factor could vary between about 53 and 380, depending on whose theory was employed. Perhaps as a consequence of this gross uncertainty with the theoretical basis of calculation, let alone the issue of appropriate geotechnical parameter selection, researchers have attempted to develop methods of end bearing capacity estimation that bypass the theory. A valuable

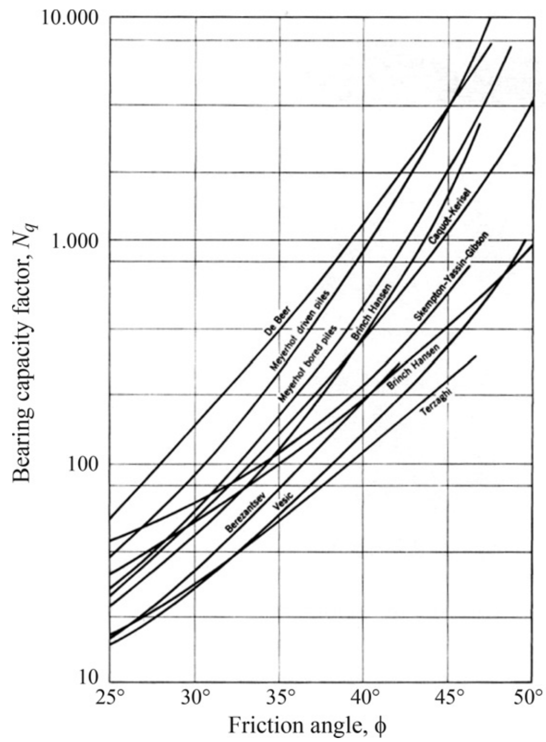

Figure 10 - Variability of theoretical solutions for bearing capacity factor N_q (Lambe & Whitman, 1969).

summary of some of these approaches is given by Seo *et al.* (2009), and again, many of these methods require cone penetration test (CPT) data.

For the same soil profile considered for shaft friction comparisons, Seo *et al.* (2009) compared the computed end bearing capacities from a number of methods for a steel H-pile, using the gross cross-sectional area of the pile in the calculations. Table 6 compares the computed end bearing values, and the measured value for a settlement of 10% of the equivalent pile diameter. It can be seen that there is a considerable scatter of the computed values and that most of the methods (except that of Jardine *et al.*, 2005) overestimate the end bearing capacity. Clearly, while there have been considerable advances in our understanding of the mechanics of pile-soil interaction, there is still a considerable uncertainty attached to our ability to predict the most fundamental characteristic of a pile, its ultimate axial load capacity.

5.7. Load-settlement curve estimation

5.7.1. Single piles

In1969 de Mello had commented on the need to develop methods of load-settlement estimation. Over the following four decades, some advances have been made in this regard, but it is interesting that the method of Seed & Reese (1955), utilizing the load transfer (or "t-z") curve concept, remains firmly embedded as one of the most commonly used approaches. Over, the past forty years, advances have

Table 6 - Measured and predicted ultimate base capacities (Seo *et al.*, 2009).

Prediction method	Base capacity using gross cross-sectional area (kN)
Fleming *et al.* (1992)	1409
Aoki & Velloso (1975) –SPT	1488
Aoki & Velloso (1975) – CPT	1306
Bustamante & Gianeselli (1982) – CPT	1260
NGI (Clausen *et al.*, 2005) - CPT	1096
Fugro (Kolk *et al.*, 2005) – CPT	1257
UWA (Lehane *et al.*, 2005) – CPT	1375
ICP (Jardine *et al.*, 2005) – CPT	853
Foye *et al.* (2009) - CPT	1204
Measured (at 10% base diameter settlement)	906

been made in the means of developing the "t-z" curves, progressing from the purely empirical methods of Coyle & Reese (1966), through the method published by Kraft *et al.* (1981) that utilized some aspects of elastic theory, to the relatively sophisticated approaches described by Randolph (2003) via his RATZ analysis. This program combines parabolic models for the shaft and base resistance responses with elastic compression of the pile, to compute the overall pile head load-settlement relationship for the pile. Figure 11 shows a satisfactory comparison between measured and predicted load-settlement behaviour for a single pile within a silty sand and sand site (Deeks *et al.*, 2005).

It is also possible to obtain good agreement between computed and measured load-settlement behaviour using a modified boundary element technique that utilizes elastic theory for the soil, but impose limiting values of shaft and base resistances, and assumed hyperbolic relationships between the local Young's modulus and local stress level. Figure 12 shows an example of a "Class A" prediction for a large diameter bored test pile for the Emirates twin tower project in Dubai, using the modified boundary element approach (Poulos & Davids, 2005). The agreement with the measured load-settlement behaviour is reasonably good, although the measured axial capacity and stiffness of the pile are clearly greater than those predicted from the design parameters.

A further development of elastic theory has been proposed by Mayne & Elkahim (2002) and Mayne & Zavala (2004), in which the elastic solutions for pile head settlement are combined with a modulus degradation function developed by Fahey & Carter (1993), namely:

$$E/E_0 = [1 - f(P/P_u)^g] \tag{18}$$

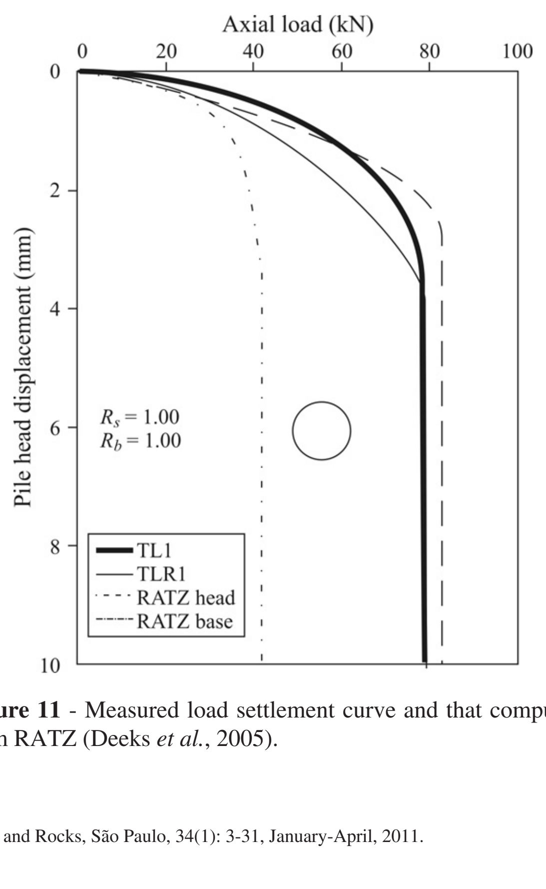

Figure 11 - Measured load settlement curve and that computed from RATZ (Deeks *et al.*, 2005).

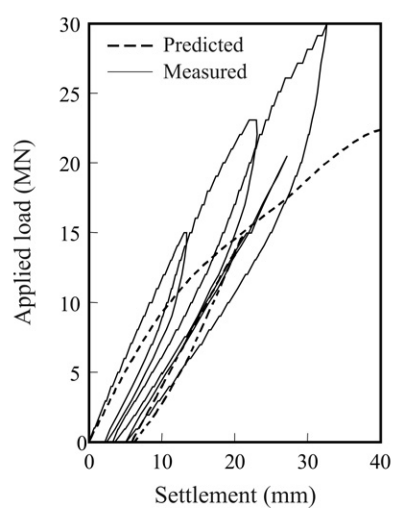

Figure 12 - Comparison between predicted and measured load-settlement behaviour for test pile at Emirates project, Dubai (Poulos & Davids, 2005).

where E_0 = small-strain Young's modulus, E = Young's modulus for an applied load P, P_u = ultimate axial load capacity, and f and g are parameters, generally taken as $f = 1$ and $g = 0.3$.

Figure 13 reproduces the measured and computed load-settlement curves for a case considered by Mayne & Elhakim (2002) in which the small-strain Young's modulus was derived from shear wave velocity measurements within the soil. The agreement can be seen to be very good, both for the overall load-settlement behaviour and for the individual shaft and base load versus settlement curves.

It appears that various methods of estimating the load-settlement behaviour of single piles have been developed since 1969, and that, provided appropriate values of pile shaft friction and end bearing, and soil stiffness, are used, these analyses can give a reasonable prediction of load-settlement behaviour.

5.7.2. Pile groups

In their 1977 state-of-the-art paper, Burland *et al.* (1977) commented that the settlement of pile groups was at that time commonly calculated from the assumption that end bearing piles are rigidly supported at the toe and that floating piles are rigidly supported at the centre of the lower third point. Since then, there have been significant developments in the prediction of the settlement of pile groups, and a number of methods are now available for practical application. A review of some of these methods has been made by Randolph (1994), Mandolini *et al.* (2005) and Poulos (2006), among others. In general, the prediction of pile group settlement is less satisfactory than for single piles, because pile group settlement is influenced not only by the shaft and base load transfer characteristics, but also by pile-soil-pile interaction, which is dependent on a number of factors, including pile spacing and configuration and the nature of the ground profile below the piles. An example of

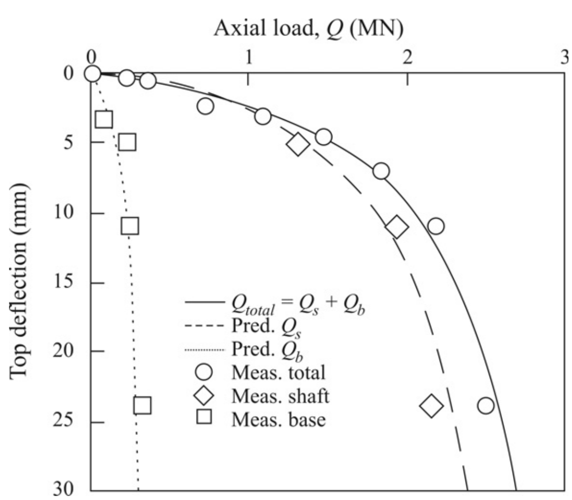

Figure 13 - Comparison between measured and calculated load-settlement behaviour for bored pile at Opelika site, Alabama (Mayne & Elhakim, 2002).

a satisfactory single pile settlement prediction, but an unsatisfactory pile group settlement prediction, is given by Poulos & Davids (2005).

There is now an increasing tendency for full three-dimensional finite element analyses to be applied to pile group settlement problems. Thus, future advances may well require more focus on proper ground characterisation and soil modelling, than on the further development of numerical techniques themselves.

5.8. Summary

Considerable research has been carried out since 1969 to improve our ability to predict pile capacity and load-settlement behaviour. Regrettably, it is not possible to claim complete success in this endeavour, as the accurate prediction of axial pile capacity remains rather elusive, despite the increased understanding of pile-soil interaction and the increased sophistication of some of the more recent methods of calculation. While some success has been achieved in predicting the load-settlement behaviour of single piles, accurate prediction of the settlement of pile groups, particularly if the piles are floating, also remains elusive. Given the high degree of sophistication that it is now possible to bring to bear on pile prediction tasks, it appears likely that the lack of consistent success may be due more to the deficiencies in characterising the ground profile, than to deficiencies in the methods of calculation.

6. Settlement Reducing Piles

6.1. Introduction

Burland *et al.* (1977) drew attention to the concept of settlement reducing piles, and commented that it should be possible to carry a substantial part of the vertical load from a pile cap or raft in the soil between the piles. They emphasized that the number of piles required to reduce settlements to an acceptable level will often be relatively small and hence the spacing of the piles within a piled raft may be relatively large. The following quotation is still as relevant today as it was in 1977:

"Traditionally engineers engaged in a pile group design have asked themselves "How many piles are required to carry the weight of the building?" When settlement is the controlling factor in the choice of piles designers should perhaps be asking the question: 'How many piles are required to reduce the settlements to an acceptable amount?' The number of piles in answer to the second question is invariably less than in answer to the first question, provided it is accepted that the load carrying capacity of each pile will probably be fully mobilized".

In many countries today, pile group design is still governed by the first question, but increasingly it is recognized that the second question is now the key design issue. This section will review, relatively briefly, some of the developments in piled raft analysis and design that have occurred over the past 33 years, and will outline some cases in which the piled raft concept has been used successfully.

6.2. Foundation concept and alternative design philosophies

Piled raft foundations utilize piled support for control of settlements with piles providing most of the stiffness at serviceability loads, and the raft element providing additional capacity at higher load levels after the capacity of the piles has been fully utilized. A geotechnical assessment for design of such a foundation system therefore needs to consider not only the capacity of the pile elements and the raft elements, but their combined capacity and their interaction under serviceability loading.

Randolph (1994) has defined clearly three different design philosophies with respect to piled rafts:

• The "conventional approach", in which the piles are designed as a group to carry the major part of the load, while making some allowance for the contribution of the raft, primarily to ultimate load capacity.

• "Creep Piling", in which the piles are designed to operate at a working load at which significant creep starts to occur, typically 70%-80% of the ultimate load capacity. Sufficient piles are included to reduce the net contact pressure between the raft and the soil to below the preconsolidation pressure of the soil.

• Differential settlement control, in which the piles are located strategically in order to reduce the differential settlements, rather than to substantially reduce the overall average settlement.

In addition, there is a more extreme version of creep piling, in which the full load capacity of the piles is utilized, *i.e.* some or all of the piles operate at 100% of their ultimate load capacity. This gives rise to the concept of using piles primarily as settlement reducers, while recognizing that they also contribute to increasing the ultimate load capacity of the entire foundation system.

Clearly, the latter approaches are most conducive to economical foundation design. However, it should be emphasized that the design methods to be discussed allow any of the above design philosophies to be implemented.

Figure 14 illustrates, conceptually, the load-settlement behaviour of piled rafts designed according to the various strategies. Curve O shows the behaviour of the raft alone, which in this case settles excessively at the design load. Curve 1 represents the conventional design philosophy, for which the behaviour of the pile-raft system is governed by the pile group behaviour, and which may be largely linear at the design load. In this case, the piles take the great majority of the load. Curve 2 represents the case of creep piling where the piles operate at a lower factor of safety, but because there are fewer piles, the raft carries more load than for Curve 1. Curve 3 illustrates the strategy of using the piles as settlement reducers, and utilizing the full capacity of the piles at the design load. Consequently,

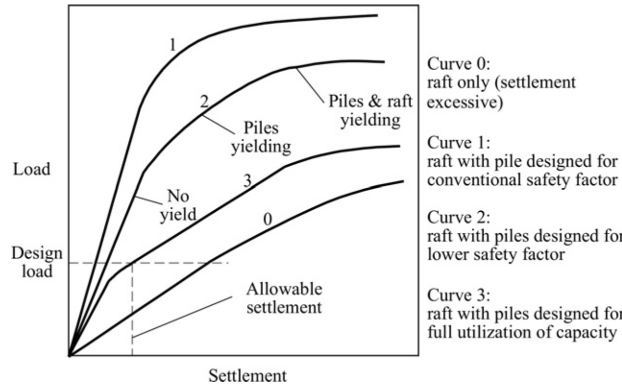

Figure 14 - Load – settlement curves for various piled raft design philosophies.

the load-settlement may be nonlinear at the design load, but nevertheless, the overall foundation system has an adequate margin of safety, and the settlement criterion is satisfied. Therefore, the design depicted by Curve 3 is acceptable and is likely to be considerably more economical than the designs depicted by Curves 1 and 2.

6.3. Favourable and less favourable circumstances for piled rafts

The most effective application of piled rafts occurs when the raft can provide adequate load capacity, but the settlement and/or differential settlements of the raft alone exceed the allowable values. Poulos (2001) has examined a number of idealized soil profiles, and found that the following situations may be favourable:

• Soil profiles consisting of relatively stiff clays

• Soil profiles consisting of relatively dense sands.

An example of the application of the piled raft concept in such circumstances was described by de Mello (1972) who developed a scheme for adding piles to control the differential settlement of a heavily loaded building.

Conversely, there are some situations which are less favourable, including:

• Soil profiles containing soft clays near the surface.

• Soil profiles containing loose sands near the surface.

• Soil profiles which contain soft compressible layers at relatively shallow depths.

• Soil profiles which are likely to undergo consolidation settlements.

• Soil profiles which are likely to undergo swelling movements due to external causes.

In the first two cases, the raft may not be able to provide significant load capacity and stiffness, while in the third case, long-term settlement of the compressible underlying layers may reduce the contribution of the raft to the long-term stiffness of the foundation. The latter two cases should be treated with caution. Consolidation settlements (such as those due to dewatering or shrinking of an active clay soil) may result in a loss of contact between the raft and the soil, thus increasing the load on the piles, and leading to increased settlement of the foundation system. In the case of swelling soils, substantial additional tensile forces may be induced in the piles because of the action of the swelling soil on the raft. Theoretical studies of these latter situations have been described by Poulos (1993) and Sinha & Poulos (1997).

6.4. Design issues and the design process

As with any foundation system, a design of a piled raft foundation requires the consideration of a number of issues, including:

1. Ultimate load capacity for vertical, lateral and moment loadings;
2. Maximum settlement;
3. Differential settlement;
4. Raft shears and moments, for the structural design of the raft;
5. Pile loads and moments, for the structural design of the piles.

In much of the available literature, emphasis has been placed on the bearing capacity and settlement under vertical loads. While this is a critical aspect, and is considered in detail herein, the other issues must also be addressed. In some cases, the pile requirements may be governed by the overturning moments and shear forces applied by wind loading, rather than the vertical dead and live loads.

It is suggested that a rational design process for piled rafts involves three main stages:

• A preliminary stage to assess the feasibility of using a piled raft, and the required number of piles to satisfy design requirements.

• A second stage to assess where piles are required and the general characteristics of the piles.

• A final detailed design stage to obtain the optimum number, location and configuration of the piles, and to compute the detailed distributions of settlement, bending moment and shear in the raft, and the pile loads and moments.

The first and second stages may involve relatively simple calculations which can usually be performed without a complex computer program. Poulos (2001) gives details of some methods that may be employed for each of the above design stages.

Once the preliminary stage has indicated that a piled raft foundation is feasible, and an indication has been obtained of the likely piling requirements, it is necessary to carry out a more detailed design in order to assess the detailed distribution of settlement and decide upon the optimum locations and arrangement of the piles. The raft bending moments and shears, and the pile loads, should also be obtained for the structural design of the foundation.

The detailed stage will generally demand the use of a suitable computer program which accounts in a rational manner for the interaction among the soil, raft and piles. The effect of the superstructure may also need to be considered. Several methods of analyzing piled rafts have been developed, and some of these have been summarized by Poulos *et al.* (1997) and Mandolini *et al.* (2005). It has been found that, despite some differences among the various methods, most of those which incorporate nonlinear behaviour give somewhat similar results, although there are significant differences among the computed raft bending moments. However, it would appear that, provided the analysis method is soundly based and takes into account the limited load capacity of the piles, similar results may be expected for similar parameter inputs.

6.5. Some characteristics of piled raft behaviour

Poulos (2001) has examined some of the characteristics of behaviour of piled rafts and the effect of the following factors on this behaviour:

1. The number of piles
2. The nature of the loading (concentrated versus uniformly distributed)
3. Raft thickness
4. Applied load level.

The following important points have been noted for practical design:

• Increasing the number of piles, while generally of benefit, does not always produce the best foundation performance, and there is an upper limit to the number of piles, beyond which very little additional benefit is obtained.

• The raft thickness affects differential settlement and bending moments, but has little effect on load sharing or maximum settlement.

• For control of differential settlement, optimum performance is likely to be achieved by strategic location of a relatively small number of piles, rather than using a large number of piles evenly distributed over the raft area, or increasing the raft thickness.

• The nature of the applied loading is important for differential settlement and bending moment, but is generally not very important for maximum settlement or load-sharing between the raft and the piles.

A particularly interesting example demonstrating the "law of diminishing returns", as applied to piled raft foundations, is described by Mandolini *et al.* (2005). They examined the effects of reducing the number of piles for the foundation of a pier of the Garigliano bridge in Italy. The conventional design approach required the addition of 144 piles to satisfy bearing capacity requirements. However, they found that a very similar settlement performance could be obtained with a significantly smaller number of piles, as shown in Fig. 15. Both their computer analysis, utilizing the program NAPRA, and a simple hand calculation method (PDR) described by Poulos (2000) showed that the settlement of the piled raft (expressed in dimensionless form in terms of the settlement of the raft alone) would be virtually unaffected if the number of piles was halved to 72. There would also be virtually no change in the load sharing between the raft and the piles.

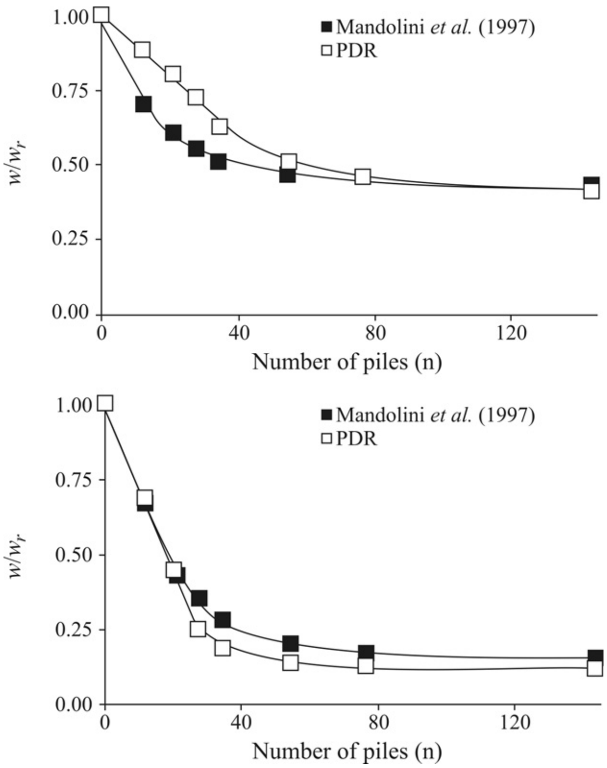

Figure 15 - The effect of number of piles on the relative settlement and load sharing (Mandolini *et al.*, 2005).

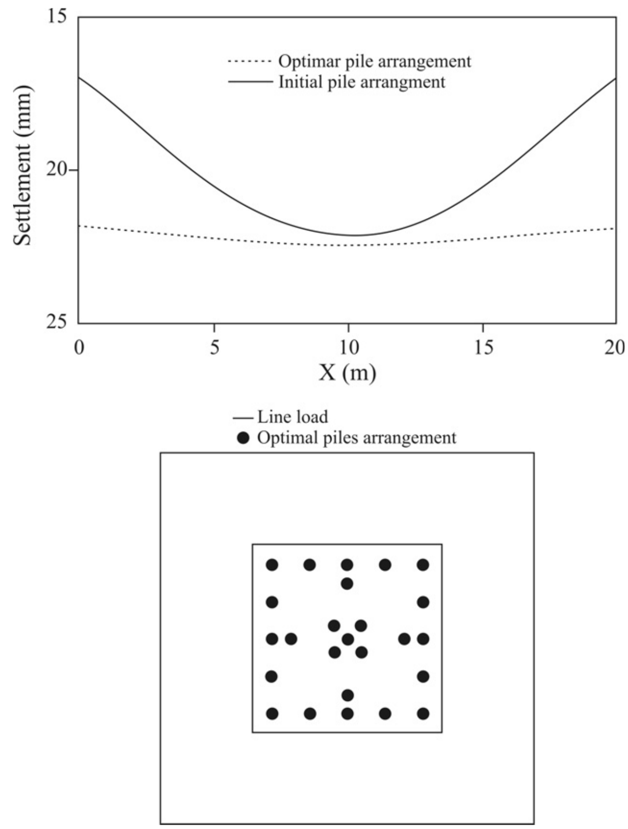

Figure 16 - The effect of pile configuration on the settlement profile below a piled raft (Fadaee & Rowhani, 2006).

It has been found that the performance of a piled raft foundation can be optimized by selecting suitable locations for the piles below the raft. In general, the piles should be concentrated in the most heavily loaded areas, while the number of piles can be reduced, or even eliminated, in less heavily loaded areas (Horikoshi & Randolph, 1998). An interesting example of pile location optimization is presented by Fadaee & Rowhani (2006), who considered a square raft with a square line load as shown in Fig. 16. The authors compared the computed distribution of settlement for two pile arrangements: 25 piles uniformly distributed across the raft, and the arrangement concentrated in the vicinity of the line load. This figure compares the computed settlement distributions, and clearly demonstrates a dramatic reduction in differential settlement with the latter pile arrangement.

Some useful further insights into piled raft behaviour have been obtained by Katzenbach *et al.* (1998) who carried out three-dimensional finite element analyses of various piled raft configurations. They used a realistic elasto-plastic soil model with dual yield surfaces and a non-associated flow rule. They analyzed a square raft containing from 1 to 49 piles, as well as a raft alone, and examined the effects of the number and relative length of the piles on the load-sharing between the piles and the raft, and the settlement reduction provided by the piles. An interaction diagram was developed, relating the relative settlement (ratio of the settlement of the piled raft to the raft alone) to the number of piles and their length-to-diameter ratio, *L/d*. For a given number of piles, the relative settlement was found to reduce as *L/d* increases. It was also found that there is generally very little benefit to be obtained in using more than about 20 piles or so, a conclusion which is consistent with the results obtained by Poulos (2001).

An interesting aspect of piled raft behaviour, which cannot be captured by simplified analyses, is that the ultimate shaft friction developed by piles within a piled raft can be significantly greater than that for a single pile or a pile in a conventional pile group. This is because of the increased normal stresses generated between the soil and the pile shaft by the loading on the raft. The results obtained by Katzenbach *et al.* (1998) indicate that the piles within the piled raft foundation develop more than twice the shaft resistance of a single isolated pile or a pile within a normal pile group, with the centre piles showing the largest values. Thus, the usual design procedures for a piled raft, which assume that the ultimate pile capacity is the same as that for an isolated pile, will tend to be conservative, and the ultimate capacity of the piled raft foundation system will be greater than that assumed in design.

6.6. Some applications of piled rafts

There are many examples of the successful use of piled rafts in practice, several of which are described in the book by Hemsley (2000). Some other cases are described briefly below.

6.6.1. Residential buildings, Sweden

An early case demonstrating the "law of diminishing returns" was provided by Hansbo (1983) who presented time-settlement curves for two similar buildings, one on 228 piles and the other on 104 piles. The first foundation system was designed as a conventional piled foundation while the second was designed using the "creep piling" concept of piled raft behaviour, as described by Burland *et al.* (1977). As shown in Fig. 17, the settlements of the two buildings were very similar, clearly indicating that the conventional design approach did not lead to any improvement in performance, despite it being more than double the cost of that using the creep piling concept.

6.6.2. Westendstrasse1, Frankfurt, Germany

The case of the Westendstrasse 1 building in Frankfurt was examined by Poulos *et al.* (1997). Figure 18 shows a plan of the tower and the 40 bored piles on which the tower was founded, and which supported an average applied pressure of about 323 kPa. Comparisons were made between the measured values of settlement and pile load, and those computed from a variety of methods, Fig. 19 shows these comparisons, from which the following conclusions can be drawn from this case:

• The measured maximum settlement is about 105 mm, and most methods tend to over-predict this settlement. However, most of the methods provide an acceptable design prediction.

• The piles carry about 50% of the total load. Most methods tended to over-predict this proportion, but from a design viewpoint, most methods give acceptable estimates.

• All methods capable of predicting the individual pile loads suggest that the load capacity of the most heavily loaded piles is almost fully utilized; this is in agreement with the measurements.

• There is considerable variability in the predictions of minimum pile loads. Some of the methods predicted larger minimum pile loads than were actually measured.

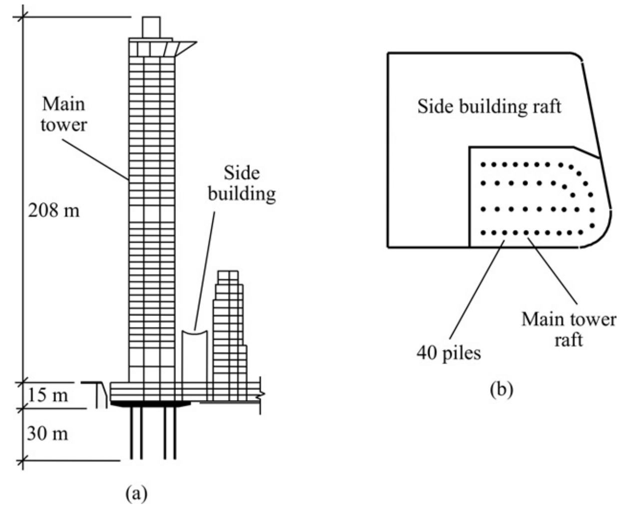

Figure 18 - Westendstrasse 1 building, Frankfurt, Germany (Franke *et al.*, 1994).

This case history clearly demonstrates that the design philosophy of fully utilizing pile capacity can work successfully and produce an economical foundation which performs satisfactorily. The available methods of performance prediction appear to provide a reasonable, if conservative, basis for design in this case.

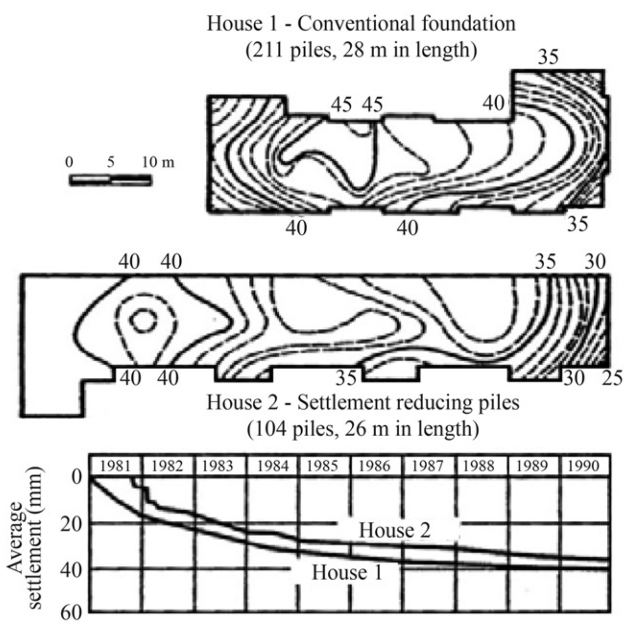

Figure 17 - Settlements for two adjacent residential buildings – (Hansbo, 1983).

6.6.3. High-rise buildings on the Gold Coast, Australia

Badelow *et al.* (2006) (Table 7) have described two cases of high-rise buildings in which the original foundation designs were carried out ignoring the presence of the raft. The first building comprised a 30 storey 176 unit residential tower located in Surfers Paradise, Queensland, where the site was underlain by alluvial sand and clay sediments, below which there was a residual soil stratum of silty clay overlying meta- siltstone rock. The second case involved a 23 storey residential tower with three levels of basement located at Tweed Heads. This site was again underlain by alluvial sand and clay layers overlying a residual silty clay layer which in turn overlaid siltstone bedrock. In both cases, the founding conditions were favourable for piled rafts.

The foundations were re-designed taking account of the presence of the raft, and Table 6 compares the original and revised designs. This table shows that significant construction cost and time savings were achieved by the use of piled raft foundation systems as alternatives to conven-

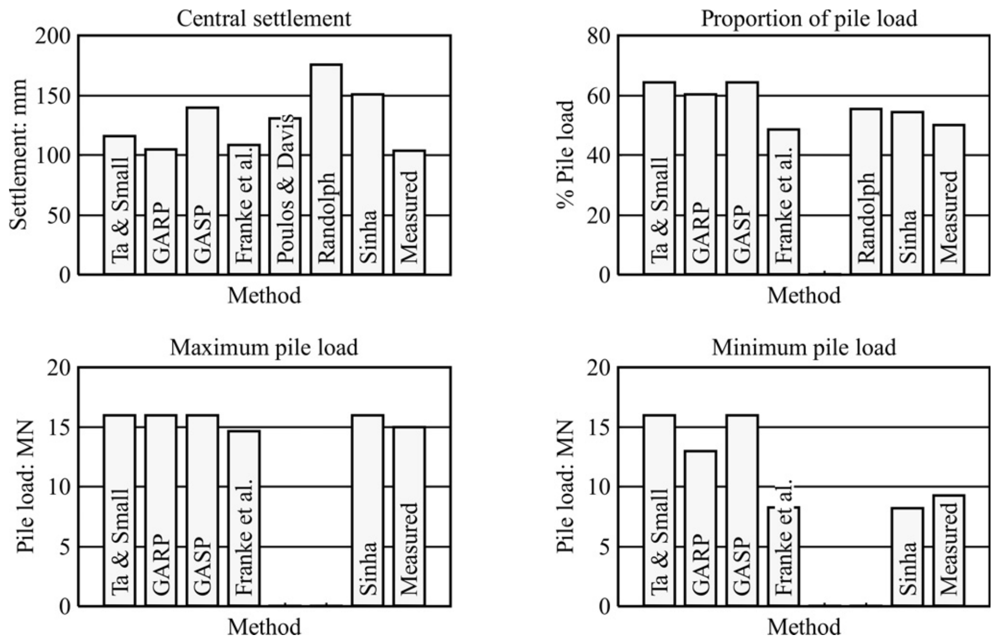

Figure 19 - Comparison of analysis methods for piled raft foundation, Westendstrasse 1 (Poulos *et al.*, 1997).

tional fully piled systems. The adoption of a piled raft resulted not only in a reduction in the number of piles required, but also in the length of the piles. In the second case, the overall foundation performance was improved because the differential settlements were reduced.

6.6.4. The Burj Dubai (Burj Khalifa)

The current world's tallest building is the Burj Dubai, re-named the Burj Khalifa at its official opening on January 4th 2010. This building is founded on a piled raft, and the design process for this foundation has been described by Poulos & Bunce (2008). Figure 20 shows a plan of the foundation, which consists of a raft 3.7 m thick and 196 piles, 1.5 m in diameter and about 50 m long, founded in a weak calcareous rock. The design of the foundation was found to be governed primarily by the tolerable settlement of the foundation rather than the overall allowable bearing capacity of the foundation. The capacity of the piles was assessed to be derived mainly from the skin friction developed between the pile concrete and rock, although limited end bearing capacity would be provided by the very weak to weak rock at depth.

The estimated maximum settlement of the tower foundation, calculated using various analysis tools, are in reasonable agreement, with the most comprehensive methods predicting a maximum long-term settlement of the order of 75-80 mm, which was considered to be within acceptable limits.

The settlements measured during construction for one of the wings of the "tripod" foundation are shown in Fig. 21 and are consistent with, but smaller than, those predicted.

Figure 22 shows contours of measured settlement. The general distribution is similar to that predicted by the various analyses.

As of mid-2009, when almost all the dead load was applied to the foundation, the maximum measured settlement was about 44 mm. On the basis of these measurements, it was estimated that the long-term settlement of the

Table 7 - Summary of Gold Coast case studies (Badelow *et al.*, 2006).

Case	Original foundation design	Revised piled raft foundation	Performance
30 storey tower, Surfers Paradise	Over 140 bored piles founded on rock at depths of 35-40 m	0.8 m thick raft on 123 0.7 m diameter CFA piles founded on stiff clay at 18 m	Saved 2767 m of pile length, and costs of about A$500,000. Maximum settlement predicted < 50 mm, maximum differential settlement < 1/400
23 storey tower, Tweed Heads	437 0.7 m and 0.9 m bored piles founded into weathered rock, and 0.45 m thick slab	0.45 m thick raft, locally thickened to 0.8 m under heavily loaded core areas, on 186 0.5 m diameter piles, and 46 0.9 m diameter CFA piles, founded on weathered rock	Savings of about A$500,000. Significant improvement in foundation performance, in terms of differential settlements between columns. Maximum predicted settlement < 50 mm

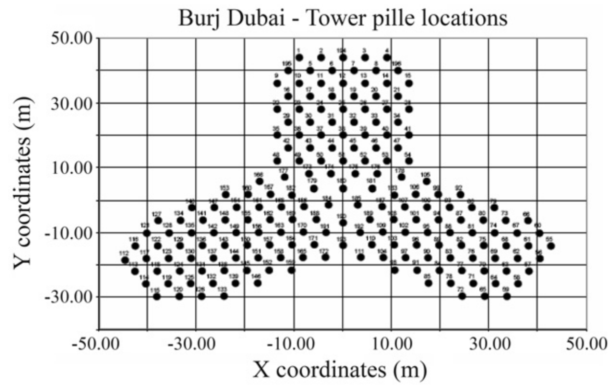

Figure 20 - Foundation layout for Burj Dubai.

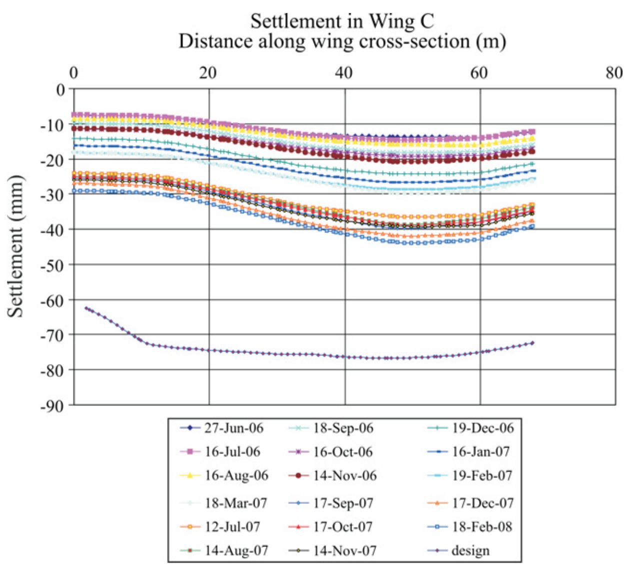

Figure 21 - Measured and computed settlements – wing C.

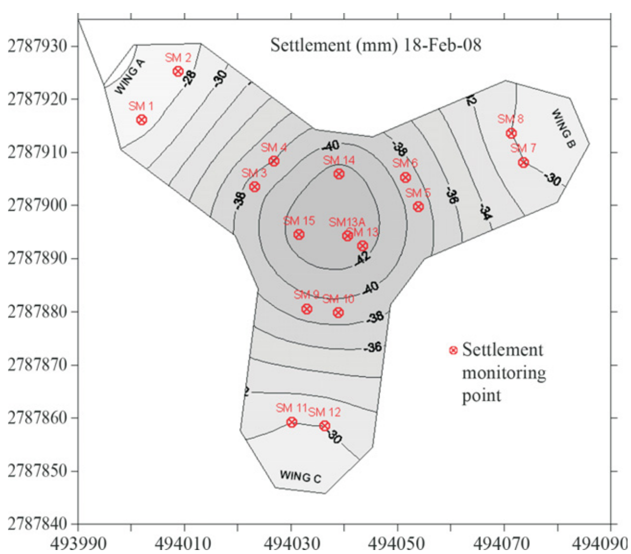

Figure 22 - Measured settlement contours for the Burj Dubai (now the Burj Khalifa).

foundation would be of the order of 55 mm, somewhat less than the predicted 75 mm.

Overall, the performance of the piled raft foundation system has exceeded expectations to date.

6.6.5. Piled rafts on very soft soils

As mentioned earlier, soft clay sites do not provide ideal ground conditions for piled rafts, but nevertheless, it is sometimes necessary to cope with such circumstances. As pointed out by Poulos (2005), possible foundation solutions may include:

- A compensated raft foundation;
- A piled raft foundation;
- A compensated raft foundation.

Compensated piled rafts involve the excavation of soil, before or after piles are installed, in order to reduce the net increase in load applied by the foundation to the underlying soft soil. The removal of soil reduces the vertical effective stress in the soil, thus putting it in an over- consolidated state and reducing its compressibility. The subsequent loadings of the foundation will therefore tend to cause less settlement than if no excavation of the soil had been carried out.

The key issues to be addressed in the design of compensated piled rafts are as follows:

- The maximum depth to which an excavation can be carried out.
- The effect of the overconsolidation caused by the excavation on the stiffness and ultimate load capacity of the raft.
- The effect of the overconsolidation on the stiffness and ultimate load capacity of the piles.

As a first approximation, it would appear reasonable to make the following assumptions with respect to raft behaviour to allow for the possible effects of excavation:

- The modulus of the soil used to compute the raft stiffness is the unload/reload value until the average contact pressure below the raft reaches the “preconsolidation” pressure, *i.e.* the footing pressure required to cause virgin (first-time) loading of the footing to occur. For average contact pressures in excess of this “preconsolidation pressure”, the first loading modulus value is used.
- The ultimate bearing capacity of the raft is unaffected by the excavation process, other than for the effect of embedment, which will tend to increase its capacity.

The possible effects of excavation on the soil modulus around the piles have been ignored, since the process of pile installation generally causes a significant “preloading” of the soil around and below the pile shaft. Moreover, the simplifying assumption is made that the ultimate axial capacity of the piles is also unaffected by excavation.

6.6.6. Application to La Azteca building case

The case of the La Azteca building was described by Zeevaert (1957) (Fig. 23). The building exerted a total average loading of about 118 kPa, and was located on a deep highly compressible clay deposit which was also subjected to ground surface subsidence arising from groundwater extraction. The building was founded on a compensated piled raft foundation, consisting of an excavation 6 m deep with a raft supported by 83 concrete piles, 400 mm in diameter, driven to a depth of 24 m (*i.e.* the piles were about 18 m long below the raft).

Figure 22 shows details of the foundation, the soil profile, the settlement computed by Zeevaert, and the measured settlements. The settlement without piles computed by Zeevaert (from a one-dimensional analysis) was substantial, but the addition of the piles was predicted to reduce the settlement to less than half of the value without piles. The measured settlements were about 20% less than the calculated settlements, but nevertheless confirmed the predictions reasonably well.

An approximate analysis by the author was applied to this case, excluding the effects of ground settlements, which were not detailed by Zeevaert in his paper. The following approach was adopted:

1. The one dimensional compressibility data presented by Zeevaert was used to obtain values of Young's modulus of the soil at various depths, for the case of the soft clays in a normally consolidated state. A drained Poisson's ratio of 0.4 was assumed. The modulus values thus obtained were typically very low, of the order of 0.5-1.0 MPa, and lower than would have been anticipated on the basis of the measured shear strength of the clay.

2. The bearing capacity of the raft was estimated from the shear strength data provided by Zeevaert, and was found to be about 200 kPa. This represented a factor of safety of about 1.7 on the average applied loading of 118 kPa.

3. The settlement of an uncompensated raft was computed using these modulus values together with conventional elastic theory. A very large settlement, in excess of 2.3 m, was obtained for the final settlement.

1. The settlement of a compensated raft was computed, assuming a 6 m depth of excavation, and assuming that the soil modulus values for the overconsolidated state were 10 times those for the normally consolidated state (based on the oedometer data presented by Zeevaert). The additional raft pressure to recommence virgin loading conditions, p_{ec}, was taken to be zero. A settlement of the order of 988 mm was thus computed.

2. From the pile load tests reported by Zeevaert, values of the single pile capacity and stiffness were obtained, these being about 735 kN and 25 MN/m respectively.

3. For the 83 piles used in the foundation, the group stiffness was computed by using the approximation of Poulos (1989) and applying a factor of 9.1 (the square root of the number of piles, *i.e.* $83^{0.5}$) to the single pile stiffness. A group stiffness of about 230 MN/m was calculated.

4. The average settlement of the foundation for an uncompensated piled raft was computed, using the equations developed by Randolph (1994) for the piled raft stiffness. A settlement of about 1.08 m was obtained. The analysis indicated that, in this case, the raft would carry only about 4% of the load under elastic conditions, and that the capacity of the piles would be mobilized fully under the design load of about 78 MN.

5. The effects of carrying out a 6 m deep excavation (as was actually used) was simulated by reducing the thickness of the soil profile accordingly, and again assuming that, for the raft, the soil Young's modulus for the overconsolidated state was 10 times that for the normally consolidated state (based on the laboratory oedometer data published by Zeevaert). The stiffness of the raft was thus in-

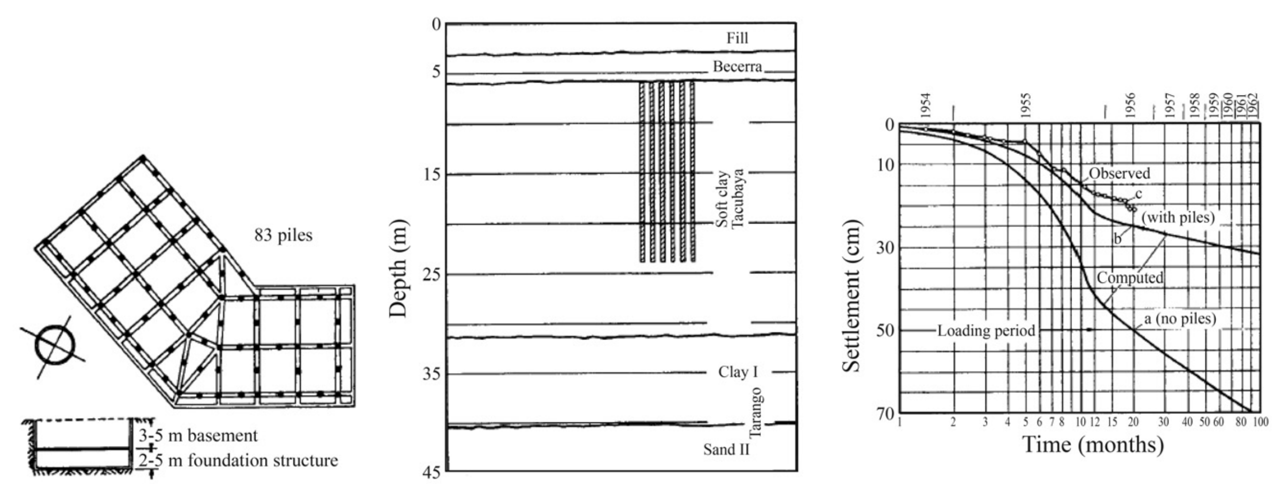

a) Foundation plan & pile layout b) Subsoil profile c) Settlement curves

Figure 23 - Details of La Azteca building on compensated piled raft (Zeevaert, 1957).

creased significantly, leading also to a significant increase in the stiffness of the piled raft foundation, to about 300 MN/m. The raft, at the design load, was found to carry about 40% of the total load, and the computed settlement under that load was reduced to about 280 mm.

The analysis results are summarized in Table 8. It can be seen that the settlement of the compensated piled raft is about 26% of the settlement of the piled raft without compensation, 29% of the settlement of the compensated raft alone, and only about 12% of the value for the uncompensated raft. Zeevaert's calculations gave larger settlements than those computed above, being about 1000 mm for the compensated raft alone, and about 370 mm for the compensated piled raft. This represented a reduction in settlement of about 63% in using the compensated piled raft rather than the compensated raft alone. This compares reasonably well to the 71% reduction in settlement computed from the present approach. It is also interesting to note that the measured settlements about 2 years after the commencement of construction were about 20% less than those predicted by Zeevaert. At that stage, the measured settlement was about 205 mm and the computed settlement from Zeevaert was 250 mm, *i.e.* about 68% of the final predicted settlement. Assuming a similar rate of settlement, the prediction made by the author's approach for the settlement after 2 years would be about 192 mm, in fair agreement with, but somewhat less than, the measured 205 mm.

Clearly, the combined use of piles and compensation via excavation, leads to a foundation that provides a superior performance to that of an uncompensated piled raft or a compensated raft alone.

6.6.7. Piled raft cases in Malaysia

Tan *et al.* (2004, 2005) have described the application of conventional piled raft foundations to cases in Malaysia involving a series of 2-storey and 5-storey apartment buildings founded on a relatively deep layer of soft silty clay. The soil profile consisted of 25-30 m of very soft to firm silty clay with some intermediate sandy layers, underlain by silty sand. Figures 24 and 25 show the variation of compressibility and strength parameters with depth at the site.

The site was subjected to filling of 0.5 to 1 m in thickness, together with temporary surcharging having heights varying from 2 m to 5 m. After the subsoil had achieved a specified percentage of settlement, the surcharging fills were removed and construction of the foundation system was commenced.

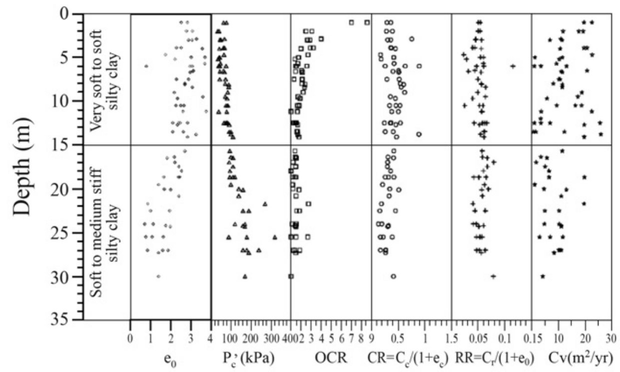

Figure 24 - Compressibility parameters for Klang clay (Tan *et al.*, 2004, 2005).

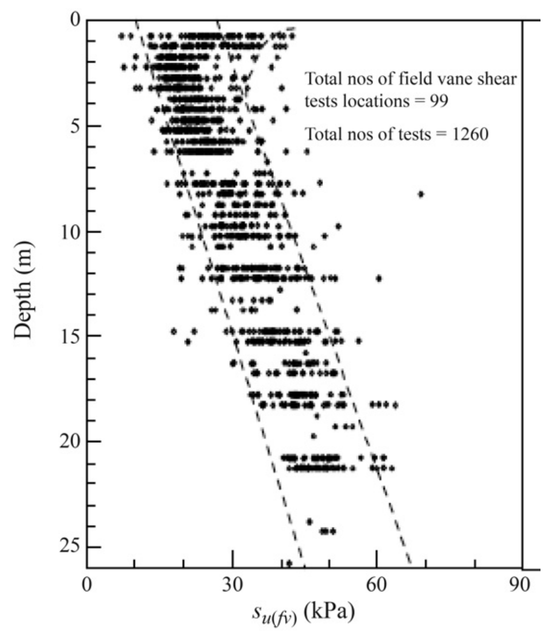

Figure 25 - Undrained strength and sensitivity of Klang clay (Tan *et al.*, 2004, 2005).

For the 2-storey buildings, piled raft foundations were used with relatively short friction piles of equal length. For the 5-storey buildings, piled rafts were also used, but the pile lengths were considerably longer and the pile length was varied, depending on the location.

Table 8 - Summary of computed average settlements.

Case	Computed average final settlement (mm)	Ratio of settlement to settlement of compensated raft
Raft alone, no compensation	2342	2.37
Raft alone, with compensation	988	1.0
Piled raft, no compensation	1084	1.10
Piled raft, with compensation	283	0.29

In their analysis of the foundation systems, Tan *et al.* used a combination of techniques to estimate the overall settlement behaviour and the pile-soil interaction. The overall settlement behaviour was computed from the conventional Terzaghi one-dimensional settlement analysis while the pile-soil interaction analysis involved iterative application of a simplified pile group analysis based on the work of Randolph & Wroth (1979), together with a commercially available finite element analysis of the raft slab.

2-Storey Buildings

For the 2-storey buildings, the column loads ranged from 10 kN to 360 kN, and the line loadings from the brick walls were from 9 kN/m to 16 kN/m. A uniform live loading of 2.5 to 3.0 kN/m^2 was assumed to act over the ground floor raft.

The foundation system consisted of a 150 mm thick raft slab thickened to a total of 600 mm over strips 350 mm wide below the column locations. 150 mm square reinforced concrete piles, 9 m long, were located below the columns (Fig. 26).

Settlements were monitored over a 6-month period, from the completion of construction of the ground floor columns to the commencement of installation of the architectural finishes. Figure 27 shows typical time-settlement relationships for one of the buildings. During the observation period, the settlements increased relatively rapidly with time, due to the increasing loads applied during construction, and at the end of the observation period, the maximum settlement was about 17 mm, with a maximum angular distortion of only 1/2850.

5-Storey buildings

For the 5-storey buildings, the column loadings ranged from 100 to 750 kN, and the line load from the brick walls was 9 kN/m. A uniform live loading of 2.7 kPa was assumed for the ground floor. The primary design criterion was to limit the angular distortion to a maximum of 1/350 to prevent cracking in walls and partitions.

The foundation system developed consisted of a 300 mm thick raft with thickened strips 350 mm wide by 700 mm deep, supported by 200 mm square section reinforced concrete piles with lengths varying from 18 m to 24 m. The longer piles were located below the central portion of the buildings, as shown in Fig. 28. In this case, the designers followed the principle set out by Reul & Randolph (2004) of reducing the differential settlements by concentrating the stiffness provided by the piles towards the centre of a loaded area.

Settlements were monitored at various locations over a 10 month period from when the building had reached the 3rd floor to more than 6 months after completion of the building. Figure 29 shows the measured time-settlement behaviour of the various locations. These measurements revealed that, while the observed settlements were relatively large, the maximum angular distortions over the period of measurement were of the order of 1/1000.

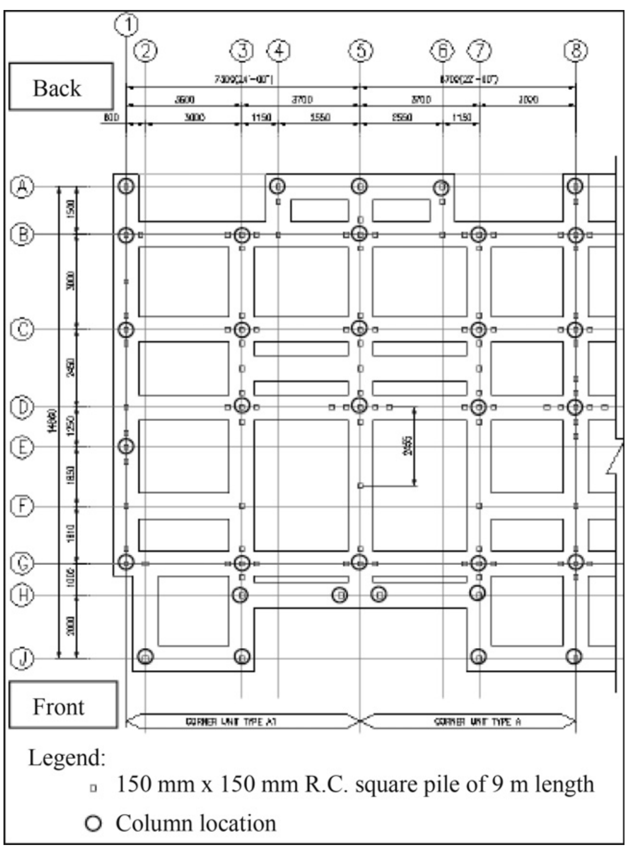

Figure 26 - Typical column and pile layout for 2-storey building (Tan *et al.*, 2004, 2005).

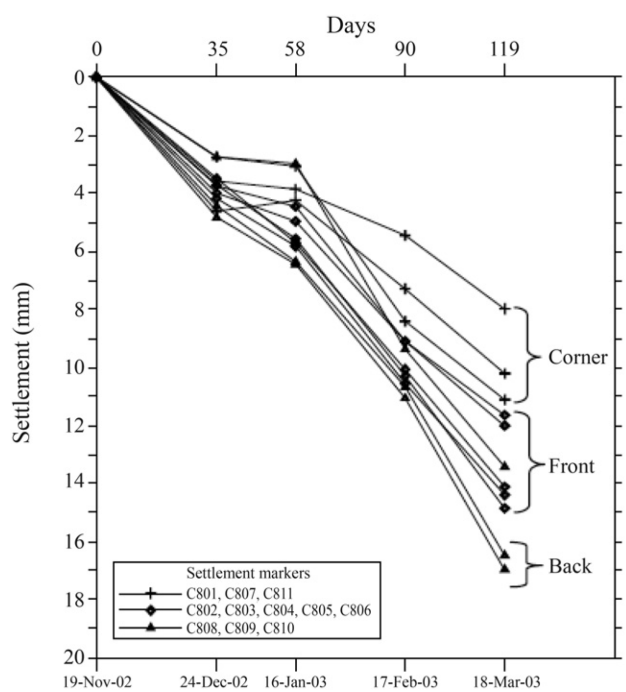

Figure 27 - Time-settlement monitoring results for typical 2-storey block (Tan *et al.*, 2004, 2005).

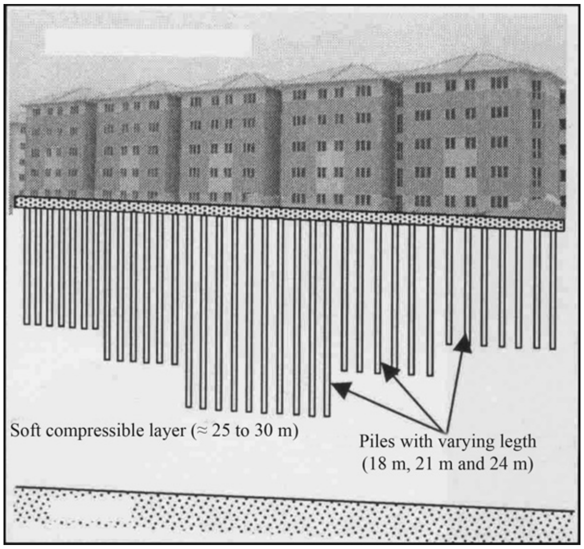

Figure 28 - Foundation system for 5-storey blocks with variable pile lengths.

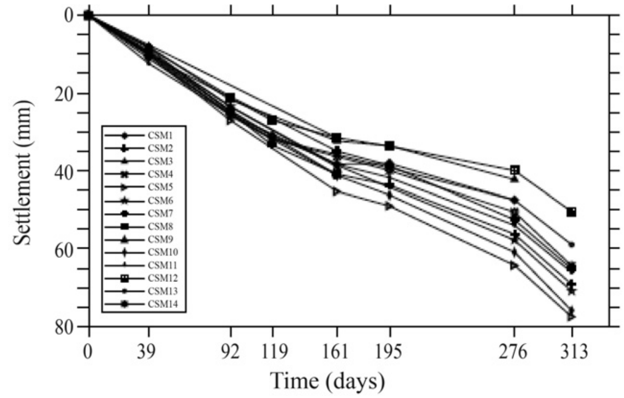

Figure 29 - Time-settlement measurements for 5-storey blocks.

Analysis of Malaysian Cases

The Malaysian cases have been analysed using a simplified analysis for pile rafts (Poulos, 20001). On the basis of the available information, the following assumptions have been made in the analyses:

1. The undrained shear strength s_u of the clay increases linearly with depth, according to the relationship $s_u = 16 + 1.6z$ kPa, where z = depth below ground surface in metres.

2. The thickness of the soft compressible clay is 30 m.

3. The long-term drained Young's modulus for the clay = $100s_u$ for calculating the settlement the raft and $200s_u$ for the calculation of pile settlements.

4. The average loading applied to the foundation by the buildings is 25 kPa for the 2-storey buildings and 62.5 kPa for the 5-storey buildings (*i.e.* 12.5 kPa per storey).

5. The raft for the 2-storey buildings is rectangular, with dimensions 80 m by 15 m.

6. The raft for the 5-storey buildings is rectangular, with dimensions 75 m by 25 m.

7. The settlement ratio for the pile groups, R_s, is approximated as $n^{0.5}$, where n = number of piles (Poulos, 1989).

8. Interaction among adjacent blocks is ignored.

Table 9 summarizes the results of the calculations for the average settlement of each building when supported by the piled raft system actually used. Also shown in this table are the settlement computed for a raft without piles, and the settlement computed if no account is taken of the presence of the raft. It can be seen that the use of piles in conjunction with the raft has resulted in a substantial reduction in the settlement, by a factor of about 3, as compared to the case of the raft alone, and by about 30%-40% compared to the piles without the raft.

Table 9 also shows the range of measured settlement reported by Tan *et al.* (2004, 2005) at the end of the settlement observation periods. The computed settlements for the piled raft are of a similar order to those measured, bearing in mind that the measured settlements were still increasing significantly with time when the observations ceased. The cases reported by Tan *et al.* therefore clearly demonstrate the feasibility of employing piled raft systems to support structures on soft clays.

6.7. Summary

The concept of settlement reducing piles, advocated by Burland *et al.* (1977) has become recognized as a potentially economical and effective type of foundation which has been used successfully in a variety of ground condi-

Table 9 - Summary of computed and measured settlements for buildings in Malaysia.

Case	Settlement mm	
	2-storey buildings	5-storey buildings
Calculated final average settlement for raft without piles	128	329
Calculated final average settlement for piles without raft	63	132
Calculated final average settlement for piles with raft	43	99
Range of measured settlements at end of monitoring period	8-22	50-78

tions. It is not uncommon for savings in the cost of the foundations of about 30% to be achieved by using piled rafts instead of conventional fully piled solutions.

Several of the world's tallest buildings in the Middle East are founded on this type of foundation, while many buildings in Frankfurt have functioned successfully on piled rafts, despite the fact that total settlements in excess of 100 mm have occurred. Piled rafts are most effective when the ground conditions near the underside of the raft are favourable and allow the raft to develop considerable stiffness and bearing capacity. However, in recent years, they have also found application in very soft clays. The cases in Malaysia demonstrate that low-to-medium rise buildings on very soft clays can be supported by piled raft foundations in which the raft is relatively thin, and the piles are engineered to obtain acceptable settlement and differential settlement performance.

Compensated piled raft foundations can be an effective foundation solution for very soft soils and have been used successfully in Mexico City. They combine the relief of overburden stress as a result of excavation, with the additional capacity and stiffness that can be provided by combining piles with a mat or raft foundation.

7. Conclusions

Victor de Mello developed a philosophy of foundation design that incorporated both common sense and sound theory. He questioned a number of conventional design approaches and pointed out their shortcomings. In particular, he was highly critical of codes that were poorly conceived and inflexible, and that led to uneconomical designs. The shortcomings that he identified in design methods included the following:

1. The use of traditional bearing capacity theory to estimate the ultimate load capacity of shallow foundations. Subsequent research has found that the traditional rigid plastic theory can be unconservative in that the effects of soil compressibility can reduce the bearing capacity very markedly, and that the theoretical size effect for foundations on sand (in which larger footings can develop larger bearing capacities) is not borne out in practice. However, on the positive side, the simple procedures adopted in practice to handle eccentric loading and applied moment appear to have been verified by subsequent research using sophisticated three-dimensional numerical analysis.

2. The commonly used "α method" for estimating the ultimate shaft friction of piles in clay is not always reliable. While considerable research has been carried out since 1969 to improve our ability to predict pile capacity and load-settlement behaviour, the accurate prediction of axial pile capacity remains rather elusive, despite the increased understanding of pile-soil interaction and the increased sophistication of some of the more recent methods of calculation. While some success has been achieved in predicting the load-settlement behaviour of single piles, accurate prediction of the settlement of pile groups, particularly if the piles are floating, also remains elusive. Given the high degree of sophistication that it is now possible to bring to bear on pile prediction tasks, it appears likely that the lack of consistent success may be due more to the deficiencies in characterising the ground profile, than to deficiencies in the methods of calculation.

3. The concept of settlement reducing piles, advocated by Burland *et al.* (1977) has become recognized as a potentially economical and effective type of foundation which has been used successfully in a variety of ground conditions. It is not uncommon for savings in the cost of the foundations of about 30% to be achieved by using piled rafts instead of conventional fully piled solutions. There is also potential for a compensated piled raft foundation to reduce both the absolute settlement and the differential settlement between the foundation and the surrounding soft soil. It therefore provides a means of developing a foundation that works and settles "with the ground", rather than one which "fights the ground".

It is sobering to reflect on the almost despairing question asked by de Mello in 1995 "*Quo vadis, Geotecnica?*" It may be argued that our capacity to solve numerical and analytical problems in geotechnical engineering has developed enormously in the 15 years since he asked that question. Yet, it may also be argued that our ability to make realistic predictions of foundation performance has barely improved. This lack of progress may be attributed to a number of factors, but perhaps the most pertinent of these are:

1. The enduring difficulty of carrying out adequate ground investigations to properly characterise a site. Despite the ground conditions often being the most potent risk factor in an engineering project, ground investigation is still generally treated as a commodity to be obtained at the cheapest price, rather than as a vital component of the engineering design process.

2. The difficulty of quantifying the soil and rock properties, taking into account the multitude of geological, environmental and geotechnical features that influence the ground behaviour. There is likely to be an optimal level of characterization that can be sought, perhaps analogous to the story of Goldilocks and the three bears. There can be too little effort expended ("the porridge is too cold") and so key aspects of behaviour are overlooked or not described adequately. There can be too much effort expended ("the porridge is too hot"), in which enormous effort is expended on every conceivable type of in-situ and laboratory test, and then tries to incorporate every conceivable physical phenomenon into the ground model. In such cases, the translation of the results into a practical ground model is either too lengthy or else it may still miss the key features of the problem. Then there is the optimal solution ("the porridge is just right") in which experience and judgement are combined with sound in-situ and laboratory testing to produce an adequate ground model that suits the key features of the prob-

lem, without trying to cover irrelevant aspects of behaviour.

3. The enduring difficulty of honestly evaluating our ability to do "Class A" predictions. De Mello commented on, and despaired of, the lack of success of experts in prediction events. It would no doubt be gratifying to him if there was a concerted effort made to make performance measurements and comparisons between anticipated and measured behaviour, a routine part of the construction and operation process.

4. Perhaps because of the increasingly large number of geotechnical researchers and the current publishing imperative, much of the geotechnical research is directed towards what may be termed "the last 2%" of a problem, *i.e.* the refinement of analyses and design procedures that are more than adequate for practical purposes. What is needed far more in research is another concerted effort to close the gap between theory and practice and to identify what combinations of ground investigation quantification and design method give reliable outcomes. It may well be time to heed de Mello's pleas and discard some of the old traditional theories (for example, the Terzaghi bearing capacity theory) and to stop the perpetuation of teaching of such theories simply because they appear in text books that have been written without an adequately critical appraisal of their applicability to geotechnical reality.

It would be highly instructive for students to be directed back to the writings of such giants of the profession as Terzaghi, Casagrande, Taylor, Skempton and de Mello. There they would find a great deal of wisdom and guidance that would assist them in understanding what is significant in a geotechnical problem and what is not. Then, in combination with properly digested and calibrated modern theories and design methods, they could achieve improved capabilities in designing foundation according to the 5 design principles of de Mello set out in Section 2.

It may be appropriate to conclude by appreciating the broader legacy that Victor de Mello left to our profession and recalling the following words from his Presidential address at the 1985 International Conference in San Francisco:

"Engineering uses art and science, intuition, and of course, the rational analyses of the day: all these are means. But the end is creativity, often inventiveness, ingenious. Engineering is the end product of design + construction + operation, a live function to be continually reviewed and revised in order to preserve or enhance the intent. As a community of engineers, we must urgently repel the widespread notion of our acting on certainty, and providing static, permanently valid projects".

Acknowledgments

I am grateful to Prof. John Small for reviewing this paper, and am indebted to many of my colleagues over many years for their support and advice, both in academia and consulting practice. Perhaps above all, three persons have had a major influence on my career: the late Professor E.H. Davis, who was my mentor, colleague and friend during the early part of my career, Professor T. William Lambe, who gave me the opportunity to become involved in the prediction of the performance of foundations and embankments, and the Late Professor Victor de Mello, who was an early supporter of my research and who subsequently provided continual support, advice and stimulation.

References

Altaee, A.; Evgin, E. & Fellenius, B.H. (1993) Axial load transfer for piles in sand. III: Load transfer for piles in sand and the critical depth. Canadian Geotechnical Journal, v. 30:3, p. 455-463.

Akbas, S.O. & Kulhawy, F.H. (2009) Axial compression of footings in cohesionless soils. II: Bearing capacity. Jnl. Geot. & Geoenv. Eng., ASCE, v. 135:11, p. 1575-1582.

Aoki, N. & Velloso, D.A. (1975) An approximate method to estimate the bearing capacity of piles. Proc. 5th Pan American Conf. Soil Mechs. Found. Eng., Buenos Aires, pp. 367-376.

Badelow, F.; Poulos, H.G.; Small, J.C. & Moyes, P. (2006) Economic foundation design for tall buildings. Proc. 10th Int. Conf. Piling and Deep Founds., Amsterdam, DFI, pp. 200-209.

BCP Committee (1971) Field tests on piles in sand. Soils and Founds, v. 11:2, p. 29.

Burland, J.B. (2008) Reflections on Victor de Mello, friend, engineer and philosopher. Soils and Rocks, v. 31:3, p. 111-123.

Burland, J.B.; Broms, B.B. & De Mello, V.F.B. (1977) Behaviour of foundations and structures. Proc. 7th Int. Conf. Soil Mechs. Found. Eng., Tokyo, v. 1, pp. 495-548.

Burland, J.B. & Wroth, C.P. (1974) Settlement of buildings and associated damage. In: Settlement of Structures. Pentech Press, London, pp. 611-654.

Burland, J.B. & Burbridge, M.C. (1985) Settlements of foundations on sand and gravel. Proc. I.C.E., v. 1, pp. 1325-1381.

Bustamante, M. & Gianeselli, L. (1982) Pile bearing capacity prediction by means of static penetrometer CPT. Proc. ESOPT II, Amsterdam, v. 2, pp. 492-500.

Carter, J.P.; Randolph, M.F. & Wroth, C.P. (1979b) Stress and pore pressure changes in clay during and after the expansion of a cylindrical cavity. Int. J. Num. and Anal. Methods in Geomechanics, 3: 305-322.

Clausen, C.J.F.; Aas, P.M. & Karlsrud, K. (2005) Bearing capacity of driven piles in sand, the NGI approach. Proc. 1st Int. Symp. On Frontiers in Offshore Geotechnics, Perth, Balkema, pp. 677-681.

Coyle, H.M. & Reese, L.C. (1966) Load transfer for axially loaded piles in clay. Jnl. Soil Mechs. Founds. Divn., ASCE, 92:SM2, p. 1-26.

Davis, E.H. & Booker, J.R. (1971) The bearing capacity of strip footings from the standpoint of plasticity theory. Proc. First Australia-New Zealand Conference on Geomechanics, v. 1, pp. 276-282.

Decourt, L. (2008) Loading tests: interpretation and prediction of their results. Geot. Spec. Pub. No. 180, J.E. Laier *et al.* (ed), ASCE, pp. 452-470.

Deeks, A.D.; White, D.J. & Bolton, M.D. (2005) A comparison of jacked, driven and bored piles in sand. Proc. 16th Int. Conf. Soil Mechs. Geot. Eng., Osaka.

De Mello, V.F.B. (1969) Foundations of buildings in clay. State-of-the art report, Proc. 7th Int. Conf. Soil Mechs. Found. Eng., Mexico City, SOA Volume, pp. 49-136.

De Mello, V.F.B. (1971) The standard penetration test. Proc. 4th Pan American Conf. Soil Mechs. Found. Eng., San Juan Puerto Rico, ASCE, v. 1, pp. 1-86.

De Mello, V.F.B. (1972) Thoughts on soil engineering applicable to residual soils. Proc. 3rd SouthEast Asian Conf. On Soil Eng., Hong Kong, pp. 5-34.

De Mello, V.F.B. (1983) Present criteria for design and construction of high-capacity piles. Conf. 25 Anniv. Soc. Venezolana de Mech. Del Suelo e Ing. de Fundaciones, Caracas, pp. 107-127.

De Mello, V.F.B. (1984) Design decisions, design calculations and behaviour prediction computations; referred to statistics and probabilities. Proc. 6th Danube Conf. Soil Mechs. Found. Eng., Budapest, Ed. G. Petrasovits, pp. 37-44.

De Mello, V.F.B. (1992) Revisiting conventional geotechnique after 70 years. US/Brazil Geot. Workshop on Applicability of Classical Soil Mechanics Principles to Structured Soils, pp. 22-61.

De Mello, V.F.B. (1994) Revisiting our origins. In: Terzaghi Oration. Proc. 13th Int. Conf. Soil Mechs. Found. Eng., New Delhi, pp. 13-34.

De Mello, V.F.B. (1995) Revisitations on sample foundation designs. Solos e Rochas, v. 18:2, p. 75-92.

De Mello, V.F.B. (2000a) Reflections on needed logical unifying of basic geotechnical prescriptions: simple examples. Libro Homenaje a Jose Antonio Jiminez Salas, Geotecnia en al ano 2000, CEDEX, pp. 7-16.

De Mello, V.F.B. (2000b) Overview of hypotheses not plucked or pursued. Merit recanting or chanting? Geotech. Year 2000, Developments in Geot. Eng., Bangkok, pp. 355-372.

Fadaee, M.J. & Rowhani, M. (2006) Optimization of piled raft foundations using generic algorithm and neural networks. 10th East Asia Pacific Conf. on Struct. Eng. and Constrn., Bangkok.

Fellenius, B. & Altaee, A.A. (1994) Critical depth: how it came into being and why it does not exist. Proc. Instn. Civ. Engrs., Geot. Eng., v. 113:April, p. 107-111.

Fleming, W.G.K.; Weltman, A.J. & Randolph, M.F. (1992) Piling Engineering. 2nd ed, Halsted Press, New York.

Foye, K.C.; Abou-Jaoude, G.; Prezzi, M. & Salgado, R. (2009) Resistance factors for use in load and resistance factor design of driven pipe piles in sands. Jnl. Geot. Geoenv. Eng., ASCE, v. 135:1, p. 1-13.

Franke, E.; Lutz, B. & El-Mossalamy, Y. (1994) Measurements and numerical modelling of high-rise buildings on Frankfurt clay. ASCE Spec. Pub. v. 40:2, p. 1325-1336.

Gavin, K.; Adekunte, A. & O'Kelly, B. (2009) A field investigation of vertical footing response on sand. Geotechnical Eng., ICE, v. 162:GE5, p. 257-267.

Hansbo, S. & Källström, R. (1983) A case study of two alternative foundation principles. Väg-och Vattenbyggaren v. 7-8, p. 23-27.

Horikoshi, K. & Randolph, M.F. (1998) A contribution to the optimum design of piled rafts. Geotechnique, v. 48:2, p. 301-317.

Jardine, R.J. & Chow, F. (1996) New design methods for offshore piles. MTD Pub. 96/103, Marine Technology Directorate, London.

Jardine, R.J.; Chow, F.; Overy, R. & Standing, J. (2005) CP design methods for driven piles in sand and clays. Thomas Telford, London.

Karlsrud, K.; Clausen, C.J.F. & Aas, P.M. (2005) Design criteria for pipe piles in clay, the NGI approach. Proc. 1st Int. Symp. On Frontiers in Offshore Geotechnics, Balkema, Perth, Australia, pp. 677-681.

Katzenbach, R.; Arslan, U.; Moorman, C. & Reul, O. (1998) Piled raft foundations: interaction between piles and raft. Darmstadt Geotechnics, Darmstadt University of Technology, v. 4, p. 279-296.

Kerisel, J. (1961) Fondations profondes en milieu sableux. Proc. 5th Int. Conf. Soil Mechs. Found. Eng., Paris, v. 2, p. 73-83.

Kerisel, J. (1965) Vertical and horizontal bearing capacity of deep foundations in clay. Proc. Symp. On Bearing Capacity and Settlement of Foundations, Duke University, Durham, NC, pp. 45-52.

Kolk, H.J.; Baaijens, A.E. & Senders, M. (2005) Design criteria for pipe piles in silica sands. Proc. 1st Int. Symp. On Frontiers in Offshore Geotechnics, Balkema, Perth, Australia, pp. 711-716.

Lam, T.S.K. & Johnston, I.W. (1982) A Constant normal stiffness direct shear machine. Proc. 7th S.E. Asian Conf. on Soil Eng., Hong Kong, pp. 805-820.

Lambe, T.W. & Whitman, R.V. (1969) Soil Mechanics. John Wiley, New York.

Lehane, B.M.; Schnieder, J.A. & Xu, X. (2005) The UWA-05 method for prediction of axial capacity of driven piles in sand. 1st Int. Symp. On Frontiers in Offshore Geotechnics, Balkema, Perth, Australia, pp. 683-689.

Kraft, L.M.; Kagawa, T. & Ray, R.P. (1981) Theoretical t-z curves. Jnl. Geot. Eng., ASCE, 107:11, p. 1543-1561

Kulhawy, F.K. (1984) Limiting tip and side resistance: fact or fallacy? Anal. and Des. of Pile Founds., J.R. Meyer, ed., ASCE, pp. 80-98.

Mandolini, A.; Russo, G. & Viggiani, C. (2005) Pile foundations: experimental investigations, analysis and design. Proc. 16th Int. Conf. Soil Mechs. Geot. Eng., Osaka, Millpress, Rotterdam, v. 1, pp. 177-213.

Mayne, P.W. & Elhakim, A. (2002) Axial pile response evaluation by geophysical piezocone tests, Proceedings, Ninth International Conference on Piling & Deep Foundations, DFI, Nice, Presses de l'ecole nationale des Ponts et Chaussees, pp. 543-550.

Mayne, P.W. & Zavala, G. (2004) Axial shaft response from seismic piezocone tests. Proceedings, GeoSupport 2004, Joint ADSC-ASCE GeoInstitute Conference, Orlando.

Meyerhof, G.G. (1951) The ultimate bearing capacity of foundations, Géotechnique, v. 2, p. 301-332.

Meyerhof, G.G. (1953) The bearing capacity of foundations under eccentric and inclined loads. Proc. 3rd Int. Conf. Soil Mechanics and Foundation Engineering, Zurich, v. 1, pp. 440-445.

Meyerhof, G.G. 1976. Bearing capacity and settlement of pile foundations. Jnl. Geot. Eng. Div., ASCE, v. 102:GT3, p. 195-228.

O'Neill, M.W. (2001) Side resistance in piles and drilled shafts. Int. Geot. and Geoenv. Eng., ASCE, v. 127:1, p. 3-16.

Ooi, L.H. & Carter, J.P. (1987) A constant normal stiffness direct shear device for static and cyclic loading. Geot. Testing Jnl., ASTM, v. 10, p. 3-12.

Poulos, H.G. (1993) Settlement of bored pile groups. Proc. BAP II, Ghent, Balkema, Rotterdam, pp. 103-117.

Poulos, H.G. (1994b) Settlement prediction for driven piles and pile groups. Spec. Tech. Pub. v. 40:2, p. 1629-1649.

Poulos, H.G. (1989) Pile behaviour – Theory and application. 29th Rankine Lecture. Géotechnique, v. 39:3, p. 65-415.

Poulos, H.G. (2000) Pile-raft interaction – Alternative methods of analysis. Devels. in Theoretical Geomechs., ed. D.W. Smith & J.P. Carter, Balkema, Rotterdam, pp. 445-463.

Poulos, H.G. (2001) Piled raft foundations – Design and applications. Geotechnique, v. 51:2, p. 95-113.

Poulos, H.G. (2004) An approach for assessing geotechnical reduction factors for pile design. Proc. 9th Australia-New Zealand Conf. on Geomechanics, Auckland, v. 1, pp. 109-115.

Poulos, H.G. (2005) Pile behavior – Consequences of geological and construction imperfections. 40th Terzaghi Lecture, Jnl. Geot. & Geoenv. Eng., ASCE, v. 131:5, p. 538-563.

Poulos, H.G. (2006) Pile group settlement estimation – Research to practice. Keynote Paper, Foundation Analysis and Design, Innovative Methods, ED. R.L. Parsons *et al.*, ASCE GSP No. 153, pp. 1-22.

Poulos, H.G. & Bunce, G. (2008) Foundation design for the Burj Dubai – The world's tallest building. Proc. 6th Int. Conf. Case Histories in Geot. Eng., Arlington, VA, Paper 1.47, CD-Rom.

Poulos, H.G.; Carter, J.P. & Small, J.C. (2002) Foundations and retaining structures – Research and practice. State of the Art Lecture, Proc. 15th Int. Conf. Soil Mechs, Found. Eng., Istanbul, v. 4, pp. 2527-2606.

Poulos, H.G. & Chua, E.W. (1985) Bearing capacity of foundations on calcareous sand. Proc. 11th Int. Conf. Soil Mech. Found. Eng., San Francisco, v. 3, pp. 1619-1622.

Poulos, H.G. & Davids, A.J. (2005) Foundation design for the Emirates Twin Towers, Dubai. Can. Geot. Jnl., v. 42, p. 716-730.

Poulos, H.G. & Davis, E.H. (1968) The settlement behaviour of single axially-loaded incompressible piles and piers. Geotechnique, v. 18, p. 351-371.

Poulos, H.G. & Davis, E.H. (1980) Pile Foundation Analysis and Design. New York, John Wiley.

Poulos, H.G.; Small, J.C.; Ta, L.D.; Sinha, J. & L. Chen (1997) Comparison of some methods for analysis of piled rafts. Proc. 14th Int. Conf. Soil Mechs. Foundn. Eng. Hamburg, Balkema, Rotterdam, v. 2, pp. 1119-1124.

Randolph, M.F. (1994) Design methods for pile groups and piled rafts. Proc. 13th Int. Conf. S.M. & Found. Eng., v. 5, pp. 61-82.

Randolph, M.F. (2003) Science and empiricism in pile foundation design. 43rd Rankine Lecture, Geotechnique, v. 53:10, p. 847-875.

Randolph, M.F.; Carter, J.P. & Wroth, C.P. (1979) Driven piles in clay – The effects of installation and subsequent consolidation. Géotechnique, v. 29:4, p. 361-393.

Randolph, M.F. & Wroth, C.P. (1979) An analysis of the vertical deformation of pile groups. Géotechnique, v. 29:4, p. 423,439.

Reul, O. & Randolph, M.F. (2004) Design strategies for piled rafts subjected to non-uniform vertical loading. Jnl. Geot. & Geoenv. Eng., ASCE, v. 130:1, p. 1-13.

Seed, H.B. & Reese, L.C. (1955) The action of soft clay along friction piles. Proc. ASCE, 81, Paper 842.

Seo, H.; Yildrim, I.Z. & Prezzi, M. (2009) Assessment of the axial load response of an H pile driven in multilayered soil. Jnl. Geot. Geoenv. Eng., ASCE, v. 135:12, p. 1789-1804.

Sinha, J & Poulos, H.G. (1997) Piled raft foundation systems in swelling and shrinking soils. Proc. 14th Int. Conf. Soil Mechs. Found. Eng., Hamburg, v. 2, pp. 1141-1144.

Skempton, A.W. & MacDonald D.H. (1956) The allowable settlements of buildings. Proc. Instn. Civ. Engrs., v. III:5, p. 727-768.

Tabucanon, J.T.; Airey, D.W. & Poulos, H.G. (1995) Pile skin friction in sands from constant normal stiffness tests. Geot. Testing Jnl., ASTM, v. 18:3, p. 350-364.

Taiebat H. & Carter J.P. (2000) Numerical studies of the bearing capacity of shallow footings on cohesive soil subjected to combined loading. Géotechnique, 50:4, p. 409-18.

Tan, Y.C.; Chow, C.M. & Gue, S.S. (2004) A design approach for piled raft with short friction piles for low rise buildings on very soft clay. Proc. 15th Southeast Asian Geot. Soc. Conf., Bangkok, v. 1, pp. 171-176.

Tan, Y.C.; Chow, C.M. & Gue, S.S. (2005) Piled raft with different pile length for medium-rise buildings on very soft clay. Proc. 16th Int. Conf. Soil Mechs. Found. Eng., Osaka, v. 3, pp. 2045-2048.

Terzaghi, K. (1943) Theoretical soil mechanics. John Willey, New York.

Vesic, A.S. (1969) Experiments with instrumented pile groups in sand. ASTM, STP v. 444, pp. 177-222.

Vesic, A.S. (1973) Analysis of ultimate loads of shallow foundations, Jnl Soil Mechanics and Foundation Division, ASCE, v. 99, p. 45-73.

Zeevaert, L. (1957) Compensated friction pile foundation to reduce settlement of buildings on the highly compressible volcanic clay of Mexico City. Proc. 4th Int. Conf. SMFE, London, v. 2, pp. 81-86.

Zhang, L. & Ng, A.M.Y. (2006) Limiting tolerable settlement and angular distortion for building foundations. Probabilistic Applications in Geotechnical Engineering, GSP 170, ASCE (CD-Rom).

Articles

Effects of the Construction Method on Pile Performance: Evaluation by Instrumentation. Part 1: Experimental Site at the State University of Campinas

Paulo José Rocha de Albuquerque, Faiçal Massad, Antonio Viana da Fonseca, David de Carvalho, Jaime Santos, Elisabete Costa Esteves

Abstract. This paper reviews the behavior of three types of piles (bored, CFA and Omega piles), installed in the experimental site of Unicamp (State University of Campinas). Unicamp subsoil is characterized by non-saturated diabasic soil, lateritic in its surface layer. Extensive data from geotechnical investigation is presented, expressed in parameters derived both from *in situ* and laboratory tests. Static load tests with electrical extensometers were performed along the depth of instrumented piles. It was observed that most of the loads applied were transferred by lateral friction. An analysis of load transfer functions was made, which displayed a very good definition of both shaft friction and tip interaction, namely the ultimate resistance. The average maximum unit shaft friction resistance of the piles was 41 kPa, 58 kPa and 86 kPa for bored, CFA and Omega piles, respectively. Maximum tip reaction was 87 kPa, 491 kPa and 1665 kPa, for bored, CFA and Omega piles, respectively. This paper also emphasizes the relevance of extracting each pile after completion of the test in order to inspect the pile facies and characteristics. This enabled checking the shape of tips and size of shafts. Part 2 of this paper will review the tests performed at the Experimental Field of FEUP (Faculty of Engineering of the University of Porto/Portugal).

Keywords: construction techniques, pile performance, bored pile, CFA pile, Omega pile, precast pile, instrumentation.

1. Introduction

Most constructions use deep foundations, mainly piles. This type of foundation can be executed either by extracting soil or by displacing soil. The first category includes bored piles, Strauss piles, CFA piles, etc; the second category includes other types of piles: driven piles (precast concrete or steel piles), Franki piles, Omega piles, etc. The technical community is aware that the pile execution procedure conditions the behavior in the load-displacement mechanism, and, therefore, in its load capacity. The purpose of this study is to analyze the performance of three kinds of piles executed in diabasic, porous and lateritic soil, at 17 m-deep water level. The static pile load tests (SPLT) were carried out in three classes of deep foundations: bored piles, CFA and Omega helical type, in Campinas, São Paulo State, Brazil. These piles were instrumented as described below. From field and laboratory tests plus pile extractions, soil conditions around pile shafts will be evaluated.

This paper was developed together with researchers from Brazil (Unicamp and Poli-USP) and from Portugal (FEUP and IST – Upper Technological Institute – Lisbon/Portugal). It reviews the behavior of CFA, Omega, bored and precast piles, instrumented in depth. This article deals with the results obtained at the Experimental Field of Unicamp, whereas part 2 will describe the results obtained at the Experimental Field of FEUP for CFA, Omega and bored piles.

2. Piles Instrumented In Depth: Cases To Be Analyzed

Instrumentation is determinant to evaluate the load transfer mechanism in pile foundations. This technique has been used for over 30 years, initially with mechanical extensometers and, more recently, with electrical extensometers. In Brazil, the first reports on pile instrumentation date back from 1975, in Prof. Dirceu Velloso's study in Rio de Janeiro, performing instrumentation of a pile with tell-tales (Velloso *et al.*, 1975). Since then, this technique has evolved with the growing demand for pile instrumentation. Nowadays, the technique employed, although it involves extra costs, since it uses electrical extensometers that can be installed in different ways, provides valuable additional information.

Paulo José Rocha de Albuquerque, D.Sc, Faculdade de Engenharia Civil, Arquitetura e Urbanismo, Universidade Estadual de Campinas, Av. Albert Einstein 951, 13083-852 Campinas, SP, Brazil. e-mail: pjra@fec.unicamp.br.
Faiçal Massad, D.Sc., Escola Politécnica, Universidade de São Paulo, Av. Professor Almeida Prado 271, Trav. 2, Cidade Universitária, 05508-900 São Paulo, SP, Brazil. e-mail: faical.massad@poli.usp.br.
Antonio Viana da Fonseca, D.Sc., Faculdade de Engenharia, Universidade do Porto, Rua Dr. Roberto Frias 4200-465, Porto, Portugal. e-mail: viana@fe.up.pt.
David de Carvalho, D.Sc, Faculdade de Engenharia Agrícola, Universidade Estadual de Campinas, Av. Marechal Rondon 501, 13083-875 Campinas, SP, Brazil. e-mail: david@feagri.unicamp.br.
Jaime Santos, D.Sc., Instituto Superior Técnico, Universidade Técnica de Lisboa, Av. Rovisco Pai 1049-001, Lisbon, Portugal. e-mail: jaime@civil.ist.utl.pt.
Elisabete Costa Esteves, M.Sc., Instituto Superiorde Engenharia do Porto, Rua Dr. Antonio Bernardino de Almeida 431, 4200-072 Porto, Portugal. e-mail: efm@isep.ipp.pt.
Submitted on September 30, 2009; Final Acceptance on June 11, 2010; Discussion open until August 31, 2011.

In this study, three SPLT's were considered, all executed in an experimental site located in the State University of Campinas (Unicamp), in Brazil (Fig. 1). The local instrumentation that was used consisted of electrical resistance extensometers installed along the entire pile length, which enabled thorough quantification of pile shaft strain.

3. Unicamp Experimental Site

3.1. Geological and geotechnical characteristics

The regional subsoil was formed by the decomposition of basic magmatic rocks, along with basic intrusive units (diabasic). The rock formations cover 98 km^2 of Campinas region, corresponding to 14% of the total area. The subsoil of the experimental site consists of a diabasic soil profile, including a 6.5 m thick surface layer, constituted of highly porous silty clay, overlaying a residual diabasic soil (with clayey silt) horizon down to 20 m. Water level is 17 m below the surface.

The geotechnical characterization of the soil of Unicamp Experimental Site is described in Giacheti (1991), Monacci (1995), Albuquerque (1996) and Peixoto (2001) as part of a research program on tropical soils for foundation purposes (Carvalho *et al.* 2000). Figure 2 shows an outline of the geotechnical profile with some characteristics of the subsoil. The physical parameters of the soil were obtained by performing tests in undisturbed samples of soil collected after a 16 m deep well was dug.

Several field tests were performed: dynamic sounding, standard penetration test including torque measurements (SPT-T), cone penetration tests (CPT), flat dilatometer tests (DMT), pre-bored pressure meters (PMT), among others. The location of CPT and SPT tests along with tested piles are shown in Fig. 3. SPT-T and CPT profiles are shown in Fig. 4. The location of piles at the Experimental Field can also be seen. The CFA, Omega and bored piles are 2.4 m (6ϕ) far from the neighboring reaction piles. We can also see a precast concrete pile measuring 0.18 m diameter and 14 m length, instrumented in depth, 12 m far from the Omega 3 pile. The results of the precast pile are shown and analyzed in Albuquerque & Carvalho (1999).

Figure 1 - Location of the city of Campinas.

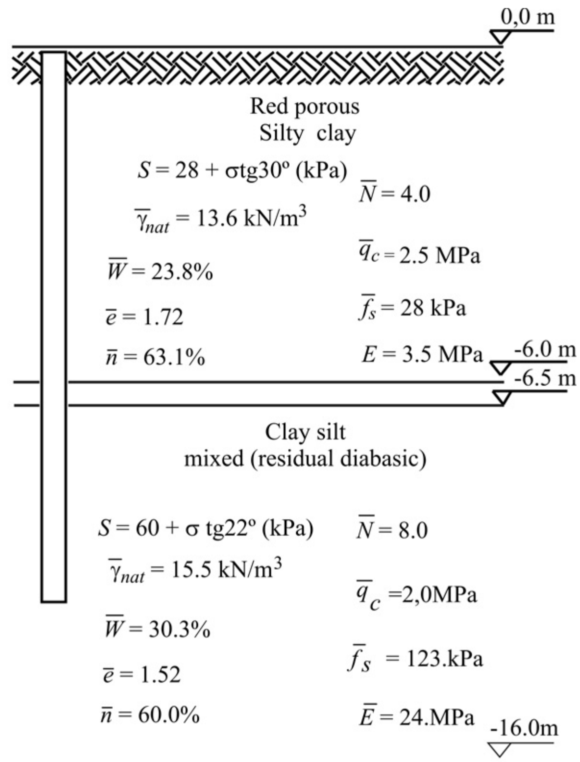

Figure 2 - Experimental site average geotechnical properties.

3.2. Results of load tests

Nine pile load tests were performed following prescriptions of Brazilian Standards (NBR 12.131/92) and adopting the slow maintained load method, considered the "Standard Loading Procedure" in opposition to other less universal tests, such as constant rate of penetration or quick

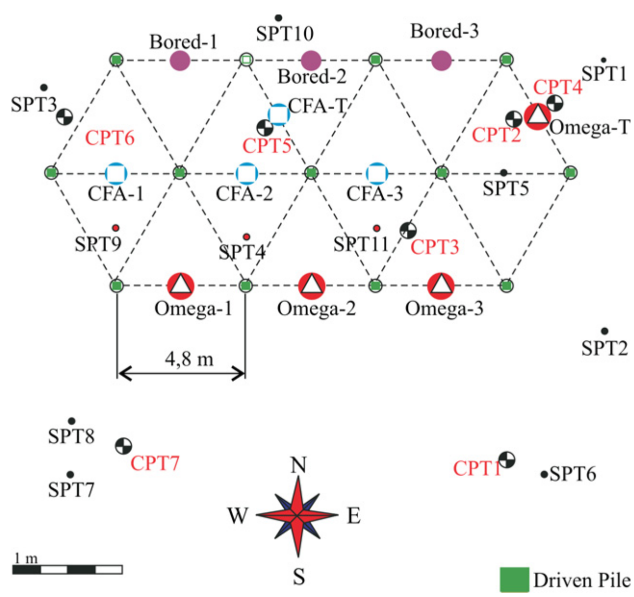

Figure 3 - Location of piles in the Experimental Site.

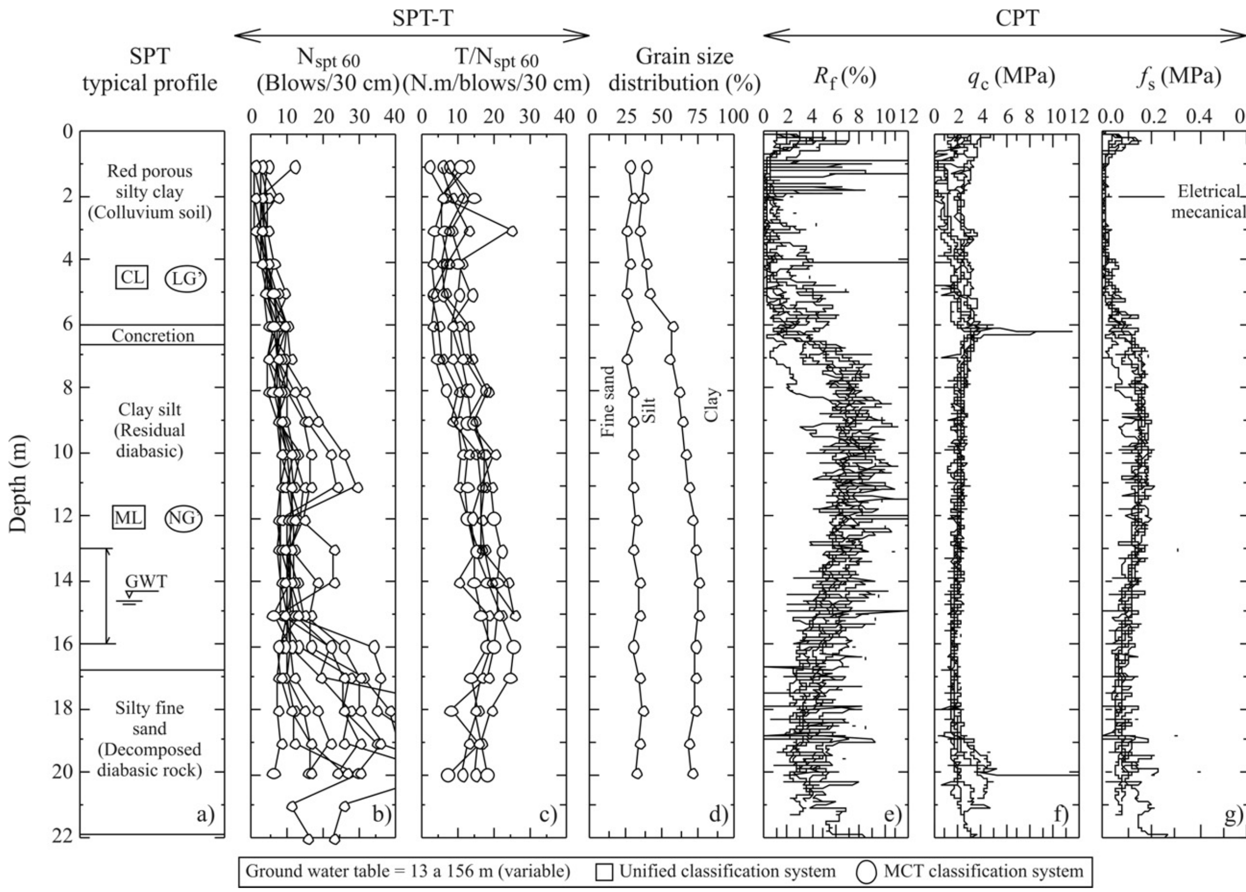

Figure 4 - SPT-T and CPT (Electrical) tests results (adapted from Giacheti *et al.*, 2004).

maintained load test. Maximum stabilized loads for each pile are shown in Table 1 and load *vs.* displacement curves in Fig. 5.

3.3. Case 1 - Bored pile

3.3.1. Execution technique

The bored piles were executed by gradually removing the soil and advancing the auger in depth with up and down movements. Care was taken not to allow the soil removed to fall back into the hole. Concrete was placed by a steel funnel, to ensure no soil got impregnated in the concrete mass.

Table 1 - Maximum load and displacement values obtained in load tests.

Pile	Maximum load (kN)	Maximum displacement (mm)
Bored 1	684	112.48
Bored 2	670	107.70
Bored 3	693	65.94
CFA 1	960	80.24
CFA 2	975	85.62
CFA 3	720	88.23
Omega 1	1545	64.57
Omega 2	1420	61.83
Omega 3	1320	22.52

3.3.2. Execution process

Three conventional bored piles (0.40 m diameter and 12 m deep) were executed. The upper 6 m were reinforced with four steel bars 16 mm diameter ($\cong$ 8 cm^2). Stirrups with 6.3 mm diameter spaced in 20 cm (Steel CA-50) completed the reinforcement. The concrete had a characteristic resistance to compression (fck) of 15 MPa and slump of around 70 mm. For the pile cap (0.7 m x 0.7 m x 0.7 m) a concrete with fck = 25 MPa was used.

3.3.3. Instrumentation response

Piles were instrumented along the shaft in the following depths: 0.30 m (reference section); 5.0 m; 11.1 m and 11.7 m. The process used consisted of instrumented steel bars with strain-gages connected in complete bridge, made by Unicamp technicians. (Figs. 6a and 6b) (Albuquerque, 2001).

To have a reliable value of the in-cast concrete Young's modulus (E), a gage level was placed below the pile cap, in the so called "reference section", where the load

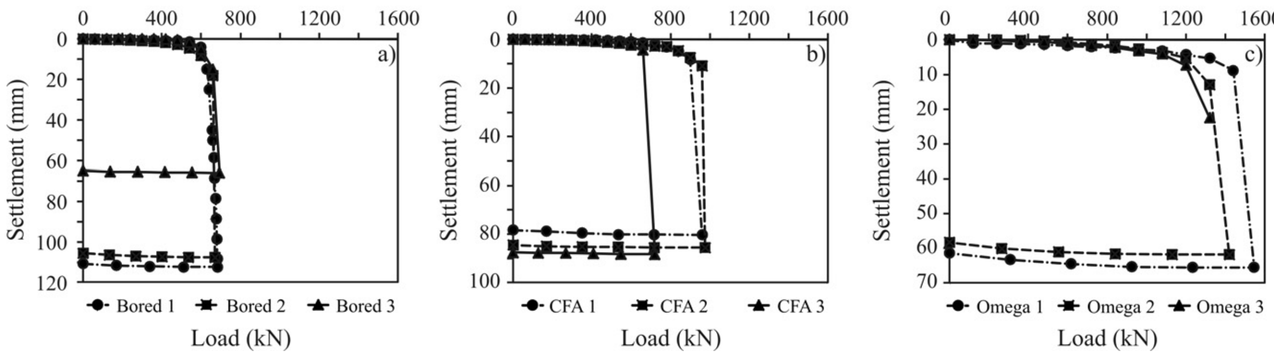

Figure 5 - Load-movement curves.

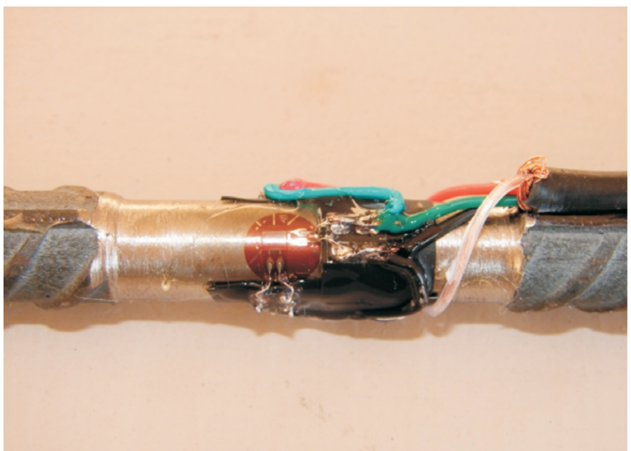

a) Strain-gage

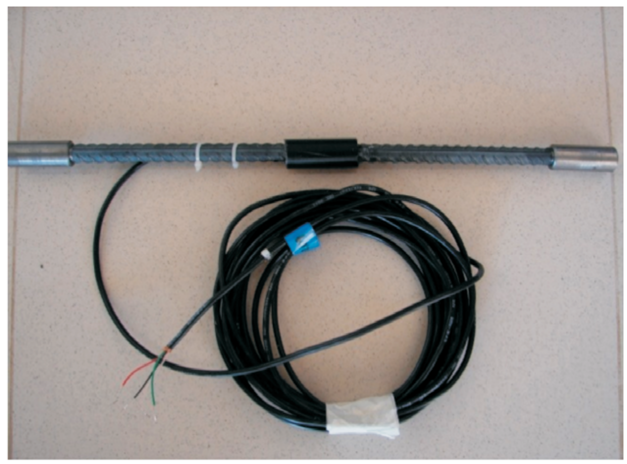

b) Instrumented steel bar

Figure 6 - Instrumentation details.

in the pile is the same as the load applied to the top face of the pile cap. Table 2 shows values obtained for the 3 instrumented bored piles. This approach to estimate Young's modulus is shown in plots (a) and (b) of Figs. 7, 8 and 9, constituting a graphical representation of the Tangent Modulus Method proposed by Fellenius (1989). This method is summarized below.

The equation for the tangent modulus line is:

$$M = \frac{d\sigma}{d\varepsilon} = A\varepsilon + b \quad (1)$$

Which can be integrated to:

$$\sigma = A\varepsilon^2 + B\varepsilon \quad (2)$$

Table 2 - Young's modulus of concrete as determined by strain gages and coefficient of variation for the three piles.

Pile	E_{min} (GPa)	E_{max} (GPa)	E (GPa)	CV(%)
Bored 1	24.2	29.9	27.4	6.6
Bored 2	23.1	24.5	23.8	2.1
Bored 3	26.4	31.9	29.1	5.5

However,

$$\sigma = E_s\,\varepsilon \quad (3)$$

Therefore,

$$E_s = 0.5A\varepsilon + B \quad (4)$$

where M = tangent modulus, E_s = secant modulus, σ = stress, $d\sigma = (\sigma_{n+1}-\sigma_1)$ = change in stress from one reading to the next, A = slope of the tangent modulus line, ε = measured strain, $d\varepsilon = (\varepsilon_{n+1} - \varepsilon_1)$ = change in strain from one reading to the next, B = y-intercept of the tangent modulus line (*i.e.*, initial tangent modulus).

$$\frac{dP_0}{d\varepsilon} = E_s\,S \quad (5)$$

Knowing the strain-dependent secant modulus ratio, the measured strain values are converted to the stress in the pile at the gage location. The load at the gage is then obtained by multiplying the stress by the pile cross sectional area.

With the values of $E_s.S$ included in these plots, where S is the cross sectional area of the pile in the gage levels and

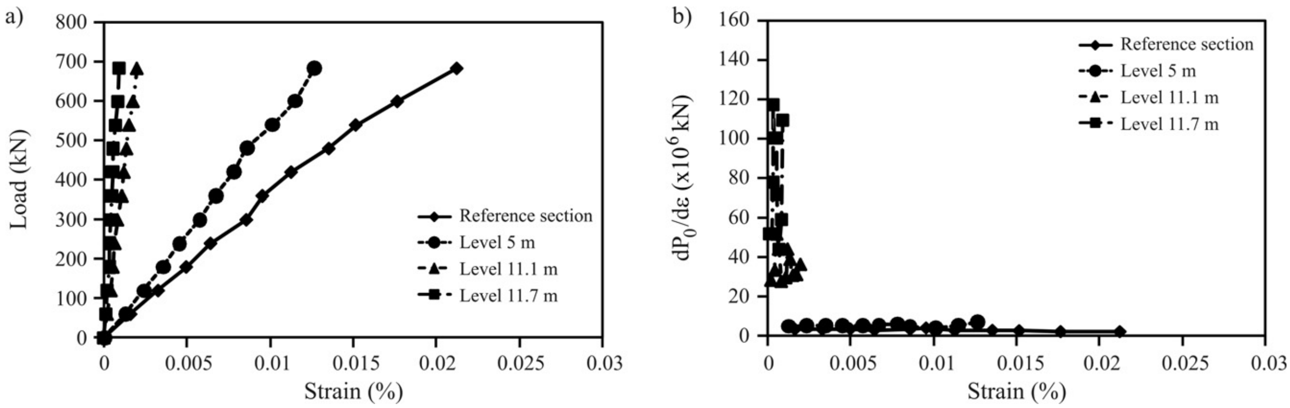

Figure 7 - Results of intrumentation analysis for Bored pile 1.

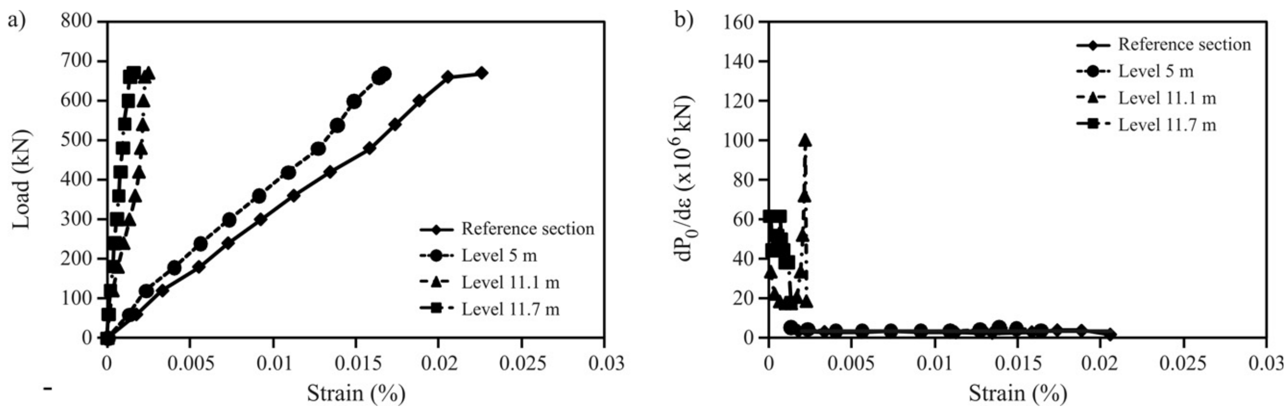

Figure 8 - Results of intrumentation analysis for bored pile 2.

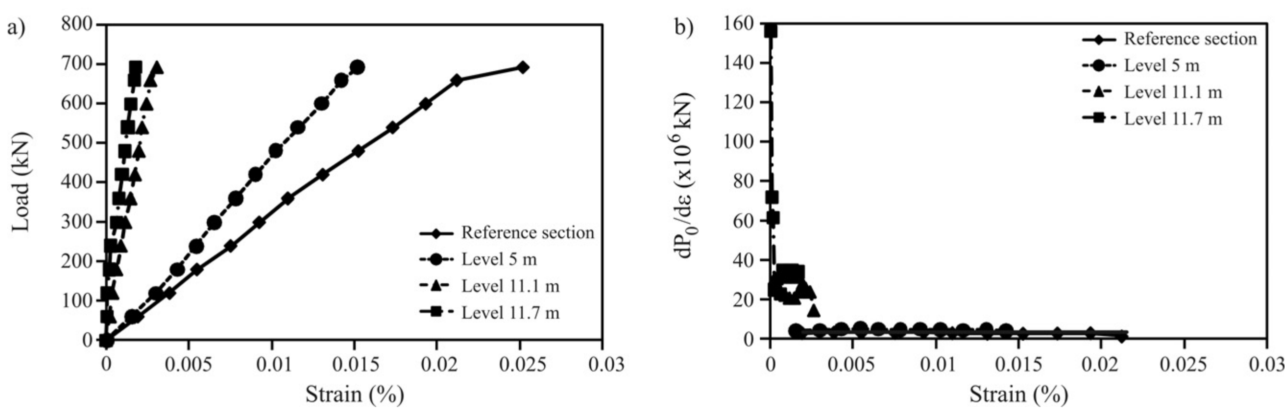

Figure 9 - Results of intrumentation analysis for bored pile 3.

E_s is the secant modulus, it is possible to build the plot of the load-transfer diagrams for piles.

From the results shown in Table 2 it can be concluded that concrete Young's modulus values are similar for the three types of piles, with very low variations. These results indicate good performance of the gages installed at the upper levels of the piles.

Analyzing the figures mentioned before, a reduction in strain levels along the depth (level 5 m, 11.1 m and 11.7 m) can be detected. It can be noticed that load transfer was more significant between the 5 m and 11.7 m depth levels. This fact was already expected, since soil at the 5 m level is more resistant than the upper layer. Observing instrumentation behavior close to pile tip, strains were very small, which indicates that at this level induced stress is very low.

As the upper 6 m were reinforced with steel bars, the increase in Young's modulus was calculated as 6% in comparison to the remaining part of the pile.

3.4. Case 2 - CFA pile

3.4.1. Execution technique

The continuous flight auger piles (CFA) are cast in place by drilling the soil through a continuous auger with a 'corkscrew' around a central hollow tube. After reaching the bottom level, while the auger is pulled up, the soil is replaced with concrete pumped down through the hollow tube. To prevent soil or water from entering the hollow tube, there is a metal cap (plug) at the bottom, which is opened, like a valve, by the injected concrete. As the auger is removed, the soil confined between the 'corkscrews' is also replaced by the concrete being injected from the tip level upwards. The concrete is characterized by a mixture of small aggregate and sand with cement (minimum consumption of 400 kg/m^3) and a value of slump of 240 mm, following prescriptions from the Brazilian Association of Foundations Companies Procedures Manual (ABEF, 1999). The advantages of using this type of pile are: reduced work schedule; applicability in rather different types of soils (except for rocks or soils with boulders); lack of disturbances and little vibration in the terrain, in opposition to percussion driving techniques, and absence of soil decompression and contamination when bentonite or other slurries are used. Disadvantages are associated to the need of flat terrain to allow the equipment to move easily; the demand for a concrete center close to the work; the need of a shovel loader to remove and clean the soil extracted while drilling; the demand for a minimum number of piles to justify the displacement of equipment to optimize the cost-benefit ratio; and, last but not least, the limitation of pile length and reinforcement, which may be considered determinant in certain projects. Special attention should be paid to the production process, particularly to control shaft continuity and disturbance of the subsoil when drilling. It is also important to observe that, in weak soils, concrete injected at high pressure may lead to soil rupture and high consumption. Another key advantage of CFA piles is the possibility of continuous electronic monitoring of the execution of piles, which can be easily accessed for corrections. The following parameters are registered: date and time; digging depth; penetration speed; torque; concrete volume and pressure; pile diameter; and pile extraction velocity.

3.4.2. Information on execution

Three CFA piles (0.40 m diameter and 12 m depth) were executed. Four reinforcing bars (16 mm diameter ($\cong$ 8 cm^2) and 6 m length) were used. Stirrups with 6.3 mm diameter, spaced in 20 cm (Steel CA-50) completed the reinforcements. A MAIT HR-200 drill was used to make the pile, with torque ranging from 220 kN.m to 380 kN.m, according to rotation speed and the diameter of piles employed.

3.4.3. Effects of installing piles in the subsoil

In order to evaluate the effects of installing piles, CPT tests were carried out both in the soil in the vicinity of the pile shafts and well distanced from them. From the two conditions, shaft and tip resistances of the CPT were obtained. The values related to the undisturbed soil, *i.e.*, the results obtained in the tests conducted far from the influence zone, were used for comparison to the analysis of the CPTs next to the pile.

The CPT-5 was 0.25 m far from CFA-T shaft, a non tested pile. It was decided not to run tests closer since piles or CPT rods might incline, which could damage the equipment.

Plots of unit lateral friction (f_s) and cone point (q_c) resistances are shown in Figs. 10 and 11. In general, f_s and q_c values lie in the range of maximum and minimum limits of undisturbed soil. It can be noticed that, while in the first 6 m values related to the distance of 0.25 m were closer to the minimum limits, in the last 6 m they tend to the maximum limits. It may be concluded that the installation of piles seemed to have no significant influence in the surrounding soil.

3.4.4. Response to instrumentation

Strain gages were installed in the CFA piles in the same way and depths as in the bored piles.

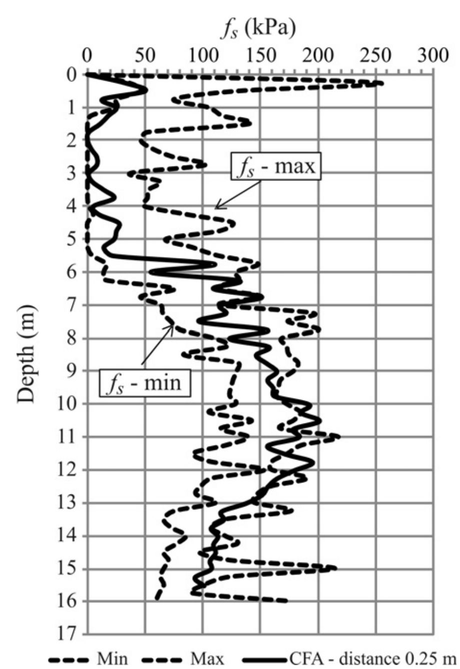

Figure 10 - f_s variation in depth.

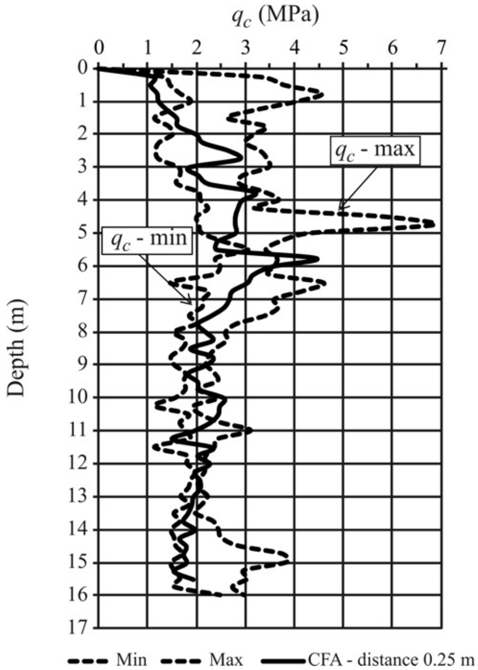

Figure 11 - q_c variation in depth.

Table 3 shows the values of the Young's modulus for each pile, obtained by applying the aforementioned method. The gage level at 0.3 m gave a load equal to the applied load at pile head. Plots (a) and (b) of Figs. 12, 13 and 14 were prepared based on the tangent modulus method of Fellenius (1989). It can also be seen that the elasticity modulus of CFA 3 was lower than those obtained for the same type of pile. This fact can only be related to the characteristics of the concrete of these piles, which came from a different lot.

3.5. Case 3 - Omega pile

3.5.1 Execution technique

The Omega pile, also called screw pile, is a soil displacement auger pile based on a screwing in – screwing out sequence. The execution can be outlined as follows: the auger head is inserted into the soil by rotation (Fig. 15), and the same CFA piles machine may be used; the soil is displaced downward and aside of the hole by the oriented slots fixed on the auger's head at different well-selected locations on the flanges; when drilling is over, as the auger is removed by rotation, concrete is injected under pressure. Concrete, with values of slump of around 240 mm, will have a minimum consumption of cement of 400 kg/m^3. Limitations to the use of this type of pile are the machine torque, which must be higher than 150 kN.m, and maximum shaft length of 30 m. At present, diameters may range from 310 to 660 mm. During the execution, monitoring is essential to differ depth parameters, torque, penetration rate and concreting characteristics. The difference between Omega and CFA piles is related to removal of soil to the surface; while the first type does not remove soil (except for the small quantity that is entrapped around the outer part of the auger), which remains compressed around the pile shaft, the second technique removes most of the soil with the up and down movement. Van Impe (1988) emphasizes these differences between the two modes of execution. Omega piles were not mentioned in this paper, but a similar pile, "Atlas" pile, was referred. Its configuration may be associated to Omega, despite some clear differences: cone shape and screw "pace" variation has peculiar characteristics but also move soil downward and to the sides (Fig. 16). The advantages of using Omega piles are their fast execution, low noise and high loading capacities (Bustamante & Gianeselli, 1998). The 8 h daily production ranges from 120 to 200 linear meters. Concrete "over consumption"

Table 3 - Concrete Young's modulus as determined by strain gages and coefficient of variation for the three piles.

Pile	E_{min} (GPa)	E_{max} (GPa)	E (GPa)	CV(%)
CFA 1	22.8	24.3	23.5	2.0
CFA 2	20.7	21.9	21.4	1.7
CFA 3	14.6	16.6	15.6	4.3

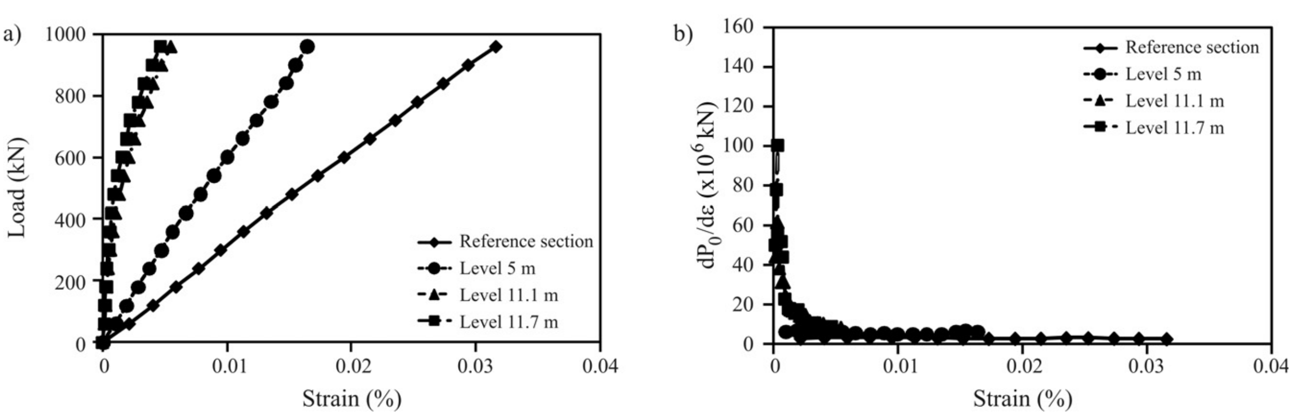

Figure 12 - Results of intrumentation analysis for CFA pile 1.

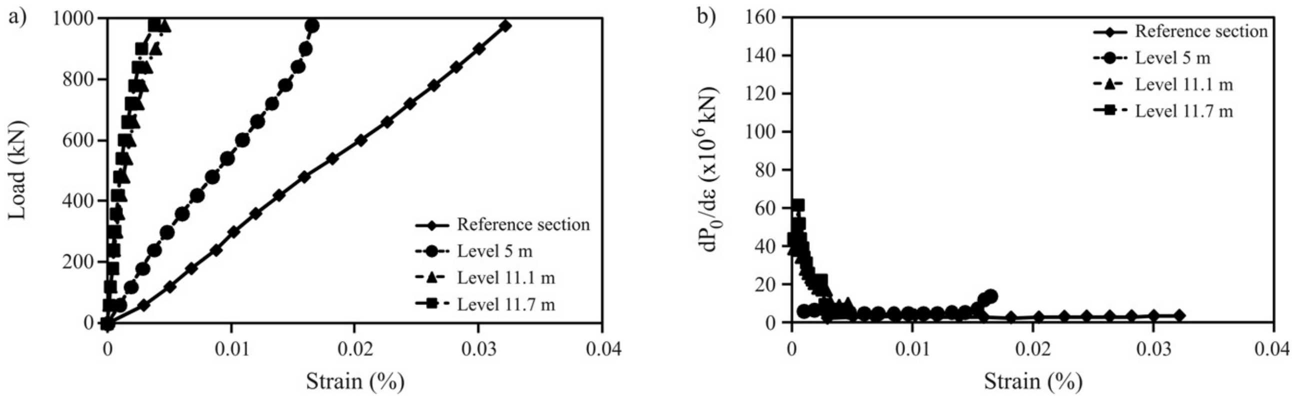

Figure 13 - Results of intrumentation analysis for CFA pile 2.

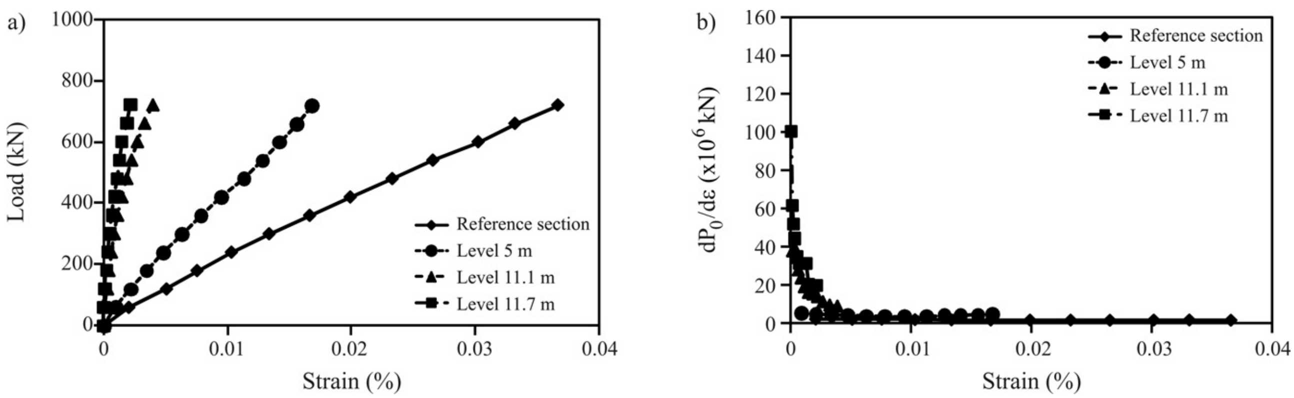

Figure 14 - Results of intrumentation analysisfor CFA pile 3.

ranges from 5 to 30%, depending on the soil, with a representative value of 15%. Some considerations about the execution of these piles can be made (Van Impe *et al.*, 1998): the shape of the perforating element brings numerous benefits to penetration, but the increase in load capacity could not be proved. The author points out the need for more work; maximum machine torque is very important to the execution; penetration rate depends on pile diameter and soil type; more energy is spent to move soil than to overcome friction between the drilling element and the soil; and this kind of pile does not present problems when executed

Figure 15 - Omega pile drilling.

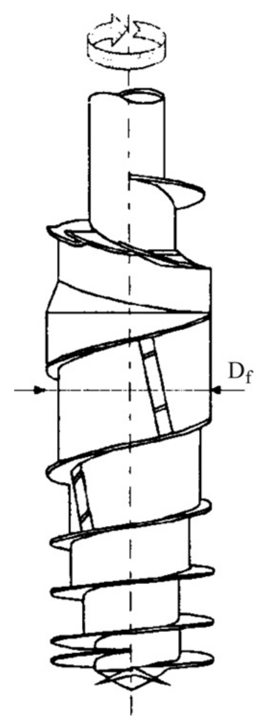

Figure 16 - Detail of the bit shape (FUNDESP, 2001).

in saturated and soft granular regions, while the fact that the soil is not dug brings several benefits.

3.5.2. Information on execution

Three 12 m deep Omega piles with 0.37 m diameter were executed. Concrete and reinforcement steel had the same characteristics and properties as those used in CFA pile.

3.5.3. Effect of installing piles in the subsoil

Similarly to what had been done to CFA piles, CPT tests were performed after installation of Omega-T pile. The results are shown in Figs. 17 and 18. It can be noticed that, in general, f_s and q_c values were between the maximum and the minimum limits of undisturbed soil. Moreover, in the first 6 m depth, CPT 4 values in the distance 0.15 m to the pile exceeded the maximum limits in some points along the pile length. Such fact was more evident in friction resistance (f_s), as it should be expected; it was verified, though, that f_s curves in a distance of 0.4 m (in CPT 2) were within the limit intervals, indicating that, for such distance, it seems that there is no pile influence. Based on these results, it is possible to conclude that, in the first 6 m depth, friction (f_s) and tip (q_c) resistances, in distance of 0.15 m from the Omega pile, exceeded the maximum values obtained for undisturbed soil (first layer). Below 6 m, f_s and q_c, resistances were within the limits of variation for undisturbed soil (the horizon of residual soil), although there was still a slight tendency of these parameters, particularly f_s, to approximate to the upper limit.

As it will be mentioned further on in the text, the Omega pile was extracted from the ground. It was observed that soil close to the shaft was more compacted than the soil located farther away. It was decided to collect samples at 5 cm and at 50 cm, from the shaft at 11 m depth. Tests were performed to determine natural volume weight (γ), water content (w) and void ratio (e). The results are shown in Table 4.

From this analysis, with emphasis on void ratio (e), it can be concluded that soil samples collected closer to the pile are denser, confirming the evaluation made by visual inspection. Based on the values presented above and those obtained in the consolidation test carried out in the natural soil (Table 5), in an exercise for a mere qualitative estimation of the vertical stress needed to change void ratio from 1.60 to 1.23, the value obtained was 682 kPa, which is over 4 times the effective overburden stress at 11 m depth.

In this context, it can be stated that installing Omega piles caused major changes around the pile shaft.

3.5.4. Response to instrumentation

Extensometers were installed in the Omega piles in the same way and same depths as in the bored and CFA

Table 4 - Physical indexes of soil samples, extracted at 11 m of depth.

Shaft distance	γ (kN/m^3)	w (%)	e
5 cm	17.5	31.1	1.23
50 cm	16.1	33.5	1.48

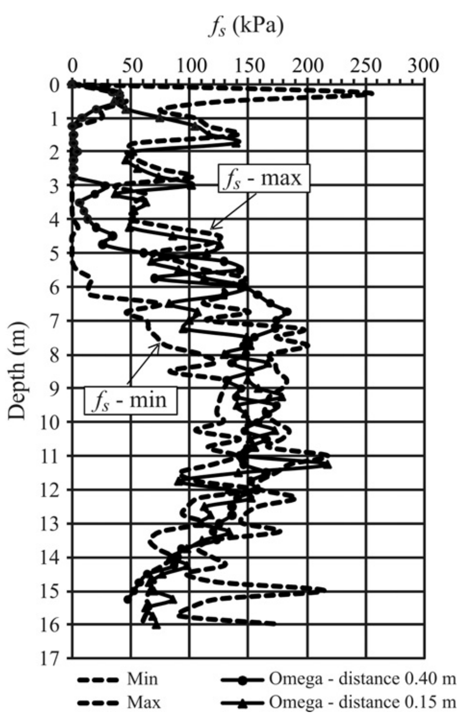

Figure 17 - f_s variation in depth.

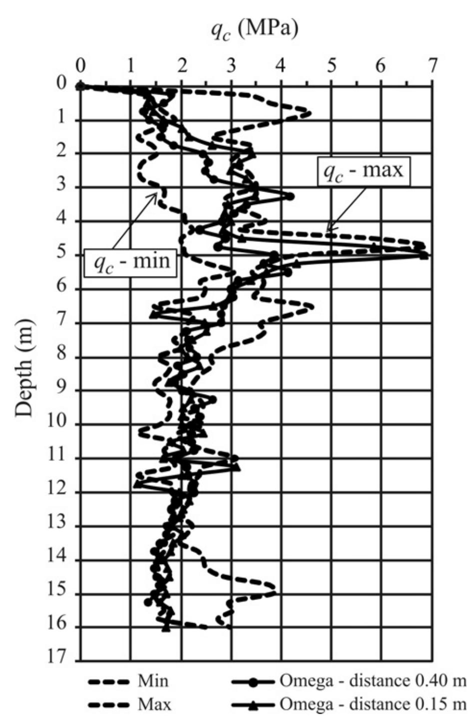

Figure 18 - q_c variation in depth.

Table 5 - Parameters used to calculate vertical stress.

Parameter	Used value
e_o	1.60
C_c	0.6
$\overline{\sigma}'_a$	140 kPa
γ	15.0 kN/m^3

e_o = baseline index of voids. C_c = compression index, $\overline{\sigma}'_a$ = pre-consolidation stress (mean), γ = specific natural weight of soil.

piles. The elastic modules (Young's modulus) were obtained in the same way.

Table 6 shows values for elastic modulus obtained for each pile, and plots (a) and (b) of Figs. 19, 20 and 21 were again prepared based on the tangent modulus method of Fellenius (1989).

In Figs. 19, 20 and 21, $E_s.S$ keeps constant values, but it did not correspond to the curves for deepest levels (11.1 and 11.7 m). This may be due to the sudden rupture when it moved from the second to the last load applied to each pile that was analyzed. If the load increase had been smoother from the next to last load increment, the constancy of this product would have been revealed. An observation of

Table 6 - Young's modulus of concrete as determined by strain gages and coefficient of variation for the three piles

Pile	E_{min} (GPa)	E_{max} (GPa)	E (GPa)	CV(%)
Omega 1	24.9	31.3	28.4	7.5
Omega 2	37.8	52.0	45.9	9.9
Omega 3	28.2	28.6	28.4	0.5

Table 6 shows that the value of Young's modulus of the Omega 2 pile is much higher than that of the other two piles. This is associated to the characteristics of different lots of concrete.

3.5.5. Unit shaft friction resistance

Values of maximum unit shaft friction resistance (f_{max}) are shown in Table 7 for all instrumented piles, including a precast concrete pile installed in the experimental site (Albuquerque, 1996). They were computed for 2 segments: 0 to 5 m and 5 to 12 m, related to the two soil horizons previously described. The table also shows average values along the entire length of the shaft for each type of pile (Albuquerque, 1996).

We were not able to get skin friction for the segments 0 to 5 m and 5 to 12 m of Omega 1 and 2 piles because the

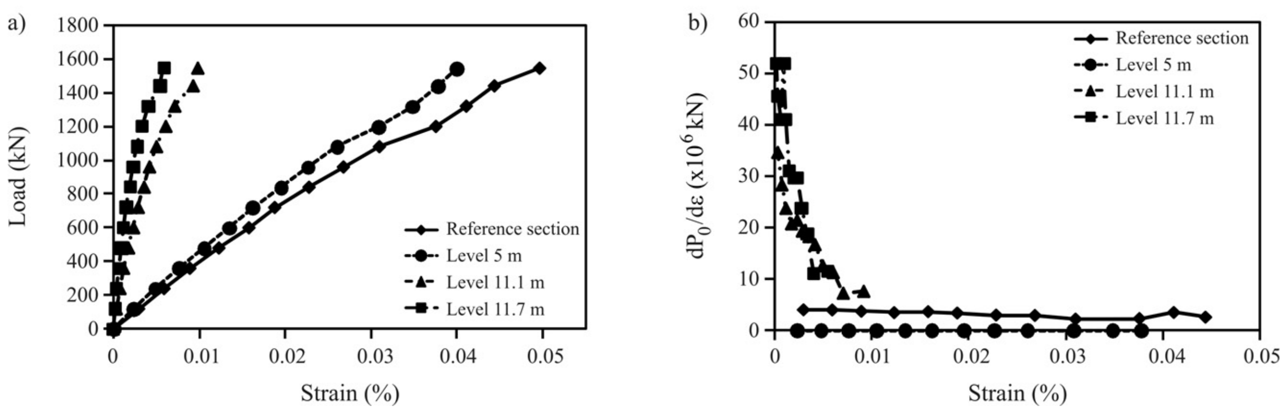

Figure 19 - Results of intrumentation analysis for Omega pile 1.

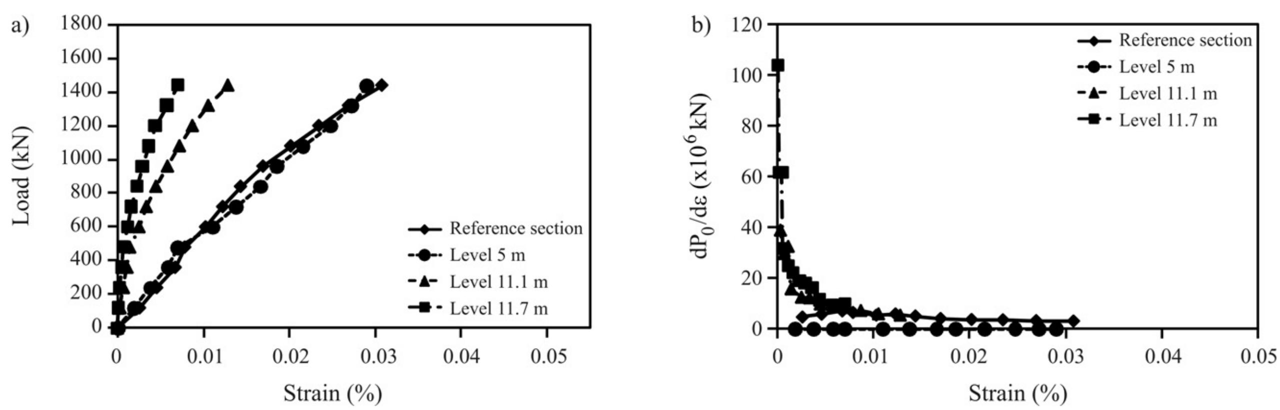

Figure 20 - Results of intrumentation analysis for Omega pile 2.

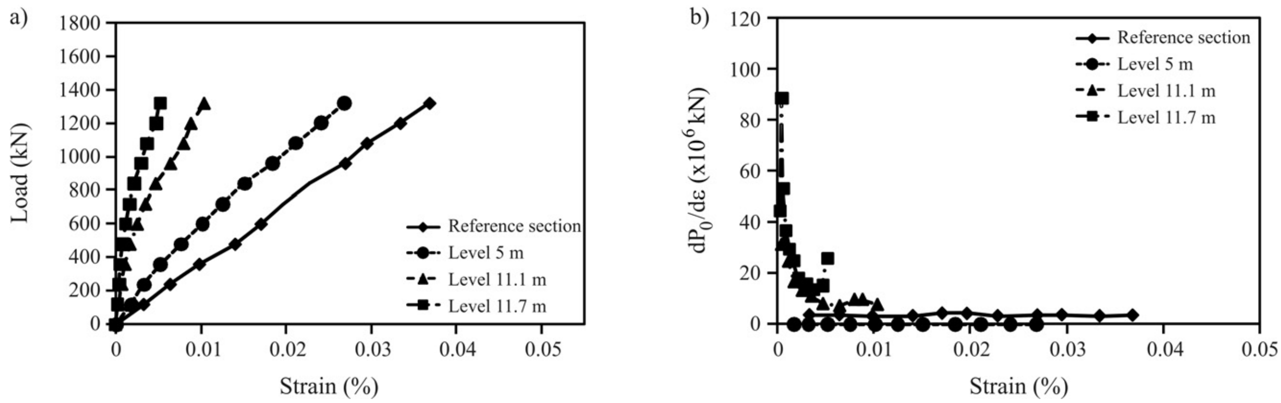

Figure 21 - Results of intrumentation analysis for Omega pile 3.

Table 7 - Maximum Unit Lateral Resistances (f_{max} in kPa).

Pile/Segments	0-5 m	5-12 m	0-12 m (average)	0-5 m (average)	5-12 m (average)	0-12 m (overall average)
Bored 1	39	44	40			
Bored 2	21	54	40	32	48	41
Bored 3	35	46	41			
CFA 1	80	47	60			
CFA 2	80	53	63	76	45	57
CFA 3	69	36	49			
Omega 1	-	-	97			
Omega 2	-	-	80	45	108	86
Omega 3	45	108	82			
Precast	24*	43**	29	-	-	29

* Segment 0-10 m ** Segment 10-14 m.

instrument located 5 m deep for both piles did not produce consistent data.

An analysis of these results shows that in the first segments (0-5 m), where soil is weaker, the average value of f_{max} for CFA piles was 76 kPa, exceeding not only the values of 32 kPa for the bored pile and 45 kPa for Omega 3 pile, but also the value of 45 kPa, associated to the second segment of the CFA piles, respecting the residual soil profile; this singular behavior was due to variation in diameter of the shaft of CFA pile.

It will be shown later (item 3.6B) that, in the execution of CFA piles, the diameter in the first meters increases bulging effect, which turns to be the main reason for the increase in lateral friction.

The increased skin friction was above the expectation, even if we consider the mean increase in pile diameter. This may be due to the tapered shape of the pile in the segment, which may have mobilized the passive thrust, as shown in Nordlund (1963) in his mathematical model for calculation of rupture of tapered piles. However, if this factor is not taken into consideration, it can be said that lateral friction values for the first segment (0 to 5 m), observed in CFA piles, without taking the bulging effect into account, may situate these type of piles at the same level as bored piles, with general values of 32 kPa, therefore, lower than Omega piles.

As for the second segment (5 to 12 m), CFA and bored piles provided friction values of the same order of magnitude, *i.e.*, 45 kPa and 48 kPa, respectively.

As for the Omega helical pile, an average value of f_{max} of 45 kPa was derived for the first segment (Table 7), roughly 40% higher than the corresponding value for the bored piles (32 kPa). In the second segment (5-12 m), this difference increased considerably, from 48 kPa in bored piles to 108 kPa in the Omega piles, which is 125% higher. This ratio increases to 140% when comparing Omega to with CFA piles.

Comparing the overall averages (Table 7), it may be concluded that f_{max} of Omega piles was 110% and 50% higher than the values of bored and CFA piles, respectively.

This confirms that the execution process of Omega piles significantly changed soil characteristics and increased soil resistance.

As far as the precast driven pile is concerned, it was not possible to compare the values indicated in Table 7, at least for the first segment because the shaft got detached due to driving vibration: the porous soil detached from the shaft (Albuquerque, 1996). This effect was also observed by Menezes (1997) in driven piles in porous soil in Ilha Solteira (SP). As to the second segment, the friction made by precast driven piles (43 kPa) was close to that of bored piles (48 kPa) and CFA piles (45 kPa), but it was far from the friction of Omega piles (108 kPa).

3.5.6. Tip unit resistance

In what follows, an analysis of the behavior of pile tips – specifically in what respects to tip bearing capacity – is presented based on the values of tip unit resistance (Rp) and maximum tip reaction, taken as the ratio of the maximum load applied to the pile tip, which is included in Table 8. Attention should be paid to the dispersion of values for each type of pile. The last line refers to the precast pile, driven in the same site and with the same length as the other piles. Rp values refer to the maximum load obtained from the load tests.

These results show that, in average, the unit tip resistance (maximum) for the Omega piles was 3.4 and 19.1 higher than the values of the CFA and bored piles. It was also revealed to be of the same magnitude as the unit tip resistance of the precast pile.

Another conclusion that could be inferred from Table 8 is related to the important design factor, *i.e.*, the expected ratio between maximum tip reactions (effective stress transmitted to the base of the pile) and the maximum loads applied to the top cap. The largest value corresponded to the precast pile (16.4%), as expected from the nature of the execution process, but with very close values for the Omega piles (13.9%), which could be considered a "good" surprise. On the other side, CFA piles (with a ratio of around 7.0%) and bored piles (with 2.0%) reflected the already foreseen incapacity of mobilizing significant tip reactions, at least for acceptable overall displacements.

Summing it up, it can be said that, as far as tip behavior is concerned, CFA piles behaved between bored piles and displacement piles, and Omega piles showed a clear improvement, typical of displacement piles.

We can see that the tip load is not mobilized to the corresponding load at 50% of the maximum load of the test.

Figure 22 shows the variation in maximum unit skin friction (mean) and the tip resistance (maximum) of each pile.

3.6. Analysis of pile shape after extraction from the terrain

After the load tests, three piles were extracted from the terrain, one of each type (bored 1, CFA 2 and Omega 2) (Fig. 23).

After cleaning the shafts, it was possible to analyze their characteristics (Figs. 24 to 31). Figure 32 shows the diameters along the length of the piles.

A detailed inspection provided important information about shaft surface, geometry and tip shape.

A) Bored pile:

Table 8 - Tip unit resistance (Rp), tip displacement and ratio of tip reaction.

Pile	R_p-max (kPa)	50% Q_{cap}-max (kPa)	δ_{tip} max (mm)	δ_{tip} for 50% Q_{cap}-max (mm)	Q_p/Q_{cap} max (%)
Bored 1	21	9	8.6	0.00	0.5
Bored 2	83	24	17.4	0.60	2.0
Bored 3	157	42	14.4	0.01	3.6
Average	87	25	13.5	0.20	2.0
CFA 1	760	77	7.3	0.00	10.6
CFA 2	530	91	6.5	0.43	7.3
CFA 3	182	19	3.5	0.13	3.2
Average	491	62	5.8	0.19	7.0
Omega 1	1411	251	7.1	0.38	10.9
Omega 2	2430	401	4.6	0.78	20.5
Omega 3	1153	250	6.7	0.75	10.4
Average	1665	300	6.1	0.64	13.9
Precast	1690	275	2.1	0.73	16.4

R_p = tip unit resistance.
Q_{cap} = maximum cap load.
δ = tip displacement.
Q_p/Q_{cap} = Tip reaction as a (%) of the load applied on the pile cap.

• the diameter ranged from 42.4 cm to 45.9 cm, averaging 45.0 cm with standard deviation of 0.96 cm;

• the effective average diameter was about 13% higher than the nominal diameter;

• the tip had sharp geometry in one of the sides (asymmetric) (Fig. 24); and,

• the shaft surface was clearly rough (Fig. 25).

B) CFA pile:

• the pile tip was molded by using a drilling bit (Fig. 26), diverging from the cone-shaped tip, as reported by Souza (2006);

• 'strips' were formed by the auger drilling all along the pile length (Fig. 27);

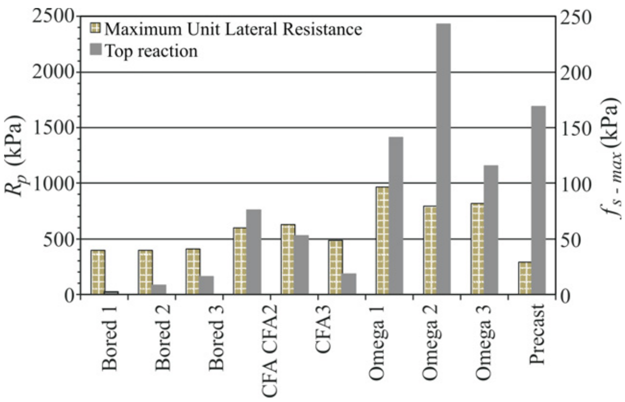

Figure 22 - Variation of maximum unit lateral resistance (average) and tip reaction.

Figure 23 - Pile extraction.

• a bulb-shaped bulge was observed, which means an increase in the diameter of a pile segment between 1.5 and 3.0 m depths;

• the diameter ranged from 37.9 cm to 48.9, averaging 40.4 cm with standard deviation of 2.78 cm.

C) Omega pile:

• the shaft had a screw spiral-shape (like a 'nervure'), with a 'pace' of 30 cm through the first 6 m (Fig. 28) and of

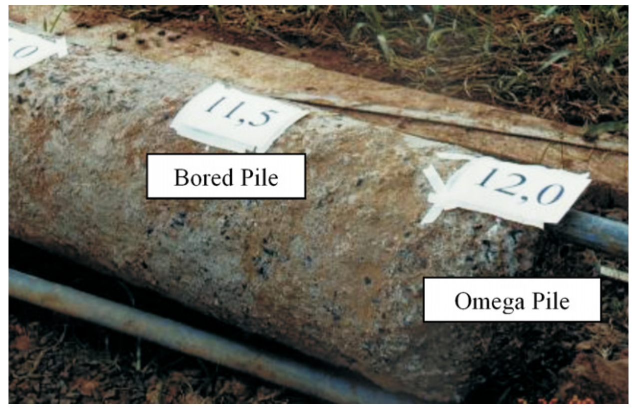

Figure 24 - Bored 1 pile tip.

Figure 25 - Shaft view in bored 1 pile (2nd plan) and in Omega 2 pile (1st plan).

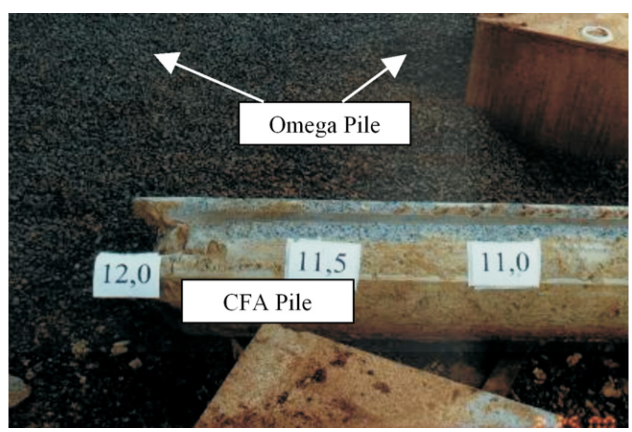

Figure 26 - CFA 2 pile tip.

Figure 27 - Shaft view in CFA 2 pile (1st plan).

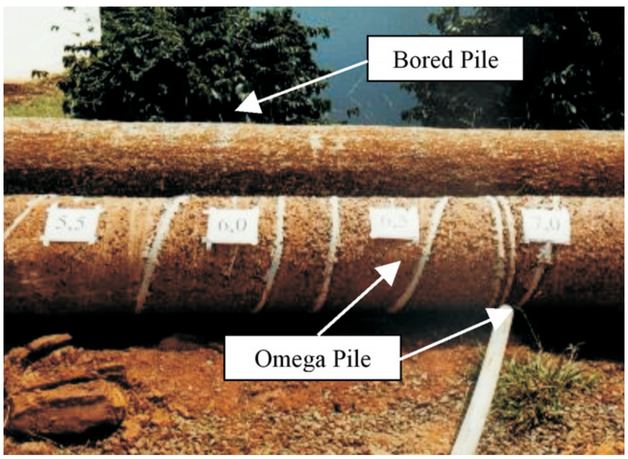

Figure 28 - Omega pile in 5.5 to 7.5 m depth segment.

12 cm through the last 6 m (Fig. 29); this may be due to the difference in the auger penetration velocity along the two layers of soil;

• Shaft surface roughness is high, caused by small gravels used in the concrete, as if they were detached from the cement paste and compacted against shaft wall;

• the soil was strongly adhered to the shaft, firmly compacted, with thickness ranging between 5 and 8 cm (Fig. 30);

• the rounded shape of the pile tip (Fig. 31); and,

• the diameter ranged from 37.8 cm to 41.7 cm, averaging 39.2 cm with standard deviation of 1.11 cm; the shape of the tip was rounded, as shown in Fig. 32.

We can see that only the actual mean diameter of the CFA pile was equal to the nominal diameter (Table 9).

By calculating unit skin friction using the actual mean value obtained for the bored and Omega piles, we get the values shown in Table 10.

Table 10 indicates reduced skin friction because of the increased side area due to a greater diameter. This causes a reduction in lateral friction of approximately 12% for bored piles and 9% for Omega piles.

Figure 29 - Omega pile in 9.0 to 10.5 m depth segment.

Figure 30 - Soil adherence in shaft of Omega 2 pile.

Figure 31 - Omega 2 pile tip characteristic.

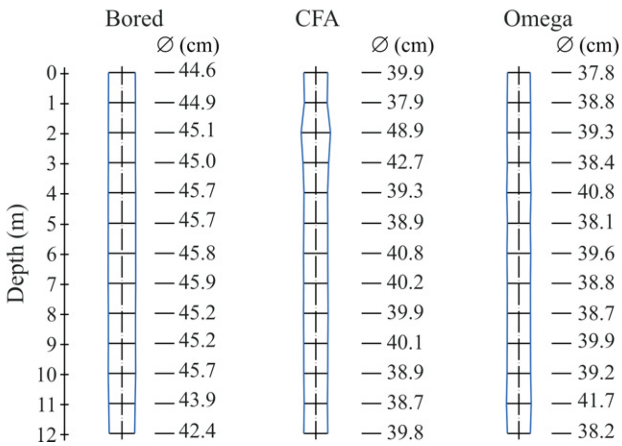

Figure 32 - Diameters measured after pile extraction.

Table 9 - Values of mean nominal and actual diameters of piles extracted from the soil.

Pile	Nominal (m)	Actual (m)
Bored 1	0.40	0.44
CFA 2	0.40	0.40
Omega 2	0.37	0.39

Table 10 - Maximum unit skin resistances of actual diameter of bored and Omega piles (f_{max} in kPa).

Pile/segments	0-5 m	5-12 m	0-12 m (average)
Bored 1	35	39	36
Omega 2*	-	-	76

*The Omega 2 pile has no friction values presented in the intermediate segments, because of the instrument located 5 m deep did not produce consistent data.

4. Conclusion

This study reviewed the influence of construction techniques on the behavior of piles by means of instrumentation along the shaft. Based on the analyses performed, the following conclusions stated below could be drawn. The values shown for skin friction and tip resistance refer to load mobilized to the maximum load applied in the test.

4.1. Tip resistance

The maximum load transfer to the base of piles was relatively small: an average of 2% for the bored pile, 7% to the CFA pile and 14% for the Omega pile. The latter ratio is similar to the one seen in the precast driven pile tested in the same site. The construction processes of bored piles strongly disturb the soil around the tip and leave it unstructured, leading to low tip resistance (87 kPa). In this aspect, the CFA pile had an intermediary behavior (491 kPa) and the Omega pile showed a high value (1665 kPa), very similar to the concrete precast pile (1690 kPa). Low values for bored piles were also obtained by Branco (2006), who presented a detailed study on shaft and tip load transfer in this type of piles.

The pile tip mobilization to the three types of piles was low for 50% of the maximum load of the test.

4.2. Unit shaft friction resistance

As expected, the unit shaft friction resistance (f_{max}) increased with depth for bored and Omega piles: the deeper soil layer is more resistant than the more superficial one. For the CFA pile, side friction was higher in the upper segments of the pile due to the formation of a bulb-shaped bulge, which was clearly observed in this area. For the 5 to 12 m depth horizon, values of f_{max} were 48 kPa for the bored pile and 45 kPa for the CFA pile. If the mentioned bulge effect is ignored, it may be concluded that both types of piles have similar behavior in terms of lateral resistance. The Omega pile, with 'nervures', intense roughness and densified soil around the shafts presented average f_{max} value of 86 kPa, much higher than the other piles: 41 kPa for the bored pile and 57 kPa for the CFA pile.

4.3. Pile extraction

After extraction, it was observed that the bored and the CFA piles presented little roughness. In the latter, strips were clearly seen along the shaft. Moreover, the CFA pile displayed a bulb-shaped bulge from 1.5 to 3.0 m depths;

Roughness of the Omega pile was higher, due to the presence of small gravels along the length; spaced nervures measuring 30 cm in the first 6 m and 12 cm in the last 6 m were also observed, with soil strongly adhered and compacted to the shaft.

The tips had different shapes, sharp in the bored pile, similar to drill edge in CFA pile and rounded in the Omega pile.

4.4. Instrumentation along the depth

The use of extensometers (strain-gages) fixed in steel bars showed that this technique gives a high return value, since the data obtained proved to be very consistent with other results and evidence in overall behavior (Albuquerque, 2001).

The results show different behaviors of piles with values for tip resistance and skin friction not known yet for this type of soil. This demonstrates the importance of performing load tests in foundation engineering.

References

Associação Brasileira de Empresas de Fundações (ABEF) (1999) Manual de Especificações de Produtos e Procedimentos, 2ª ed. ABEF, São Paulo, 282 pp.

Albuquerque, P.J.R. (1996) Análise do Comportamento de Estaca Pré-Moldada de Pequeno Diâmetro, Instrumentada, em Solo Residual de Diabásio da Região de Campinas. M.Sc. Thesis, Faculdade de Engenharia Agrícola, Universidade Estadual de Campinas, Campinas, 170 pp.

Albuquerque, P.J.R. & Carvalho, D. (1999) Análise de transferência de carga de estaca pré-moldada em solo residual de diabásio. Solos & Rochas. v. 22:2, p. 125-136.

Albuquerque, P.J.R. (2001) Estacas Escavadas, Hélice Contínua e Ômega: Estudo do Comportamento à Compressão em Solo Residual de Diabásio, Através de Provas de Carga Instrumentadas em Profundidade. PhD. Thesis, Escola Politécnica, Universidade de São Paulo, São Paulo, 263 pp.

Associação Brasileira de Normas Técnicas (ABNT) (1992) NBR 12131: Estacas: Prova de Carga Estática. Rio de Janeiro.

Branco, C.J.M.C. (2006) Provas de Carga Dinâmica em Estacas Escavadas de Pequeno Diâmetro com Ponta Modificada. PhD. Thesis, Escola de Engenharia de São Carlos, Universidade de São Paulo, São Carlos, 192 pp.

Bustamante, M. & Gianeselli, L. (1998) Installation parameters and capacity of bored piles. Proc. 3rd International Geotechnical Seminar on Deep Foundations on Bored and Auger Piles, Ghent, pp. 95-108.

Carvalho, D.; Albuquerque, P.J.R. & Giacheti, H.L. (2000) Campo experimental para estudos de mecânica dos solos e fundações em Campinas-SP. In: Seminário de Engenharia de Fundações Especiais – SEFE IV, Seminário Brasileiro de Investigações de Campo - BIC. São Paulo, v. 3, pp. 90-100.

Fellenius, B.H. (1989) Tangent modulus of piles determined from strain data. ASCE, Geotechnical Engineering Division, the 1989 Foundation Congress, v. 1, pp. 500-510.

Fundesp (2001) Fundações Especiais, 1st ed. Fundesp, São Paulo, 62 pp.

Giacheti, H.L. (1991) Estudo Experimental de Parâmetros Dinâmicos de Alguns Solos Tropicais do Estado de São Paulo. PhD Thesis, Escola de Engenharia de São Carlos, Universidade de São Paulo, São Carlos, 232 pp.

Giacheti, H.L.; Peixoto, A.S.P. & Mondelli, G. (2004) Comparação entre resultados de ensaios de penetração com os cones mecânico e elétrico em solos tropicais. Solos & Rochas, v. 27:2, p. 191-200.

Menezes, S.M. (1997) Análise do Comportamento de Estacas Pré-Moldadas em Solo de Alta Porosidade do Interior do Estado de São Paulo. PhD Thesis, Escola Politénica, Universidade de São Paulo, São Paulo, 377 pp.

Monacci, M.D. (1995) Estudo da Colapsibilidade de um Solo do Campo Experimental da Faculdade de Engenharia Agrícola – Unicamp. M.Sc. Thesis, Faculdade de Engenharia Agrícola, Universidade Estadual de Campinas, Campinas, 114 pp.

Nordlund, R.L. (1963) Bearing capacity of piles in cohesion less soils. Journal of the Soil Mechanics and Foundation Division, v. 89:3, p. 1-35.

Peixoto, A.S.P. (2001) Estudo do Ensaio SPT-T e sua Aplicação na Prática de Engenharia de Fundações. PhD Thesis, Faculdade de Engenharia Agrícola, Universidade Estadual de Campinas, Campinas, 468 pp.

Souza, R.N. (2006) Observação do contato concreto-solo da ponta de estacas hélice contínua. Anais. XIII Congresso Brasileiro de Mecânica dos Solos e Engenharia Geotécnica, Curitiba, v. 2, pp. 1253-1258.

Van Impe, W.F. (1988) Considerations on the auger pile design. Proc. 1st International Geotechnical Seminar on Deep Foundations on Bored and Auger Piles, Ghen, pp. 193-218.

Van Impe, W.F.; Van Impe, P.O.; Viggiani, C.; Russo, G. & Bottiau, M. (1998) Load-settlement behavior versus distinctive Ω-pile execution parameters. Proc. 3rd International Geotechnical Seminar on Deep Foundations on Bored and Auger Piles, Ghent, pp. 355-366.

Velloso, D.A.; Aoki, N.; Lopes, F.R. & Salomon, J.A (1975) Instrumentação simples para provas de carga em tubulões e estacas escavadas. Simpósio Sobre Instrumentação de Campo em Engenharia de Solos e Fundações, Rio de Janeiro, v. 1, pp. 269-280 (In Portuguese).

Effects of the Construction Method on Pile Performance: Evaluation by Instrumentation. Part 2: Experimental Site at the Faculty of Engineering of the University of Porto

Paulo José Rocha de Albuquerque, Faiçal Massad, Antonio Viana da Fonseca, David de Carvalho, Jaime Santos, Elisabete Costa Esteves

Abstract. Three different types of piles (bored, CFA and precast driven) were installed in the experimental site located in the Campus of the Faculty of Engineering of the University of Porto to study the effects of the construction method on pile performance. The subsoil is a residual granitic soil reaching depth levels over 20 m. In this site, several field and laboratory tests were conducted to obtain the local geotechnical parameters. Static pile load tests with load-unload cycles were performed. Bored and CFA piles were instrumented along the depth, with installation of retrievable sensors; a flat-jack load cell was inserted at the bottom of the bored pile. Load tests results demonstrated that bored and CFA piles show similar behavior: i) the applied load reaching the pile tip was about 42%, ii) and the average mobilized lateral resistance was about 60 kPa. After the tests were completed, piles were extracted for further inspection of shaft and load cell conditions. The driven pile although having a smaller cross-section showed a stiffer response and higher resistance than the other two piles, which are a clear indication that the installation effects play an important role in the pile response. The results are compared to those obtained in Part 1 of this article relating to tests performed at the Experimental Field of Unicamp (State University of Campinas).

Keywords: construction technique, bored pile, CFA pile, precast pile, instrumentation, granitic residual soil.

1. Introduction

The use of deep foundations in the City of Porto, in the North of Portugal, has been very frequent, mainly due to the particular geotechnical conditions of that area and the great development of means and processes of construction for this type of ground conditions. Therefore, knowledge of operation and calculation parameters used in design is essential. Many factors influence the behavior of deep foundations, some of which are difficult or even impossible to be characterized, so that the design methods for piles, especially in residual soils, still remain undefined. Thus, it became important to conduct axial compressive load tests on three different piles: bored with temporary casing, CFA and precast square. Piles were executed under the same current practice conditions and utilizing internal instrumentation at depth, allowing the assessment of load distribution along the shaft. Tests were conducted at the Experimental site of the Faculty of Engineering of the University of Porto, where a broad geotechnical site investigation was carried out, including a significant number of *in situ* and laboratory tests. The experimental site is composed of granitic subsoil, characterized by a very heterogeneous residual soil (saprolitic).

This study was conducted within a project supported by specialized companies and integrated in an International Prediction Event (Class A). The event was organized by the Faculty of Engineering of the University of Porto (FEUP) and the High Technical Institute of the Technical University of Lisbon (IST-UTL) in collaboration with the TC18 of the ISSMGE and the organizers of the ISC'2 Conference in Porto in September 2004 (Viana da Fonseca & Santos, 2008).

2. Experimental Site of Feup

2.1. Geological-geotechnical characteristics

In the northern region of Portugal, granitic residual soils prevail, reaching depths over 20 m. These soils have particular characteristics as a consequence of the variability and heterogeneity in macroscopic level and, on the other hand, by the inter-particles spatial arrangement and distribution. In Portugal, a country that has temperate weather, residual soils are generally found in the northern coast, characterized by a high rainfall rate with moderate temperatures and low gradients (Costa Esteves, 2005).

Paulo José Rocha de Albuquerque, D.Sc, Faculdade de Engenharia Civil, Arquitetura e Urbanismo, Universidade Estadual de Campinas, Av. Albert Einstein 951, 13083-852 Campinas, SP, Brazil. e-mail: pjra@fec.unicamp.br.
Faiçal Massad, D.Sc., Escola Politécnica, Universidade de São Paulo, Av. Professor Almeida Prado 271, Trav. 2, Cidade Universitária, 05508-900 São Paulo, SP, Brazil. e-mail: faical.massad@poli.usp.br.
Antonio Viana da Fonseca, D.Sc., Faculdade de Engenharia, Universidade do Porto, Rua Dr. Roberto Frias 4200-465, Porto, Portugal. e-mail: viana@fe.up.pt.
David de Carvalho, D.Sc, Faculdade de Engenharia Agrícola, Universidade Estadual de Campinas, Av. Marechal Rondon 501, 13083-875 Campinas, SP, Brazil. e-mail: david@feagri.unicamp.br.
Jaime Santos, D.Sc., Instituto Superior Técnico, Universidade Técnica de Lisboa, Av. Rovisco Pai 1049-001, Lisbon, Portugal. e-mail: jaime@civil.ist.utl.pt.
Elisabete Costa Esteves, M.Sc., Instituto Superiorde Engenharia do Porto, Rua Dr. Antonio Bernardino de Almeida 431, 4200-072 Porto, Portugal. e-mail: efm@isep.ipp.pt.
Submitted on February 4, 2010; Final Acceptance on September 20, 2010; Discussion open until August 31, 2011.

The experimental site is located in the University Campus at the Faculty of Engineering of the University of Porto, Portugal. Its location is shown in Figs. 1 and 2, where the geological map of the Porto Region and the Experimental site is also shown.

It can be noticed that the site is located in a region where igneous rocks predominate: medium or medium to fine grained granite named Porto's granite. Subsoil is constituted by medium to fine particle sand (young residual soil) up to 1.5 m to 2 m thick, followed by a layer of approximately 13 m of residual soil composed of medium to fine sand (structured residual soil). Between 15 and 20.5 m, a medium particle and very weathered granite is found. Ground water table can be found at 8.5 m to 11.5 m, depending on the period of the year. Several in situ tests were conducted (SPT, CPTU, DMT, PMT and seismic tests) to characterize the soil. Laboratory tests were performed on undisturbed samples obtained from the studied site: triaxial, resonant column and oedometric tests, besides usual identification tests. The localization of these tests is represented together with the tested piles in Fig. 3. Figures 4, 5 and 6 show the variation of N_{SPT}, q_c and f_s with depth, respectively.

2.2. Execution of piles characteristics

In this experimental site, a total of 14 piles were executed; 10 were 600 mm diameter bored piles, installed using a temporary steel casing, two of which were shorter, 6 m long (E0 and E9) and eight were 22 m long. These were used as reaction piles (E1 to E8); two 600 mm diameter

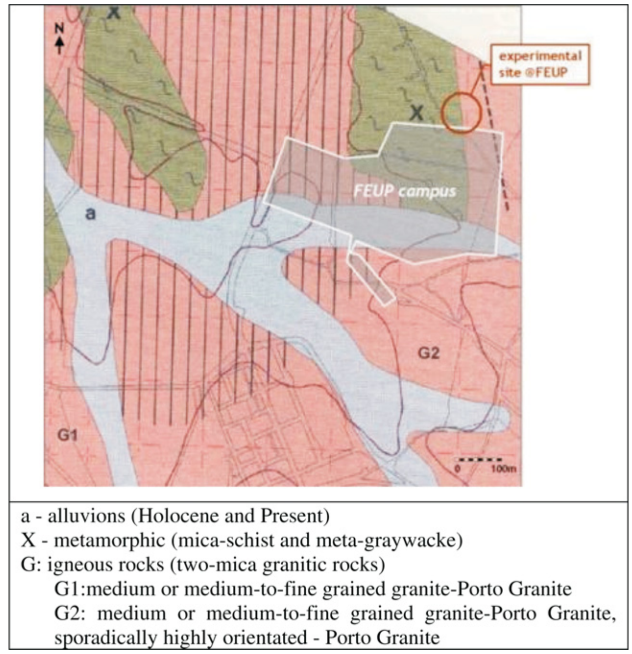

Figure 2 - Geological map of the experimental site (Viana da Fonseca *et al.*, 2004).

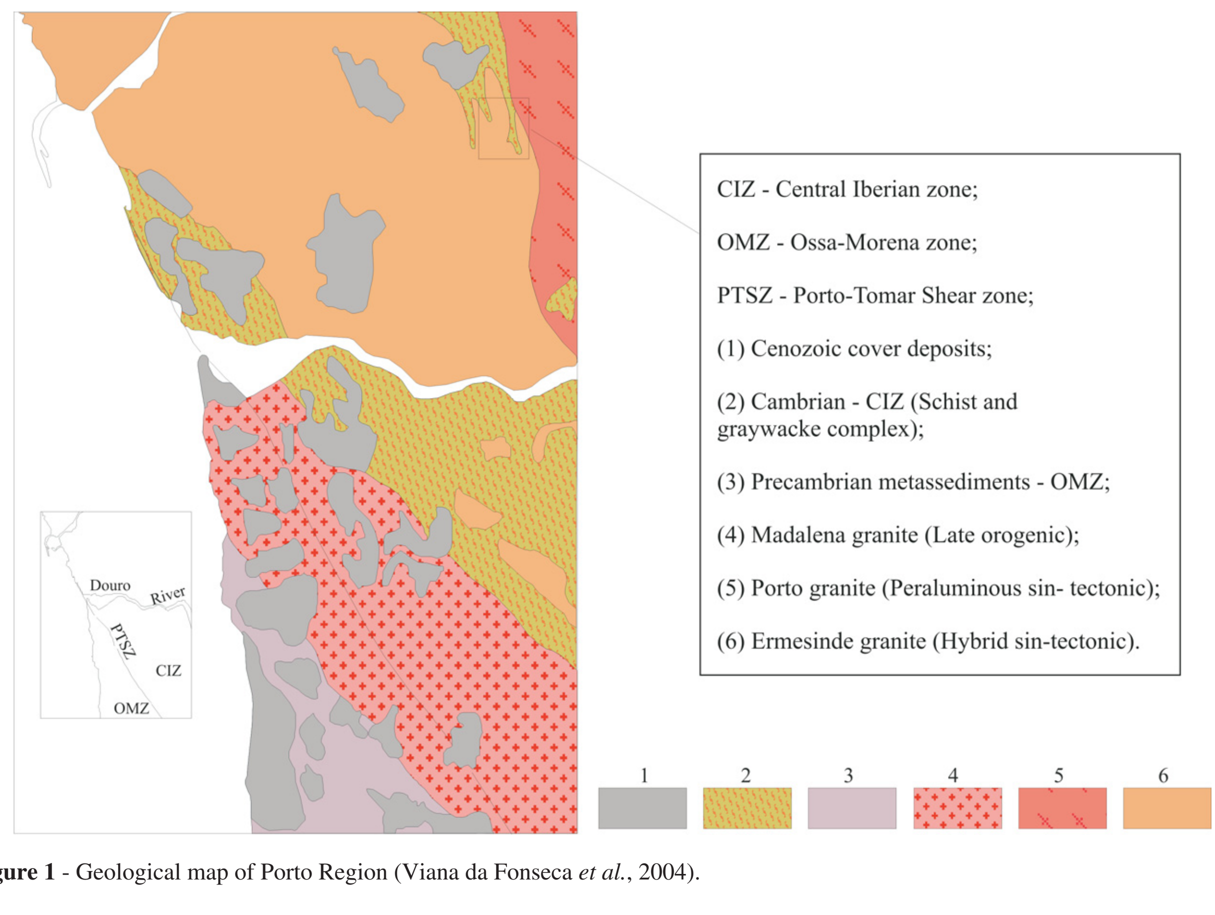

Figure 1 - Geological map of Porto Region (Viana da Fonseca *et al.*, 2004).

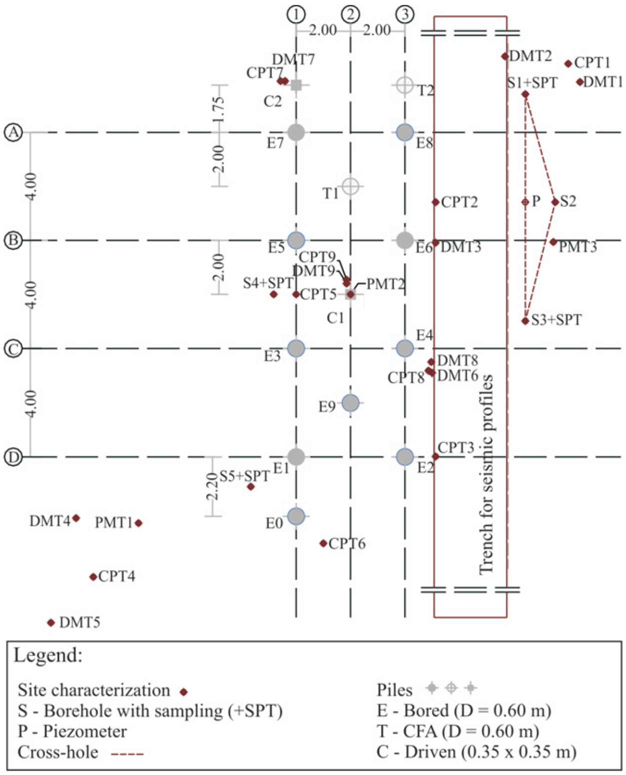

Figure 3 - Layout of the experimental site (Viana da Fonseca *et al.*, 2004).

CFA piles were installed to 6 m depth (T1 and T2) and two 350 mm square precast (C1 and C2) were precast to a depth of 6 m. Piles followed a predefined alignment and spacing between piles axis was variable but not lower than the usual recommended spacing (around three diameters).

In the static load tests, the reaction system was materialized by the eight bored and longer piles already mentioned and shown in Fig. 3 (E1 to E8 with 22 m embedded length in the soil). The test piles E9, C1 and T1 were executed with 6 m of embedded length in the saprolitic soil. Characteristics of the piles are summed up in Table 1. Details of installation of each type of pile are given in items 2.4, 2.5 and 2.6.

2.3. Load tests results

The test procedures tried to meet ISSMGE-ERTC3 (De Cock *et al.*, 2003), ASTM D 1143/94 and NBR 12.131/92 recommendations. The piles were loaded in increments with unloading cycles and for each loading stage the load was maintained until the displacement rate became less than 0.3 mm/h, with a minimum of 0.5 h and a maximum of 2 h. Maximum loads established for each pile are shown in Table 2 and load-settlement curves in Fig. 7.

2.4. Case 1 – Bored pile with temporary casing

2.4.1. Execution technique

Bored piles installed with a temporary casing are those which cause reduced soil displacement, thus, stress

Table 1 - Pile characteristics (Costa Esteves, 2005).

Piles [*]	Name	Type	Cross-section (mm)	L(m)	Longitudinal reinforcement	Transverse reinforcement	f_{ck} [***] (MPa)	f_{cm} [***] (MPa)
Reaction (tension)	E1 to E8	bored	Circular (ϕ 600)	< 12	A500 12ϕ25	ϕ12 with a 10 cm spacing	27.7	30.9
				12 < L < 22	A500 6ϕ25	ϕ12 with a 20 cm spacing		
Static (compression)	E9	Bored	Circular (ϕ 600)	6	A500 12ϕ25	ϕ12 with a 10 cm spacing	27.7	30.9
Static and dynamic (compression)	C1, C2	precast	Square (350x350)	6	A400 8ϕ16	A235 ϕ6 with a 16 cm spacing[**]	45	48
Static and dynamic (compression)	T1, T2	CFA	Circular (ϕ 600)	6	A500 12ϕ25	ϕ10 with a 10 cm spacing	44	52.6

[*] behavior of piles under dynamic compressive loading or horizontal loading will be the purpose of another study.
[**] 8 cm spacing near pile head.
[***] f_{ck} and f_{cm}: characteristic value and average value of the concrete compressive resistance.

state is slightly changed due to the installation of the drive tube. This kind of pile has the advantage of producing little soil displacement and its use is recommended when minimum reduction of movements and soil disturbance is necessary useful or even imperative. Its use is particularly recommended when the hole is supposed to be kept stable in non-cohesive, submerged soils, etc.

2.4.2. Execution information

The steel drive tube has high resistance and a 'cork-screw' around a central hollow tube to facilitate penetration (Fig. 8).

Soil penetrated in the drive tube, under static compression, with small rotations and counter rotations, is

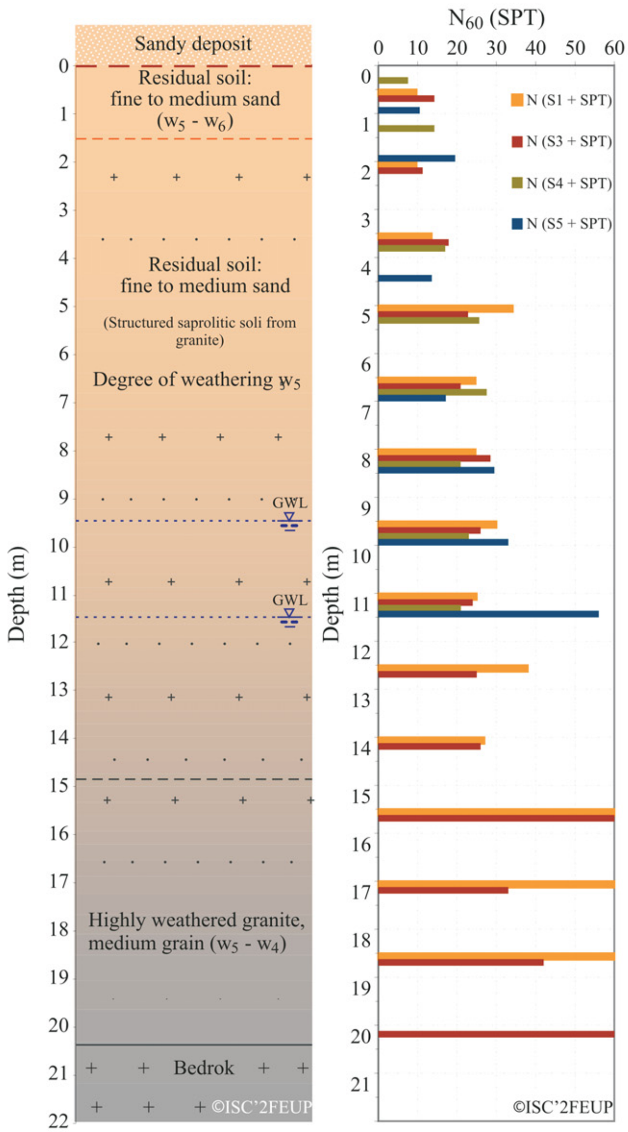

z (m)	N_{60} (SPT) S1	S3	S4	S5
0.35			8	
0.85	10	14		11
1.35			14	
1.85				20
2.35	10	11		
2.85				
3.35				
3.85	14	18	17	
4.35				14
4.85				
5.35	34	23	26	
5.85				
6.35				
6.85	25	21	28	17
7.35				
7.85				
8.35	25	29	21	29
8.85				
9.35				
9.85	30	26	23	33
10.35				
10.85				
11.35	25	24	21	56
11.85				
12.35				
12.85	38	25		
13.35				
13.85				
14.35	27	26		
14.85				
15.35				
15.85	60 (29 cm)	60 (42 cm)		
16.35				
16.85				
17.35	60 (28 cm)	33		
17.85				
18.35				
18.85	60 (26 cm)	42		
19.35				
19.85				
20.35		60 (24 cm)		
20.85				
21.35				
21.85				

Borehole S3

Figure 4 - Geotechnical profile and photos of the samples obtained in boreholes (Viana da Fonseca & Santos, 2008).

withdrawn by internal cleaning device, always maintaining the tube in an advanced position in relation to the borehole and cleaning device (Fig. 9). These piles are cast in place and the steel drive tube can be withdrawn or discarded after the pile is executed. In this case, it was withdrawn during the concreting process. The withdrawal process is also made by increasing static compression and tube rotation, but on a random basis, which influences pile shaft, as it can be seen in the final texture of the concrete.

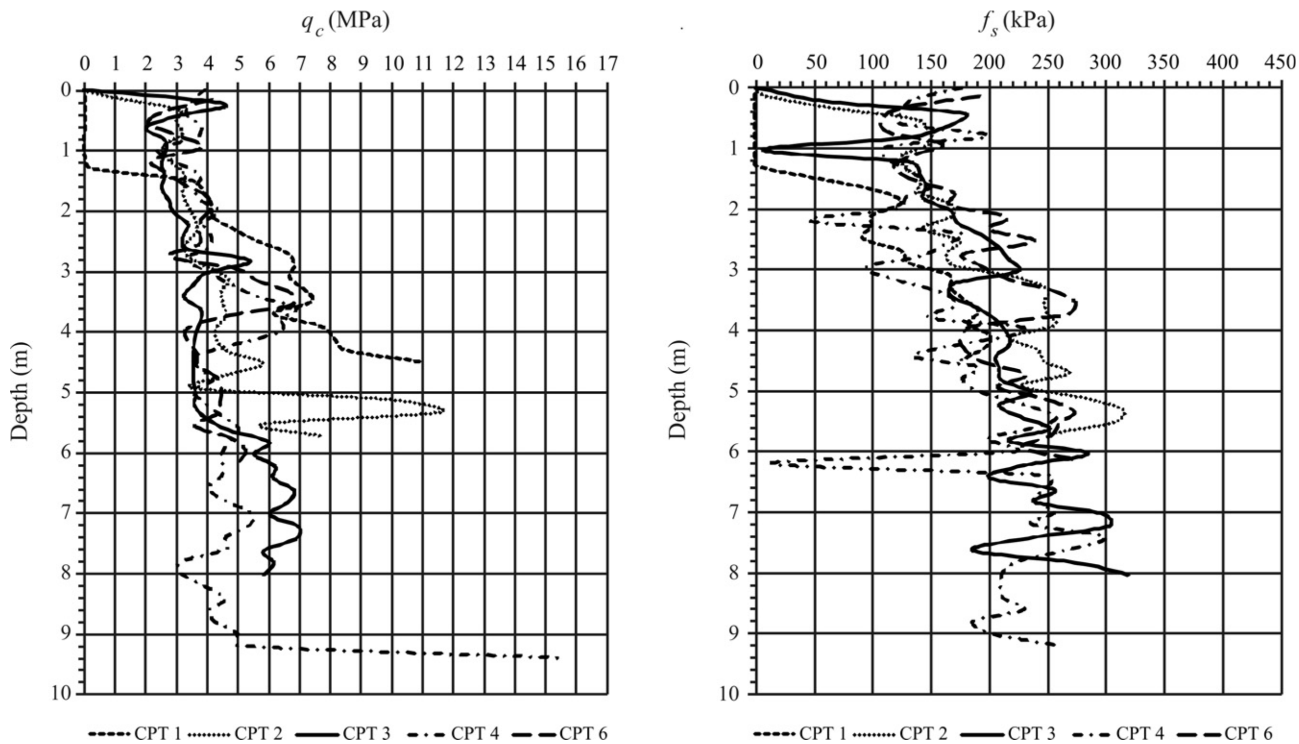

Figure 5 - Variation of q_c and f_s with depth from CPT tests (before pile execution).

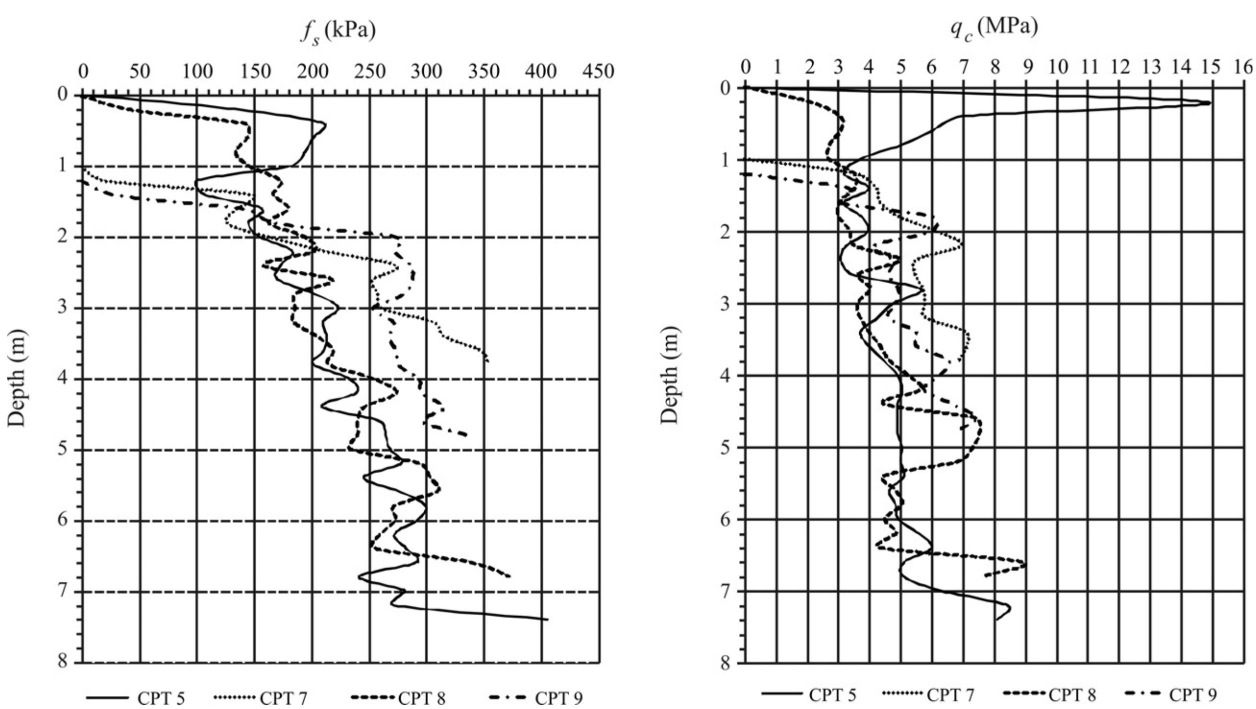

Figure 6 - Variation of q_c and f_s with depth from CPT tests (after piles execution).

As already mentioned, eight piles were used as reaction for the static loading tests; only one bored pile, E9, was tested under static compressive load, and one of these reaction piles was instrumented in order to measure lateral resistance under tension loading.

As it can be seen in Fig. 10, after removing soil from the driving tube down to a slightly higher depth (20 cm) than the final column concrete base (and with careful cleaning of the bottom), the reinforcement was installed and properly guided. Only then concreting was started, using a 'tremi' tube from the base to the top on a continuous basis

Table 2 - Load-settlement values obtained from pile load tests.

Pile	Load (kN)	Settlement (mm)
Bored – E9	900(*)	39.7
	1350(**)	155.1
CFA – T1	900(*)	10.8
	1175(**)	95.4
Precast – C1	1427	

(*)4th cycle. (**)5th cycle.

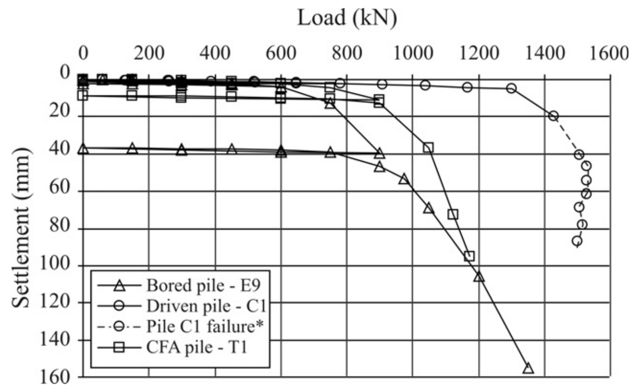

Figure 7 - Load-settlement curves from static load tests.

a) b) c)

Figure 8 - a) and b) Steel drive tube; c) Detail of the metal drive tube base (Costa Esteves, 2005).

a) b) c)

Figure 9 - Cleaning of the tube: a) and b) Borehole; c) Cleaning device (Costa Esteves, 2005).

a) b) c)

Figure 10 - a) and b) Reinforcement installation; c) Final positioning of the reinforcement (Costa Esteves, 2005).

and trying to maintain (this condition is very important) the flow of the concrete mass (Fig. 11).

2.4.3. Instrumentation

In the static axial loading tests, the load was measured using hydraulic manometers of the system and an electric load cell. Axial and transverse displacements of the pile cap were also measured in several points and with two parallel acquisition systems, assuring redundant independence which allowed to control displacements and rotations in vertical and horizontal directions, as well as the time for each measurement.

Data acquisition was automatically got with detailed temporal scanning depth.

Besides the pile cap instrumentation, six internal sensors were installed in E9 and T1 piles (Geokon *retrievable extensometer*). The sensors were inserted in PVC Hidronil tube with a 2” diameter and 6 m of length embedded in the pile. Sensors were connected to a reading unit (Geokon data logger) by an extension or electric cable from the pile cap. Figure 12 shows some details regarding the installation of the sensors and Fig. 13 shows its position in depth.

At the bottom of pile E9 a flat-jack load cell was installed with an electric cable coming up to the top of the pile to connect to the reading unit.

The load cell composed by a high resistant membrane filled with oil was placed between two 25 mm thick, 450 mm diameter steel plates. In Fig. 14b, it can be noticed that mastique was applied to avoid insertion of soil between the plates. Finally, a pressure transducer was linked to the cell (Fig. 14c).

The cell pressure measured in the static loading test multiplied with the total pile cross sectional area was assumed to correspond to the portion of applied load reaching the pile tip. In Fig. 14 (d, e, f) procedures for the installation of the already mentioned load cell are shown.

The characteristics of the pressure transducer and load cell can be seen in Table 3.

Four linear variable differential transducers (LVDT) were installed in the three studied piles with 50 mm range and 0.01 mm precision for the measurement of vertical displacements and two transducers with the same characteristics for the measurement of horizontal displacements. Simultaneously and for redundancy reasons, two mechani-

a) b) c)

Figure 11 - a) and b) Piles concreting; c) Finalized concreting (Costa Esteves, 2005).

a) b) c) d)

Figure 12 - Internal instrumentation: a) Anchor; b) Sensor c) Installation of sensors inside PVC tube; d) Sensors connections to reading unit (Costa Esteves, 2005).

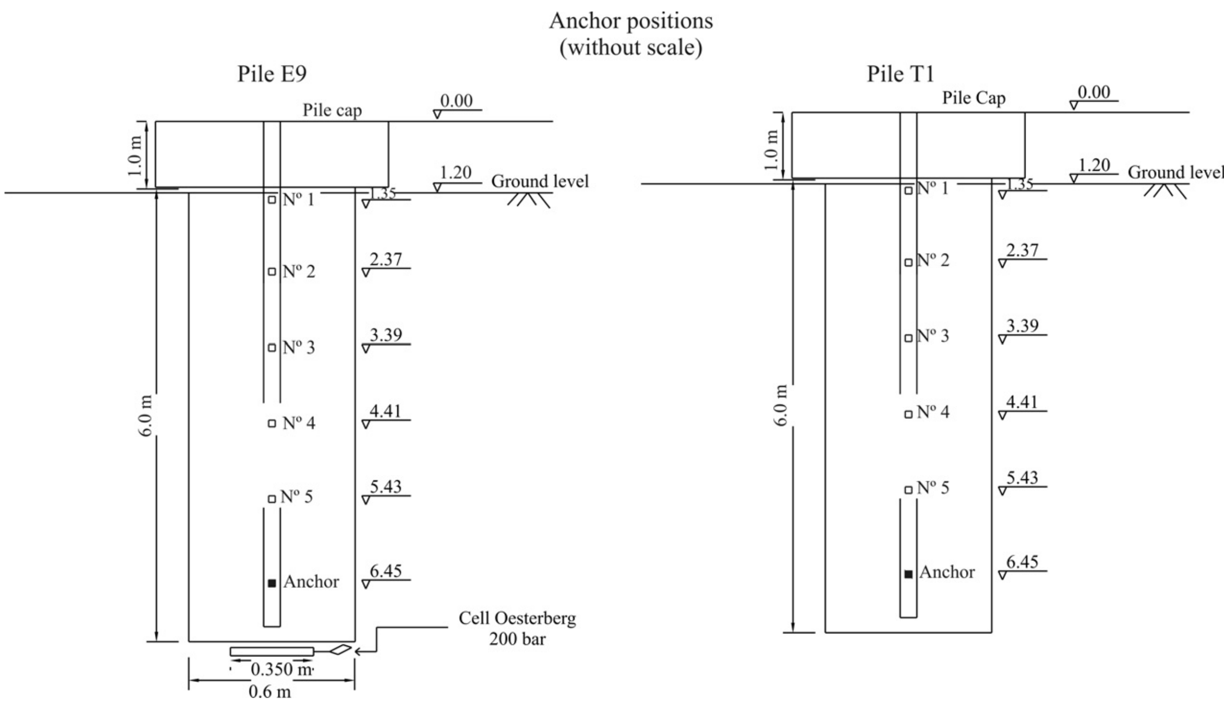

Figure 13 - Location of sensors (retrievable extensometer) (Costa Esteves, 2005).

cal dial gage devices (DG) were installed in order to check the results obtained by the electronic transducers (Fig. 15).

Converting measurements of strain to load is frequently thought to require knowledge of pile cross section and Young modulus.

The Young modulus of the pile was obtained from the slope of the strain on the instrument installed in the reference section of the pile – Level 1 (Fig. 16).

The slopes of the shortenings curves (kN/mm) are proportional to the axial stiffness, EA, of the pile. The slope corresponding to modulus value of 20 GPa is indicated under assumption that the pile diameter is equal to the nominal 600 mm value and the distance between gages points of 1020 mm.

Figure 16 shows the shortenings-load curves for each instrumented level of the bored pile.

2.5. Case 2 – CFA pile

2.5.1. Execution technique

The continuous flight auger piles (CFA) are cast in place by drilling the soil through a continuous auger, with a 'corkscrew' around a central hollow tube. After reaching the bottom level, while the auger is pulled up, the soil is replaced with concrete, pumped down through the hollow

a) b) c)

d) e) f)

Figure 14 - Load cell installation (Costa Esteves, 2005).

Table 3 - Load cell characteristics.

Pressure transducer		Load cell	
Type	Weight-resistivity	Plate diameter [m]	0.45
Range [MPa]	0-25	Load cell diameter [m]	0.35
Sensitivity to mA [MPa/mA]	1.5625	Load cell area [m^2]	0.096

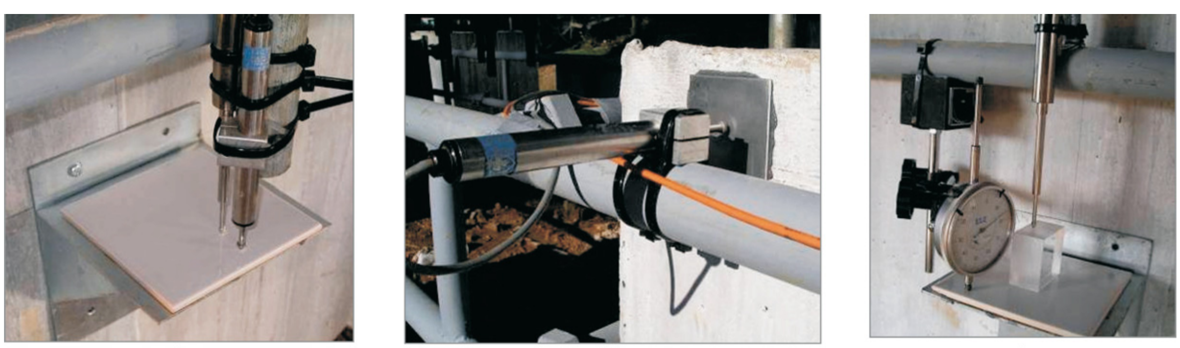

a) b) c)

Figure 15 - Pile cap instrumentation: a) and b) LVDT transducers; c) DG devices (Costa Esteves, 2005).

tube. There is a metal cap (plug) in its bottom, which opens, like a valve, by the injected concrete to prevent soil or water from entering the hollow tube. As the auger is removed, soil confined between ‘corkscrews’ is also replaced by the concrete being injected from the tip level upwards. The concrete is characterized by a mixture of small aggregate and sand with cement (minimum consumption of 400 kg/m^3) and a value of slump of 190 mm, following prescriptions from The Brazilian Association of Foundations Companies Procedures Manual (ABEF, 1999). The advantages of using this type of pile are: reduced work schedule; applicability in rather diversified classes of terrains (except for rocks or soils with boulders); lack of disturbances and low vibration level in terrain, in opposition to percussion driving

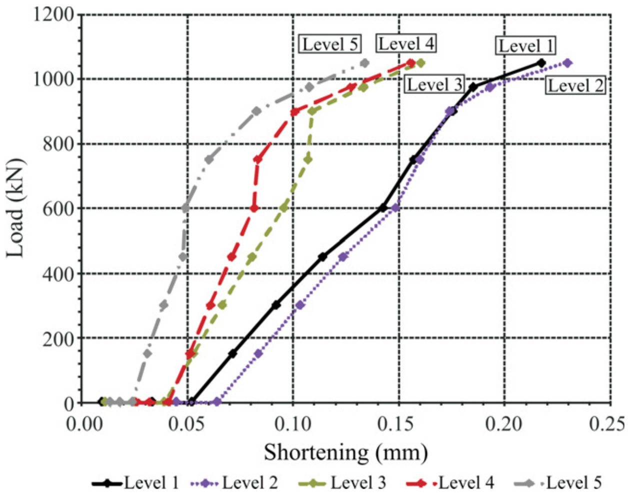

Figure 16 - Shortening-Load curves (bored pile).

techniques; and, absence of soil decompression and contamination when bentonite or other slurries are used. Disadvantages are associated to the need for a plain terrain allowing the equipment to move easily; the demand for a concrete plant close to the work; the need of a shovel loader for soil cleaning and removal, extracted during the drilling; the demand for a minimum volume of piles to justify the equipment mobilization in cost-benefit optimization; and, last but not least, the limitation of pile length and reinforcement, which may be considered determinant in certain projects. The production process must receive special attention, especially for shaft continuity control and subsoil disturbance on drilling. It is also important to observe that, in weak soils, concrete injected with high pressure may lead to soil rupture and high consumption. In these situations pressure is due to be moderate and thoroughly controlled by experience. Another important advantage of CFA piles is the possibility of continuous electronic monitoring, providing pile execution monitoring, which will be easily accessed and allow an eventual correction. The following parameters are registered: date and time; digging depth; penetration speed; torque; concrete volume and pressure; pile diameter; and pile extraction velocity.

2.5.2. Information on execution

Three CFA piles with 0.60 m diameter and 6 m depth were executed. Twelve reinforcing bars 25 mm diameter ($\cong$ 59 cm^2) and 6 m length were used. Stirrups with 10.0 mm of diameter, spaced in 10 cm completed the reinforcements. The concrete resistance (fck) was 44.0 MPa.

2.5.3. Instrumentation

In this item, the data obtained from the pile instrumentation are presented. Five retrievable extensometers were installed at depth as previously described and according to Fig. 13.

The slope corresponding to modulus value of 40 GPa is indicated under assumption that the pile diameter is equal to the nominal 600 mm value and the distance between gages points of 1020 mm.

Figure 17 shows the shortenings-load curves for each instrumented level and loading cycle.

2.6. Case 3 – Precast pile

2.6.1. Execution technique

The precast pile was installed by impact percussion and it is included in the group named 'displacement piles'. Precast piles can be made of reinforced and pre-stressed concrete compacted by vibration or centrifugation. The main disadvantage of concrete precast piles is the difficulty of adapting to unpredicted soil variations. If pile length is not carefully studied, an amendment or cut will be necessary, which will interfere on the costs and schedule for job execution. When precast, these piles cause vibrations and may cause soil compaction. They need to be reinforced in order to resist to bending moments originated from lifting and transportation, driving and lateral forces from the supported structure (Fig. 18).

2.6.2. Information on execution

Driven precast concrete piles were made under rigorous control of materials, resulting in high quality reinforced concrete. The equipment used for driving the precast piles was a 40 + 10 kN hydraulic hammer. The pile had a square cross-section (350 mm x 350 mm) and was precast down to the desired depth to an embedded length of 6 m. After driving, the pile was cut off to the desired level.

3. Analysis of Data Obtained From Instrumentation

As stated before, bored and CFA piles were instrumented along the depth, with installation of retrievable sensors. A flat-jack load cell was inserted at the bottom of the

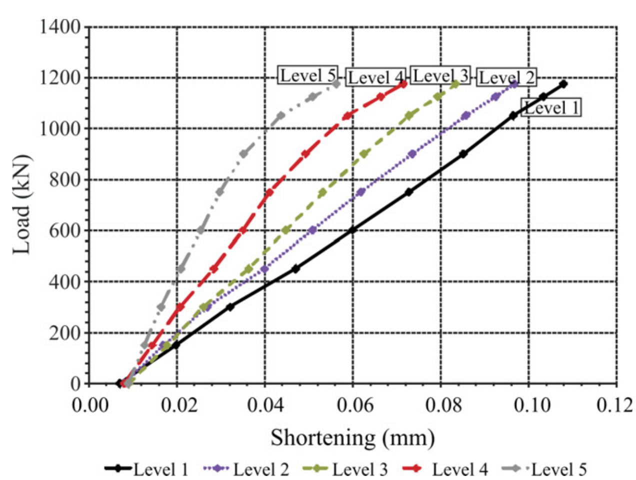

Figure 17 - Shortening-Load curves (CFA pile).

a) b)

Figure 18 - Precast pile: a) Positioning b) Driving (Costa Esteves, 2005).

bored pile. The evaluation of extensometer measurements for piles E9 and T1 to load distributions indicated apparent values of shaft and tip resistances. However, residual loads were present in the piles before the static test. This effect is much more important for the driven pile C1. The analysis of axial loaded pile response can be made from diverse methods. Analysis based on soil parameters determined in laboratory or in situ tests rely on simple total stress (alpha) or effective stress (beta) methods, or on more sophisticated numerical finite element method.

The data obtained in this experimental site was analyzed by Fellenius *et al.* (2007) and Viana da Fonseca *et al.* (2007). Fellenius *et al.* (2007) used the beta-method and special preference was given to analysis based on CPTU data, for its continuous and representative scanning of the ground spatial variations. Viana da Fonseca *et al.* (2007) used a mathematical model developed by Massad & Lazo (1998) and Marques & Massad (2004), called "Modified Two Straight Lines Method" for rigid or short piles.

These analyses provided similar and consistent results regarding the mobilized lateral and tip resistances. For the bored and CFA piles the maximum load at each pile head are from a settlement of about 100 mm, chosen to ensure that both piles are evaluated at the same pile settlement. Table 4 summarizes the values obtained by Fellenius *et al.* (2007) and Viana da Fonseca *et al.* (2007).

The estimated unit shaft resistance was about 60 kPa and the applied load reaching the bored and CFA piles tip was 42%. The driven pile although having a smaller cross-section (43.3%) showed a stiffer response and higher resistance than the other two piles, which are a clear indication of installation effects and its importance in the pile response.

4. Evaluation of Piles After Removal of Soil

In order to inspect the geometrical characteristics of the executed piles and to confirm their integrity, phased excavation of the soil around the piles was carried out, aiming not only at obtaining a good visual characterization but also successive samples of blocks for laboratory testing. This was done up to approximately 6 m depth. For this removal, a study had to be conducted on the possible ways of extraction, since this is a complex and expensive process. Following, all the excavations steps are described.

To remove the piles, it was necessary, as already mentioned, to excavate the surrounding soil. This excavation should be phased, not only to avoid risks associated with instability of excavation ramps but also to enable pile removal with minimum possible damage.

For pile removal, the selection of the retro-excavator to be used (arm length and capacity) was carefully made, considering the weight and the length of all elements (piles and cap block). In Fig. 19, the beginning of excavation is shown with the chosen retro-excavator, with a 6 m length arm.

Two distinct situations were considered in this process: one regarding the removal of the 6 m long piles and the other removal of 22 m long piles to avoid any interference with future constructions in the area. Although it would be interesting to remove all the piles, this was not considered necessary, since the deepest objects would not affect future constructions. Thus, the 6 m long piles were removed as a whole while the others were cut-off approximately at the 5 m portion (from soil level) and then removed. Figure 20 shows the schematic procedure utilized to remove the 6 m long piles and Fig. 21 shows the adopted procedure for the 22 m long piles.

After pile removal, relevant geometrical characteristics were measured after properly cleaning the piles from existing soil in the shaft length. It was observed that geometrical characteristics for bored and CFA piles diameters

Table 4 - Load Distribution for 100 mm pile head settlement.

Pile	Viana *et al.* (2007)			Fellenius *et al.* (2007)		
	Q_l (kN)	Q_p (kN)	Total load (kN)	Q_l (kN)	Q_p (kN)	Total load (kN)
E9 (Bored)	696	481	1177	700	500	1200
T1 (CFA)	703	499	1202	700	500	1200
C1 (Precast)	511 to 1021	1004 to 494	1515	520	980	1500

a) b) c)

Figure 19 - Excavation: a) beginning of job; b) c) steps for soil removal (Costa Esteves, 2005).

a) b) c) d) e) f)

Figure 20 - Pile extraction (6 m): a) beginning of excavation; b) and c) and d) removal of pile from the soil; e) transportation of pile to the warehouse; f) general view of the pile after removal (Costa Esteves, 2005).

were slightly higher than the initial nominal diameter (605 mm and 611 mm, respectively).

It is important to highlight that the shaft surface of CFA piles was smoother than the bored pile executed with temporary casing (Fig. 22) and that the last 20 cm to 30 cm of the bored piles showed a significantly reduced diameter, reaching 12% of reduction in pile E9 (525 mm), as it can be seen in Fig. 23.

As reported in item 2.4.2, removal of drive tube in bored piles is made by ascending static pressure and tube rotation, but on a random basis, which does not promote a perfectly smooth shaft texture in bored piles, as shown in Fig. 22.

This study on pile removal also enabled to check conditions of the load cell utilized at the base of pile E9. The load cell was well positioned at the pile base, as seen in Fig. 24.

5. Comparison with Results Obtained in the EF-Unicamp

Based on the results presented in Part 1 of this paper, the following observations are made:

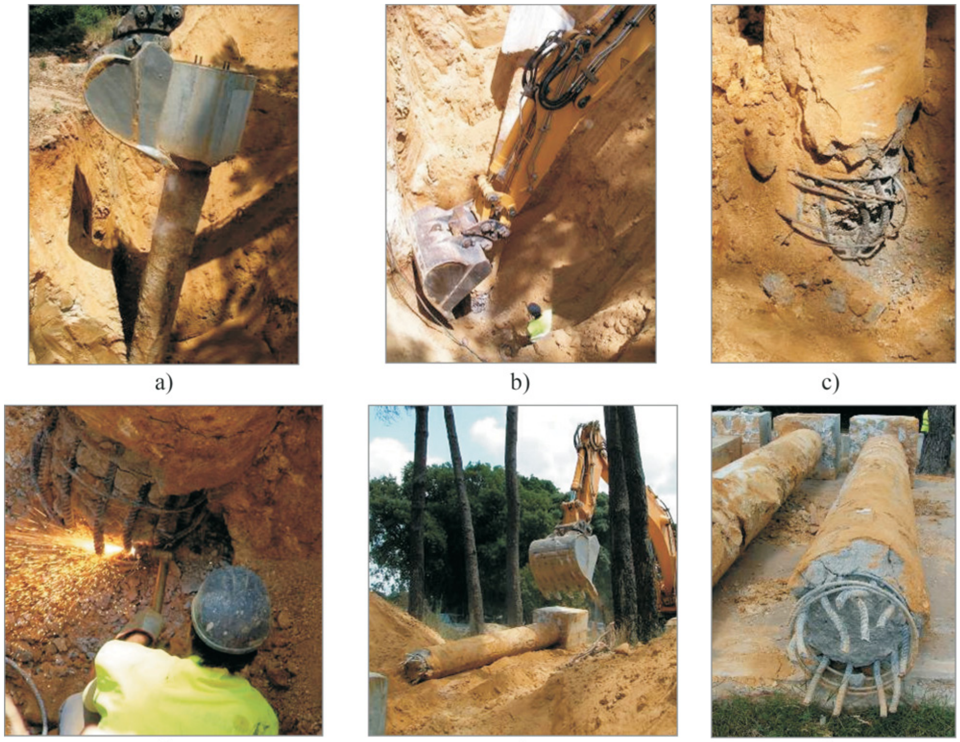
a) b) c)
d) e) f)

Figure 21 - Pile extraction (22 m): a) and b) pile cut-off at portion 5 m; c) and d) detail of the cut pile e) removal of pile from the soil; f) general view of the pile after removal from the soil (Costa Esteves, 2005).


a) b)

Figure 22 - Detail of pile shaft texture: a) bored; b) CFA (Costa Esteves, 2005).

Figure 23 - Bottom of the bored pile E9 (Costa Esteves, 2005).

As for piles executed at the Experimental site of FEUP, it was found that, unlike pile behavior at the Experimental site of Unicamp, the tip of the piles absorbed high loads of around 29% for bored and CFA piles, at Unicamp the average values were about 2% and 7% for bored and CFA piles.

This difference between the values obtained for load absorption at the tip in both experimental fields is explained by the difference between the two soils, which have distinct genesis and resistance. While the pile tip region at the Experimental Site of Unicamp has N_{SPT} average values of 10 blows and cone resistance of 2 MPa, in the EF-FEUP, average N_{SPT} values of 25 blows and cone resistance of 4 MPa are found.

In the site of EF-FEUP, both CFA and bored piles behaved similarly in terms of lateral friction. The same happened to the CFA and bored piles in the EF-Unicamp.

Two different techniques were utilized for instrumentation of pile shafts; the process executed by Unicamp researchers was a rather ‘handicraft’ one, while the one used by FEUP's researchers utilized electric removable extensometers manufactured by a specialized company. Equipment installation techniques on piles were very similar, *i.e.*, from insertion of the tube in piles. In spite of utilizing distinct techniques, it was observed that both techniques are

Figure 24 - Load cell and the pile base (Costa Esteves, 2005).

good in terms of measuring load distribution in a deep foundation.

6. Conclusions

From the assessment of results obtained from the performed tests, the following conclusions can be drawn:

Based on the results obtained from the bored and CFA piles, it seems that the execution process of CFA pile did not provide differences on behavior regarding shaft resistance of this type of foundation, which means, it behaved as a bored pile.

Regarding the tip resistance results obtained from CFA and bored piles, both showed similar values, but soil on CFA pile tip was less disturbed, while in the bored pile the soil gradually became stiffer as successive loadings occurred.

After the loading tests the piles were extracted and inspected. The pile surfaces were smooth and the actual diameter of piles was very close to the nominal value.

Evaluation of extensometer measurements for piles E9 and T1 to load distributions indicated values of shaft and tip resistances. However, residual loads were present in the piles before the static test, for which the actual magnitude was estimated after trial-and-error back-analysis. The estimated unit shaft resistance was about 60 kPa and the applied load reaching the pile tip was 42%.

The precast pile C1 although having a smaller cross-section showed a stiffer response and higher resistance than the other two piles. This is a clear indication that the installation effects play an important role in the pile behavior. In this case, the pile driving process should have induced significant changes in the surrounding soil affecting the shaft resistance and inducing residual loads.

References

American Society of Civil Engineers (ASTM) (1994) D 1143-81: Piles under static axial compressive load. Standard test method. In: Annual Book of ASTM Standards, Philadelphia, v. 04.08, pp. 96-106.

Associação Brasileira de Empresas de Fundações (ABEF) (1999) Manual de Especificações de Produtos e Procedimentos, 2ª ed. ABEF, São Paulo, 282 pp.

Associação Brasileira de Normas Técnicas (ABNT) (1992) NBR 12131: Estacas: Prova de Carga Estática. Rio de Janeiro.

Costa Esteves, E. (2005) Ensaios e Análise de Resposta de Estacas em Solo Residual do Granito sob Acções Verticais. MSc Thesis, Faculdade de Engenharia, Universidade do Porto, Porto, 322 pp.

De Cock, F.; Legrand, C. & Huybrechts, N. (2003) Axial static load test (ASPLT) in compression or in tension – Recommendations from ERTC3-Piles, ISSMGE Subcommittee. Proc of the XIII ECSMGE, Prague. v. 3, pp. 717-741.

Fellenius, B.H.; Santos, J.A. & Viana da Fonseca, A. (2007) Analysis of piles in a residual soil – The ISC'2 prediction. Canadian Geotechnical Journal, v. 44, p. 201-220.

Marques, J.AF. & Massad, F. (2004) Provas de carga instrumentadas com bulbos, executadas na região praieira de Maceió, Alagoas. Solos e Rochas, v. 27:3, p. 243-260.

Massad, F. & Lazo G. (1998) Método gráfico para interpretação da curva carga-recalque de provas de carga verticais em estacas rígidas ou curtas. Anais do XI Congresso Brasileiro de Mecânica dos Solos e Engenharia Geotécnica, Brasília, v. 3, pp. 1407-1414.

Viana da Fonseca, A.; Carvalho, J.; Ferreira, C.; Tuna, C.; Costa Esteves, E. & Santos, J.A. (2004) Geothecnical characterization of a residual soil profile: the ISC'2 experimental site. Proc. ISC'2 Geothecnical and Geophysical Site Characterization, Rotterdam, v. 2, pp. 1361-1369.

Viana da Fonseca, A.; Santos, J.A.; Costa Esteves, E. & Massad, F. (2007) Analysis of piles in residual soil from granite considering residual loads. Soils and Rocks, v. 30:1, p. 63-80.

Viana da Fonseca, A. & Santos, J.A. (2008) International Prediction Event. Behaviour of Bored, CFA and Precast Piles in Residual Soil. ISC'2 Experimental Site. University of Porto and Tech. Univ. of Lisbon, Porto and Lisbon, 699 pp.

Evaluation on the Use of Alternative Materials in Geosynthetic Clay Liners

P.M.F. Viana, E.M. Palmeira, H.N.L. Viana

Abstract. Geosynthetic clay liners (GCL) have been increasingly used in barrier systems of waste disposal areas and in hydraulic works. However, sometimes they are discarded as possible barrier solutions in these works because of their greater costs in comparison with other solutions (geomembranes or compacted clay liners). This paper presents a laboratory study to investigate the technical feasibility of mixing alternative materials to bentonite for the production of alternative low cost GCLs. The alternative materials used were sand, clay and tire grains. Direct shear, consolidation, and expansibility tests were carried out on bentonite mixtures with varying percentages in mass of the alternative material. Ramp tests and expansibility tests were also performed on alternative GCLs manufactured with these types of mixtures. The results obtained showed that the presence of the alternative materials in the bentonite increased the shear strength and the permittivity of the mixture and reduced its expansibility. The tests on the bentonite-tire grains mixtures suggest that alternative GCLs manufactured with this type of mixture may be used in less critical barrier systems (particularly under high stress levels) and as bedding/protective layers underneath geomembranes, also providing a better use for wasted tires in environmental terms.

Keywords: GCL, alternative materials, laboratory tests, ramp tests.

1. Introduction

Geosynthetic Clay Liners (GCLs) are relatively thin geosynthetic products used as barriers in hydraulic and waste disposal works. They consist of a layer of bentonite enveloped by geosynthetic layers (usually geotextiles). Variations are possible, like products consisting of a layer of bentonite on a geomembrane (Koerner, 2005).

The use of GCLs as barriers in environmental protection projects has increased markedly in the last decade, mainly due to its low hydraulic conductivity (typically $\leq 10^{-11}$ m/s), easy and quick installation, self-healing capacity in case of damage during installation and good overall performance. Several works can be found in the literature reporting successful applications of GCL in environmental protection works (Reuter & Markwardt 2002, Didier & Nassar 2002, Rowe & Orsini 2003 and Shan & Chen 2003, Touze-Foltz *et al.*, 2006).

Hydraulic conductivity is a major factor to be considered when using GCLs in hydraulic and environmental projects. The low permeability of the bentonite guarantees a satisfactory performance as a barrier if damages during transport of the product to the job site and installation are avoided or minimised. In this sense, the self-healing capacity of GCLs is a great advantage in comparison to other barrier systems. Shan & Daniel (1991) and Sivakumar Babu *et al.* (2001) have shown that cracks in a GCL, as a consequence of a dry period, were closed in a subsequent wetting period, without compromising its barrier function. Expansion of the GCL due to hydration may increase its thickness significantly, depending on the stress level on the GCL, reducing even further its permittivity. Permittivity (ψ) values of GCLs are typically lower than 10^{-9} s^{-1}.

Besides low hydraulic conductivity and self-healing capacity, the internal shear strength of GCLs products is of utmost importance in the design of lining systems on slopes, because of the low shear strength of bentonite, particularly when hydrated. The internal shear strength of a GCL depends on the bentonite shear strength and on the strength of the fibres used to fix its cover and carrier layers, as well as on the manufacturing process used (stitching or needle-punching). Chiu & Fox (2004), Fox & Stark (2004) and Viana & Palmeira (2009) discussed the importance of the internal shear strength of GCLs and how it can be severely reduced due to hydration. However, the internal shear strength of GCL products can be markedly increased depending on how they are manufactured and on the mechanical strength of the fibres used to fix the geotextile cover layers (Bouazza, 2002, Bouazza & Vangpaisal, 2007, Müller *et al.*, 2008).

Some materials can be mixed to the bentonite as a way to reduce the GCL cost, improve some of its relevant properties and, in the case of waste materials, to provide a better and more environmentally friendly destination of such materials (Viana & Palmeira 2008, Viana & Palmeira 2009, Ikizler *et al.* 2009). For instance, the mixture of fine sand to the bentonite can increase its internal shear strength and resistance against perforations and cuts, without compromising its low hydraulic conductivity. However, the manufacturing process and costs may be influenced by the presence of sand mixed to the bentonite. Besides, the

P.M.F. Viana, DSc., Associate Professor of Civil Engineering, Departamento de Engenharia Civil, Universdade de Goiás, Anápolis, GO, Brazil. e-mail: paulo.viana@ueg.br.
E.M. Palmeira, PhD., Professor of Civil Engineering, Departamento de Engenharia Civil e Ambiental, Universidade de Brasília, Brasília, DF, Brazil. e-mail: palmeira@unb.br.
H.N.L. Viana, DSc., Geotechnical Engineer, Secretaria de Infra-Estrutura Hídrica, Ministério da Integração Nacional, Brasilia, DF, Brazil.
Submitted on May 17, 2010; Final Acceptance on November 3, 2010; Discussion open until August 31, 2011.

expansibility, and by so the permittivity, of the alternative GCL may be affected because of the addition of a non expansive material and this should be properly evaluated.

This paper examines the influence of adding non conventional materials to bentonite to form alternative and low cost GCLs and the repercussion of the addition of these materials on the hydraulic and strength properties of the GCLs. Two commercially available conventional GCLs were used as references for comparisons. Small and large scale laboratory tests were performed in this study and the experimental methodology and results obtained are presented and discussed in the following sections.

2. Experimentals

2.1. Materials used in the experiments

2.1.1. Bentonite

A sodic bentonite (code BTN), produced by Bentonit Nordeste Ltd., Brazil, was used in the tests and its main properties are summarized in Table 1. X rays diffractometry tests showed that the bentonite was predominantly composed by sodium montmorillonite with some illite, calcite and quartz.

2.1.2. Materials used in the bentonite mixtures

Three materials were mixed to the bentonite (BTN) to form the alternative GCL products. These materials were a fine sand (code SND), a clay (kaolinite, code CLY) and tire grains (code TG) from wasted automobile tires. Table 2 presents the main properties of these materials. Figure 1 shows views of the materials mixed to the bentonite.

Table 1 - Physical properties of the bentonite used in laboratory testing.

Grain unit weight (kN/m^3)	26.60
Liquid limit (%)	381.0
Plastic limit (%)	133.0
Plasticity index (%)	248.0
Initial water content (%)	14.0%
Minimum dry unit weight (kN/m^3)	7.3

*Chemical composition: 60.2% de SiO_2, 18.5% Al_2O_3, 7.2% Fe_2O_3, 2,5% de Na_2O, 2.4% de CaO, 2.0% MgO e 0.53% K_2O.

2.1.3. GCLs tested

Two commercially available GCLs (codes GCLA and GCLB) manufactured with sodic bentonite and three

Table 2 - Physical properties of the materials used in the tests.

Property	Sand	Clay	Tire grains
D_{10} (mm)[1]	0.08	0.02	0.12
D_{60} (mm)	0.25	0.07	0.48
D_{85} (mm)	1.00	0.08	0.60
Particle unit weight (kN/m^3)	26.8	28.2	11.5
CU[2]	3.10	3.50	4.0
Friction angle (degrees)	34[3, 4]	34.1[6]	23[3,7]
Cohesion (kPa)	-	6.14[5,6]	-
Maximum void ratio	0.93	-	-
Minimum void ratio	0.63	-	-
Liquid limit (%)	-	36	-
Plastic limit (%)	-	26	—
Optimum moisture content (%)[8]	-	23	—
Maximum dry unit weight (kN/m^3)[8]	16.3	14.9	4.9
Percentage of carbon (%)	-	-	> 80

Notes: (1) D_n - diameter for which n%, in mass, of the remaining soil particles are smaller than that diameter; (2) Coefficient of uniformity (= D_{60}/D_{10}); (3) Friction angle obtained in direct shear tests for a stress level ranging from 15 kPa to 200 kPa (4) For a sand unit weight of 16.3 kN/m^3; (5) From drained direct shear tests for a stress level ranging from 15 kPa to 200 kPa; (6) Under optimum moisture conditions (clay dry unit weight of 14.9 kN/m^3); (7) For a tire grains unit weight of 4.9 kN/m^3; (8) Normal Proctor compaction energy.

(a) (b) (c)

Figure 1 - Materials mixed with the bentonite to produce the alternative GCLs: (a) Tire grains (TG); (b) Sand (SND) and (c) Clay (CLY) - 50x enlargement.

alternative GCLs with cores consisting of mixtures of bentonite with sand, clay or tire grains were tested. The alternative GCLs had cores consisting of 50% (in mass) of the alternative material (sand – code GCL-SND, clay – code GCL-CLY or tire grains – code GCL-TG). This percentage of alternative material was adopted based on results of tests performed with varying percentages of alternative materials that will be presented and discussed later in this paper. Table 3 summarises the main properties of the GCLs tested.

The alternative GCLs using cores with different mixtures of bentonite, sand, clay and tire grains were manufactured in the laboratory. Woven and a nonwoven geotextiles, whose main properties are listed in Table 4, were used as carrier and cover layers of these GCLs, as in conventional products. The geotextiles were stitch-bonded to form the GCL with 25 mm spacing between stitch-bonding rows, as shown in Fig. 2. Initially, a study on the influence of the stitching process was carried out, with products being manufactured with spacing between stitches equal to 2 mm, 4 mm and 8 mm. Based on this study, the 8 mm spacing was adopted for the manufacture of the GCL specimens that were subjected to expansibility and inclined plane tests.

2.2. Equipment used in the experimental programme

2.2.1. Expansion test cells

Free expansion tests on bentonite-alternative materials and on alternative GCLs were carried out for the evaluation of the influence of the type of bentonite mixture used on the product's expansibility potential. Figure 3 shows the equipment used in these tests. Each GCL specimen, 100 mm in diameter, was accommodated in the testing cell with natural moisture content. The specimen was then inundated for 96 h without any confinement and its vertical expansion was measured with dial gauges until readings stabilisation.

2.2.2. Consolidation and hydraulic conductivity tests

Consolidation and hydraulic conductivity tests under confinement on bentonite mixtures and on the alternative materials described above were performed using a standard soil consolidation testing cell. The GCL specimens were 75 mm in diameter, 20 mm thick and during the tests were subjected to normal stresses up to 200 kPa. Initially, the specimens were hydrated under a vertical stress of 5 kPa for 48 h. This period of time was adopted based on results from preliminary tests that showed that to be sufficient for mixture expansion stabilisation. After specimen expansion had been completed, the loading stages were applied, as in conventional one-dimensional soil consolidation tests. At the end of each loading stage the hydraulic conductivity of the mixture was assessed by performing a variable water head test using ports connected to the cell ends.

Table 4 - Properties of the geotextiles of the GCLs.

Property	Woven	Nonwoven
Polymer type	Polypropylene	Polypropylene
Mass per unit area (g/m^2)	110	350
Tensile strength (kN/m^2)$^{(1)}$	10/10$^{(2)}$	17/14$^{(2)}$
Filtration opening size (μm)$^{(3)}$	NA$^{(5)}$	1.2 x 10^{-5}
Permittivity (s^{-1})$^{(4)}$	NA	1.31

Notes: (1) Wide-strip tensile tests according to ASTM D4595; (2) Number on the left is the tensile strength along the warp direction while number on the right is the tensile strength along the weft direction; (3) According to NF EN ISO 12956; (4) According to ASTM D4491; (5) Not available.

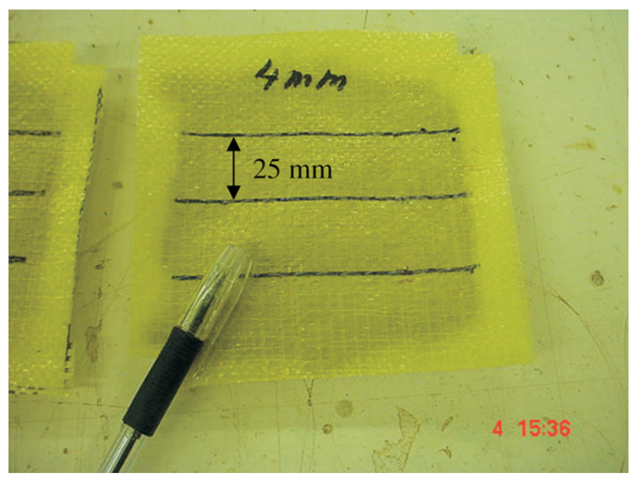

Figure 2 - Alternative GCL product.

Table 3 - Properties of the GCLs used in the tests.

Property	GCLA	GCLB	GCL-SND	GCL-CLY	GCL-TG
Bentonite type	sodic	sodic	sodic	sodic	sodic
Core dry minimum density (kN/m^3)	7.3	7.3	10.6	9.2	6.1
Thickness (mm)	6-7	6-7	6-7	6-7	6-7
Mass per unit area (g/m^2)	5000	4500	6858	5948	3965
Moisture content (%)	13.6	13.4	12.7	12.7	8.6
Manufacturing process	Stitch bonded	Needle punched	Stitch bonded	Stitch bonded	Stitch bonded

Note: The percentage (in mass) of sand, clay and tire grains in GCL-SND, GCL-CLY and GCL-TG, respectively, was equal to 50%.

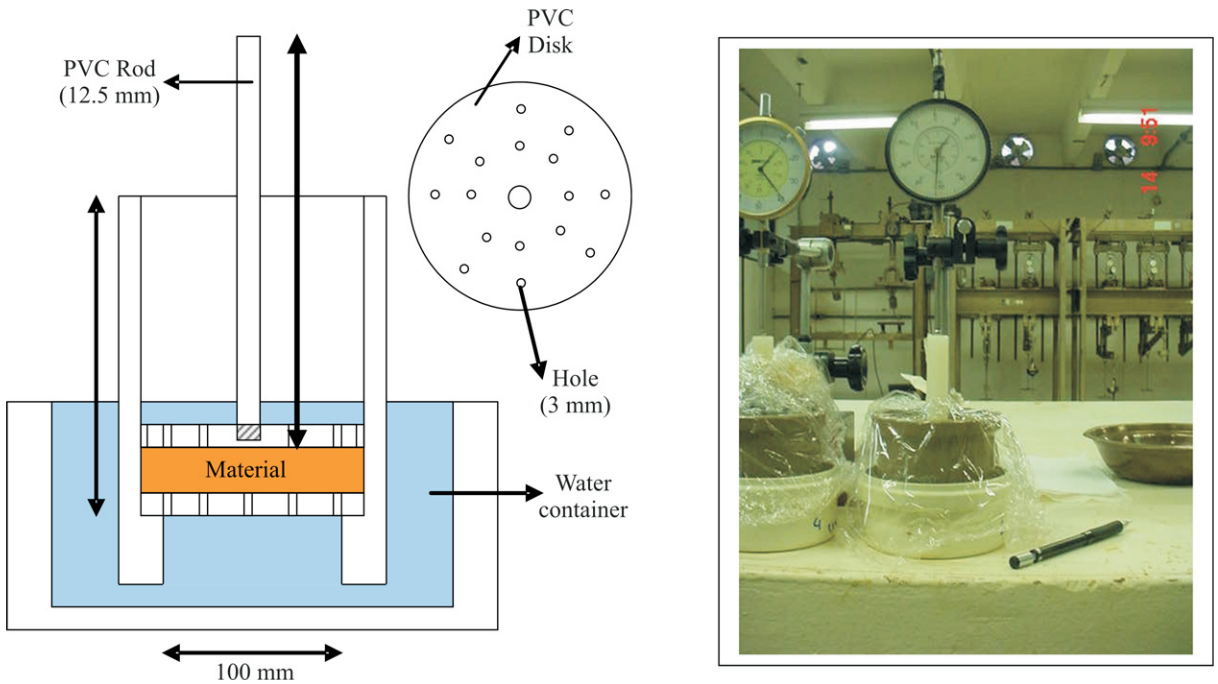

Figure 3 - Free expansion test apparatus.

2.2.3. Direct shear tests

Conventional direct shear tests were performed on the bentonite mixtures used in the experimental programme. The dimensions of the specimens tested in the conventional direct shear apparatus were 100 mm x 100 mm. Dry (under natural moisture content) bentonite mixtures were tested under minimum dry unit weight condition (loosest state) using a test speed of 0.3 mm/min. Tests on hydrated mixtures were also carried out after a period of 48 h of specimens submersion in water. A test speed of 0.03 mm/min was used for the hydrated specimens (ASTM D 6243). Vertical stresses up to 200 kPa were applied to the specimens during the tests and the procedure used was that used in conventional soil direct shear tests. Post-test investigations included assessing the shear zone at the specimen mid-height. Figure 4 shows the region of the shear zone in one of the specimens after the end of the test.

2.2.3. Ramp tests

The ramp (inclined plane) test equipment used (Fig. 5) is capable of testing GLC specimens with dimensions up to 0.6 m x 2.2 m. In this equipment the specimen can be fixed to the ramp along its entire length or to have one end anchored to the ramp (Palmeira *et al.* 2002, Palmeira & Viana 2003, Palmeira 2009, Viana & Palmeira 2010). The latter case was the one adopted in the present work. In the series of tests described in this work the dimensions of the specimens tested were 0.6 m (width) x 1.0 m (length). Tests with normal stresses up to 10 kPa were carried out. The interface between the GCL specimen and the smooth metal ramp surface was lubricated with double layers of plastic films and grease to minimise friction along this interface. Concrete blocks accommodated in a rigid box were used to provide vertical stresses on the GCL specimen. Displacement transducers allowed for the measurement of the displacements of this box during the tests and a load cell fixed to the anchored GCL end measured the tensile forces mobilised in the specimen. In these tests the upper geotextile layer was cut and only the bottom one (carrier layer) was anchored to the ramp extremity. This procedure was adopted to favour internal failure of the GCL. Tests on dry and on hydrated GCL specimens were carried out. For the latter case a water filled container was installed on the ramp for the hydration of the specimen prior to testing.

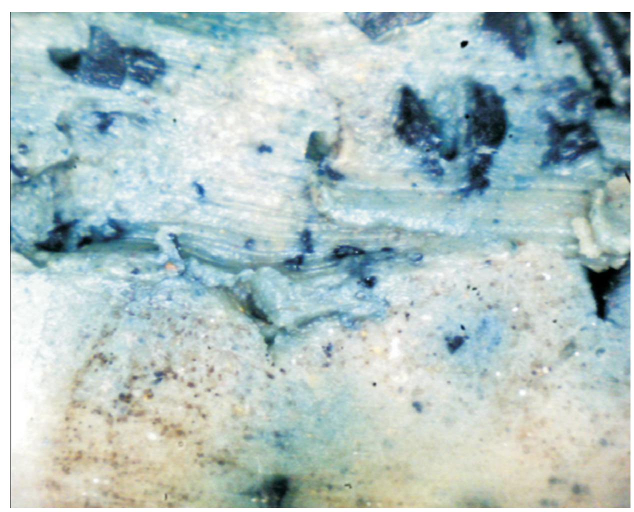

Figure 4 - Shear zone region in a test on GCL-TG 50% (50% in mass of tire grains) at the end of a direct shear test.

Figure 5 - Large scale ramp test equipment.

3. Results Obtained

3.1. Tests on bentonite mixtures

Direct shear, expansion and consolidation tests were performed in the mixtures of bentonite with sand, clay or tire grains for percentages (in mass) of these materials in the mixtures equal to 25%, 50% and 75%. Tests on each individual material were also carried out and their results were used as references for comparisons.

3.1.1. Direct shear tests

Figures 6(a) to (c) shows typical shear stress – shear displacement curves obtained in conventional direct shear tests (100 mm x 100 mm specimens) carried out on "dry" (natural moisture content) bentonite mixtures, containing 50% of the alternative material in mass, under a normal stress of 100 kPa, as well as results of tests on each individual component of the mixture. Table 5 shows the initial conditions of the specimens in terms of moisture contents and void ratios. The mixture specimens were prepared under the loosest stated possible by gently placing the mixture in the testing cell (no compaction). The results in Fig. 6 show the beneficial aspects brought by the presence of the alternative material to the increase of the shear strength of the mixture. The presence of these materials reduced the mixture void ratio, increasing the shear strength of the mixture. This increase is more clearly visualised at later stages of the tests on the BTN-SND and BTN-CLY mixtures (Figs. 6a and 6b). Regarding the BTN-TG mixture, gains of shear strength with respect to test on the bentonite alone only occurred after large shear displacements (above 5 mm, Fig. 6c). This was in part due to the compressibility and to the greater values of initial void ratios of the mixture with tire grains.

Figure 7 summarises the results of friction angles of the dry bentonite mixtures obtained in the direct shear tests. In this figure, R_ϕ is the ratio between the tangent of the mixture friction angle and the tangent of the friction angle of the bentonite alone. It can be noted that R_ϕ tends to increase with the increase of the percentage of the alternative material in the mixture, with greater gains in friction angle for the BTN-SND and BTN-CLY mixtures. The presence of a coarser material mixed with bentonite will provide greater strength along the shear plane. This can be observed in Fig. 8, which shows views (50x enlargement) of shear zones at the end of tests on hydrated BTN-TG mixtures for percentages of tire grains of 25%, 50% and 75%. It is interesting to note the reduction on the value of R_ϕ for the test on the tire grains alone (R_ϕ = 0.7) in Fig. 7. This was due to the large value of void ratio (e = 4.6) of the tire grains specimen, as shown in Table 5.

Very low values of cohesion intercept were obtained in direct shear tests on dry bentonite mixtures. These intercepts were negligible for BTN-SND and BTN-TG mixtures. For BTN-CLY mixtures it varied between 0 and 6.1 kPa, depending on the percentage of clay in the mixture.

Figure 9 presents values of mixture friction angle and R_ϕ obtained in conventional direct shear tests on hydrated (after 4 days under submersion) specimens. In general,

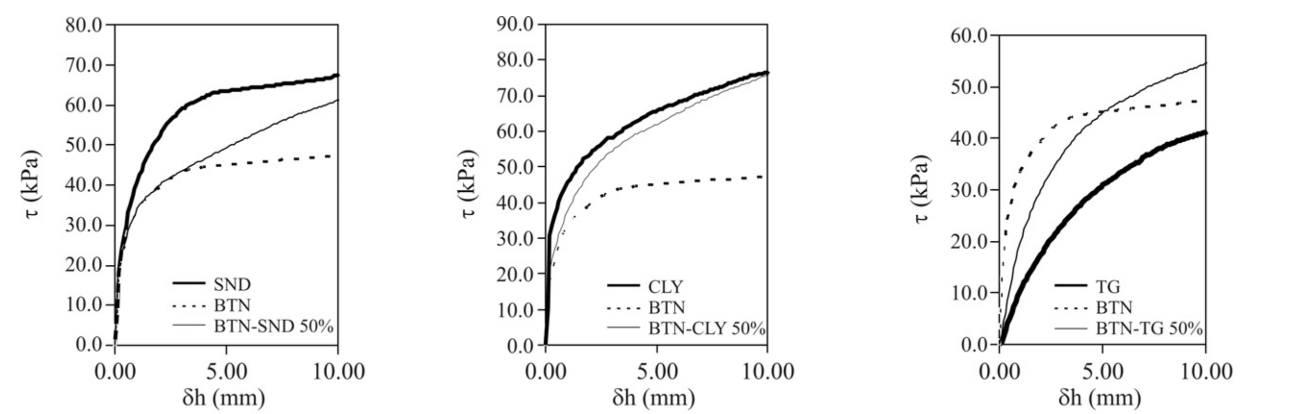

(a)Bentonite-sand mixture (BTN-SND 50%) b) Bentonite-clay mixture (BTN-CLY 50%) c) Bentonite-tire grains mixture (BTN-TG 50%)

Figure 6 - Typical shear stress-shear displacement curves obtained in tests on bentonite mixtures containing 50% (in mass) of bentonite.

Table 5 - Moisture content and void ratio of the mixtures tested.

Material	% of BTN (%)	$w_i^{(1)}$ (%)	w_{4d} (%)	e_o	e_{4d}
BTN	100	12	139	3.3	7.5
CLY	0	1	57	1.2	1.2
SND	0	0	22	0.9	0.9
TG	0	1	40	4.6	4.6
BTN-CLY 25%[(2)]	75	10	123	3.1	7.3
BTN-CLY 50%	50	8	123	2.8	6.5
BTN-CLY 75%	25	8	103	2.6	5.6
BTN-SND 25%	75	11	117	2.8	6.3
BTN-SND 50%	50	10	112	2.5	5.6
BTN-SND 75%	25	7	107	1.9	3.5
BTN-TG 25%	75	10	123	3.2	7.3
BTN-TG 50%	50	9	111	3.0	7.3
BTN-TG 75%	25	6	79	2.9	5.1

Notes: (1) w_i = natural moisture content, w_{4d} = moisture content after 4 days of inundation, e_o = initial void ratio, e_{4d} = void ratio after 4 days of inundation; (2) Number on the right indicates the percentage of alternative material, in mass, mixed to the bentonite.

hydration caused a drastic reduction on mixture friction angles. The low friction angle obtained in the test with the bentonite alone is consistent with values reported in the literature (Fox *et al.* 1998, Thiel *et al.* 2001, Fox & Stark 2004, Viana & Palmeira 2009). A more significant increase on R_ϕ was observed for the mixture BTN-TG with a percentage of tire grains greater than 50%. In spite of the reduction of the friction angle caused by hydration, the addition of alternative material led to greater shear strength of the mixture in comparison to that of the bentonite alone.

The variation of the cohesion intercept with the percentage of alternative material in the mixture obtained in the direct shear tests on hydrated specimens is depicted in Fig. 10. It can be noted that the cohesion intercept decreases from the value (~12 kPa) obtained for the bentonite alone with the increase of mass of alternative material. For values up to 75% of alternative material in the mixture, the cohe-

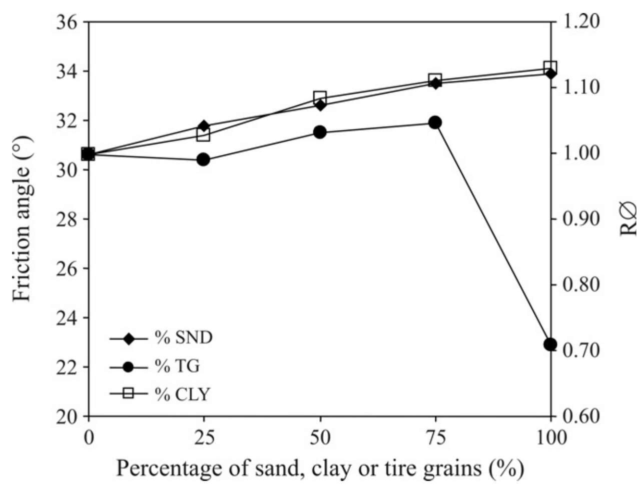

Figure 7 - Bentonite mixture friction angles for different percentages of alternative materials.

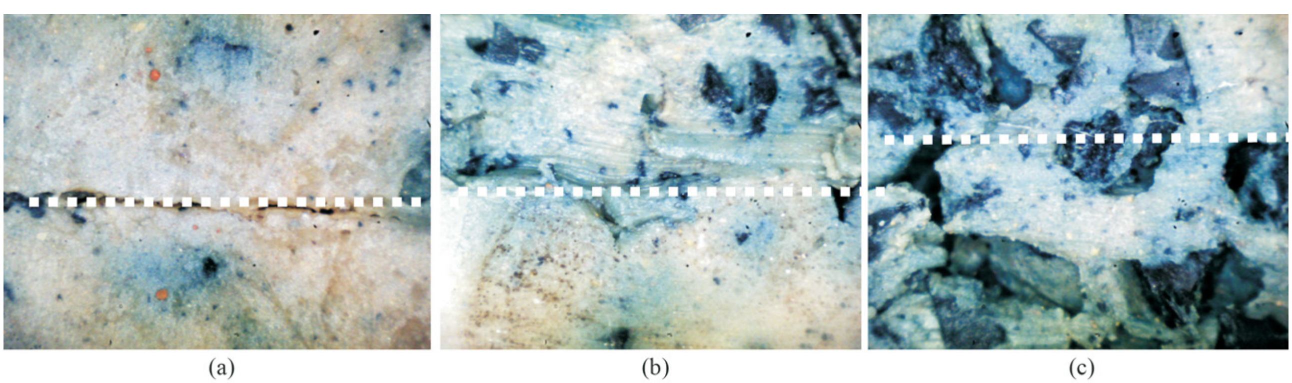

Figure 8 - Shear zones in specimens of BTN-TG mixtures (50x enlargement) at the end of tests with different values of tire grains content, (a) 25%, (b) 50% and (c) 75% of TG.

sion intercept varied between 7 kPa and 10 kPa (between 17% and 40% less than the value for the bentonite alone), depending on the material considered and its percentage in the mixture.

3.1.2. Consolidation, hydraulic conductivity and permittivity tests

The results obtained in consolidation tests on the bentonite mixtures are shown in Figs. 11(a) to (c) in terms of specimen vertical strain (equal to $\Delta e/(1 + e_o)$, where Δe is the void ratio variation and e_o is the initial void ratio) *vs.* vertical effective stress. For clarity sake the unloading stages of the tests are not presented in those figures. Greater expansions (negative values of $\Delta e/(1 + e_o)$) due to specimen inundation under the low initial vertical stress of 5 kPa were observed for the BTN-CLY mixtures (Fig. 11b). In spite of different initial values of vertical strain due to different expansion levels, the patterns of variation of e *vs.* σ of the mixtures are similar. The results obtained for the BTN-CLY specimens were little affected by the percentage of clay in the mixture, in contrast to what was observed for the other mixtures.

Table 6 presents results of hydraulic conductivity tests on bentonite mixture specimens for normal stresses

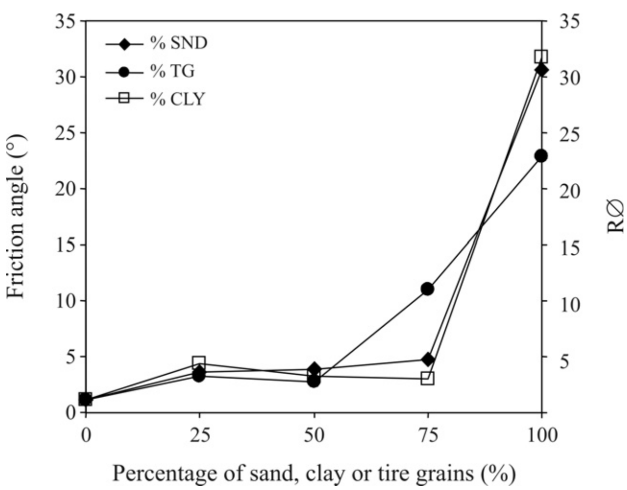

Figure 9 - Friction angles of bentonite mixtures after hydration.

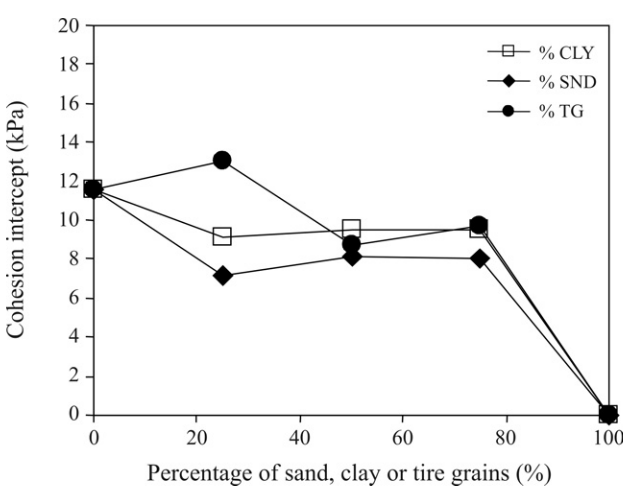

Figure 10 - Cohesion intercept obtained in direct shear tests on hydrated specimens.

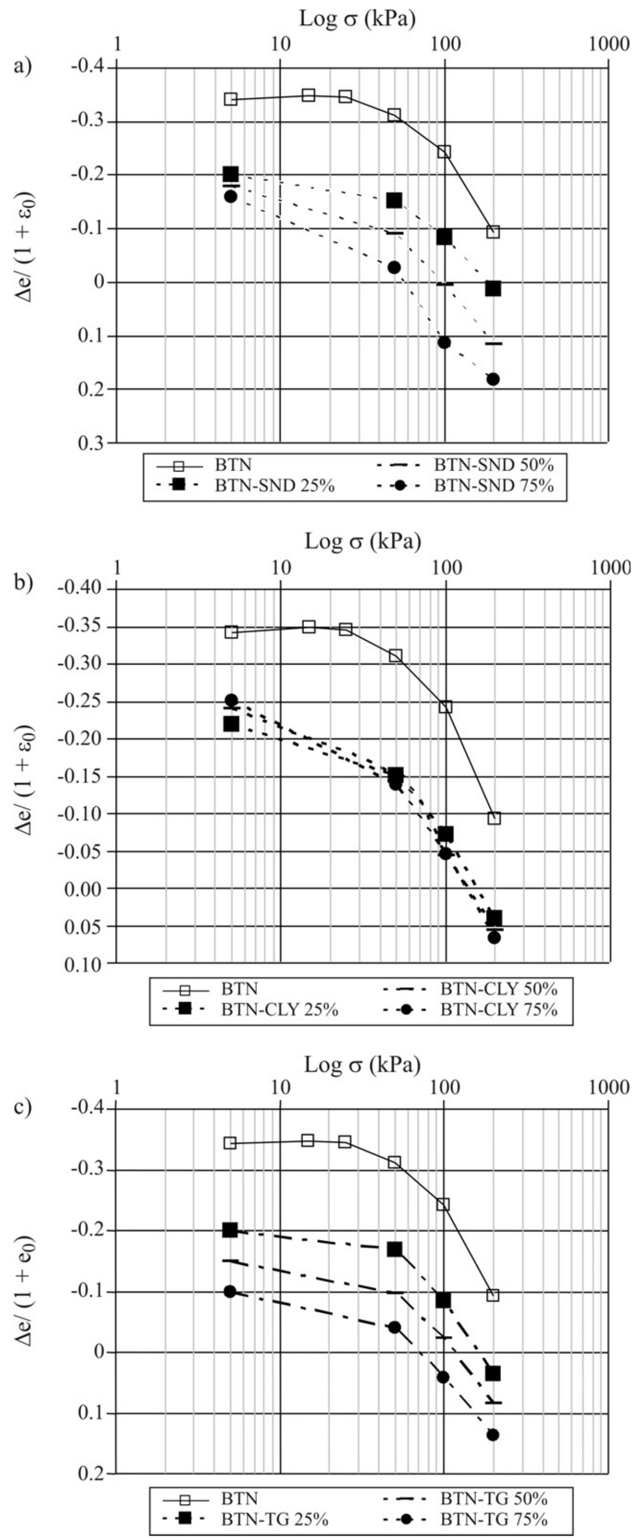

Figure 11 - Results of consolidation tests.

Table 6 - Hydraulic conductivity (k_N, cm/s) *vs.* normal stress (σ_N, kPa).

σ_N (kPa)	BTN (k_N x 10^{-9})	BTN-SND (k_N x 10^{-8})			BTN-CLY (k_N x 10^{-8})			BTN-TG (k_N x 10^{-8})		
		25%	50%	75%	25%	50%	75%	25%	50%	75%
50	3.3	2.3	2.3	2.4	5.2	4.6	5.2	3.4	4.0	4.9
100	3.0	1.4	2.3	1.1	2.0	1.0	2.1	2.0	1.6	4.2
200	2.0	1.4	2.3	1.1	2.0	1.0	2.1	1.6	1.6	2.1

varying from 50 kPa to 200 kPa. It can be noted that the hydraulic conductivity (k_N) of the bentonite alone was less sensitive to the normal stress than those of the mixtures. The values of k_N for the mixtures were 3.3 to 15.8 times greater than that of the bentonite alone, depending on the mixture and normal stress considered.

The hydraulic conductivity alone is not sufficient to assure a good performance of a material as a barrier, as its thickness plays also a fundamental role in the process. In this context, the permittivity (ratio between a medium hydraulic conductivity and its thickness, ψ) of the material provides a better measurement of the difficulty that a fluid will face to cross it. Figures 12 and 13 show the variations of permittivity and of permittivity ratio (R_ψ, ratio between mixture permittivity and bentonite permittivity) with normal stress, respectively, obtained from consolidation tests. A rather large scatter of test results can be observed and this is a consequence of the natural scatter of results of hydraulic conductivity in permeability tests, associated with the variability of the initial thickness of the mixtures under very loose states, depending on the type and content of the alternative material used. Figure 12 shows that the permittivity of the bentonite alone is less sensitive to the normal stress (ψ varying between 1.1 x 10^{-10} s^{-1} and 2.6 x 10^{-10} s^{-1}). For the bentonite mixtures, ψ varied between 7.4 x 10^{-9} s^{-1}, for the BTN-SND 75% mixture under 5 kPa normal stress (Fig. 12a) and to 6 x 10^{-10} s^{-1}, for BTN-CLY 50% mixture under 200 kPa normal stress (Fig. 12b). The ratio (R_ψ) between permittivity values of the mixture and of the bentonite alone varied between 5 and 29 (Figs. 13a to c), depending on the mixture and stress level considered. For a normal stress of 200 kPa the mixture permittivity was 5 to 12 times greater than that of the bentonite alone, depending on the alternative material considered, with lower values of ψ for mixtures of bentonite with clay. Despite the greater permittivity values of the mixtures, the results obtained show that the use of bentonite mixtures may be interesting in less critical barrier problems, particularly under stress levels greater than 100 kPa.

As permittivity is a function of the layer thickness, for larger thicknesses than the ones tested in the present study significantly lower values of permittivity could be obtained for the mixtures. Thus, thicker layers of bentonite-alternative material mixtures could function as a barrier as well as traditional (even thicker) compacted clay layers. In this sense, thicker bentonite-tire grains mixtures would consume a greater number of tires, which would be beneficial to the environment regarding a better use for this type of

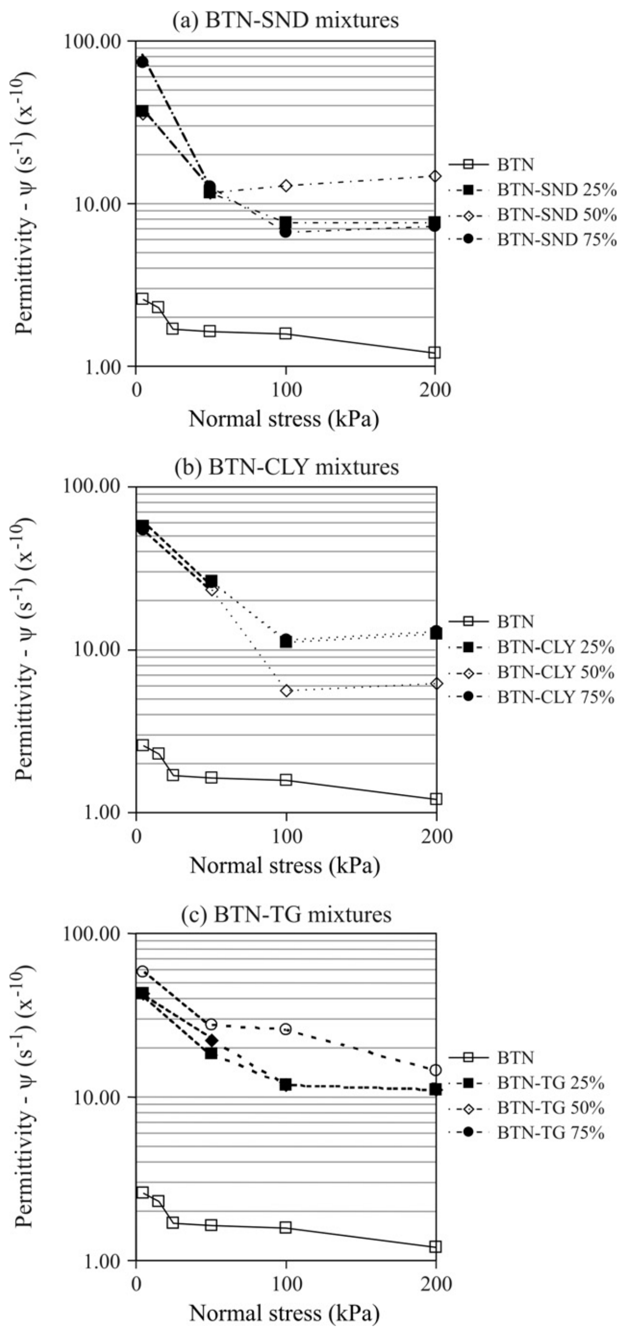

Figure 12 - Permittivity of mixtures *vs.* normal stress.

waste. However, obviously the cost of this alternative solution would have to be compared to those of other traditional solutions (compacted clay liner, GCL) to check its economical feasibility as a barrier.

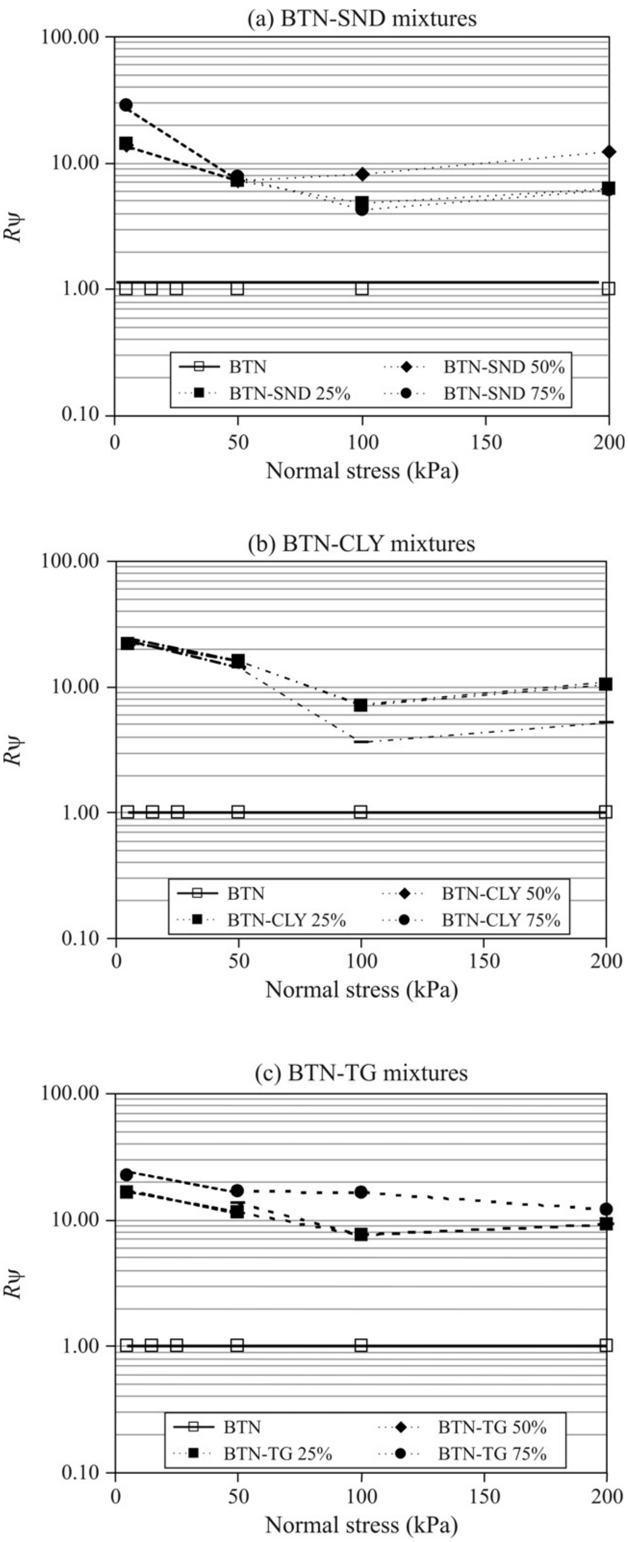

Figure 13 - Permittivity ratio *vs.* normal stress.

3.1.3. Expansibility tests

Figures 14(a) to (c) present the final relative expansion of the mixtures after 4 days under submersion in distilled water *vs.* confining normal stress ($\leq$ 5 kPa). In these figures relative expansion is defined as the ratio between the specimen thickness increase and its initial thickness (prior to inundation). As expected, the expansibility of the mixture decreases with the increase of the amount of alter-

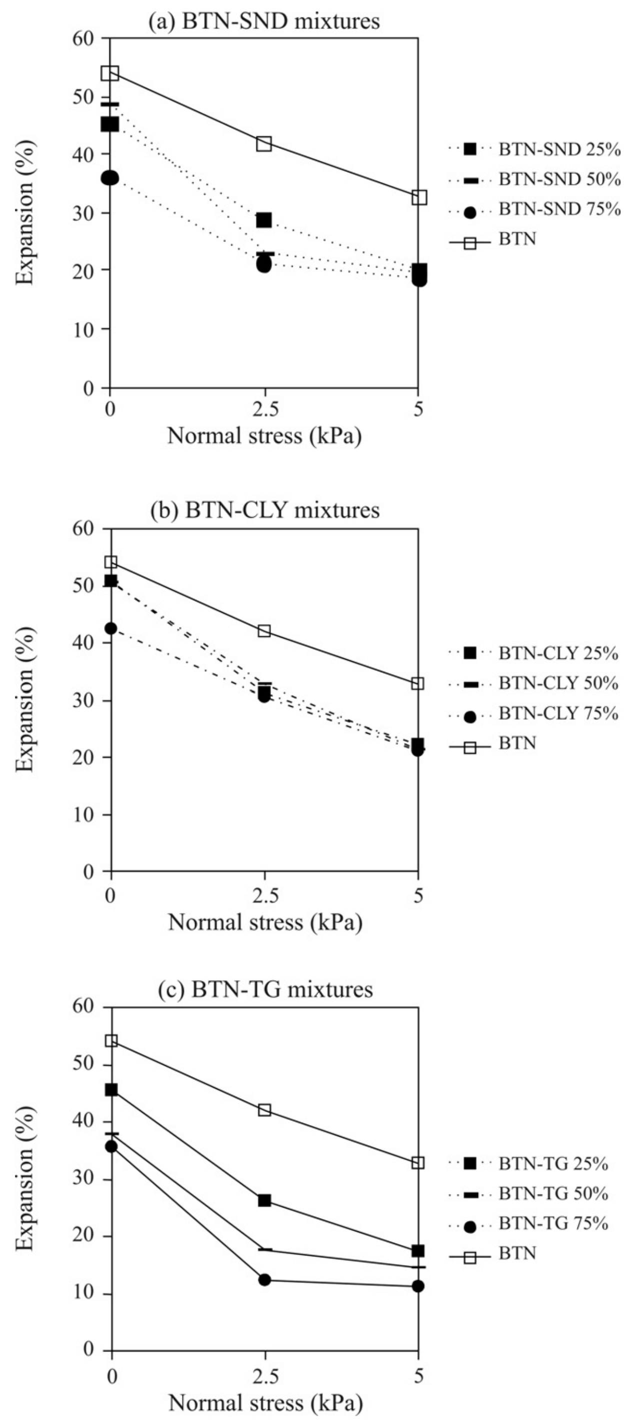

Figure 14 - Mixture expansion *vs.* normal stress.

native material in the mixture and with the increase of confining stress. The BTN-TG mixtures were the ones that presented the smallest expansions, which may be associated with the smaller water retention capacity and large initial void ratios of these mixtures.

Figure 15 shows the value of the ratio (R_e) between the final expansion of the mixture and the final expansion of the bentonite alone for each mixture tested. As expected, R_e decreased with the confining stress and, for a given alternative material, with the percentage of that material in the mixture. A more significant reduction on the value of R_e with the percentage of alternative material in the mixture was observed for the BTN-TG mixtures. This is in part a consequence of the smaller dry specific unit weight of this mixture.

3.2. Performance of GCLs with alternative core materials

3.2.1. Tests on alternative GCLs

Based on the results of the tests carried out on the bentonite mixtures presented in the previous section, a 50% percentage in mass of alternative material was chosen for the production of the alternative GCLs. This percentage is a compromise between the use of a great percentage of the alternative material in the mixture and less losses of relevant geotechnical and hydraulic parameters for barrier systems. Three alternative GCLs (GCL-SND 50%, GCL-CLY 50% and GCL-TG 50%) and the conventional GCL A and B were subjected to free expansion tests and to ramp tests (0.6 m x 1.0 m size specimens).

3.2.1.1. Free expansion tests

Figure 16 presents the results obtained in the free expansion tests performed. This figure shows that the GCLs with cores resulting from the mixtures of bentonite and alternative materials (50% in mass) presented less expansion than that of the conventional commercial products GCL A and GCL B. This was a consequence of the non expansive

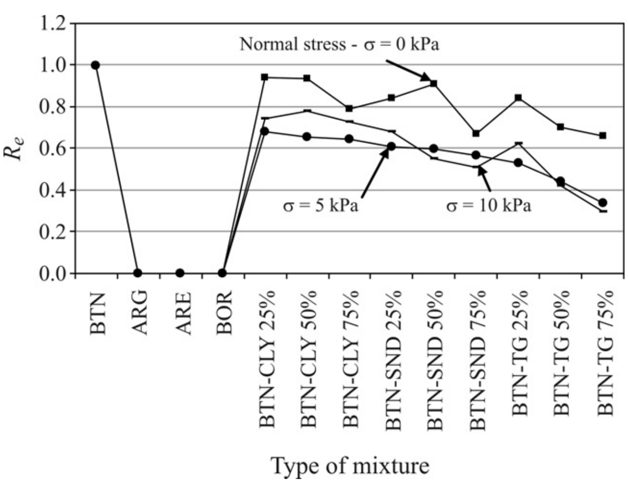

Figure 15 - Value of the ratio R_e for different types of mixtures.

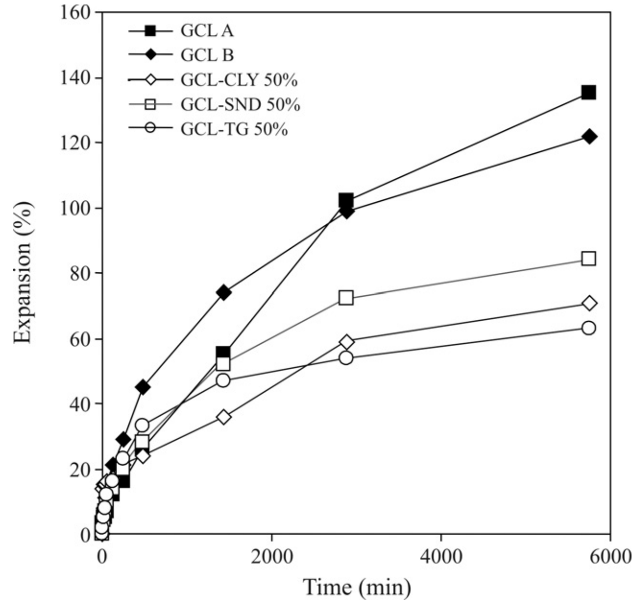

Figure 16 - GCL free expansion *vs.* time.

nature of the alternative materials employed. GCL BTN-TG 50% was the one showing less expansion, of the order of half the expansion observed for the conventional products.

3.2.1.2. Ramp tests

Figure 17 shows the relationship between shear stress and normal stress on the GCL under dry conditions and after hydration for 24 h ("H") obtained at the end of the ramp tests. It is important to point out that only for GCL B tested after hydration this relationship represents a failure envelope, because of internal shear failure having been reached in this case. For the other products tested internal failure was not obtained in the ramp tests because of the contribution from the stitches' strength. In these cases, the maximum inclination imposed to the ramp was of the order of 50°. As a result, for a given normal stress, similar mobilized shear stresses were obtained for GCL A (dry or hydrated), GCL B (dry) and the alternative GCLs. This shows that for the conditions of the test the presence of the alternative materials did not influence the GCL internal strength, in part because in these cases the internal shear strength was controlled by the strength of the stitches. For the same reason, hydration had little effect on the behaviour of the alternative GCLs in comparison with the reference commercial GCLs used in this experimental programme.

The stitch filaments can have a marked effect on the internal shear strength and on the shear stiffness of the GCL. For the ramp tests carried out, internal failure occurred only for hydrated GCL B. In this case, it was observed that the expansion of the bentonite of GCL B caused failure of some stitches, which yielded to lower internal shear strength. This reduction on the internal shear strength of the GCL may compromise the stability of the lining system in a slope, if this aspect is not properly considered in the design. Figures 18(a) and (b) show enlarged views of stitches in GCLs A and B, respectively. Figure 18(b) shows a stitch filament that failed during hydration of GCL B. This failure mechanism can be minimized or avoided if hydration takes place under high stress levels, because under such conditions the expansion of the bentonite will be inhibited to some extent. Therefore, the critical conditions will take place under low stress levels and in this case the ramp test on hydrated GCLs can provide important information on the internal strength of the GCL under normal stresses closer to those expected in the field.

Figure 19 presents maximum values of mobilized tensile load on the lower (carrier) geotextile of the GCL *vs.* normal stress at the end of the ramp tests. In all cases, except for hydrated GCL B, the mobilized tensile force increased with normal stress with little difference among results of tests on different GCLs. The results obtained for the GCL with BTN-TG 50% mixture were close to those of GCLA. The rather constant value of mobilized tensile load with normal stress for the hydrated GCL B was due to internal failure having occurred prior to significant mobilization of force in the carrier geotextile of this product.

The variation of shear displacement (difference between displacements of the cover and carrier geotextiles of the GCL) with normal stress at the end of the ramp tests is depicted in Fig. 20 for each GCL tested. It can be noted that hydration slightly increased the relative displacement between cover and carrier geotextiles of GCL A. Under dry conditions the variation of these displacements with normal stress was similar for GCLs A and B for normal stresses greater than 2.5 kPa. However, hydration caused catastrophic internal failure of GCL B, with relative displacements in excess of 100 mm. With the exception of GCL B

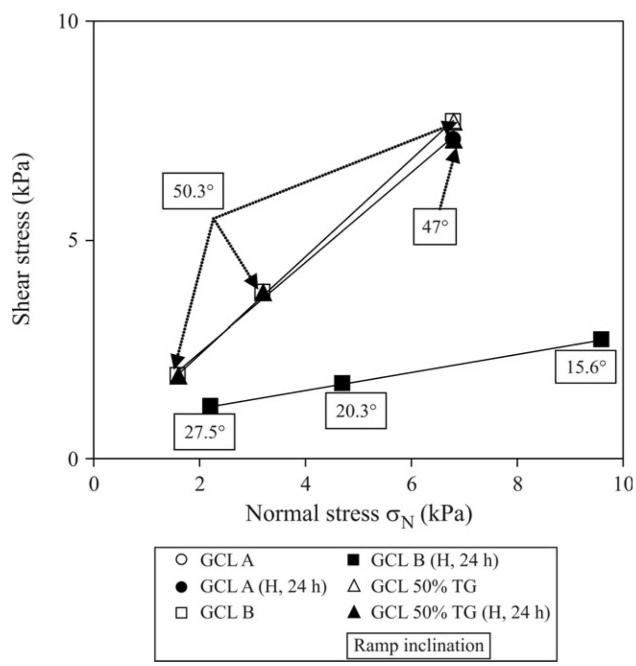

Figure 17 - Mobilised shear stress *vs.* normal stress on the GCL for dry and hydrated specimens.

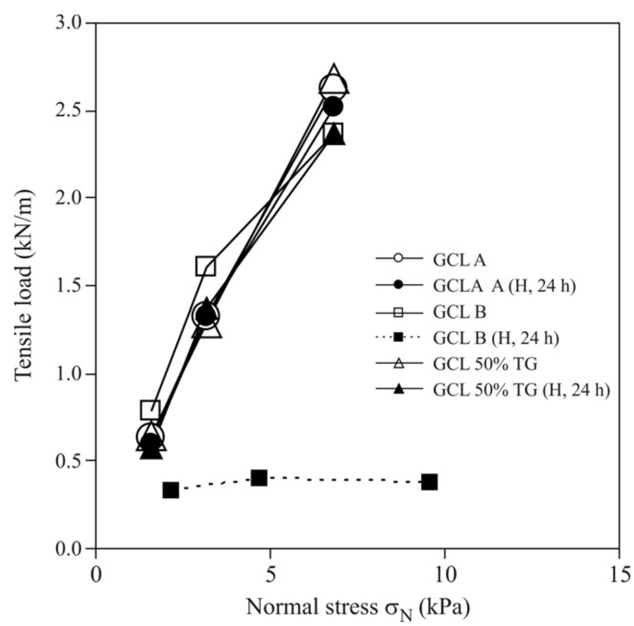

Figure 19 - Maximum mobilised tensile force *vs.* normal stress.

Figure 18 - Stitches of GSLs A and B after hydration: (a) GCL A stitch after hydration; (b) Failed stitch in GCL B after hydration.

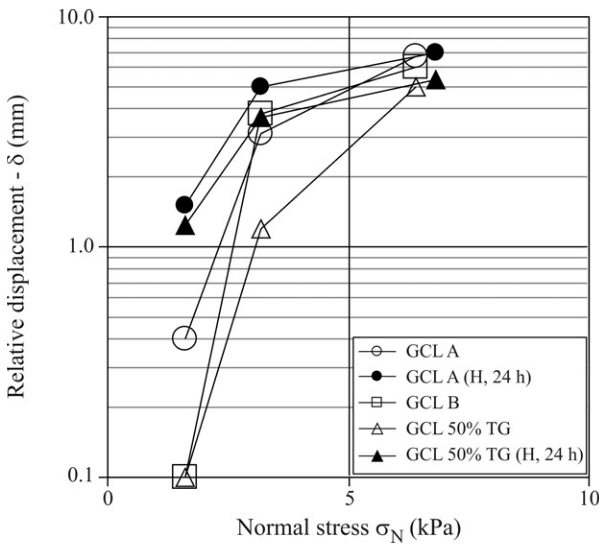

Figure 20 - Relative displacement *vs.* normal stress in ramp tests.

(H, 24 h), the maximum relative displacement for the range of normal stresses used was approximately 7 mm. Similar results of maximum relative displacements were obtained for the alternative GCLs independent on the material (tire grains, sand or clay) mixed to the bentonite, with maximum values below 5.5 mm for dry and hydrated conditions. Great distortions of the GCL will increase the deformation of the lining system as a whole, which may favour the formation of cracks in compacted soil layers overlying the GCL and increase the tensile load in the geomembrane (if present) on the GCL at the anchorage region.

4. Conclusions

This paper presented results of a laboratory study on the use of alternative materials mixed to bentonite in GCLs. The main conclusions obtained are summarised below.

The presence of the alternative materials (sand, clay or tire grains) increased the shear strength of the mixture. For the mixture with tire grains the shear strength increase was observed at the late stages of direct shear tests, mainly due to the compressible nature of the tire grains, which increased the deformability of the mixture. The friction angles of the mixtures were also greater than that of the bentonite alone under dry and hydrated conditions, although for the latter condition the values were still low. Under hydrated conditions, the cohesion intercept obtained for the mixtures were smaller than that of the bentonite alone, being between 17% and 40% smaller than the value obtained for the bentonite, depending on the mixture considered.

The compressibility of the mixtures was greater than that of the bentonite. This was due to the loose state of the specimens tested and compressibility of individual grains, like in the case of the tests with tire grains.

The addition of alternative materials to the bentonite reduced the expansibility and increased the permittivity of the mixture. Permittivity values of the mixtures were 5 to 29 times greater than that of the bentonite alone, depending on the mixture and stress level considered. In general, the greatest increases on permittivity were observed for the bentonite-tire grains mixtures. Even so, the permittivity of bentonite-tire grains mixtures for percentages (in mass) of tire grains up to 50%, and normal stresses above 100 kPa, were of the order of 10^{-9} s^{-1} (0.18 x 10^{-9} s^{-1} for the bentonite alone). The expansions of the hydrated alternative GCLs manufactured in the laboratory were also smaller than those of the two commercial conventional GCLs tested.

The internal shear strength, as measured in ramp tests, was controlled by the strength of the stitches of the GCLs. Only commercial GCL B failed in this type of test. The results obtained for the alternative GCL made with core consisting of a mixture of bentonite and tire grains (50% in mass) were similar to those presented by commercial GCL A, under dry and hydrated conditions, in terms of mobilised shear stresses and mobilised tensile loads in the carrier geotextile.

The results obtained showed that the mixture of the alternative materials used in this research programme with bentonite can increase the internal shear strength of an alternative low cost GCL made with those mixtures, but degraded some other important parameters for barrier applications, such as GCL expansibility and permittivity. Increases in the cost of manufacturing the alternative GCLs should also be taken into account before assuming that the use of less bentonite alone will result in a cheaper GCL, particularly for the case o mixtures involving bentonite and sand. Some practical aspects also need investigation, such as the possibility of segregation of the alternative material used in the GCL during transportation, handling and installation in the field. This segregation can be minimised or avoided depending on the manufacturing process used to produce the GCL, but this can also yield to additional costs to produce the alternative GCL product.

Despite presenting greater permittivity and lower expansibility than conventional GCLs, alternative products with mixtures of bentonite and tire grains may be considered for less critical barrier systems and as bedding/protective layers underneath geomembranes, particularly under confining stresses above 100 kPa, which are easily reached in waste disposal areas. In addition, this type of use of tire grains provides a more environmentally friendly use of wasted tires. However, despite some encouraging results obtained in this work, further research is required for a better understanding on the behaviour of alternative GCL products.

References

ASTM D 6243 (2009) Standard test method for determining the internal and interface shear resistance of geosynthetic clay liner by the direct shear method. ASTM International, West Conshohocken, PA, USA.

ASTM D 4595 (2009) Standard Test Method for Tensile Properties of Geotextiles by the Wide-Width Strip Method. ASTM International, West Conshohocken, PA, USA.

ASTM D4491 (2009) Standard Test Methods for Water Permeability of Geotextiles by Permittivity. ASTM International, West Conshohocken, PA, USA.

Bouazza, A. (2002) Review article: geosynthetic clay liners. Geotextiles and Geomembranes, v.20, 13, pp. 3-17.

Bouazza, A. & Vangpaisal, T. (2007) Gas permeability of GCLs: effect of poor distribution of needle-punched fibres. Geosynthetics International, v. 14:4, p. 127-142.

Chiu, P. & Fox, P.J. (2004) Internal and interface shear strengths of unreinforced and needle-punched geosynthetic. Geosynthetics International, v. 11:3, p. 176-199.

Didier, G & Al Nassar, M. (2002) Hydraulic performance of geosynthetic clay liners some French laboratory test methods. Clay Geosynthetics Barriers. Zanzinger, Koerner, Gartung (eds), pp. 249-273.

Fox, P.J.; Rowland., M.G. & Scheithe, J.R. (1998) Internal shear strength of three geosynthetic clay liners, Journal of Geotechnical and Geoenvironmental Engineering, ASCE, v. 124:10, p. 933-944.

Fox, P.J. & Stark, T.D. (2004) State-of-the-art report: GCL shear strength and its measurement. Geosynthetics International, v. 11:3, p. 117-151.

Ikizler, S.B.; Aytekin, M. & Vekli, M. (2009) Reductions in swelling pressure of expansive soil stabilized using EPS geofoam and sand. Geosynthetics International, v. 16:3, p. 216-221.

Koerner, R.M. (2005) Design with geosynthetics. 5th ed. Prentice Hall New Jersey, USA, 816 pp.

Müller, W.; Jakob, I.; Seeger, S. & Tatzky-Gerth, R. (2008) Long-term shear strength of geosynthetic clay liners. Geotextiles and Geomembranes, v. References and further reading may be available for this article. To view references and further reading you must this article. 26:2, p. 130-144.

NF EN ISO 12956 (2010) Géotextiles et produits apparentés – Détermination de l'ouverture de filtration caractéristique.

Palmeira, E.M. (2009) Soil-geosynthetic interaction: modelling and analysis. Geotextiles and Geomembranes, v. 27:5, p. 368-390.

Palmeira, E.M.; Lima Junior, N.R. & Mello, L.G. (2002) Interaction between soil and geosynthetic layers in large scale ramp tests. Geosynthetics International, v. 2:9, p. 149-187.

Palmeira, E.M. & Viana, H.N.L (2003) Effectiveness of geogrids as inclusions in cover soils of slopes of waste disposal areas. Geotextiles and Geomembranes, v. 21:5, p. 317-337.

Reuter E. & Markwardt N. (2002) Design of landfill cover lining systems with geosynthetic clay liners (GCLs). 7th International Conference on Geosynthetics, Nice, France, v. 1, pp. 573-576.

Rowe, R.K. & Orsini, C. (2003) Effect of GCL and subgrade type on internal erosion in GCLs under high gradients, Geotextiles and Geomembranes, v. 21:1, p. 1-24; References and further reading may be available for this article. To view references and further reading you must this article.

Shan, H-Y & Daniel, D. E. (1991) Results of laboratory tests on a geotextile/bentonite liner material. Geosynthetics 91', IFAI, Atlanta, GA, v. 2, pp. 517-535.

Shan, H,Y. & Chen, R.H. (2003) Effect of gravel subgrade on hydraulic performance of geosynthetic clay liner. Geotextiles and Geomembranes, v. 21:6, p. 339-354.

Sivakumar Babu, G.L., Sporer, H., Zanzinger, H. & Gartung, E. (2001) Self-healing properties of geosynthetic clay liners. Geosynthetics International, v. 8:5, p. 461-470.

Thiel, R.; Daniel, D. E.; Erickson, R. B.; Kavazanjian, E. Jr & Giroud, J.P. (2001) The GSE GundSeal GCL Design Manual, GSE Lining Technology, Inc., Houston, TX, USA.

Touze-Foltz, N.; Duquennoi, D. & Gaget, E. (2006) Hydraulic and mechanical behavior of GCLs in contact with leachate as part of a composite liner. Geotextiles and Geomembranes, v. 24:3, p. 188-197.

Viana, H.N.L. (2007) A study on the stability and hydraulic conductivity of conventional and alternative barrier systems for waste disposal areas, PhD. Thesis, Graduate Programme of Geotechnics, University of Brasilia, 201 pp. (in Portuguese).

Viana, H,N.L. & Palmeira, E.M. (2010) Influence of geogrid geometrical and mechanical properties on the performance of reinforced veneers. Soils and Rocks, v. 33:1, p. 33-44.

Viana, P.M.F. & Palmeira, E.M. (2009) Evaluation of GCL internal shear strength in inclined plane tests. GeoAfrica 2009, Cape Town, South Africa, 8 pp.

Viana, P.M.F. & Palmeira, E.M. (2008) Evaluation of the interface and internal strength of alternative barrier systems incorporating geosynthetics. Internal Report, Graduate Programme of Geotechnics, University of Brasilia, Brazil, 57 pp. (in Portuguese).

CPT and T-bar Penetrometers for Site Investigation in Centrifuge Tests

M.S.S. Almeida, J.R.M.S. Oliveira, H.P.G. Motta, M.C.F. Almeida, R.G. Borges

Abstract. Geotechnical design is based on site investigations which provide a reasonable overview of the soil profile and a realistic estimate of the geotechnical properties of each component layer. Nevertheless, when centrifuge modelling is involved, *in situ* tests become an additional challenge mainly because of limitations of in-flight procedures, but also due to the miniaturization of regular tools. As centrifuge modelling is becoming widespread, mostly as a result of decreasing electronic and computer costs, miniature site investigation tools are being designed to provide proper geotechnical information about model layers. This paper examines the development of site investigation tools to assess the strength of models during centrifuge tests. These tools are a T-bar penetrometer and a Cone Penetration Test (CPT) apparatus capable of measuring the resistance of clay and granular soils, respectively. These tools were used in a number of centrifuge tests on clay soils and silty tailings respectively. Both tools were tested and the results compared with centrifuge tests, *in situ* conventional tests, triaxial and direct shear laboratory tests showing an overall consistency and reliability of the measured data.

Keywords: penetrometer, CPT, T-bar, centrifuge test, soft clay, mine tailings.

1. Introduction

Physical modelling plays an important role in modern geotechnics as it aims to create a scaled model able to provide a physical understanding of a phenomenon associated with a real problem.

Within physical modelling, centrifuge modelling has becoming increasingly important due to its flexibility regarding the simulation of various engineering problems while keeping critical parameters invariable. The basic principle in centrifuge tests consists of submitting a reduced model (N times smaller than the prototype) to an acceleration N*g*, thus providing an inertial field similar to the gravitational field experienced by the prototype (Schofield, 1980).

Advances in centrifuge research have led to the need for a reliable resistance profile of the soil models, leading to the conception of in-flight penetration tests in order to describe the variation in the soil properties with depth.

A major difficulty in carrying out in-flight tests is the miniaturization of tools and their actuations. As a result, routine procedures such as SPT, for example, can become extremely complex. Early developments in in-flight site investigation in centrifuge tests made use of the vane test and cone penetration test (*e.g.*, Almeida & Parry, 1984, 1987; Esquivel & Ko, 1995) to measure the undrained strength of soil models and also sands (*e.g.*, Almeida, 1984; Bolton *et al.* 1999). Subsequent developments used the T-bar (Stewart & Randolph, 1991) to assess the undrained strength of clay soils. This paper presents the experience of the development of T-bar and CPT probes to measure the strength of models used in the mini-drum centrifuge at the Alberto Luiz Coimbra Institute – Graduate School and Research in Engineering (COPPE) in Rio de Janeiro. Test results and their interpretation are presented for clay and silty tailings soils.

2. Coppe'S Geotechnical Centrifuge

The COPPE geotechnical centrifuge (Gurung *et al.*, 1998), shown in Fig. 1, is a 1.0 m diameter mini-drum with a full load capacity of 90 *g*-ton. It comprises 20 slip rings, 16 data acquisition channels, a linear actuator, and a turntable on which the linear actuator is mounted.

The COPPE centrifuge has been used in studies on pipeline movements (Oliveira, 2005; Pacheco, 2006), stability of solid waste fills (Calle, 2007), and the behaviour of iron tailings materials (Motta, 2008).

A strongbox with dimensions 260 mm length, 210 mm width, and 178 mm height has been used for the tests performed so far in COPPE's centrifuge. Use of the whole centrifuge channel is also possible but such a procedure would require a very large amount of soil to be tested. A new, larger strongbox is now in use for pipeline studies.

Currently the main tool used in the centrifuge for clayey soils is the T-bar penetrometer. Its use is similar to that of the cone with the advantage that it does not need any area correction as the soil resistance is obtained directly from a simple equation. The use of the T-bar (Stewart & Randolph, 1991) is indicated only for clay soils, once the theoretical interpretation of the mobilized resistance was deduced solely for this type of soil. The tool considered

M.S.S. Almeida, PhD, Professor, Universidade Federal do Rio de Janeiro, COPPE-Programa de Engenharia Civil, Rio de Janeiro, RJ, Brazil. e-mail: almeida@coc.ufrj.br.
J.R.M.S. Oliveira, DSc, Professor, Instituto Militar de Engenharia, Seção de Fortificação e Construção, Rio de Janeiro, RJ, Brazil. e-mail: jrmso@terra.com.br.
M.C.F. Almeida, DSc, Professor Adjunto, Departamento de Engenharia Civil, Escola Politécnica, Universidade Federal do Rio de Janeiro, Rio de Janeiro, RJ, Brazil. e-mail: mariacascao@globo.com.
R.G. Borges, MSc, CENPES-PETROBRAS, Rio de Janeiro, RJ, Brazil. e-mail: garske@petrobras.com.br.
Submitted on October 1, 2009; Final Acceptance on March 8, 2010; Discussion open until August 31, 2011.

Figure 1 - COPPE/UFRJ Geotechnical centrifuge.

most suitable to evaluate the behaviour of granular soils is the cone penetration test (CPT). This paper examines the use of the T-bar and the CPT for the site investigation of clay and granular type soils respectively.

3. T-Bar Tests In Clay Soils

A T-bar with a 15.2 mm diameter adapted to a rigid shaft was used in the present study (Fig. 2). The vertical force was measured using a manufactured 50 N tension and compression load cell, which compensates bending moments and thermal variations (Fig. 2). One pore-pressure transducer was positioned inside the soil layer for monitoring the consolidation phase.

3.1. Reconstituted clay and sample preparation

The natural clay from Guanabara Bay in Rio de Janeiro/RJ consists of lightly overconsolidated highly compressible soft clay with water content in the range 150%-200% and close to the liquid limit. A number of tests were used to assess the *in situ* undrained strength of the natural clay and it was found by Almeida *et al.* (2001) that the undrained strength profile (Fig. 3) could be well described by Eq. (1), in kPa, where z is the depth in m.

$$S_u = 0.126 + 1.373z \quad (1)$$

For the centrifuge tests described below the natural clay was collected *in situ* and transformed into slurry by increasing the water content up to 1.5 times the liquid limit. The slurry was then placed in-flight inside the strongbox through a specially designed rotating joint. After the consolidation, this process produced a smooth and regular surface, adequate for the shallow tests.

During the 10 h consolidation flight, the clay slurry settled down from a 105 mm height into a 71 mm clay layer height. Figure 4 shows the measured pore pressures 10 mm above the clay layer bottom. A specially prepared program (Oliveira, 2005) has been developed, based on Terzaghi theory but combined with large deformation and centrifuge issues, in order to calculate total and effective stresses, pore pressure, water content and undrained shear strength variations, throughout the layer, during the tests at the centrifuge particular conditions. A pore pressure dissipation prediction curve has been added to Fig. 4, based on the clay parameters and the consolidation conditions.

The parameters of the reconstituted natural clay are summarized in Table 1. Figure 5 presents a final water content profile in prototype (real) scale.

Each test was divided into two phases: consolidation at 100 g followed by vertical and lateral actuations at 30 g. All samples reached around 90% consolidation during 10 h flight (Oliveira *et al.*, 2006). Enough time was allowed for pore-pressure dissipation during the centrifuge decelera-

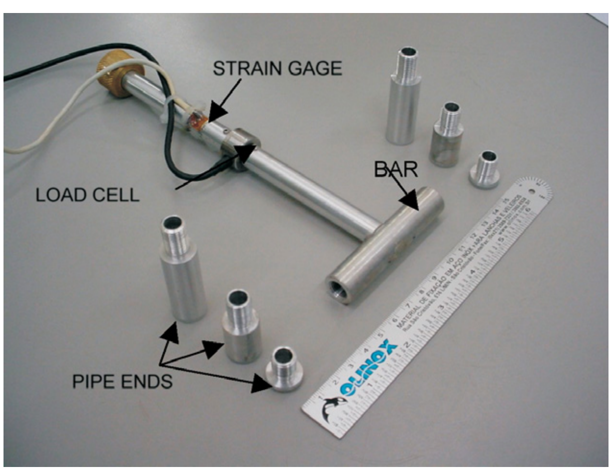

Figure 2 - Instrumented T-bar.

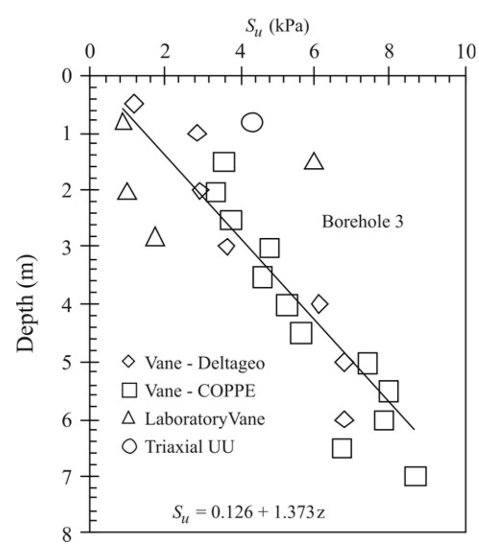

Figure 3 - Undrained strength profiles for a representative borehole (Almeida *et al.*, 2001).

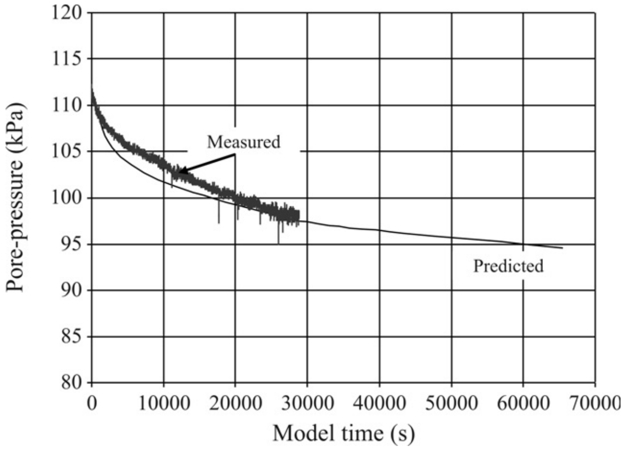

Figure 4 - Measured and predicted pore-pressure dissipation during consolidation.

Table 1 - Summary of the reconstituted clay properties.

Soft clay properties	Data
Liquid limit w_L	174%
Plasticity Index I_p	90%-120%
Solids specific weight G_s	2.60
Bulk weight (*)	12.0 kN/m^3
Voids ratio e	3.6-4.5
CR = C_c / (1 + e_0)	0.36
OCR	≈ 1.3
Coefficient of consolidation c_v	4.8 x 10^{-8} m^2/s

tion from 100 g to 30 g. After that, the T-bar was driven into the soil (Fig. 6). The vertical penetration of the T-bar allowed the measurement of the undrained strength and this is described next.

3.2. Vertical actuation

As the bar penetrates the soil, the whole setup (Fig. 2) can be employed as a T-bar penetrometer (Stewart & Randolph, 1991), and the load cell measurements can be used to estimate the undrained shear strength of the soil profile. The following equation is used to obtain S_u from T-bar measurements:

$$S_u = \frac{V}{N_b \; D^* L} \tag{2}$$

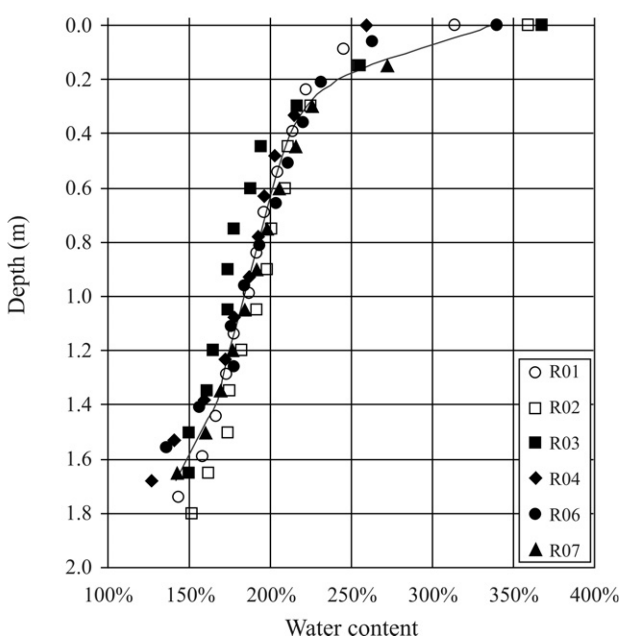

Figure 5 - Water Content Profile for clay centrifuge tests (prototype scale).

where V is the vertical force measured during penetration, L is the T-bar length, and N_b is the T-bar factor, with N_b = 10.5 the recommended value (Randolph & Houlsby, 1984; Randolph, 2004) for deep penetration. Shallow depths require different T-bar factors for each depth. In addition, the contact area increases as the bar is pushed into the soil, also increasing the amount of material involved in the failure process. For deep bar penetration D^* is the bar diameter D. For shallow embedment ratios a modified bar diameter D^* is used once the contact area between bar and soil varies with depth, and it has a direct relationship with strength. To take this variation into account, the following relation was used to express the horizontal projection of the contact area of the bottom half of the bar with the soil (Fig. 7).

$$D^* = 2\sqrt{H\,(D-H)} \tag{3}$$

where H is the distance between the soil surface and the bottom of the bar.

When the bar is just touching the soil surface, the cylindrical shape can be assumed to have a flat plate foundation, therefore associating this condition with Terzaghi's bearing capacity factor N_b = 5.14 for a purely cohesive ma-

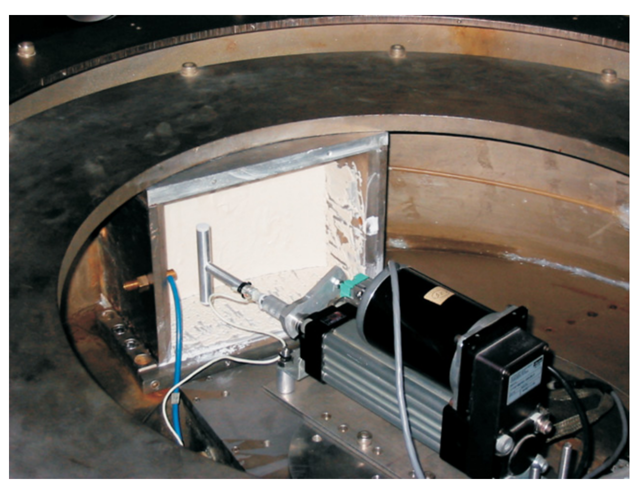

Figure 6 - T-bar in position for actuation phase.

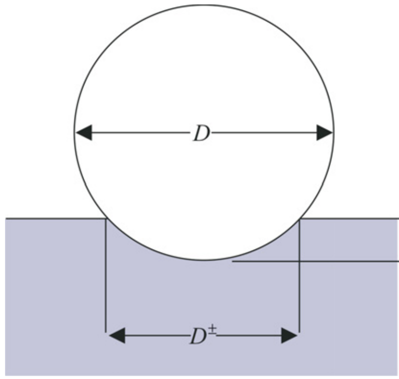

Figure 7 - Horizontal projection of the bar bottom contact area with soil.

terial. However, it is important to evaluate the burial depth at which the T-bar factor reaches its full value and how this variation develops. A numerical approach is proposed below.

3.3. Numerical simulation to evaluate N_b

The vertical penetration phase was numerically simulated (Oliveira, 2005) in order to evaluate the variation in the T-bar factor N_b with the embedment ratio H/D. In this way, numerical analyses have been carried out with the embedment ratio H/D varying from 17% to 600%. In each case, the T-bar was pushed into the soil until yield of the soil was achieved.

A finite element code for geotechnical applications (Costa, 1984), incorporating geometric and physical non-linearities with iterative-incremental integration algorithms, was used. For the soft clay soil the elastic perfectly plastic Von Mises model was adopted, with $E_u = 300\ S_u$ (Almeida & Marques, 2002), $\nu = 0.5$, and a unitary strength profile of $S_u = 1$ kPa, which makes it easier to normalize the vertical force against S_u. In these finite element analyses using the code developed by Costa (1984), three adhesion factors α were used to simulate the soil-bar interface: $\alpha = 1.0$, $\alpha = 0.5$, and $\alpha = 0.2$. Figure 8 shows the displacement vectors output for the numerical simulation of a fully buried T-bar penetrometer.

Figure 9 presents the numerical results of the T-bar factor (N_b) for the three adhesion factors computed with Eq. (2) using the numerical value of V, S_u equal to unity, and D^* defined by Eq. (3). The results in Fig. 9 indicate that the T-bar factors show a major variation for H/D in the range 0%-300% and just a minor increase for H/D greater than 400%. The initial value is around 5.24, which is close to the expected Terzaghi's bearing capacity factor, 5.14. The final value for the same adhesion factor is around 10.5, which is the same value as that proposed by Randolph (2004). A similar range of values has also been obtained by Barboza-Cruz & Randolph (2004) using a remeshing technique for smooth and rough cylinder surfaces.

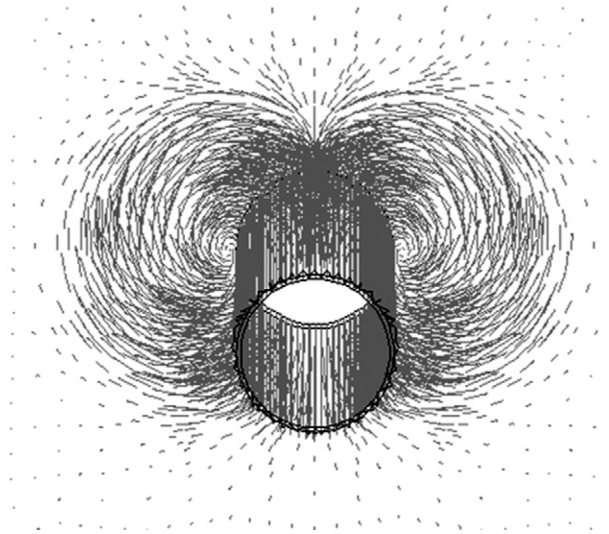

Figure 8 - Numerical displacement vectors for a 500% buried T-bar (Borges *et al.*, 2005).

3.4. Undrained strength from T-bar tests

T-bar tests were interpreted using Eq. (2), with N_b factors provided by Fig. 9, as shown in Fig. 10. The penetration rate used in all tests was 0.50 mm/s. The linear fit through S_u data of the five tests with H/D varying between 17% and 124% is given by the equation below (Oliveira *et al.*, 2006) with a linear coefficient of correlation greater than 0.99.

$$S_u = 0.1002 + 1.283z \tag{4}$$

with S_u in kPa and depth z in m. Values of S_u obtained according to Eq. (4) compare reasonably well with the *in situ* values given by Eq. (1), although the penetration depth of the model tests (around 1.0 m) is much smaller than the penetration depth of the field tests (around 6.0 m). As the sample has been consolidated at 100 g, and the penetration phase has been done at 30 g, the S_u/σ'_{v0} ratio of 0.64 is compatible with that of the Rio de Janeiro clays for an OCR ≈ 3 (Almeida, 1982).

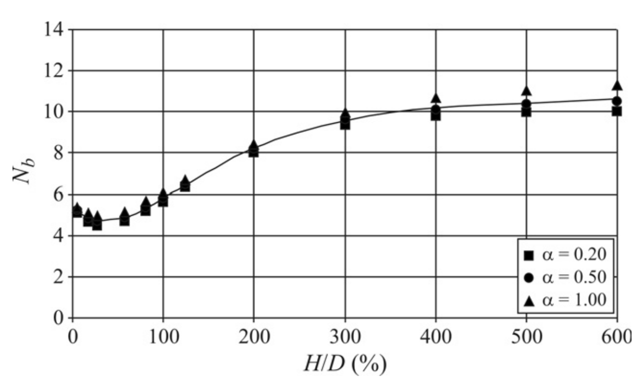

Figure 9 - Variation of the T-bar factor (N_b) with burial depth.

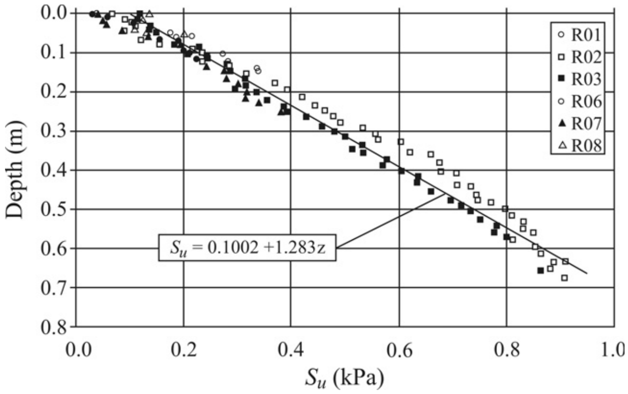

Figure 10 - T-bar tests data in prototype scale.

In an attempt to overview the whole S_u behaviour, all *in situ* and laboratorial undrained strength results on undisturbed samples have been plotted against their respective water content values on Fig. 11. In addition, centrifuge tests strength profiles on reconstituted samples have also been included in the same plot.

However, some corrections were necessary, since field samples are undisturbed, whereas centrifuges samples were reconstituted and tested in 15 h. Almeida & Marques (2002) report sensitivity values up to 4.4 measured in vane tests. Reconstituted samples used in the centrifuge are consolidated, *i.e.*, some restructuration is allowed, which needs to be taken into account. Therefore an average sensitivity value of 2.0 was adopted as a multiplying factor for the centrifuge values.

Using the critical state soil mechanics equation, which associates undrained shear strength with water content, and adopting the critical state parameters, for the same soil, obtained by Almeida (1982), a theoretical curve, based on Eq. (5), was plotted on the chart of Fig. 11.

$$S_u = 0.59 e^{\left(\frac{5.80-2.60w}{0.90}\right)} \tag{5}$$

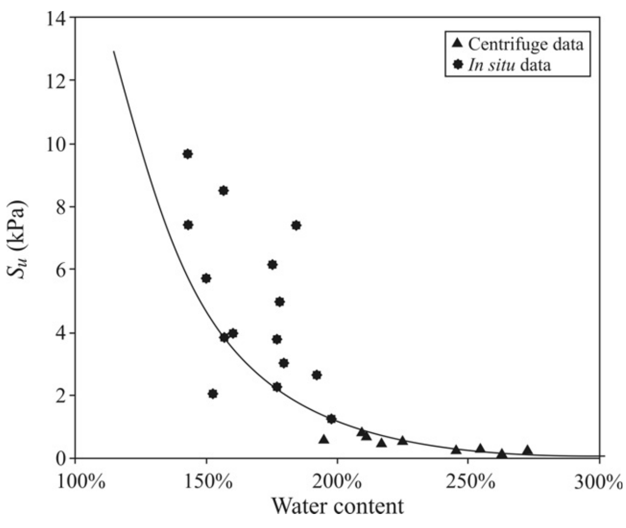

Figure 11 - Consolidation of centrifuge and *in situ* undrained shear strength versus water content data.

The centrifuge and the *in situ* data shows good agreement with the critical state theory curve, indicating that the procedures adopted for the shear strength analysis of the T-Bar measurement con-ducted to a set of reasonable values.

Figure 12 shows the centrifuge and the *in situ* liquidity index and shear strength data. These values compared well with Wood & Wroth (1978) equation keeping a clear linearity.

These clay beds have been subjected to lateral actuation of pipelines and the results of these tests are shown in Oliveira *et al.* (2005) and Oliveira *et al.* (2010).

4. Cpt Tests In Fine Tailings

4.1. Characteristics of the fine tailings

The fine tailings studied in this work came from the exploitation of iron ore by Samarco Mineração S.A., located in the city of Mariana, State of Minas Gerais, Brazil. The main minerals present are haematite, goethite (limonite), and magnetite. For the purpose of the tests carried out here the fine tailings were dried in an oven and homogenized to obtain representative samples. The grain size analysis resulted in the following percentages: clay 7%, silt 71%, and fine sand 22%. The X-ray diffraction indicated predominance of haematite Fe_2O_3 and quartz silica, confirmed by the chemical analysis, which resulted in 40.9% Fe_2O_3 and 53.6% silica.

The fine iron tailings were found to be non-plastic. Geotechnical properties of the studied soil are: specific gravity G_s = 3.22; minimum dry density = 1.36 g/cm^3; maximum dry density = 2.16 g/cm^3; field density = 1.6 to 2.2 g/cm^3 (average 1.97 g/cm^3); coefficient of consolidation c_v = 0.5-3.0 x 10^{-6} m^2/s (average 1.4 x 10^{-6} m^2/s); coefficient of permeability = 5-8 x 10^{-6} m/s; and compression ratio CR = $C_c/(1 + e_o)$ = 0.05, characteristic of a low compressibility soil.

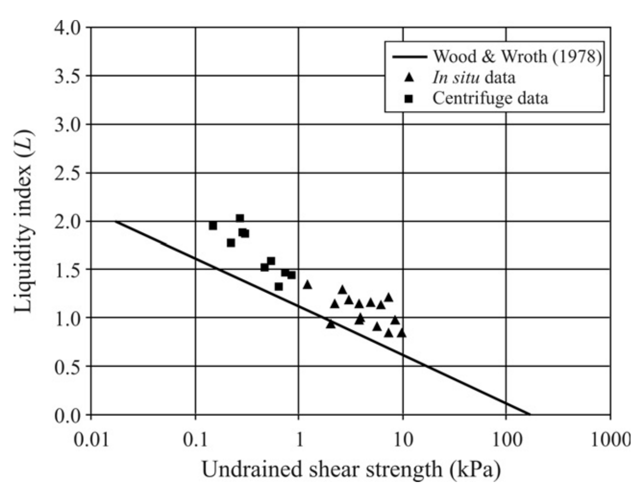

Figure 12 - Comparison between liquidity limit and undrained shear strength.

4.2. CPT design and assembly

The design of the mini-CPT penetrometer had to take into account a number of factors such as the maximum driving capacity of the radial centrifuge actuator (2000 N), the measuring capacity of the load cells (125 N), the maximum travel length of the tool (less than 18 cm), and the high resistance of the soil material to be tested. Also, the tool should be as light as possible, but still capable of measuring the soil resistance.

The mini-CPT was designed to measure the point load Q_b plus the total load Q_t which is the sum of Q_b and Q_s, the lateral load. Thus, the mini-CPT was designed with a 9 mm cone diameter, a 5 mm internal shaft diameter, 165 mm total length (including total load cell), and approximately 70 mm of free driving shaft (Fig. 13). These dimensions took into account the possibility of buckling of the CPT shaft, predicted according to Euler's formulation. The total weight of the mini-CPT including load cells was 323 g.

A general view of the developed mini-CPT can be seen in Fig. 14, where the location of the load cells installed in the equipment is shown. The point load cell positioned inside the metallic body is attached to the inner shaft and the cone tip. The total load cell bears both the point load and the shaft load.

4.3. Modelling of models

New centrifuge tests tools are usually verified using the "modeling of models technique" (Schofield, 1980).

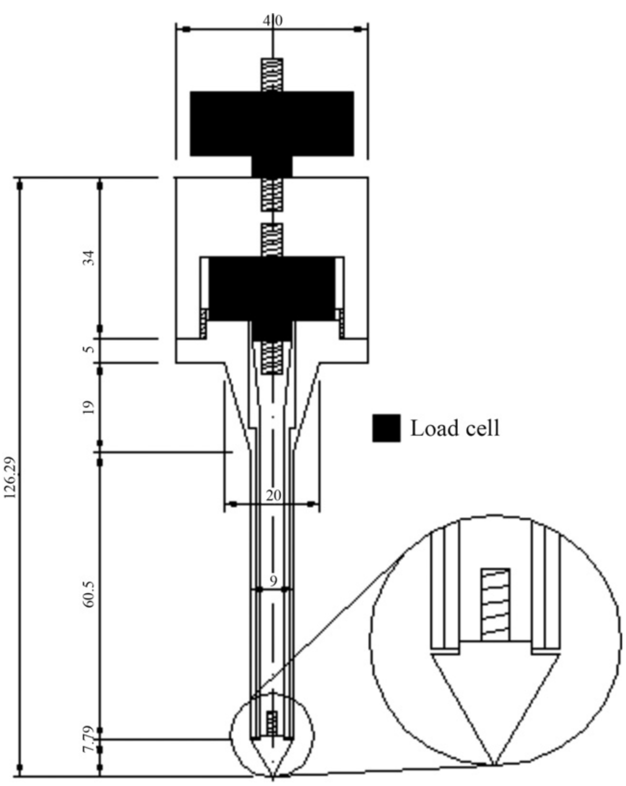

Figure 13 - Mini-CPT schematics (measurements in mm).

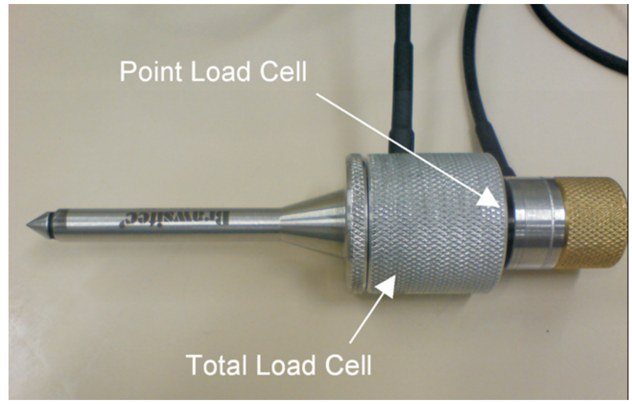

Figure 14 - General view of mini-CPT.

This procedure is realized by carrying out tests with different accelerations.

The tests were carried out using the tool in the silty tailings materials. The soil layers were moulded inside the strongbox with the centrifuge fully stopped. After that, the equipment was set to spin and the samples were consolidated at 50 *g* for 30 min, which is enough time to allow full consolidation. The final layers had a total height of 9 cm and average dry density equal to 1.80 g/cm^3 (relative density of 55%).

These test penetration velocities were standardized with the normalized velocity $V = 0.5$, defined by the expression (Finnie & Randolph, 1994):

$$V = \frac{vD}{c_v} \quad (6)$$

where v is the rate of cone penetration, D is the cone diameter, and c_v is the coefficient of consolidation. This value of $V = 0.5$ assures a fully undrained behaviour. The maximum penetration in the model was 6 cm, which corresponds to prototype depths of 1.5 m, 3.0 m, and 4.5 m for the 25 *g*, 50 *g*, and 75 *g* accelerations respectively.

Figure 15(a) shows the model scale point resistance profiles for test accelerations of 25 *g*, 50 *g*, and 75 *g*. Figure 15(b) presents the same point resistance profiles in prototype scale. All tests show good agreement, except for a slight deviation to the right in the 25 *g* test. This apparent increase in soil resistance is related to the overconsolidation conditions for the 25 *g* test, once the consolidation phase took place at 50 *g*. The good agreement observed in Fig. 15 is in accordance with a successful modelling of the model's procedure. Similar results were previously obtained for sands (Almeida, 1984).

Almeida (1984) used an in-flight mini-CPT apparatus to assess the strength profile of a Leighton Buzzard 30/52 uniform medium sand layer at centrifuge accelerations of 25 *g*, 50 *g* and 100 *g*. The samples were carefully prepared by placing the sand with a scoop, in submerge conditions, reaching a relative density of 47.8% and a void's ratio of 0.668. Figure 16 shows the results obtained by Almeida

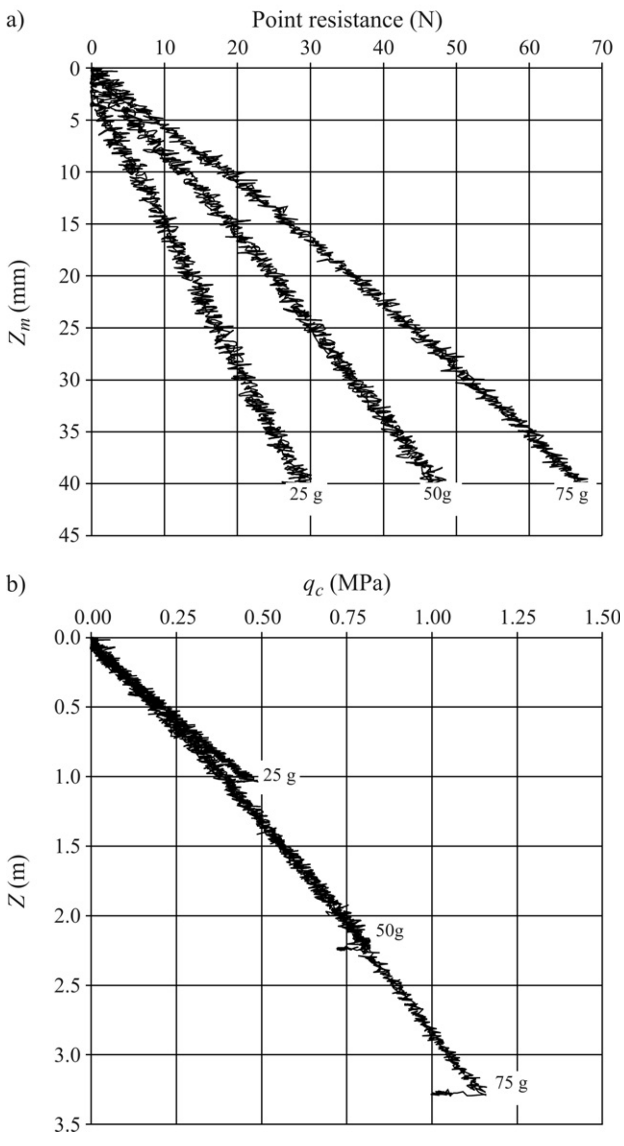

Figure 15 - Mini-CPT modelling of models tests with silty tailings: (a) point resistance in model scale and (b) q_c in prototype.

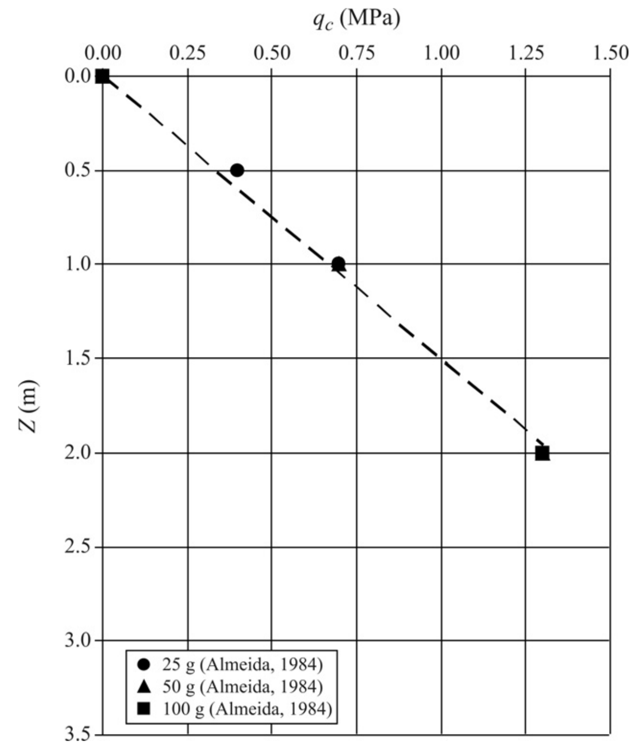

Figure 16 - Mini-CPT modelling of models tests for Leighton Buzzard sand (after Almeida, 1984).

(1984), which are very similar to those described in this work, despite of the different nature of the tested materials.

4.4. Strength parameters of the silt tailings

Strength parameters obtained from the mini-CPT tests are compared herein with the strength parameters measured in direct shear tests and triaxial tests, which are described first.

4.4.1. Direct shear tests on centrifuge samples

The preparation of centrifuge samples was similar to preparation of the samples for the mini-CPT test. After the consolidation stage and the complete drainage of the water, the centrifuge was halted and placed in a 90° position so that five test specimens could be extracted as shown in Fig. 17. The direct shear test moulds were inserted at a depth corresponding to twice their height in order to avoid surface interference.

The direct shear tests were carried out at vertical stresses of 100, 200, 300, and 400 kPa on saturated specimens and the results are shown in Table 2. These data presented negligible dilation and a mean effective friction angle $\phi' = 31.5°$. However strength data at low stress levels relevant to the centrifuge tests give $\phi' = 34.6°$ and this is the value to be compared with friction angles obtained from CPT tests performed in the tailings soil.

4.4.2. Triaxial tests

A set of CD triaxial tests were undertaken in silty tailings samples statically compacted at the optimum water content. The mean dry density obtained with this process was $\rho = 2.09$ g/cm^3. The confining pressures adopted for the tests were 100, 200, 300 and 400 kPa. The volumetric strain behaviour shows an overconsolidated material with an initial increase in volume followed by a small decrease. Figu-

Table 2 - Data from direct shear tests in the tailings soil.

Test	σ (kPa)	τ (kPa)	τ/σ	ϕ' (°)
1	115	80	0.69	34.6
2	232	147	0.63	32.4
3	350	197	0.56	29.4
4	462	260	0.56	29.4

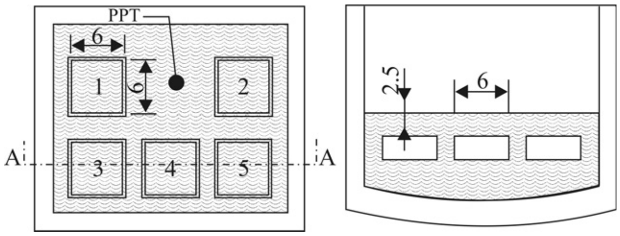

Figure 17 - Location of the direct shear specimens: (a) plan view and (b) cross section AA (dimensions in cm).

re 18 presents the triaxial CD results, displaying an internal friction angle of 41° and no cohesion.

4.4.3. Friction angles from CPT tests

A number of authors have developed theories or correlations between CPT tests and friction angles for non-cohesive soils. The methods proposed by Durgunoglu and Mitchell (1975) and Robertson & Campanella (1983) are quite often used (Schnaid, 2009; Lunne *et al.*, 1997) to estimate friction angles from CPT data. The method by Durgunoglu & Mitchell (1975) is based on bearing capacity theory. The method developed by Robertson & Campanella (1983) is based on correlations with CPT tests performed in calibration chambers on normally consolidated sands of medium compressibility. Both methods are based on the ratio between the measured point resistance q_c and the vertical *in situ* stress σ_{vo}. For $c' = 0$ soils, the bearing capacity factor N_q is equal to q_c/σ'_{v0}, which is the ratio between the measured point resistance q_c and the vertical effective stress σ'_{v0}. Chen & Huang (1996) have expressed these two methods using the equation

$$\tan\phi' = \frac{1}{C_1}\ln\left(\frac{\dfrac{q_c}{\sigma'_V}}{C_2}\right) \tag{7}$$

where the coefficients C_1 and C_2 are expressed as shown in Table 3.

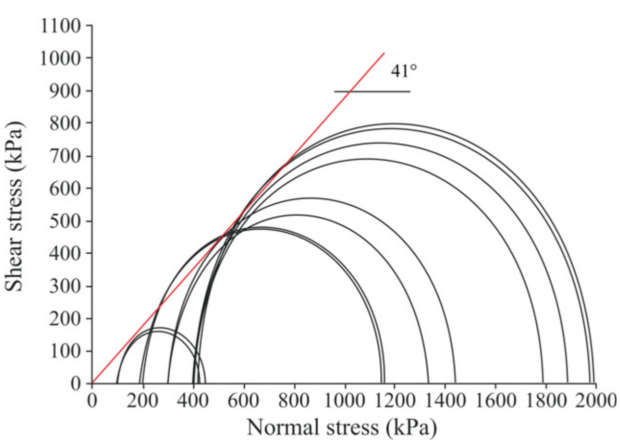

Figure 18 - Triaxial CD tests in silty tailings samples.

Table 3 - Coefficients for q_c-tan f ' correlations.

Method	C_1	C_2
Durgunoglu & Mitchell (1975)	7.629	0.194
Robertson & Campanella (1983)	6.820	0.266

According to Chen & Huang (1996), Durgunoglu & Mitchell's method (1975) is suitable for low compressibility sands and Robertson & Campanella's method (1983) is suitable for medium compressibility sands. Although the above methods have been developed for sands, they will be applied for the non-plastic silty soil studied here. This is a soil with granular behaviour ($c' = 0$), and thus this application appears to be reasonable.

The 50 *g* test was used to estimate the soil friction angle. Table 4 summarizes the values of point resistance and σ'_{v0} obtained at the prototype depths 0.5, 1, 1.5, and 2 m. Values of σ'_{v0} considered in Table 4 take into account the small non-linearity of σ'_{v0} with the centrifuge radius (Schofield, 1980) important in small centrifuges. Data of $N_q = q_c/\sigma'_{v0}$ are also shown in Table 4.

Values of friction angles using the two methods are presented in Table 5. It is observed in Table 5 that values of ϕ' appear to decrease slightly with depth and the average friction angles ϕ' obtained by the two methods are quite close and are also in agreement with $\phi' = 34.6°$ obtained in direct shear tests at low stress levels. Higher values in CPT tests for loose samples are expected once a relative compaction of the soil ahead of the cone can increase the friction angle.

Friction angle values associated with the triaxial tests (41°) are higher than those from direct shear and CPT tests.

Table 4 - Point resistance, vertical stresses and bearing capacity factors.

Depth (m)	q_c (kPa)	σ'_V (kPa)	$N_q = q_c/\sigma'_{v0}$
0.5	190.3	5.3	36
1.0	390.1	10.8	36
1.5	579.0	16.4	35
2.0	738.2	22.1	35

Table 5 - Data for friction angles from CPT tests.

Depth (m)	ϕ' (°) - D&M	ϕ' (°) - R&C
0.5	34.4	35.7
1.0	34.4	35.8
1.5	34.3	35.6
2.0	34.0	35.3
Average values	34.3	35.6

This result is probably related with the high relative density (91%) obtained with the static compaction procedure, which is much higher than those obtained in the centrifuge tests (55%).

5. Conclusions

The design and development of instrumentation for centrifuge geotechnical purposes requires the best tools to measure the desired parameter. Also it demands that the variables involved, such as the materials to be tested and equipment limitations, are very well known and controlled.

The T-bar penetrometer developed for this research was used in centrifuge tests to measure the undrained strength of reconstituted samples of Guanabara Bay clay.

Numerical analyses were carried out with the aim of obtaining a variation in the factor N_b with the normalized depth, which was shown to be consistent with the extreme values available in the literature for shallow and deep cases. Based on this formulation the undrained strength profile was calculated for a number of tested samples. The T-bar centrifuge test data carried out for high water content values were complemented by measurements of water content values for the clay.

The measured centrifuge S_u profile agreed well with the field profile obtained by a vane and triaxial tests. Also the relationship between water content and S_u seemed to be coherent with the *in situ* measurements.

Additionally, a comparison between liquidity limit and undrained shear strength show a clear linear behaviour that is very close to the line proposed by Wood & Wroth (1978). All these evidences confirm the overall consistency of the measured data.

The mini-CPT apparatus developed for this research was designed for the specific purpose of testing embankments in silty tailings materials. The tests showed the efficiency of the miniature tool, as well as the possibility of assessing a continuous resistance profile of in-flight layers.

The modelling of the models technique, a highly established procedure to evaluate consistency in centrifuge modelling simulations, was applied in 3 different *g* levels leading to coherent results. Strength parameters were also obtained from the mini-CPT tests and compared with strength parameters measured in direct shear tests and triaxial, leading to consistent results.

The strength profile was also compared with other centrifuge mini-CPT tests in sand soil confirming the expected behaviour.

Finally, both tools developed for in flight strength profile measurements in clayey and sandy soils were tested and the results compared with conventional tests showing an overall consistency and reliability of the measured data.

References

Almeida, M.S.S. (1982) The undrained behaviour of the Rio de Janeiro clay in the light of Critical State theories. Solos e Rochas, v. 5:2, p. 3-24.

Almeida, M.S.S. (1984) Stage Constructed Embankments on Soft Clays. Ph.D. Thesis, University of Cambridge, Cambridge.

Almeida, M.S.S. & Parry, R.H.G. (1984) Penetrometer apparatus for use in the centrifuge during flight. Symposium on the Application of Centrifuge Modelling to Geotechnical Design, Manchester University, Manchester, pp. 47-66.

Almeida, M.S.S. & Parry, R.H.G. (1987) Miniature vane and cone penetration tests during centrifuge flight. Proc. International Symposium on Laboratory and Field Vane Shear Strength Testing, Tampa, Flórida, ASTM ASTP 1014, pp. 209-219.

Almeida, M.S.S.; Costa, A.M.; Amaral, C.S.; Benjamin, A.C.; Noronha Jr, D.B.; Futai, M.M. & Mello, J.R. (2001) Pipeline failure on very soft clay. Proc. 3rd International Conference on Soft Soil Engineering, Hong Kong, Balkema, pp. 131-138.

Almeida, M.S.S. & Marques, M.E.S. (2002) The behaviour of Sarapuí soft organic clay. International Workshop on Characterisation and Engineering Properties of Natural Soils, Singapore, v. 1, pp. 477-504.

Barboza-Cruz, E.R. & Randolph, M.F. (2005) Bearing capacity and large penetration of a cylindrical object at shallow embedment. Frontiers in Offshore Geotechnics, Perth, Australia, pp. 615-621.

Bolton, M.D.; Gui, M.W.; Garnier, J.; Corte, J.F.; Bagge, G.; Laue, J. & Renzi, R. (1999) Centrifuge cone penetration test in sand. Geotechnique, v. 49:4, p. 543-552.

Borges, R.G.; Amaral C.S.; Costa A.M.; Oliveira, J.R.M.S.; Almeida, M.S.S. & Almeida M.C.F. (2005) Avaliação Numérica da Reação do Solo para Comparação com Testes Centrífugos de Dutos. RT MC no 037/2005 PETRO-BRAS/CENPES.

Calle, J.A.C. (2007) Comportamento Geomecânico de Resíduos Sólidos Urbanos. D.Sc. Thesis, Universidade Federal do Rio de Janeiro, Rio de Janeiro.

Chen, J.W. & Juang, C.H. (1996) Determination of drained friction angle of sands from CPT. Journal of Geotechnical Engineering, ASCE, pp. 374-381.

Costa, A.M. (1984) Uma Aplicação de Métodos Computacionais e Princípios de Mecânica das Rochas no Projeto e Análise de Escavações Destinadas à Mineração Subterrânea. D.Sc. Thesis, Universidade Federal do Rio de Janeiro, Rio de Janeiro.

Durgunoglu, H.T. & Mitchell, J.K. (1975) Static penetration resistance soil. I: Analysis. Proc. ASCE Spec. Conf. On In-Situ Measurement of Soil Parameters, ASCE, v. 1, pp. 151-171.

Esquivel, E.R. & Ko, H. Y.. (1995) Interpretation of Piezocone Results from Centrifuge Testing. Proc. International Symposium on Cone Penetration Testing CPT'95, Linkoping, Balkema, pp. 13-18.

Finnie, I.M.S. & Randolph, M.F. (1994) Punch-through and liquefaction induced failure of shallow foundations on calcareous sediments. Proc. International Conference on Behaviour of Off-Shore Structures – BOSS'94, Boston, v. 1, pp. 217-230.

Gurung, S.B.; Almeida, M.S.S. & Bicalho, K.V. (1998) Migration of zinc through sedimentary soil models. Proc. International Conference Centrifuge 98, Tokyo, v. 1, pp. 589-594.

Lunne, T.; Robertson, P.K. & Powell, J.J.M. (1997) Cone penetration testing in geotechnical practice. 1st edn., London, Blackie Academic & Professional.

Motta, H.P.G. (2008) Comportamento de um Rejeito de Transição em Centrífuga Geotécnica. M.Sc. Dissertation, Universidade Federal do Rio de Janeiro, Rio de Janeiro.

Oliveira, J.R.M.S. (2005) Modelagem em Centrífuga de um Problema de Interação Solo-Estrutura. D.Sc. Thesis, Universidade Federal do Rio de Janeiro, Rio de Janeiro.

Oliveira, J.R.M.S.; Almeida, M.S.S.; Almeida, M.C.F. & Marques, M.E.S. (2006) Undrained strength of very soft clay soils used in pipeline studies centrifuge, ICPMG, Hong Kong, v. 2, pp. 1355-1360.

Oliveira, J.R.M.S.; Almeida, M.S.S.; Almeida, M.C.F.; Borges, R.G.; Amaral, C.S. & Costa, A.M. (2005) Physical and numerical modelling of lateral buckling of a pipeline in very soft clay. ISFOG-2005.

Oliveira, J.R.M.; Almeida, M.S.S.; Almeida, M.C.F. & Borges, R.G. (2010) Physical Modelling of Lateral Clay-Pipe Interaction. Journal of Geotechnical and Geoenvironmental Engineering, ASCE, July 2010, in press.

Pacheco, L.A. (2006) Modelagem Física e Numérica de um Duto Enterrado em Areia Sujeito a Deslocamento Lateral. M.Sc. Dissertation, Universidade Federal do Rio de Janeiro, Rio de Janeiro.

Randolph, M.F. & Houlsby, G.T. (1984) The limiting pressure on a circular pile loaded laterally in cohesive soil. Geotechnique, v. 34:4, p. 613-623.

Randolph, M.F. (2004) Characterization of soft sediments for offshore applications. Proc. Geotechnical and Geophysical Site Characterization, Rotterdam, Millpress, pp. 209-232.

Robertson, P.K. & Campanella, R.G. (1983) Interpretation of cone penetration tests. Part I: Sand. Canadian Geotechnical Journal v. 20:4, p. 718-733.

Schnaid, F. (2009) *In-Situ* Testing in Geomechanics. Francis and Taylor, 320 pp.

Schofield, A.N. (1980) Cambridge geotechnical centrifuge operations. Géotechnique, v. 25:4, p. 743-761.

Stewart, D.P. & Randolph, M.F. (1991) A new site investigation tool for the centrifuge. International Conference on Centrifuge Modelling, Boulder, pp. 531-538.

Technical Note

Soils and Rocks
v. 34, n. 1

The Influence of Laboratory Compaction Methods on Soil Structure: Mechanical and Micromorphological Analyses

Flavio A. Crispim, Dario Cardoso de Lima, Carlos Ernesto Gonçalves Reynaud Schaefer,
Claudio Henrique de Carvalho Silva, Carlos Alexandre Braz de Carvalho,
Paulo Sérgio de Almeida Barbosa, Elisson Hage Brandão

Abstract. This paper addresses the influence of the static and dynamic laboratory compaction procedures in the compaction curves and mechanical strength of two residual soils from the Zona da Mata Norte, in the state of Minas Gerais, Brazil. The laboratory testing program was directed to: (i) two gneissic residual soils, respectively, with silty-sandy clay and clayey-silty sand textures; (ii) compaction of specimens at the standard Proctor compaction effort and at the optimum water content (w_{ot}), as well as at w_{ot} - 3% and w_{ot} + 2%; (iii) determination of the unconfined compressive strength of the compacted specimens; (iv) micromorphological analysis of thin sections of the compacted specimens using optical microscopy; (v) statistical analysis of the laboratory testing program data. Conclusions are, as follows: (i) there was statistically significant influence of the compaction procedures on the optimum compaction parameters; (ii) for both soils, significant structural changes represented by variations in the unconfined compression strength were observed evidencing the importance of the soils formation processes in their mechanical responses when compacted; and (iii) differences in the soils structures produced by the static and dynamic compaction procedures were identified through incorporation of the micromorphological analysis.

Keywords: tropical soils, static and dynamic laboratory compaction curves, unconfined compressive strength, statistical and micromorphological analyses.

1. Introduction

Compaction can be understood as a procedure that causes reduction of soil volume without variation in its water or mass content; therefore, it is a process that essentially alters soil structure. In the 30's, Ralph R. Proctor brought an important contribution for the development of the soil compaction technique, showing the relationship between dry apparent specific mass, water content and compaction energy.

Internationally, the most common compaction test is the Proctor, which in Brazil has been regulated by the Brazilian Association of Technical Standards (ABNT, 1986) and by the former Brazilian National Roads Department (DNER, 1994), nowadays the Brazilian National Department of Transportation Infrastructure (DNIT). However, in geotechnical laboratories, different compaction methods have been used in an attempt to come as close as possible to real field situations, and to reduce specimen compaction time.

Since compaction is a process that basically modifies soil structure, it is important to analyze the effects of applying different compaction procedures on the soil compaction curve, as well as it should be emphasized that some aspects of the mechanical response of compacted soils are still poorly understood, mainly regarding tropical soils, because morphological and microstructural features related to geotechnical behavior are rarely quantified or even observed (Schaefer, 2001; Viana *et al.*, 2004). For instance, the optical microscopy technique is a process that has rarely been used for such purpose, even though it allows the examination of soil composition in microscopic detail, such as size, arrangement and particle orientation, and the observation of soil mass pores and shear zones.

Particularly, in studies of soil morphology, the optical microscope allows images over 1,000 times bigger, although it is common to resize them from 10 to 100 (Resende *et al.*, 2002). These authors assert that image studies through optical microscopy starting from thin sections (of approximately 25 μm thick) allow for identification of the

Flavio Alessandro Crispim, Doctoral Student, Departamento de Engenharia Civil, Universidade Federal de Viçosa, 36.570-000 Viçosa, MG, Brazil. e-mail: e-mail: crispim_br@yahoo.com.br.
Dario Cardoso de Lima, Ph.D., Professor, Departamento de Engenharia Civil, Universidade Federal de Viçosa, 36.570-000 Viçosa, MG, Brazil. e-mail: declima@ufv.br.
Carlos Ernesto Gonçalves Reynaud Schaefer, Ph.D., Associate Professor, Departamento de Solos, Universidade Federal de Viçosa, 36.570-000 Viçosa, MG, Brazil. e-mail: carlos.schaefer@ufv.br.
Cláudio Henrique de Carvalho Silva, Ph.D., Associate Professor, Departamento de Engenharia Civil, Universidade Federal de Viçosa, 36.570-000 Viçosa, MG, Brazil. e-mail: silvac@ufv.br.
Carlos Alexandre Braz de Carvalho, D.Sc., Associate Professor, Departamento de Engenharia Civil, Universidade Federal de Viçosa, 36.570-000 Viçosa, MG, Brazil. e-mail: cabraz@ufv.br.
Paulo Sérgio de Almeida Barbosa, M.Sc., Assistant Professor, Departamento de Engenharia Civil, Universidade Federal de Viçosa, 36.570-000 Viçosa, MG, Brazil. e-mail: pbarbosa@ufv.br.
Elisson Hage Brandão, Civil Engineer. e-mail: elissonhage@yahoo.com.br.
Submitted on January 7, 2010; Final Acceptance on October 27, 2010; Discussion open until August 31, 2011.

organization (form) of soil particles that are over 20 μm, as well as it is harder to identify smaller particles, and almost impossible to visualize those smaller than 5 μm.

The evaluation of the influence of different compaction methods in the soil compaction curve and, consequently, in its mechanical behavior (shear strength, compressibility and permeability) is indeed a difficult task, once there is a great number of factors involved and related to the interaction and stress distribution in the solid, liquid and gas phases, capillarity phenomena and osmotic pressures. In order to advance studies on this matter, this paper addresses the influence of the static and dynamic soil compaction procedures using as elements of analysis basic soil compaction parameters, and data from unconfined compression tests and micromorphological analysis.

2. Materials and Methods

The study was carried out in the Laboratory of Civil Engineering at the Universidade Federal de Viçosa – UFV, located in the city of Viçosa, Minas Gerais state, Brazil, using two gneissic residual soils, as follows: (i) soil 1 - the soil sample was collected in the B horizon of a cut slope in the Campus of the UFV at the geographical coordinates 20°45'35" S and 42°52'28" W. It is a mature residual soil, pedologically classified as red yellow latosol (EMBRAPA, 2006), and according to Trindade (2006) in its clay fraction there is predominance of kaolinite and goethite, and traces of gibbsite, as well as after compaction there is a micro-aggregate coalescence tendency, resulting in a highly cohesive and compact structure; (ii) soil 2 - the soil sample was collected in the C horizon of a cut slope in the Secundino Village located in the Campus of the UFV at the geographical coordinates 20°45'38" S and 42°52'25" W. It is a young residual soil, and following Trindade (2006) description its sand and silt fractions are constituted, basically, by quartz, mica and feldspars, and its clay fraction is predominantly composed by kaolinite with traces of goethite. Structurally, this soil shows a bridge structure (argillaceous bridges connecting the grains) involved in scarce plasma.

The geotechnical characterization of soils 1 and 2 followed the ABNT technical standards including grain size distribution (ABNT, 1984a), liquid limit (ABNT, 1984b), plastic limit (ABNT, 1984c), and specific gravity of soil solids (ABNT, 1984d).

In an attempt to reproduce the compaction effort and water content commonly used in the field compaction of landfills and sub-grade soil layers, all specimens were compacted at the standard Proctor compaction effort (ABNT, 1986) adopting nine repetitions of the compaction curve at the following water contents: optimum (w_{ot}); optimum minus 3% (w_{ot} -3%); and optimum plus 2% (w_{ot} + 2%). All specimens were compacted 24 h after mixing in order to reach equilibrium water content in the soil mass. The compaction tests were carried out through dynamic and static compaction laboratory procedures, as follows: (i) dynamic compaction (ABNT, 1986) using the standard Proctor compaction cylinder to produce three-layer compacted specimens 0.100 m in diameter and 0.127 m in height and determining the dry unit weight (γ_d) at each selected water content; (ii) static compaction using a hydraulic press to impose the required force to each layer of three layer specimens in order to produce the desired γ_d determined via dynamic compaction at the selected water contents. It should be emphasized that in the static compaction procedure there was no control of the applied force to the specimen; therefore, only the mass and height layers were controlled. The acceptance criteria adopted for specimen preparation was water content maximum deviation of ± 0.3%.

The unconfined compression strength (UCS) of the compacted specimens was determined following the ABNT (1992) at the deformation rate of 1.25 x 10^{-5} m/s. The statistic tests t and F were applied to the UCS data in order to evaluate the influence of the compaction procedures in the soils structures, considering the 5% probability level in all analyses.

As illustrated in Fig. 1, the micromorphological study was directed to the analysis of thin sections cut from the medium section of four specimens of each soil compacted statically and dynamically at the water contents w_{ot} -3% and w_{ot}.

The micromorphological analysis was carried out using an optical microscope according to the following procedure:

• The compacted specimens were placed and kept in a 35 °C stove during two days. Subsequently, they were impregnated with the resin Revopal T-208 with Bayer blue colorant in a mixture 1:1 with styrene monomer, adding 6 drops of catalyzer for each 200 mL of mixture;

• After impregnation, 0.025 m x 0.047 m polished thin sections were taken from the direction of the specimen cylinder axis and analyzed using the optical microscope OLYMPUS DX-40 equipped with digital camera (NIKON Coopix);

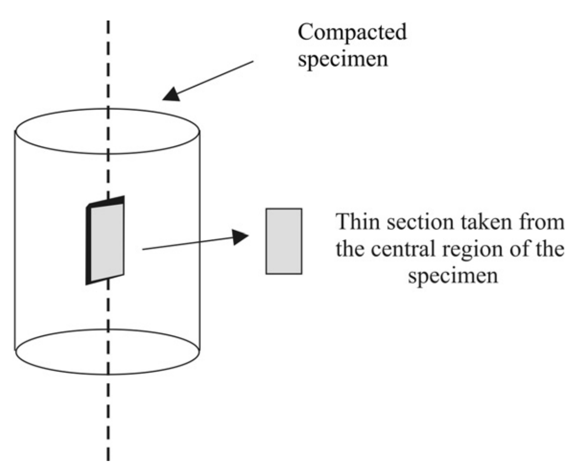

Figure 1 - Position of a thin section in the compacted specimen.

• Descriptions of microstructure and porosity followed the recommendations of Fitzpatrick (1993), and emphasizing the micromorphological and mineralogical aspects of geotechnical relevance;

• The QUANTIPORO software (Fernandes Filho & Viana, 2001) was used to measure porosity, plasma and grains adopting the average means of data from 5 to 8 photomicrographs taken from different regions of each thin section.

Figure 2 summarizes all activities developed in the research program.

3. Results and Discussions

Table 1 shows the geotechnical characterization data of soils 1 and 2, and Fig. 3 presents theirs grain size distributions according to ABNT (1995).

0 summarizes compaction data at the standard Proctor energy and water contents of w_{ot} - 3%, w_{ot} and w_{ot} + 2%, and Fig. 4 shows the compaction curves and unconfined compression data from laboratory tests performed in specimens of soils 1 and 2.

From Fig. 4, it was observed that the static compaction mode produced soil specimens with higher and lower shear strength, respectively for soils 1 and 2, emphasizing the influence of soils formation processes in their mechanical strength.

Figure 5 shows relative differences between the mean values of the parameters γ_d and UCS of soils 1 and 2, adopting the dynamic compaction data as reference. For practical engineering applications, the relative differences between the γ_d mean values are not significant, not over 1% for soil 1 and 3% for soil 2; on the other hand, regarding the UCS mean values, the relative differences are higher, reaching approximately 37% for soil 1 and 20% for soil 2, which emphasizes the significant influence of the compaction procedure on soil mechanical strength.

Table 1 - Geotechnical characterization and classifications of soils 1 and 2.

Properties	Soil 1	Soil 2
Grain size distribution (%)		
Clay ($\Phi \leq 0.002$ mm)	66	7
Silt ($0.002 < \Phi \leq 0.06$ mm)	4	25
Sand ($0.06 < \Phi \leq 2$ mm)	30	68
Gravel ($\Phi > 2$ mm)	0	0
Atterberg limits (%)		
Liquid limit (LL)	74	27
Plasticity index (PI)	48	12
Specific weight of grains (kN/m^3)		
γ_s	27.17	24.91
Soil classification		
TRB	A-7-5(20)	A-2-6(0)
USC	CH	SC
MCT (Trindade, 2006)	LG'	NA'

Table 3 introduces the results of the statistical analyses applied to γ_d and UCS data from soils 1 and 2 at the 5% significance level. Regarding the parameter $\gamma_{d,}$ there are significant statistical differences between the data from the static and the dynamic compaction procedures, except for specimens of soil 1 compacted at the water content w_{ot} + 2%; on the other hand, considering the UCS parame-

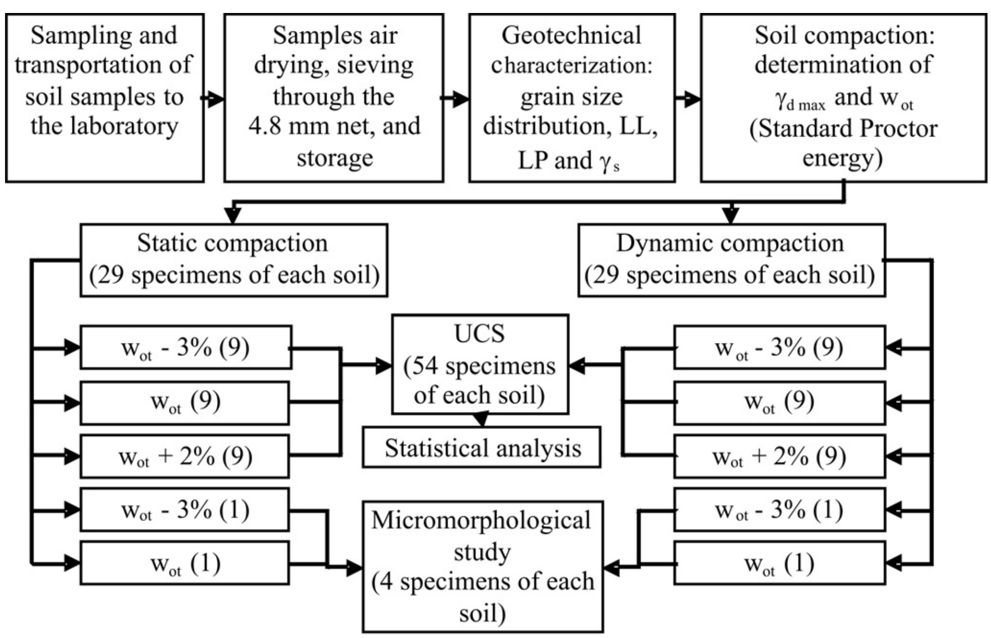

Figure 2 - Summary of the research program.

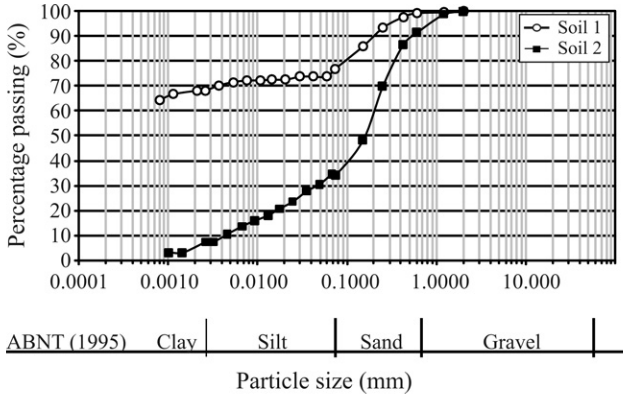

Figure 3 - Grain size distribution curves of soils 1 and 2.

ter, the results of the statistical analysis confirm that the compaction procedure affects the soils mechanical strength, except for specimens of soil 1 compacted at the water content $w_{ot} + 2\%$.

Figures 6 and 7 present photomicrographs taken from thin section of specimens from soils 1 and 2 statically and dynamically compacted at the water contents w_{ot} - 3% and w_{ot}, and Fig. 8 introduces the respective porosity data determined using the QUANTIPORO software (Fernandes Filho & Viana, 2001).

At the water content w_{ot}, Fig. 6a shows that the statically compacted specimens of soil 1 present features of original microagreggation, noticing original nodules, for-

Table 2 - Compaction data of specimens from soils 1 and 2.

Soil	w_{ot} - 3% (%)	γ_d (kN/m^3)	w_{ot} (%)	$\gamma_{d\,max}$ (kN/m^3)	w_{ot} + 2% (%)	γ_d (kN/m^3)
1	27.50	13.62	30.50	14.18	32.50	13.78
2	11.90	17.15	14.90	17.42	16.90	17.15

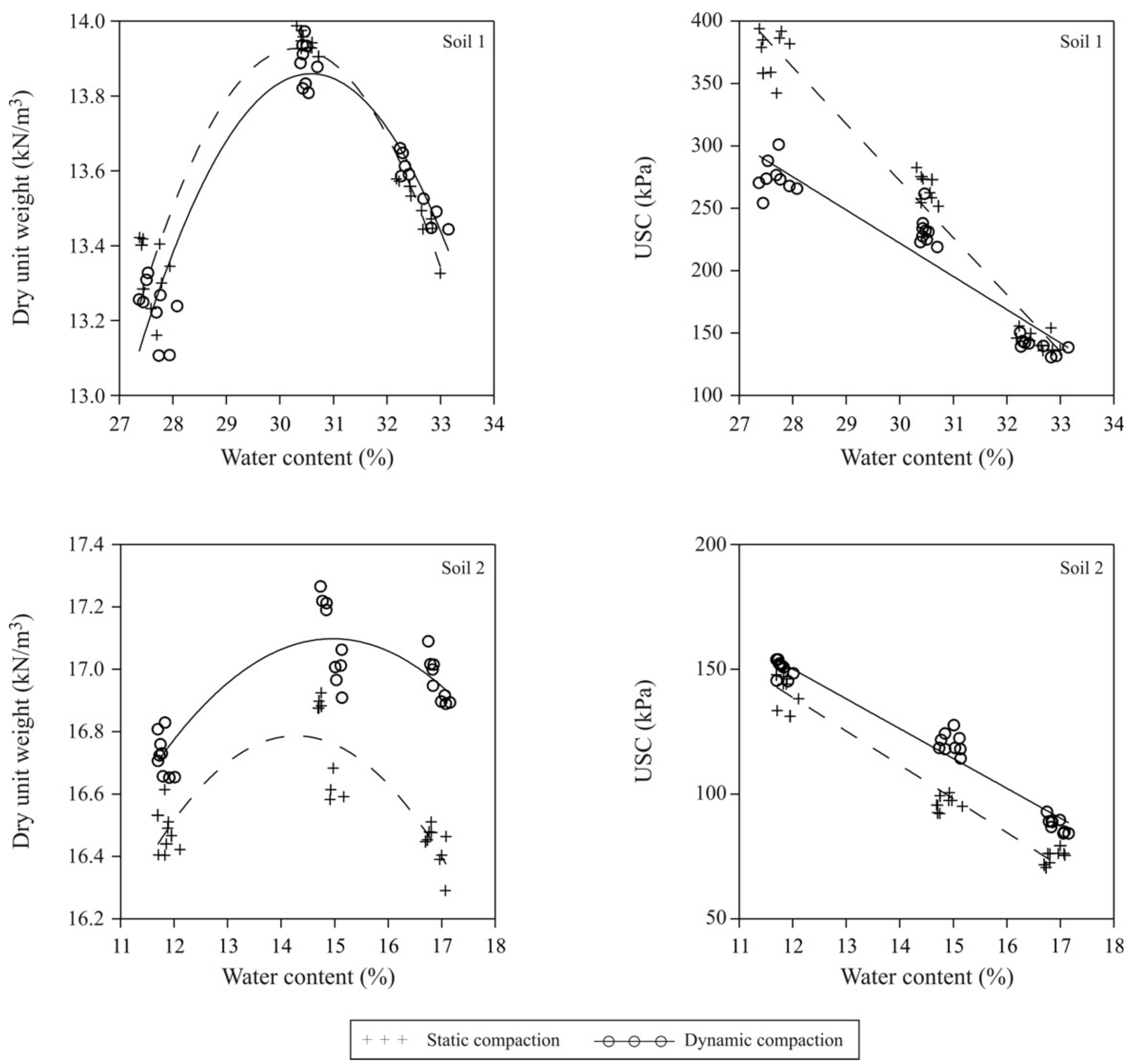

Figure 4 - Compaction curves and unconfined compressive strength (UCS) of soils 1 and 2.

Table 3 - Results from statistical analysis applied to data from soils 1 and 2 at 5% probability level.

Evaluated parameter	w_{ot} - 3%	w_{ot}	w_{ot} + 2%	w_{ot} - 3%	w_{ot}	w_{ot} + 2%
	Soil 1			Soil 2		
γ_d	*	*	Ns	*	*	*
RCNC	*	*	Ns	*	*	*

(*) indicates the occurrence of significant differences, and (Ns) that there are no significant statistical differences at 5% probability level.

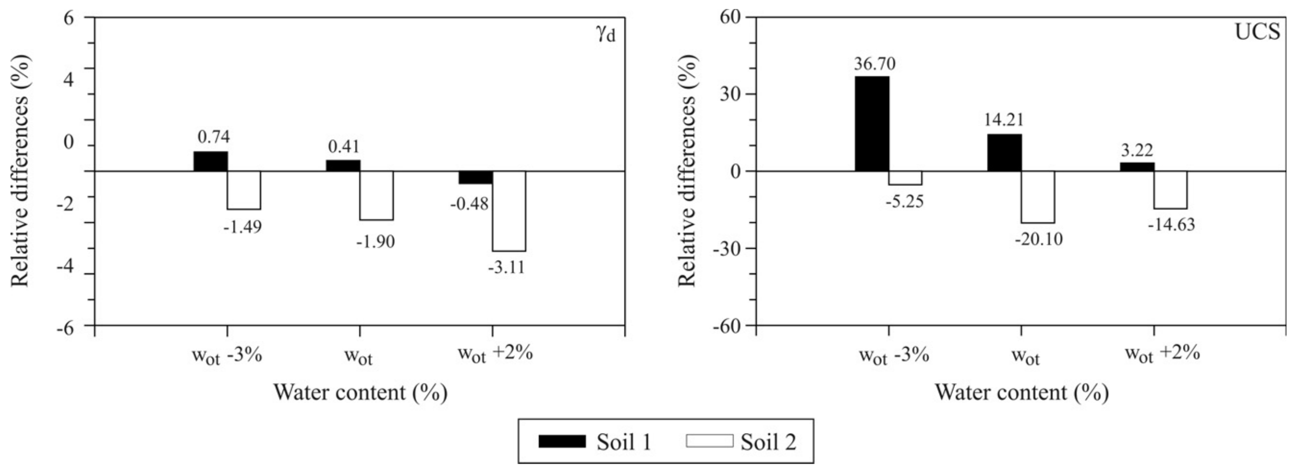

Figure 5 - Relative differences between mean values of the parameters γ_d and RCNC of soils 1 and 2, adopting the dynamic compaction data as reference.

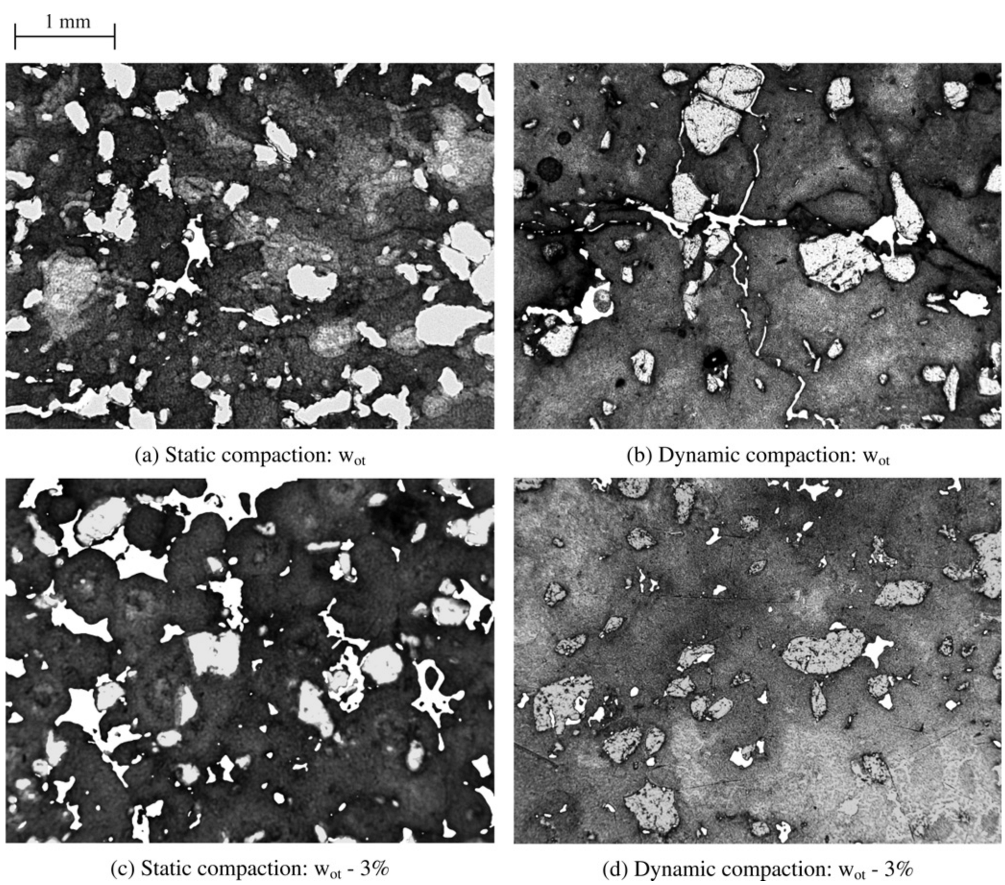

Figure 6 - Photomicrographs taken from thin section obtained from specimens of soils 1 and 2 statically and dynamically compacted at the water contents w_{ot} and w_{ot} - 3%.

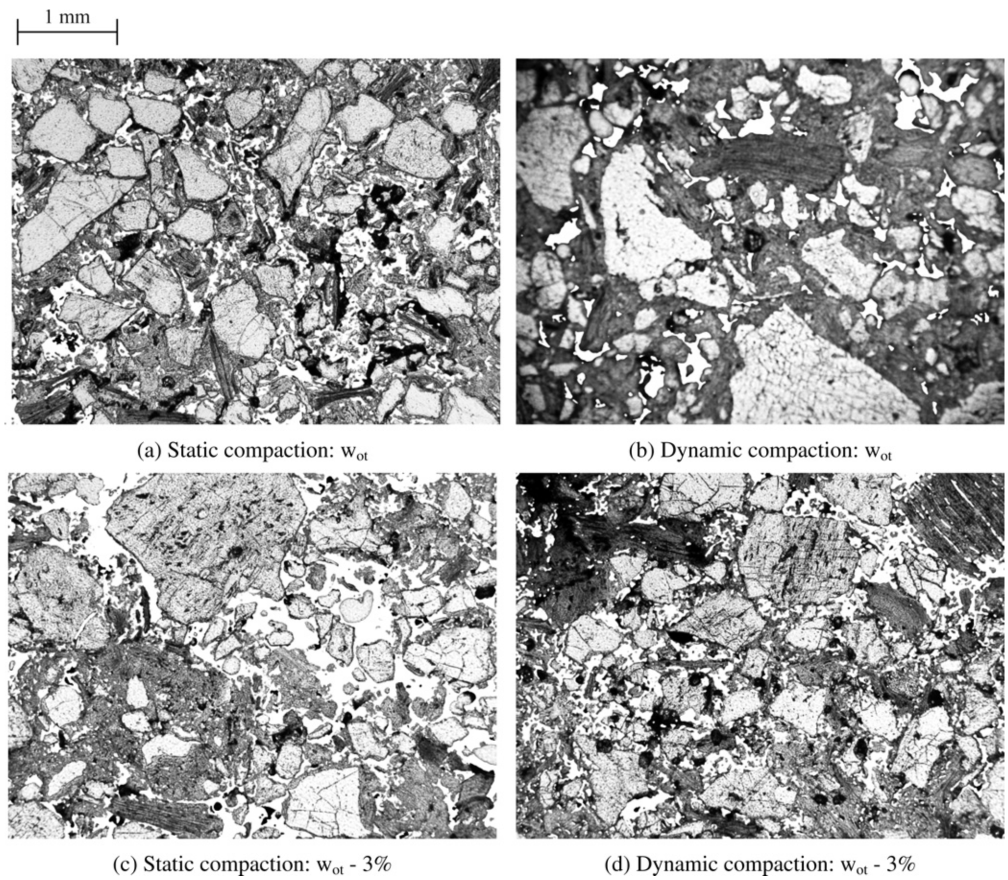

Figure 7 - Photomicrographs taken from thin section obtained from specimens of soils 1 and 2 statically and dynamically compacted at the water contents w_{ot} and w_{ot} - 3%.

mation of isolated gaps and fissured and oriented porosity, and low porosity, around 3%, as depicted in Fig. 8. On the other hand, at this same water content, Fig. 6b supports that the dynamically compacted specimens present a few original microaggregation features, with porosity almost all lost, around 2%, as presented in Fig. 8. At the water content w_{ot} - 3%, as showed in Fig. 6c and Fig. 6d, the static compaction applied to soil 1 produced structure with strong features of original microaggregation and gaps, and porosity

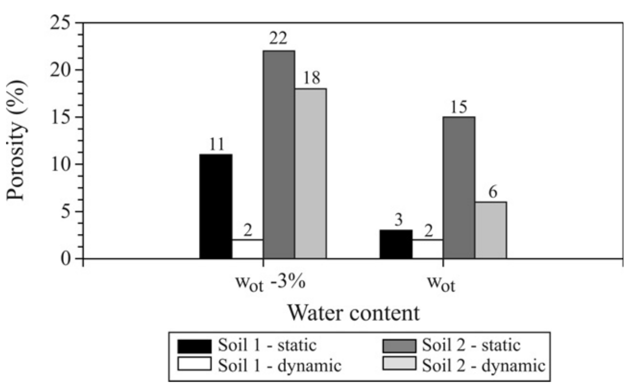

Figure 8 - Porosity data obtained from photomicrographs taken from thin sections of specimens of soils 1 and 2 statically and dynamically compacted at the water contents w_{ot} and w_{ot} - 3%.

around 11% as indicated in Fig. 8. From another standpoint, the dynamic compaction produced partially bonded microstructured argillaceous plasma (coalited), with the original microaggregation destroyed, and porosity reaching around 2%, which is much lower than the one imposed by the static compaction.

It should be emphasized that soil 1 was collected in the B horizon from the profile and exhibits silty-sandy clay texture, with significant clay fraction of 66%, accordingly to Table 1. Geotechnically, it is classified as mature residual soil, and pedologically, as red-yellow latosol, indicating occurrence of advanced pedogenetic formation processes. It also presents granular structure, with well individualized granules and highly porous aspect that can present potential collapse according to Azevedo (1999). Therefore, in soil 1 specimens there can be predominance of interparticle forces that were affected or destroyed by the dynamic compaction, producing structures with lower shear strength. This kind of behavior is compatible with the one described by Bueno *et al.* (1992) when analyzing the effect of dynamic compaction in a red-yellow latosol in comparison with its mechanical response under undisturbed field condition.

On the other hand, Soil 2 specimens compacted statically at the water content w_{ot} presented porosity close to those compacted dynamically, respectively 22% and 18% as presented in Fig. 8. However, the statically compacted specimens showed a fairly uniform distribution of porosity, and those dynamically compacted specimens presented isolated pores, as revealed in Fig. 7a and 7b. This behavior may be related to the higher mechanical strength of the specimens compacted dynamically, as presented in Fig. 4, because once the pores are isolated the soil structure (plasma and grains) can resist better to the shear effort than that permeated by an uniform pore distribution. From another standpoint, at the water content w_{ot} - 3% the static compaction produced porosity around 15%, and the dynamic compaction less than half of that, 6%, as illustrated in Fig. 8; in this case, certainly it is possible to associate the higher mechanical strength of the dynamically compacted specimens to their lower porosity.

It should be also stressed that the sample of soil 2 was collected in the C horizon from the profile and presents clayey-silty sand texture, with considerable sand fraction accordingly to Table 1 (around 68%). From the results presented in Fig. 7, it is possible to explain the higher efficiency of dynamic compaction of the specimens mainly due to the significant influence of vibration on the gradual sand particles arrangement and, consequently, on the efficiency of the compaction procedure as asserted by Rico & Del Castillo (1976), Guedes de Melo (1985) and Hilf (1991).

4. Conclusions

This research brought up the influence of the compaction mode (static and dynamic) in the compaction parameters and in the structure of two residual soils. The conclusions from this study are the following:

• Compared to the dynamic compaction, the static procedure produced specimens with higher UCS for the clayey soil (soil 1), and lower UCS for the granular soil (soil 2), bringing up the importance of soils formation processes in their mechanical responses;

• Considering the applied compaction methods, statistically significant differences were identified in the parameters γ_d and UCS of both soils, except for specimens of soil 1 compacted 2% above the optimum. Therefore, the use of the static compaction procedure in laboratory to obtain compaction and mechanical strength parameters of soils for field applications requires careful study;

• Incorporation of the micromorphological analysis to the present study allowed to identifying differences in the structures produced by the static and dynamic compaction procedures.

Acknowledgments

The authors would like to express their acknowledgments to FAPEMIG for funding this research through the Grant TEC-APQ-00378-08, and to CAPES for granting a scholarship to the first author.

References

ABNT (1984a) Solo-Análise Granulométrica. NBR 7181, Rio de Janeiro, RJ, 13 pp.

ABNT (1984b) Solo-Determinação do Limite de Liquidez. NBR 6459, Rio de Janeiro, RJ, 6 pp.

ABNT (1984c) Solo-Determinação do Limite de Plasticidade. NBR 7180, Rio de Janeiro, RJ, 3 pp.

ABNT (1984d) Grãos de Slos que Passam na Peneira de 4,8 mm – Determinação da Massa Específica. NBR 6508, Rio de Janeiro, RJ, 8 pp.

ABNT (1986) Solo-Ensaio de Compactação. NBR 7182, Rio de Janeiro, RJ, 10 pp.

ABNT (1992) Solo Coesivo – Determinação da Resistência à Compressão Não Confinada – Método de Ensaio. NBR 12770, Rio de Janeiro, Rio de Janeiro, RJ, 4 pp.

ABNT (1995) Rochas e Solos. NBR 6502, Rio de Janeiro, RJ, 18 pp.

Azevedo, M.A.A (1999) Contribuição ao Estudo Geotécnico de Solos de Viçosa-MG. MSc. Dissertation, Universidade Federal de Viçosa, Viçosa, 169 pp.

Bueno, B.S.; Lima, D.C. & Minette, E (1992) Geotechnical aspects of Viçosa soils. Proc. US/Brazil Geotechnical Workshop: Applicability of Classical Soil Mechanics Principles to Structured Soils, Belo Horizonte, Brazil, November 23-25, pp. 349-354.

DNER (1994) Solos-Compactação Utilizando Amostras Não Trabalhadas. DNER-ME 129/94, Rio de Janeiro, RJ, 7 pp.

EMBRAPA (2006) Sistema Brasileiro de Classificação de Solos. 2ª ed. Embrapa, Rio de Janeiro, 306 pp.

Fernandes Filho, E.I. & Viana, J.H.M (2001) Quantiporo: um novo programa para tratamento e quantificação de imagens digitais para aplicações em ciência do solo. Anais, 28º Congresso Brasileiro de Ciência do Solo, Sociedade Brasileira de Ciência do Solo, Londrina, pp. 224.

Fitzpatrick, E.A. (1993) Soil Microscopy and Micromorfology. John Wiley & Sons, New York, pp. 304.

Guedes de Melo, F. (1985) Compactação de Aterros de Barragens de Terra. Laboratório Nacional de Engenharia Civil (LNEC), Lisboa, Portugal, pp. 117.

Hilf, J.W. (1991) Compacted fill. Fang, H.Y. (ed.) Foundation Engineering Handbook. 2nd ed. Van Nostrand Reinhold, New York, pp. 249-316.

Resende, M *et al.* (2002) Pedologia: Base para Distinção de Ambientes. 4ª ed. NEPUT, Viçosa, MG, pp. 338.

Rico, A. & Del Castillo, H. (1976) La Ingeniería de Suelos en las Vías Terrestres. Editorial Limusa, Mexico, v. 1, pp. 459.

Schaefer, C.E.R. (2001) Brazilian latosols and their B horizon microstructure as long-term biotic constructs. Australian Journal of Soil Research, n. 39, p. 909-926.

Trindade, T.P. (2006) Caracterização Tecnológica de Solos Residuais Estabilizados Quimicamente com vistas a

Aplicações em Estradas e em Obras Geotécnicas de Caráter Ambiental. D.Sc. Thesis, Universidade Federal de Viçosa, Viçosa, 254 pp.

Viana, J.H.M.; Fernandes Filho, E.I. & Schaefer, C.*e.g.*R. (2004) Effects of wetting and drying cycles in the latosols micro granular reorganization. Brazilian Soil Science Journal, n. 28, p. 1-9.

List of Symbols

$\gamma_{d\ max}$: maximum dry unit weight
γ_d: dry unit weight
γ_s: specific weight of grains
LL: liquid limit
PI: plasticity index
w_{ot}: optimum water content
w_{ot} - 3%: optimum water content minus 3%
w_{ot} + 2%: optimum water content plus 2%
MCT: Miniatura, compactado, tropical
TRB: Transportation Research Board
UCS: Unconfined compression strength
USC: Unified Soil Classification

SOILS and ROCKS
An International Journal of Geotechnical and Geoenvironmental Engineering

Publication of
ABMS - Brazilian Association for Soil Mechanics and Geotechnical Engineering
SPG - Portuguese Geotechnical Society
Volume 34, N. 1, January-April 2011

Author index

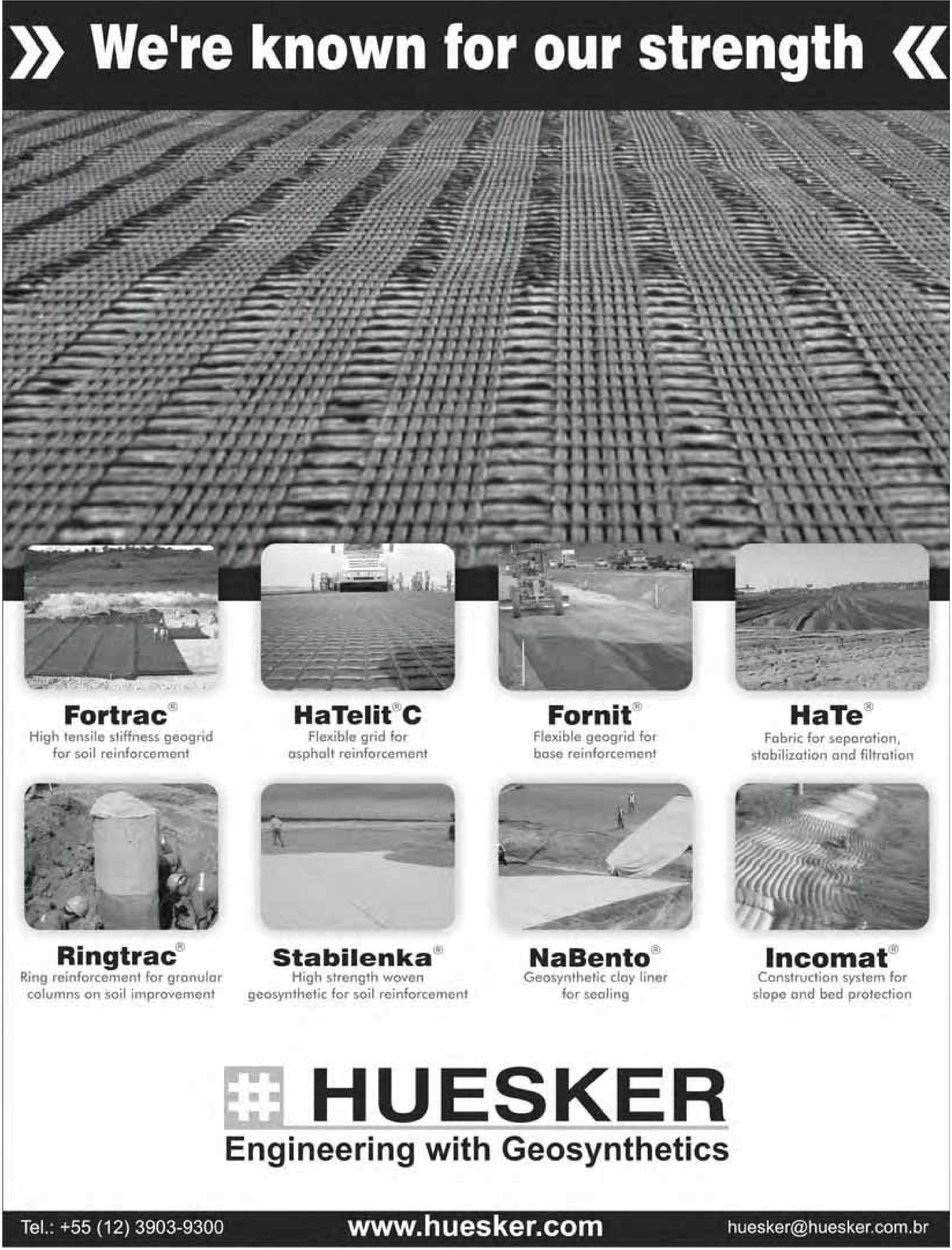
We're known for our strength
Fortrac®
High tensile stiffness geogrid for soil reinforcement
HaTelit®C
Flexible grid for asphalt reinforcement
Fornit®
Flexible geogrid for base reinforcement
HaTe®
Fabric for separation, stabilization and filtration
Ringtrac®
Ring reinforcement for granular columns on soil improvement
Stabilenka®
High strength woven geosynthetic for soil reinforcement
NaBento®
Geosynthetic clay liner for sealing
Incomat®
Construction system for slope and bed protection
HUESKER
Engineering with Geosynthetics
Tel.: +55 (12) 3903-9300
www.huesker.com
huesker@huesker.com.br


Simple drapery system


Surficial reinforcing systems


Rockfall barriers


Rockfall protection embankments

Tecnasol

Geotechnics and Foundation Engineering

Diaphragm Walls

Piles

Micropiles

Retaining Walls

Anchors

Soil nails

Monitoring

Repair Stuctures

Post tensioning

Grouting

Jet Grouting

Compensation Grouting

Tunnelling and

Underground Works

Sealing and

Waterproofing Systems

Site Investigations

Slope Stabilization

HEAD OFFICE
Edifício Edifer
Estrada do Seminário , 4 - Alfragide
2610 - 171 Amadora - PORTUGAL
Tel. 00 351 21 475 90 00 / Fax 00 351 21 475 95 00

Madrid
Calle Rodriguez Marín, Nº 88 1º Dcha
28016 Madrid – ESPANHA
Tel. 00 34 91 745 03 64 / Fax 00 34 91 411 31 87

Porto
Rua Eng. Ferreira Dias, nº 161 2º Andar
4100-247 Porto – PORTUGAL
Tel. 00 351 22 616 74 60 / Fax 00 351 22 616 74 69

Madeira
Rampa dos Piornais, n.º 5 - Sala 1
9000-248 Funchal – PORTUGAL
Tel. 00 351 291 22 10 33 / Fax 00351 291 22 10 34

Angola
Rua Alameda Van-Dúnem, n.º 265 R/c
Luanda - ANGOLA
Tel. 00 244 222 443 559 / Fax 00 244 222 448 843

Barcelona
Calle Comte d' Urgell, 204-208 6.º A
08036 Barcelona – ESPANHA
Tel. 00 34 93 419 04 52 / Fax 00 34 93 419 04 16

Sevilha
Polígono Industrial de Guadalquivir, C/ Artesania, 3
41120 Gelves (Sevilla) - ESPANHA
Tel. 00 34 955 762 833 / Fax 00 34 955 76 11 75

www.tecnasolfge.com

Instructions to Authors

Category of the Papers

Soils and Rocks is the scientific journal edited by the Brazilian Association for Soil Mechanics and Geotechnical Engineering (ABMS) and the Portuguese Geotechnical Society (SPG). The journal is intended to the divulgation of original research works from all geotechnical branches.

The accepted papers are classified either as an Article paper, a Technical Note, a Case Study, or a Discussion according to its content. An article paper is an extensive and conclusive dissertation about a geotechnical topic. A paper is considered as a technical note if it gives a short description of ongoing studies, comprising partial results and/or particular aspects of the investigation. A case study is a report of unusual problems found during the design, construction or the performance of geotechnical projects. A case study is also considered as the report of an unusual solution given to an ordinary problem. The discussions about published papers, case studies and technical notes are made in the Discussions Section.

When submitting a manuscript for review, the authors should indicate the category of the manuscript, and is also understood that they:

a) assume full responsibility for the contents and accuracy of the information in the paper;

b) assure that the paper has not been previously published, and is not being submitted to any other periodical for publication.

Manuscript Instructions

Manuscripts must be written in English. The text is to be typed in a word processor (MS Word or equivalent), using ISO A4 page size, left, right, top, and bottom margins of 25 mm, Times New Roman 12 font, and line spacing of 1.5. All lines and pages should be numbered. The text should be written in the third person.

The fist page of the manuscript is to include the title of the paper in English, followed by the names of the authors with the abbreviation of the most relevant academic title. The affiliation, address and e-mail is to be indicated below each author's name. An abstract of 200 words is to be written in English after the author's names. A list with up to six keywords at the end of the abstract is required.

Although alteration of the sequence and the title of each section may be required, it is suggested that the text contains the following sections: Introduction, Material and Methods, Results, Discussions, Conclusion, Acknowledgements, References and List of Symbols. A brief description of each section is given next.

Introduction: This section should indicate the state of the art of the problem under evaluation, a description of the problem and the methods undertaken. The objective of the work is to be clearly presented at the end of the section.

Materials and Methods: This section should include all information needed to the reproduction of the presented work by other researchers.

Results: In this section the data of the investigation should be presented in a clear and concise way. Figures and tables should not repeat the same information.

Discussion: The analyses of the results should be described in this section. **Conclusions**: The text of this section should be based on the presented data and in the discussions.

Acknowledgenments: If necessary, concise acknowledgements should be written in this section.

References: References to other published sources are to be made in the text by the last name(s) of the author(s), followed by the year of publication, similarly to one of the two possibilities below:

"*while Silva & Pereira (1987) observed that resistance depended on soil density*" or "*It was observed that resistance depended on soil density (Silva & Pereira, 1987)*."

In the case of three or more authors, the reduced format must be used, *e.g.*: Silva *et al.* (1982) or (Silva *et al.*, 1982). Two or more citations belonging to the same author(s) and published in the same year are to be distinguished with small letters, *e.g.*: (Silva, 1975a, b, c.). Standards must be cited in the text by the initials of the entity and the year of publication, *e.g.*: ABNT (1996), ASTM (2003).

Full references shall be listed alphabetically at the end of the text by the first author's last name. Several references belonging to the same author shall be cited chronologically. Some examples are listed next:

Papers: Bishop, A.W. & Blight, G.E. (1963) Some aspects of effective stress in saturated and unsaturated soils. Géotechnique, v. 13:2, p. 177-197.

Books: Lambe, T.W & Whitman, R.V. (1979) Soil Mechanics, SI Version, 2nd ed. John Wiley & Sons, New York, p. 553.

Book with editors: Sharma, H.D.; Dukes, M.T. & Olsen, D.M. (1990) Field measurements of dynamic moduli and Poisson's ratios of refuse and underlying soils at a landfill site. Landva A. & Knowles, G.D. (eds) Geotechnics of Waste Fills - Theory and Practice, American Society for Testing and Materials - STP 1070, Philadelphia, p. 57-70.

Proceedings (printed matter or CD-ROM): Jamiolkowski, M.; Ladd, C.C.; Germaine, J.T & Lancellotta, R. (1985) New developments in field and laboratory testing of soils. Proc. 11th Int. Conf. on Soil Mech. and Found. Engn., ISSMFE, San Francisco, v. 1, pp. 57-153.(specify if CD – ROM)

Thesis and dissertations: Lee, K.L. (1965) Triaxial Compressive Strength of Saturated Sands Under Seismic Loading Conditions. PhD Dissertation, Department of Civil Engineering, University of California, Berkeley, 521 p.

Standards: ASTM (2003) Standard Test Method for Particle Size Analysis of Soils - D 422-63. ASTM International, West Conshohocken, Pennsylvania, USA, 8 p.

Internet references: Soils and Rocks available at http://www.abms.com.br.

On line first publications must also bring the digital object identifier (DOI) at the end.

Figures shall be either computer generated or drawn with India ink on tracing paper. Computer generated figures must be accompanied by the corresponding digital file (.tif, .jpg, .pcx, etc.). All figures (graphs, line drawings, photographs, etc.) shall be numbered consecutively and have a caption consisting of the figure number and a brief title or description of the figure. This number should be used when referring to the figure in text. Photographs should be black and white, sharp, high contrasted and printed on glossy paper.

Tables shall be numbered consecutively in Arabic and have a caption consisting of the table number and a brief title. This number should be used when referring to the table in text. Units should be indicated in the first line of the table, below the title of each column. Abbreviations should be avoided. Column headings should not be abbreviated. When applicable, the units should come right below the corresponding column heading. Any necessary explanation can be placed as footnotes.

Equations shall appear isolated in a single line of the text. Numbers identifying equations must be flush with the right margin. International System (SI) units are to be used. The symbols used in the equations shall be listed in the List of Symbols. It is recommended that the used symbols be in accordance with Lexicon in 8 Languages, ISSMFE (1981) and the ISRM List of Symbols.

The text of the submitted manuscript (including figures, tables and references) intended to be published as an article paper or a case history should not contain more than 30 pages formatted according to the instructions mentioned above. Technical notes and discussions should have no more than 15 and 8 pages, respectively. Longer manuscripts may be exceptionally accepted if the authors provide proper explanation for the need of the required extra space in the cover letter.

Discussion

Discussions must be written in English. The first page of a discussion paper should contain:

• The title of the paper under discussion in the language chosen for publication;

• Name of the author(s) of the discussion, followed by the position, affiliation, address and e-mail. The discusser(s) should refer himself (herself, themselves) as "the discusser(s)" and to the author(s) of the paper as "the author(s)".

Figures, tables and equations should be numbered following the same sequence of the original paper. All instructions previously mentioned for the preparation of article papers, case studies and technical notes also apply to the preparation of discussions.

Editorial Review

Each paper will be evaluated by reviewers selected by the editors according to the subject of the paper. The authors will be informed about the results of the review process. If the paper is accepted, the authors will be required to submit a version of the revised manuscript with the suggested modifications. If the manuscript is refused for publication, the authors will be informed about the reasons for rejection. In any situation comprising modification of the original text, classification of the manuscript in a category different from that proposed by the authors, or refusal for publication, the authors can reply presenting their reasons for disagreeing with the reviewers' comments

Submission

The author(s) must submit for review:

1. A hard copy of the manuscript to Editors - Soils and Rocks, Av. Prof. Almeida Prado, 532 – IPT, Prédio 54 – DEC/ABMS, 05508-901 - São Paulo, SP, Brazil. The first page of the manuscript should contain the identification of the author(s), or

2. The digital file of the manuscript, omitting the authors' name and any information that eventually could identify them, should be sent to **abms@ipt.br**. The following must be written in the subject of the e-mail message: "*Paper submitted to Soils and Rocks"*. The authors' names, academic degrees and affiliations should be mentioned in the e-mail message. The e-mail address from which the digital file of the paper was sent will be the only one used by the editors for communication with the corresponding author.

Follow Up

Authors of manuscripts can assess the status of the review process at the journal website (www.soilsandrocks.com.br) or by contacting the ABMS secretariat.

Volume 34, N. 1, January-April 2011

Table of Contents